DECLARATION

I, **Sujata Das** hereby declare that the project entitled "**Production of ligninolytic enzymes from novel, wild isolates of basidiomycetes for degradation of industrial dyes**" is an authentic record of my own work carried out at School of Bioengineering and Bioscience, Lovely Professional University, Phagwara for the partial fulfilment for the award of '**Doctor of Philosophy' in Microbiology** under the guidance of **Dr. Shalini Singh.**

This work is my original work and not been submitted for any degree/diploma in this or any other university. The information furnished in this report is genuine to the best of my knowledge and belief.

Place:

Date:

Sujata Das (41200445)

CERTIFICATE

This is to certify that the thesis entitled **"Production of ligninolytic enzymes from novel, wild isolates of basidiomycetes for degradation of industrial dyes"** by **Ms. Sujata Das (41200445)** under my guidance and supervision. To the best of my knowledge, the present work is the result of their original investigation and study.

No part of the study has ever been submitted for any other degree at any university. The report is fit for submission and partial fulfilment of condition for the award of Doctor of Philosophy in Microbiology.

Date:

Supervisor signature

Dr. Shalini Singh

Associate Professor

deoaryment

Lovely Professional University

Abstract

Dyes are the important class of synthetic organic compounds used in various types of industries. They have been recognized as a significant pollutant because of the recalcitrant properties conferred by few of them. Their presence in natural water resources, on disposal of effluents from various types of industries, not only affects the aesthetic quality but also the aquatic eco-system adversely. Various types of remediation methods have been employed since many years but the demand of efficient system, which would not only reduce the possibility of secondary pollution rate but also would be economically feasible and technologically advance, has always been epicentre of recent researches. Thus, this study has endeavoured to provide a probable solution to the above problem, which not only could increase the efficiency of dye remediation but also has gone forward to propose a cost-effective advance operation technology for the effluent treatment plants.

Out of 114 samples collected, 3 isolates were obtained showing all the three ligninolytic enzyme activity under optimized condition of temperature, pH, days of incubation, yeast extract and copper sulphate concentration. One amongst the three has shown the best laccase production with 11.84 ± 0.67 IU/mL under solid state fermentation (SSF) condition. Based on the sequence comparison and phylogenetic analysis of the 18s rRNA genes with the reference taxa *Schizophyllum commune* H4-8: GCA_000143185.1, the wild isolate S4 with high laccase activity was identified as Schizophyllum-S4. It has shown around 89.52% identity in the aligned region, suggesting its novelty. On statistical method of analysis (by RSM) for its laccase production it has shown 18.47 IU/mL production of laccase.

The study has used five different dyes to exhibit the maximum adsorption capacity of wheat bran, a lignocellulosic waste, for dye decolorization by adsorption method. It has successfully given a result with maximum adsorption capacity (q_m mg/g) 19.79, 11.14, 15.17, 12.34 and 15.98 for CV, MG, CR, DDR and DO, respectively, following non-Linear Langmuir adsorption isotherm model. They have followed pseudo second order kinetic model, with, q_m mg/g, values, 12.07, 13.46, 12.26, 11.88 and 13.28 for the respective dyes indicating wheat bran to be an efficient, eco-friendly alternative for the removal of dyes from the industrial wastewater.

The study has evaluated the synergistic activity of the adsorbent (WB) and the isolate (*Schizophyllum*-S4) (WB-F biomass) obtained in the study, for the production of laccase for the purpose of dye decolorization (/ degradation) and on subsequent check on its reusability has shown that the percent decolorization by dye adsorbed bran and fungal mycelium in conjuncture was 93.98, 96.57, 98.89, 87.46 and 88.12 % for CV, MG, CR, DDR and DO, respectively. With respect to reusability it has shown the alternate adsorption and desorption mechanism of the WB-F biomass could make the biomass to be used for 5 cycles with efficiency of dye removal of around 61.89, 66.28, 68.79, 61.77 and 64.38 %, respectively, depicting the involvement of the fungal mycelium as an adsorbent along with the wheat bran in the process of decolorization. Chromatographic analysis has shown that the dye of 98% has shown degradation of around 60.94%, 62.47%, 48.26%, 51.57% and 44.01% for CV, MG, CR, DDR and DO respectively after 10 days of incubation in WB-F biomass, depicting the production of laccase enzyme responsible for the degradation.

Lastly, the study has proposed a novel architecture for system operation for a designed effluent treatment prototype by taking into consideration of the isolated novel strain, efficient lignocellulosic biomass (WB), an IoT, a cost-efficient effluent treatment plant prototype was designed. After the usage of the system, by treatment of textile effluent as a representation effluent it was observed that there was a decrease in BOD by 84.12 %, COD by, 63.92%, TDS by 54.29%, TSS by 48.23%, DO by 58.64 % and Optical Density by 93.67%. Thereby giving a unique system where a novel eukaryotic system and agro-industrial waste material could be used together for an enzyme system application in remediation purpose. Online monitoring, distribution device management and integration with a legacy system was another uniqueness of the invention. Next, being able to connect to the surrounding system, with a boundary less information flow being able to convert the legacy system to IoT based system, compatible to Bigdata or Data analytic platform and a loose coupled customer friendly invention.

Acknowledgement

First and foremost, I bestow my praises and thanks to my father, Late **Shri Radha Ballav Das**, the **Almighty**, for their showers of blessings upon me throughout my research work to complete the research successfully.

I would like to express my deep and sincere gratitude to my research supervisor, **Dr. Shalini Singh**, Associate Professor, School of Bioengineering and Biosciences, Lovely Professional University, Jalandhar, Punjab, India, for giving me the opportunity to do research under her supervision and providing invaluable guidance throughout this research and since known. Her dynamism, vision, sincerity, precision and motivation have deeply inspired me. She has taught me how to design and represent a research work with appropriate justifications and clarity. It was a great privilege and honour to work and study under her guidance. Not only in research, her support and guidance in personal life was also duly felt. I am extremely grateful for what she has offered me. I would also like to thank her for her friendship, empathy, and great sense of humour.

I am extremely grateful to my mother and mother-in law for their love, prayers, caring and sacrifices for helping me and staying beside me during this crucial phase of my life. I am very much thankful to my husband and my daughters for their love, understanding and perennial support to complete this research work. My husband, **Avijit Deb Sarkar**, has not only been a support by being a pillar and a navigator for me during this tenure by extending his unparallel help to successfully get a patent from this work but also has buffered all my emotional upheavals and continuously boosted me up with positivity.

I also extend my gratitude and thanks to my brother, **Shashank Garg,** for his immense, unconditional support during the statistical analysis done during this study. He has been a great help, without whom, this study would have been very difficult. My sincere thanks to my next brother **Sanjeev Singh**, who has always been beside me during all the ups and downs of this tenure. **Dr. Charu Khanna**, whose support and help can never be overlooked, who has been beside me as a sister to support me both emotionally and physically for the accomplishment of

my research work. I would sincerely like to thank **Dr. Joginder Singh**, for his support. He has been someone who under any situation has always tried to extend his help whenever it was required. I would like to thank **Dr. Simranjeet Singh**, who has helped me in few of the experiment analysis without any time confinement. I would like to bestow my thanks to all my colleagues, who had been always encouraging me for my work, appreciating me to boost up my quality of work, to name a few, **Dr. M.A. Khan, Dr.Arun Karnwal, Dr. Gaurav, Dr. Jastin Samuel, Dr. Shiwani Guleria, Dr. Richa Arora, Dr. Arvind, Dr. Surendra, Dr. Joydeep Dutta, Ms. Anu Bansal, Er. Chirag Chopra**. I, also express my thanks to my own brother, sister-in-law, niece and nephew for their support and valuable prayers.

I would like to extend my immense gratitude to the Dean of Lovely Faculty of Technology and Sciences, **Dr. Lovi Raj Gupta**, for his time to time appreciation, that has worked as an impetus for me to work harder. The Head of School, School of Bioengineering and Biosciences, **Dr. Neeta Raj Sharma**, for continuously relying on me and allowing me to work, day and night and utilize the lab facilities without any hindrance and always supporting me for my work with appreciation. The Head of Department, **Dr. Ashish Vyas**, for trusting on me, that inspite of the heavy tasks of teaching, the accomplishment of this project was possible by me.

I would like to extend my sincere thanks to all my lab technicians, who has always helped and provided me with all the materials whenever has been requested. To name a few I would extend my thanks to **Mr. John Masih, Mr. Sandeep Singh, Mr. Omkar Chand, Mr. Rahul Singh, Mr. Bhupender Singh, Mr. Sunny** for helping me during my experimentation by providing me all my requirements on time. I extend my thanks even to all my students, Ms.Prama Rani, Mr. Shilpa Nandi, Ms. Reema Verma, Mr. Vidhya for their kindness, support and prayer.

Finally, I owe my thanks to all the people who have supported me to complete the research work directly or indirectly.

Table of Content

Table of Content

Table of Content

Table of Content

Table of Content

List of Abbreviations

CV	Crystal Violet
MG	Malachite Green
CR	Congo Red
DDR	Disperse Dark Red
DO	Disperse Orange
WB	Wheat bran
UV-Spectroscopy	Ultra-Violet Visible Spectroscopy
FT-IR Spectroscopy	Fourier Transform Infra-Red Spectroscopy
ABTS	2,2'--azinobis(3-ethylbenzothiazoline-6-sulphonic acid)
WRF	White Rot Fungus
SSF	Solid State Fermentation
PDA	Potato Dextrose Agar
ETP	Effluent Treatment Plant
RBC	Rotatory Biological Contactor

List of Tables

List of Figures

List of Photographs

List of Appendices

List of Patent Published

1. Intellectual Property India, A communication network implementing REST based protocol. Date of publication: 26/07/2019.

List of Paper Published

1. Das S, Singh S, Garg S. 2019. Evaluation of wheat bran as a biosorbent for potential mitigation of dye pollution in industrial wastewater. Oriental Journal of Chemistry 35: 1565-1573.
2. Das S, Singh S, Sharma D, Anowar M, Kaur R and Kaur S. 2017. Bioscouring and desizing of textile fabrics using crude enzyme produced by white rot fungus (Basidiomycetes) isolated from rotten wood, International Journal of Chemical, Environmental and Biological Sciences 5 : 8-12.

List of Conferences attended

1. International Conference on Innovations in Engineering and Technology (ICIET-2017), Pattaya, Thailand, Oral Presentation on Bioscouring and desizing of textile fabrics using crude enzyme produced by white rot fungus (Basidiomycetes) isolated from rotten wood.
2. International Conference (ESDACON 2019) on Global Environmental Challenges, Human Health and Sustainable Development organized *by* Environment and Social Development Association (ESDA), Delhi in collaboration with Metropolitan University -USA; CSRD - JNU Delhi; BRAC - University of Delhi; CSIR-NEERI and GSI. Oral Presentation on Isolation and screening for laccase production by diversified species of basidiomycetes from in and around Punjab and Himachal Pradesh.

Chapter 1

Introduction

1.1 Introduction

Dye industry is a vibrant but challenging industry with a continuous streaming of new products on demand of the quickly changing world. Dyes are substances that, when applied to a substrate provides color by a process that at least temporarily alters any crystal structure of the colored substance (Othmer, 2004; Chequer et al., 2013). Dyes have a long history of usage began that with application of extracts from natural plant and insects, with a rapid switch over to synthetic process for use in number of application (Bafana, et al., 2011).

The dye manufacturing industry occupies a significant position in the chemical industries like polymer, petrochemical, paint, varnishes etc. for the industrial and economic development of the country. It is estimated that over 7×10^5 tons of synthetic dyes are produced annually, with more than 10,000 different types being used in industries like food, pharmaceutical, cosmetics, plastics, photographic, paper and textile industries (Zollinger,1991; Robinson, et al., 2001; Ogugbue and Sawidis, 2011). Of all the dyes used across the world, 11 percent has been reported to be present in industrial effluents of which around 2 percent is contributed from manufacturing and about 9 percent has been reported to be from the coloring sector of an industry (Carneiro et al., 2003). Dyes are classified either based on their chemical structure or on the substrate on which they are applied. They are composed of chromophores and auxochromes, responsible for their colour generation, and modification of ability to absorb light within the visible range (400-800nm), respectively (Chequer et al., 2013). Diverse functional groups govern these chromophore containing centers, such as azo, anthraquinone methine, nitro, aryl methane, carbonyl and others whereas, the auxochrome, that generates or intensifies the colour of the chromophore, either by electron donating or withdrawing substituents, mostly the amine, carboxyl, sulfonate and hydroxyl groups helps in imparting colour (Christie, 2001; Dos Santos et al., 2007 and Prasad et al., 2010). The

classification of dyes based on their structural and / or functional groups is standardized by the United States International Trade Commission (Table 1) (Gurses, et al., 2016).

Dye group	Description	Applications	References
Acid	Achieves affinity by salt formation between anionic and cationic groups; uses acid dyebath; water-soluble.	Wool, silk, paper, synthetics, leather, food colorings	Gregory, 1990
Azoic	Insoluble azo formulation; fiber must be treated to achieve affinity; unique colors possible due to modifications in both dye and modification chemicals; typically toxic.	Printing inks; pigments	Gupta and Suhas, 2009; Shah, 2014
Basic	Uses basic dyebath treated with acetic acid; water-soluble.	Silk, wool, cotton, acrylics, paper	Robinson, 2001; Hunger, 2003
Direct (substantive)	Uses alkaline dyebath; can also be used as biological stain.	Cotton, cellulosic and blended fiber, pH indication, paper, nylon	Burkinshaw and Salihu, 2019
Disperse	Water-soluble; dyebath may require high temperature; typically sold as powder or paste.	Synthetic fiber (esp. polyester)	Ejder-Korucu et al., 2015
Reactive	Relies on a chromophore capable of reacting directly with substrate; most permanent dye group.	Cellulosic fiber and fabric (esp. cotton)	Başer and Inanici 1990; Ferus-Comelo 2002; Pereira and Alves 2012
Sulfur	Typically dark-colored; requires two-part bath.	Cotton, cellulosic fiber	Wang et al., 2005 and Hunger, 2003
Vat	Soluble in alkaline liquor, but not water.	Cotton, cellulosic and blended fiber	Burkinshaw et al., 2019; Chakraborty 2010

Table 1.1: Classification of Dyes based on their chemical structure and applications

India has been reported to produce around 64,000 tons of dyes each year of which, 7040 tons are directly discharged into the environment in the form of industrial waste (Anonymous1, 2019). These dyes have become one of the most common sources of

industry based environmental pollution, from their synthesis till application in various industries in dyeing processes (Pereira and Alves, 2012). Dyes have affinity for the substrate they act upon forming chemical bonds by adhering to the compatible surfaces. They either form covalent bonds or complexes with salts or metals present on the substrate by physical adsorption or by mechanical retention method (Bafana et al., 2011). Based on the sources, dyes may be either natural or synthetic, the former ones are derived from natural sources such as roots, flowers, berries, leaves, bark and wood (Saxena and Raja, 2014). These natural dyes were used for thousands of years extensively until the discovery of synthetic dyes in the mid of 19^{th} century. Synthetic dyes are much more commonly used in industrial and commercial applications now a days. This is due to their colour flexibility and improved lasting power after application in comparison to natural dyes. The industrial dyes are produced, used, and tested based on the parameter listed in various standards like ISO 105-Z03, ISO 7579 and ISO 16373 (ISO16373-2, 2014) that tests for colour fastness, inter-compatibility of dyes, determination of their solubility in organic solvents, extractability, allergenic and carcinogenic properties (Anonymous 4, 2019).

Though there is no evidence that can suggest the health risks posed by most of the dyes but all dyes and chemicals must be handled with immense care as the most common hazard of reactive dyes are respiratory problems due to dye particle inhalation (Barr and Aust, 1994). At times they can affect the individual's immune system in such a manner that an individual may exhibit hypersensitivity (Rajaguru et al., 1999) , which may cause skin irritation or respiratory sensitization accompanied by the symptoms like itching, watery eyes, sneezing, blocked noses, symptoms of asthma like wheezing and coughing (Anonymous 2, 2019). Additionally, dyes have also been reported to have mutagenic agents (Mathur et al., 2012). The incidence of bladder tumors (Chung et al., 1992, and Rani et al., 2014) has been reported to be particularly higher in dye workers than in general population, which can be considered as an instance of problems lead by the presence of dyes in the wastewater (Eichlerova et al, 2006). Reports indicate that aromatic amines are generated by incomplete degradation of chemicals because of the presence of azo and nitro groups

in the organic dyes and it is this aromatic amine which is responsible for the induction of cancer and tumor in humans (Pang and Abdullah, 2013).

Heavy metals such as copper, zinc, chromium, lead, nickel and manganese are commonly associated with the dyes. The release of these heavy metals into soil and water may be dangerous to the human health and the environment (Barr and Aust, 1994). The non-biodegradable organic compounds present in dyes when mixes with natural water, on disposal, has also shown their ability to disrupt the food web leading to bioaccumulation, which can affect the water eco-system negatively.

Textile industry has been reported to be the largest consumer of dyes, (Silveira et al., 2009). Textile dyes are generally classified either in accordance with their chemical constitution, or on their application to textile fibres (Walters et al., 2005). Reactive Dyes, Vat Dyes and Azo Dyes are mainly required for dyeing and printing of fibres (Anonymous 3, 2014). Textile industries generate the largest amount of liquid waste among all the industries (Mostafa, 2015). The textile manufacturing includes, various processes of which the production of textile includes yarn formation, fabric formation & processing (Wet processing) and textile fabrication. It is during wet processing that includes, desizing, scouring, bleaching, dyeing, and printing, when they generate a large quantity of liquid waste. The dyes are released especially during the dyeing and the printing processes. The release of such effluent from the wet processing is detrimental to the environment as are disposed into the water bodies. Different types of chemicals (Saxena, 2017) comprising of unfixed dyes, auxiliary chemicals (Table 4) which are released as effluent at the final stage from the textile industries acts as contaminants for such water bodies (Babu et al., 2007). Structurally, most of the dyes are recalcitrant in nature for serving the purpose of conferring colour onto the applied materials which can ultimately show resistance towards fading on exposure to perspiration, soap, water, light or oxidizing agents. It has been reported that these dyes covalently react with the cellulosic -OH group in the fibres which results in their wash fastness (Forgacs et al., 2004). Those remain unbound gets into the wastewater generated in the wet processing contributing towards the high levels of visible colour and large amount of COD, BOD, TDS and alkalinity pH (9-11) (Table 1.2) (Gogate and Pandit, 2004).

Processes	Waste-water contaminants
Desizing	BOD from water soluble sizes; synthetic sizes; lubricants
Scouring	NaOH; disinfectant and insecticide residue; detergents; fats; oils, wax; lubricants
Bleaching	Hydrogen peroxide; sodium silicate; organic stabilizer
Merserizing	High pH; NaOH
Dyeing	Heavy metals; salts; surfactants; BOD; color
Printing	Suspended solids; urea; solvent; colour; metals; BOD
Finishing	BOD; COD; suspended solids; spent solvents

Table 1.2: Textile wet processing and associated waste -water contaminants

In developing countries, the textile operations are performed without the requisite resources for their waste treatment which ultimately contributes to environmental pollution (Sarayu and Sandhya, 2012; Saxena, Raja and Arputharaj, 2016). These effluents, generated from the wet processing, contain organic and inorganic compounds (Eliot et al., 1954). It has been reported that there are more than 10,000 dyes used in the textile manufacturing of which nearly 70% are of complex structure, carcinogenic in nature, azo dyes (Hildenbrand et al., 1999). During dyeing, of all the dyes, the unfixed dyes remains and gets washed out leading to the presence of a high concentration of these dyes in the generated effluent (Hassaan and Nemr, 2017). Around 10-15% (on an average) of unused dyes enter the wastewater after dyeing and after subsequent fabric washing (Rajamohan and Karthikeyan, 2006).The released water, affects the quality of both the surface and groundwater in the proximity of such textile facilities (Carnerio et al., 2010; Das, and Ramanathan, 2013).

Thus, the textile wastewater demands an appropriate treatment before disposal to the natural resources. Chemical and physical methods are applied for the treatment of textile effluent containing dyes but alone these methods are expensive (Robinson et al., 2001, 2002). Advanced treatment technologies like, photocatalytic degradation, electrochemical destruction etc., though, has shown an efficient removal of dyes from such effluents but green technologies such as adsorption of dyestuffs on low cost non-conventional adsorbents Crini, 2006) or on bacterial or fungal biomass (Fu and Viraraghavan, 2002) has shown a much better and promising results on the basis of

dye removal efficiency as well as economics of their use (Hameed and Lee, 2009, Hameed, 2009).

In physico-biological wastewater treatment, adsorption is one of the major technologies which have presently found an immense recognition for the waste-water treatment. The adsorbent, used either can mix with the wastewater as porous material powder or granules, as done by the activated carbon and clay or can allow the passage of the wastewater through its granular filter bed (Hussain et al., 2015). The most popular and widely used adsorbent, presently, is activated carbon but the major issue with it is, its cost, which increases with its quality along with, an additional factor of loss of adsorbent by 10-15% during its regeneration (Chen, 2017). Thus, there has been an intensive exploration for an efficient low-cost alternative material as a sorbent for dyes. In recent years, various types of biological and industrial wastes have been investigated for evaluation of their ability for dye removal from the aqueous solution. Few examples of such adsorbent are the agro-industrial waste material such as, corncob (Yatome et al., 1991), chitosan (Juang and Tseng, 1997), waste coir pith (Namasivayam et al., 2001) , giant duckweed (van den Brink et al., 1998), powdered peanut hull (Gong et al., 2005), coccinea berries (Akar et al., 2009), trees' leaves (Han et al., 2007), eggshell (Bouberka et al., 2005), modified clays (Tsai et al., 2007), fly ash (Rodriguez, 2013), beer brewery waste (Ghadiri et al., 2010), natural zeolite (Hashemian, 2007), bentonite (Hashemian et al., 2008) and rice bran (Ong et al., 2010). It has been shown in a study that barley straw, wheat straw and oat straw has a maximum adsorption capacity (q_m) around 27.72 mg/gm, 17.54 mg/gm and 8.34 g/gm for methylene blue, exhibiting their efficiency in dye removal capacity (Abdualhamid and Asil, 2012). Lignocellulosic substrate, wheat bran has been reported to be used in various studies as a cheap, natural substrate, as a growth medium because of the presence of combination of phenolic compounds (Kim et al., 2006, Murugesan et al., 2007 and Li et al., 2007) carbohydrates, proteins, amino acids and trace elements (Hashemian et al., 2008). It has also been used as a low cost adsorbent for the elimination of pollutants as well as heavy metals such as, Cr (VI) (Nameni et al., 2008), Pb (II), Cu(II) and Cd(II) (Farajzadeh and Boviery, 2004) from natural water and waste water in various studies. Conclusively, if the adsorbent is

inexpensive and does not require much pre-treatment, it can be used for remediation of dyes and industrial wastewater as such applications are economically and technologically viable and better as compared to the existing conventional methods (Namasivayam et al., 2001).

Though, the various physical and chemical methods like, membrane filtration, ion exchange, irradiation, ultrafiltration, microfiltration, nanofiltration, oxidative process, coagulation, photocatalytic degradation, electro-kinetic coagulation etc., respectively, so far reported, has shown effectivity for colour removal from the textile effluent but has also shown the possibility of further introduction of unwanted chemicals or substances in the system. The concentration or the generation of the pollutants into solid or liquid stream by such processes further demands an additional treatment or disposal methodology contributing towards the escalation of the waste-water treatment cost (Sandhya et al., 2007). Thereby, presently the major focus is on the microbiological methods being specific, less energy extensive, effective and environmentally safe as they result in a partial or complete bioconversion of organic pollutants to stable and non-toxic end products leading to the formation of water and carbon dioxide (Rekabi et al., 2001. Numerous bacterial, fungal and algal species have already been reported to show the ability to degrade and/or adsorb azo dyes (Singh et al., 2014).

For microbiological treatment, it has been reported that microbes are chosen on the basis of the structure of dye, the concentration of the dye to be decolorized, organism's absorption ability, based on cell wall composition and permeability; concentration of the biomass; presence of the electron donor species i.e. a redox mediator like, NADH, FAD, salt concentration, pH, temperature, oxygen concentration as well as the presence of the other chemical compounds. The major researches appeared to be conducted on bacteria and fungi as they have been proven to possess the ability to decolorize different types of dyes around 90% (Pandey et al., 2007).

Bacterial decolorization has been reported to be normally faster than fungal. They have the advantages of ease of cultivation, requirement of less generation time,

exhibit rapid growth both under aerobic and anaerobic conditions, and ready adaptation to a facultative environment in the effluent with high COD (Robinson, 2001). However, a disadvantage is the development of heavy sludge because of the huge development of bacterial biomass (Parmar and Shukla, 2018). The treatment an average estimation of around 0.4 gm of bacterial biomass production for every 1 gm Chemical Oxygen Demand (COD) removal (Metcalf and Eddy, 2003) has been estimated in the discharged effluent from the industries. Nearly, half of the COD which is removed from the wastewater gets transformed into new bacterial cells. The processing, treatment and disposal of such sludge poses one of the major environmental issue in numerous countries (Weemaes and Verstraete, 1998). It has been estimated that the costs involved in the treatment and disposal of excess sludge accounts for up to 60% of the total wastewater treatment costs (Canales et al., 1994). Anaerobic digestion is employed to reduce the sludge, but it has been reported to be energy consuming and cost intensive for the separation of biogas generated (Metcalf and Eddy, 2003). The treatment of, such high strength wastewater, with filamentous fungi has found to be an efficient and attractive alternative as they can be cultivated on relatively inexpensive substrates such as starch and molasses, for the production of by products like proteins and other biochemicals (Barbesgaard et al., 1992). Their application in wastewater organics not only can lead to the generation of important proteins or biochemicals but also can produce highly dewaterable fungal biomass which can also be used as a source of animal feed (Guest and Smith, 2002; Zheng et al., 2005). They also can produce a wide range of biochemicals and enzymes and has been shown to be more efficient in metabolizing complex chemicals like dyes in comparison to bacteria (Jin et al., 1998; van Leeuwen et al., 2003). Fungi are more resistant to inhibitory substances because of their hyphal growth, which provides protection to their sensitive organelles. The cell wall protects them from the inhibitory compounds by adsorption and, being eukaryotic system, they possess more genes than bacteria which make them more versatile to tolerate inhibitory compounds (Guest and Smith, 2002). The fungal mycelia have an added advantage because of their greater physical and enzymatic contact with the environment which helps them to degrade variety of organic pollutants, can solubilize the insoluble substrates, etc. Fungi also shows several advantages over bacteria in biological treatment of industrial

wastewater that helps in the biodegradation of the recalcitrant compounds such as, phenolics, dyes and polyaromatic hydrocarbons, through non-specific oxidation reactions (D'Annibale et al., 2004; Giraud et al., 2001; Jaouani et al., 2005). It has been reported that among the different fungi, white rot fungi have the greatest potential in dye degradation. They have shown the ability to decolourize various textile dyes with their lignin-degrading enzymes like, Laccase, Lignin Peroxidase and Magnesium peroxidase (Ramachandran and Gnanadoss, 2013).

White rot fungus (WRF), have earned immense attention since 1980s, with the discovery of ligninolytic enzymes. Since then, for nearly three decades, WRF have shown the ability to decolourize various textile dyes with their lignin degrading enzymes (Champagne and Ramsay, 2005). WRF constitute a varied eco-physiological group encompassing mostly basidiomycetous fungi, and to a lesser extent litter-decomposing fungus (Wang et al., 2005) which possesses the ability to degrade the heterogenous, complex and stable polymer lignin. Tien and Kirk (1983) had reported the first dye decolourization study by *Phanerochaete chrysosporium* (Robinson et al., 2001). *Hirschioporus larincinus*, *Inonotus hispidus*, *Phlebia tremellosa* and *Coriolus versicolor*, have also been reported to decolourise dye present in the industrial effluent (Banat et al, 1996). Wesenberg et al. (2003) had evaluated 29 different white rot fungi which were capable of decolorizing dyes. Several different investigators have evaluated the decolorization of various commercial dyes by different new species of white rot fungi (Levin et al., 2004). The capability of dye decolorization varies with different types of fungal species or enzymes (Tien and Kirk, 1983). The lignin degrading ability of white rot fungi is correlated with their capacity to synthesize an extracellular non-specific enzymatic complex comprising of lignin peroxidase (ligninase, LiP, EC 1.11.1.14) (Wong, 2009), manganese dependent peroxidase (MnP, EC 1.11.1.13) (Wesenberg, 2003), laccase (benzenediol: oxygen oxidoreductase, EC 1.10.3.2) (Baldrian, 2006) and versatile peroxidase (VP, EC 1.11.1.16) (Asgher, et al., 2008). They also produce the hydrogen peroxide required by peroxidases (LiP and MnP) which can link lignocellulose degradation pathways (Leonowicz et al., 2001, Robinson et al., 2001). Of all the enzymes, laccase has been

reported to possess the greatest potential for textile dye decolorization, xenobiotic removal and degradation (Strong and Claus, 2011).

For effluent treatment various types of techniques are being employed, either physical, chemical or biological processes, though it has been reported that individually they are either less efficient or economically non-viable especially when executed as a standalone process (Mehna et al., 1995). A combination of physical and biological process, on the contrary, can be explored as an efficient and economical and environmental friendly method where biosorption by lignocelluloses and subsequent utilization of the substrate as a solid substrate during solid state fermentation (Moldes et al., 2003; Boran and Yesilada, 2011) could be a significant integration for an efficient bio-decolorization process.

Bioreactors play an important role in any biotechnological application (Chisthi and Young, 2001), as they maintain the product value and the scale of the production (Jagani et al., 2010). Stirred tank reactors constitute the largest group concerning the most widespread reactor used for fungus culturing (Musoni, 2015). Immobilization of fungi at lab, at industrial scale fixed bed reactors, like rotating biological contactors (Yao et al., 2012; Kapdan and Kargi, 2002) has found few applications in industries for various types of industrial effluent treatment processes. Numerous publications have also appeared on various types of reactor designing for the lignin modifying enzyme production like, stirred tank, packed beds, air lifts, column, rotating disks etc., but still there exists a dearth of analogous reports on the usage of WRF in the reactor systems for the waste water treatment (Wesenberg et al, 2003). Application of smart technologies has the potential to enhance the output of a process. However, every technique targeted the complete removal of the dye or sustainability of the processes but the real time process operation and regulation, irrespective of the methods (physical, chemical, biological or combinations) employed is also a major area of concern during evaluation of an efficient industrial level operation. Advanced technology like Internet of Things (IoT) (Anonymous 5, 2019) of which Industrial Internet of Things (IIOT), a subset of the IOT concept has the potential to increase the output and amplify the working ability of a process or a system. IoT possesses the ability to connect physical objects and spaces to the internet for monitoring and utilize

them for more effective scale up. Cloud computing can provide an access to the remote servers hosted in the internet, whereby can store, manage and process the data on a distributed system. Thus, it enables the consumers with internet access to use applications in a secured environment (Kanday, 2012; Khalil et al., 2014).

The present investigation is thus, devoted for the evaluation of, wheat bran, a cheap and readily available, lignocellulosic waste for the removal of textile dyes, screen indigenously isolated white rot fungal strains their ligninolytic enzymes that can help degrade the dye adsorbed lignocellulosic waste to further reduce dye load from textile effluent. The dyes chosen for this study were, Crystal Violet (CV), Malachite Green (MG), Congo Red (CR), Dispersive Dark Red (DDR) and Dispersive Orange (DO), of which CV and MG, are basic dyes, CR, an azo dye, DDR and DO are disperse dye used specifically in the textile industries for dye polyesters. The first three dyes (CV, MG, CR) were lab procured whereas, DDR and DO were procured from textile industry, locally available. The study also aims to investigate the recycling potential of the adsorbent (wheat bran) and adsorbent fungal biomass in dye remediation. Based on which, a textile effluent treatment prototype will be developed.

Following are the formulated objectives of the study:

1. Isolation and screening of basidiomycetous strain for production of ligninolytic enzymes.
2. Evaluation of wheat bran as a dye adsorbent.
3. Recycling potential of spent dye adsorbed substrate-fungal biomass for dye removal
4. Designing of a cost-effective bioreactor for efficient industrial dye removal.

1.2 Reference

1. Abdulhamid SA, Asil AA. 2012. The effect of soaking process of agricultural wastes on the adsorption of methylene blue dye, *Int Food Res J* 19: 1567- 1571.
2. Akar T, Anilan B, Gorgulu, A, Akar ST. 2009. Assessment of cationic dye biosorption characteristics of untreated and non-conventional biomass: Pyracantha coccinea berries. *J of hazardous mat* 168 (2-3):1302-1309.
3. Al-Rekabi12 WS, Qiang H, Qiang WW. 2007. Improvements in wastewater treatment technology. *Pak J of Nut* 6(2):104-110.
4. An SY, Min SK, Cha IH, Choi YL, Cho YS, Kim CH, Lee YC. 2002. Decolorization of triphenylmethane and azo dyes by Citrobacter sp. *Biotechnology letters* 24(12):1037-1040.
5. Ananthashankar R. 2012. Treatment of textile effluent containing reactive red 120 dye using advanced oxidation.
6. Anonymous 1, 2019, https://www.iso.org/obp/ui/#iso:std:iso:16373:-1:ed-1:v1:en, Textiles, Dyestuffs — Part 1: General principles of testing coloured textiles for dyestuff identification, accessed on 12/02/2019.
7. Anonymous 4, 2014, https://www.iso.org/obp/ui/#iso:std:iso:16373:-2:ed-1:v1:en, ISO16373-2: 2014, Textiles-Dyestuffs-Part-2: General Method for the Determination of Extractable Dyestuffs including allergenic and carcinogenic dyestuffs (method using pyridine-water), Technical Committee ISO/TC 38, 1-20, accessed on 13/02/2019.
8. Anonymous 5, Abdulla Fatiya, 2019, https://textiles-apparels.cioreviewindia.com/cioviewpoint/role-of-iot-and-digital-technology-in-textile-industry-nid-3531-cid-1.html , Role of loT and digital Technology in textile industry, Head IT SAP Applications, D'décor Exports, accessed on 3/3/2019.
9. Anonymous 2, 1996,https://onlinelibrary.wiley.com/doi/abs/10.1111/j.14784408.1996.tb01754.x, Health and Safety Executive, HSE. Dyeing and Finishing Information

Sheet No 1- HSE information sheet, Dyes and chemicals in textile finishing, an introduction, accessed 10.10.2016.

10. Anonymous3,2014, https://www.globalspec.com/learnmore/materials_chemicals_adhesives/chemicals_raw_materials/dyes, Industrial dyes information, Engineering 360, powered by IEEE global spec, accessed on 12/03/2019.
11. Asgher M, Batool S, Bhatti HN, Noreen R, Rahman SU and Asad MJ. 2008. Laccase mediated decolorization of vat dyes by *Coriolus versicolor* IBL-04. *Int Biodet & Biodeg* 62(4):465-470.
12. Azbar N, Yonar T, Kestioglu K. 2004. Comparison of various advanced oxidation processes and chemical treatment methods for COD and color removal from a polyester and acetate fiber dyeing effluent. *Chemosphere 55*(1):35-43.
13. Azmi W, Sani RK, Banerjee UC. 1998. Biodegradation of triphenylmethane dyes. *Enz and micro tech* 22(3):185-191.
14. Bafana A, Devis SS, Chakraborty T. 2011. Azo dyes: past, present and future. *Env Rev* 19: 350-370.
15. Banat IM, Nigam P, Singh D and Marchant R. 1996. Microbial decolorization of textile-dye containing effluents: a review. *Biores tech* 58(3):217-227.
16. Barr DP, Aust SD. 1994. Pollutant degradation by white rot fungi. Int *Rev Environ Cont and Tox*, Springer, New York, NY: 49-72.
17. Boran F, Yesilada O. 2011. Enhanced production of laccase by fungi under solid substrate fermentation condition. *Biores* 6(4):4404-4416.
18. Bouberka Z, Kacha S, Kameche M, Elmaleh S, Derriche Z. 2005. Sorption study of an acid dye from an aqueous solution using modified clays. *J of Hazard Mat* 119(1-3):117-124.
19. Bulut Y, Baysal Z. 2006. Removal of Pb (II) from wastewater using wheat bran. *J of Env Manag* 78(2):107-113.
20. Bumpus JA and Brock BJ.1988. Biodegradation of crystal violet by the white rot fungus *Phanerochaete chrysosporium*. *Appl Environ Micro* 54(5):1143-1150.

21. Carrott PJM, Carrott MR, Correia PFMM. 2018. Evolution of porosity of activated carbon fibres prepared from pre-oxidized acrylic fibres. *Micro and Meso Mat* 264:176-180.
22. Castillo-Carvajal LC, Pedroza-Rodríguez AM, Barragán-Huerta BE. 2013. Adsorption and biological removal of basic green 4 dye using white-rot fungi immobilized on *Agave tequilana* weber waste. *Fres Env Bulletin* 22(8):2334-2343.
23. Cha CJ, Doerge DR and Cerniglia CE. 2001. Biotransformation of Malachite Green by the Fungus *Cunninghamella elegans*. *Appl Env Micro* 67(9):4358-4360.
24. Champagne PP, Ramsay JA. 2005. Contribution of manganese peroxidase and laccase to dye decoloration by *Trametes versicolor*. *App Micro and Biotech* 69(3):276.
25. Chequer FD, de Oliveira GAR, Ferraz EA, Cardoso JC, Zanoni MB, de Oliveira DP. 2013. Textile dyes: dyeing process and environmental impact. *Eco-friendly tex dye and finish* 6:151-176.
26. Chequer FD, de Oliveira GAR, Ferraz EA, Cardoso JC, Zanoni MB, de Oliveira DP. 2013. Textile dyes: dyeing process and environmental impact. *Eco-frien Tex Dyeing and Fin* 6:151-176.
27. Chishthi and Young M. 2001. Bioreactor design, Fundamentals. *J of Bact, of Biotech chromofuscus* 176:1339–1347.
28. Chung KT, Stevens SE, Cerniglia CE.1992. The reduction of azo dyes by the intestinal microflora. *Cri Rev in Micro* 18(3):175-190.
29. Crini G. 2006. Non-conventional low-cost adsorbents for dye removal: a review. *Biores tech* 97(9):1061-1085.
30. Dhir B and Kumar R. 2010. Adsorption of heavy metals by Salvinia biomass and agricultural residues. *I J of Env Res* 4(3):427-432.
31. Eichlerová I, Homolka, Nerud F. 2006. Synthetic dye decolorization capacity of white rot fungus *Dichomitus squalens*. *Biores Tech* 97(16):2153-2159.
32. Farajzadeh MA, Monji AB. 2004. Adsorption characteristics of wheat bran towards heavy metal cations. *Sep and Pur Tech* 38(3):197-207.

33. Faria PCC, Órfão JJM, Figueiredo JL, Pereira MFR. 2008. Adsorption of aromatic compounds from the biodegradation of azo dyes on activated carbon. *App Sur Sc* 254(11): 3497-3503.
34. Ferrero F. 2007. Dye removal by low cost adsorbents: Hazelnut shells in comparison with wood sawdust. *J of Haz Mat* 142(1-2):144-152.
35. Fu Y, Viraraghavan T. 2001. Fungal decolorization of dye wastewaters: a review. *Biores tech* 79(3): 251-262.
36. Fu Y, Viraraghavan T. 2002. Removal of Congo Red from an aqueous solution by fungus *Aspergillus niger*. *Adv in Env Res* 7(1):239-247.
37. Galindo C, Kalt A.1999. UV/H_2O_2 oxidation of azo dyes in aqueous media: evidence of a structure—degradability relationship. *Dyes and Pig* 42(3):199-207.
38. Ghadiri SK, Nabizadeh R, MahviA H, Nasseri S, Kazemian H, Mesdaghinia
39. Gong R, Ding Y, Li M, Yang C, Liu H, Sun Y. 2005. Utilization of powdered peanut hull as biosorbent for removal of anionic dyes from aqueous solution. *Dyes and Pig* 64(3):187-192.
40. Gutiérrez-Bouzán C, López-Grimau V and Vilaseca M. 2013. New Trends in Textile Wastewater Treatments. *Dyeing: Pro Tech and Appl. Fu J, Ed.* New York: Nova Science Publishers.
41. Hameed BH, Lee TW. 2009. Degradation of malachite green in aqueous solution by Fenton process. *J of Haz Mat* 164(2-3):468-472.
42. Hameed BH. 2009. Removal of cationic dye from aqueous solution using jackfruit peel as non-conventional low-cost adsorbent. *J of Haz Mat* 162(1):344-350.
43. Han R, Zou W, Yu W, Cheng S, Wang Y, Shi J. 2007. Biosorption of methylene blue from aqueous solution by fallen phoenix tree's leaves. *J of Haz Mat* 141(1):156-162.
44. Hashemian S, Dadfarnia S, Nateghi MR, Gafoori F. 2008. Sorption of acid red 138 from aqueous solutions onto rice bran. *Afr J of Biotech* 7(5):600-605.
45. Hashemian S. 2007. Study of adsorption of acid dye from aqueous solutions using bentonite. *Main Grp Chem* 6(2):97-107.

46. Hassaan MA, El Nemr A. 2017. Advanced oxidation processes for textile wastewater treatment. *Int J of Photochem and Photobio* 2(3):85-96.
47. Hildenbrand S, Schmahl FW, Wodarz R, Kimmel R, Dartsch PC. 1999. Azo dyes and carcinogenic aromatic amines in cell cultures. *Int Arch of Occ and Env Health* 72(3):52-56.
48. Hofrichter M, Lundell T and Hatakka A. 2001. Conversion of milled pine wood by manganese peroxidase from *Phlebia radiata*. *Appl Environ Microbio* 67(10):4588-4593.
49. Jebapriya GR, Gnanadoss JJ. 2013. Bioremediation of textile dye using white rot fungi: A review. *Int J of Cur Res and Rev* 5(3):1.
50. Juang RS, Tseng RL, Wu FC, Lee SH. 1997. Adsorption behaviour of reactive dyes from aqueous solutions on chitosan. *J of Chem Tech & Biotech: Int Res in Pro, Env and Clean Tech* 70(4):391-399.
51. Kapdan IK, Kargi F. 2002. Biological decolorization of textile dyestuff containing wastewater by *Coriolus versicolor* in a rotating biological contactor. *Enz and Micro Tech* 30(2):195-199.
52. Leonowicz A, Cho N, Luterek J, Wilkolazka A, Wojtas-Wasilewska M, Matuszewska A, Rogalski J. 2001. Fungal laccase: properties and activity on lignin. *J of Basic Micro: An Int J on Biochem, Phy, Gen, Mor, and Eco of Micro* 41(3-4):185-227.
53. Levin L, Papinutti L, Forchiassin F. 2004. Evaluation of Argentinean white rot fungi for their ability to produce lignin-modifying enzymes and decolorize industrial dyes. *Biores Tech* 94(2):169-176.
54. Manzoor J and Sharma M. 2020. Impact of Textile Dyes on Human Health and Environment. *Impact of Textile Dyes on Public Health and the Environment*. IGI Global. 162-169.
55. Mehna A, Bajpai P, Bajpai PK. 1995. Studies on decolorization of effluent from a small pulp mill utilizing agri residues with *Trametes versicolor*. *Enz and Micro Tech* 17(1):18-22.
56. Messner K, Ertler G, Jaklin-Farcher S, Boskovsky P, Regensberger U & Blaha A. 1990. Treatment of bleach plant effluents by the MYCOPOR

system. In Biotechnology in Pulp and Paper Manufacture. *Butterworth-Heinemann* : 245-251.

57. Moldes D, Gallego PP, Couto SR, Sanromán A. 2003. Grape seeds: the best lignocellulosic waste to produce laccase by solid state cultures of *Trametes hirsuta*. *Biotech Let* 25(6):491-495.
58. Moreira MT, Feijoo G, Lema JM. 2003. Fungal bioreactors: applications to white-rot fungi. *Rev in Env Sc and Biotech* 2(2-4):247-259.
59. Mostafa M. 2015. Waste-water treatment in textile Industries-the concept and current removal technologies. *J Biodivers Environ Sci* 7(1):501-525.
60. Musoni M, Destain J, Thonart P, Bahama JB, Delvigne F. 2015. Bioreactor design and implementation strategies for the cultivation of filamentous fungi and the production of fungal metabolites: from traditional methods to engineered systems. BASE.
61. Namasivayam C and Kavitha D. 2002. Removal of Congo Red from water by adsorption onto activated carbon prepared from coir pith, an agricultural solid waste. *Dyes and Pig* 54(1):47-58.
62. Namasivayam C, Radhika R and Suba S. 2001. Uptake of dyes by a promising locally available agricultural solid waste: coir pith. *Waste Manag* 21(4):381-387.
63. Nazmara S. 2010. Methyl tert-butyl ether adsorption on surfactant modified natural zeolites. *Ira J of Env Health Sc Eng*, 7:241–252.
64. Neilson, AH, Allard, AS. 1997. Microbial Metabolism of PAHs and Heteroarenes. *PAHs and Related Compounds: Biology 3*(Part J):1.
65. Nyanhongo GS, Gomes J, Gübitz GM, Zvauya R, Read J, Steiner W. 2002. Decolorization of textile dyes by laccases from a newly isolated strain of *Trametes modesta*. *Wat Res* 36(6):1449-1456.
66. Ong S, Keng P, Chong A, Lee S, Hung YT. 2010. Tartaric acid modified rice hull as a sorbent for methylene blue removal. *A J of Env Sc* 6(3):244-248.
67. Othmer K. 2004. Encyclopedia of Chemical Technology. *Wiley International Science*, 5th Edition (7).

68. Rajaguru P, Fairbairn LJ, Ashby J, Willington MA, Turner S, Woolford LA, Rafferty JA. 1999. Genotoxicity studies on the azo dye Direct Red 2 using the in vivo mouse bone marrow micronucleus test. *Mut Res Gen Tox and Env Mut* 444(1):175-180.
69. Rajamohan N and Karthikeyan C. 2006. Kinetic studies of dye effluent degradation by Pseudomonas stutzeri. *J Solid Waste Technol Manag* :1-5.
70. Rani B, Kumar V, Singh J, Bisht S, Teotia P, Sharma S, Kela R. 2014. Bioremediation of dyes by fungi isolated from contaminated dye effluent sites for bio-usability, *Bra J of Micro* 45 (3):1055-1063.
71. Robinson T, McMullan G, Marchant R, Nigam P. 2001. Remediation of dyes in textile effluent: a critical review on current treatment technologies with a proposed alternative. *Biores Tech* 77(3):247-255.
72. Rodriguez-Couto S. 2013. Treatment of textile wastewater by white-rot fungi: still a far-away reality. *Tex and Light Ind Sc and Tech* 2(3):113-119.
73. Strong PJ and Claus H. 2011. Laccase: a review of its past and its future in bioremediation. *Cri Rev in Env Sc and Tech* 41(4):373-434.
74. Tien M, Kirk TK. 1983. Lignin-degrading enzyme from the *Hymenomycete Phanerochaete chrysosporium* Burds. *Sc* 221(4611):661-663.
75. Tsai WT, Hsu HC, Su TY, Lin KY, Lin CM. 2008. Removal of basic dye (methylene blue) from wastewaters utilizing beer brewery waste. *J of Haz Mat* 154(1-3):73-78.
76. van Gorcom RF, van den Hondel CA, Punt PJ. 1998. Cytochrome P450 enzyme systems in fungi. *Fun Gene and Bio* 23(1):1-17.
77. Wang S, Boyjoo Y, Choueib A, Zhu ZH. 2005. Removal of dyes from aqueous solution using fly ash and red mud. *Wat Res* 39(1):129-138.
78. Waranusantigul P, Pokethitiyook P, Kruatrachue M, Upatham ES. 2003. Kinetics of basic dye (methylene blue) biosorption by giant duckweed (*Spirodela polyrrhiza*). *Env Pol* 125(3): 385-392.
79. Wesenberg D, Kyriakides I, Agathos SN. 2003. White-rot fungi and their enzymes for the treatment of industrial dye effluents. *Biotech Adv* 22(1-2):161-187.

80. Wesenberg D, Kyriakides I, Agathos SN. 2003. White-rot fungi and their enzymes for the treatment of industrial dye effluents. *Biotech Adv* 22(1-2):161-187.
81. Yao S, Lai H, Shi Z. 2012. Biosorption of methyl blue onto tartaric acid modified wheat bran from aqueous solution. *Ira J of Env H Sc & Eng* 9(1):16.
82. Yatome C, Ogawa T, Koga D, Idaka E. 1981. Biodegradability of azo and triphenylmethane dyes by *Pseudomonas pseudomallei* 13NA. *J of the Soc of Dyers and Col* 97(4):166-169.
83. Yatome C, Ogawa T, Matsui M. 1991. Degradation of crystal violet by *Bacillus subtilis*. *J of Env Sc & Health* Part A 26(1):75-87.
84. Yatome C, Yamada S, Ogawa T, Matsui M. 1993. Degradation of crystal violet by *Nocardia corallina*. *App Micro and Biotech* 38(4):565-569.
85. Zheng Z, Levin RE, Pinkham JL, Shetty K. 1999. Decolorization of polymeric dyes by a novel Penicillium isolate. *Pro Biochem* 34(1):31-37.
86. Zhou Q, Gong WQ, Li YB, Chen SH, Yang DJ, Bai CP, Xu N. 2011. Biosorption of Methylene Blue onto spent corncob substrate: kinetics, equilibrium and thermodynamic studies. *Wat Sc and Tech* 63(12):2775-2780.
87. Zollinger H. 1987. Properties of Organic Dyes and Pigments. *Col Chem, New York, USA, VCH Publishers*: 92-102.
88. Zollinger H. 1991. Colour Chemistry: Synthesis. *Pro and App of Org Dyes and Pig* : 496.

Chapter 2

Isolation and screening of basidiomycetous strain for production of ligninolytic enzymes

2.1 Introduction

Basidiomycetes are characterized as such, as they produce their sexual spores, usually in four (basidiospores) on a cell called, basidium usually in fours. The basidium is the cell in which karyogamy (nuclear fusion) and meiosis occur, and on which usually four haploid basidiospores are formed on the tips of sterigmata. Sterigmata are small spike like projections that originate from the basidium. Millions of these spores are present together in the hymenium, which covers the exposed or enclosed surfaces of the sporocarp, which are quite variable in form (Coelho et al., 2017). Many, but not all, have clamp connections. No other group of fungi has these structures (Hood et al., 2006). The basidiomycetes make up a huge variety of fungi (ca. 23,000 species are known). Like other fungi, different basidiomycetes feed saprophytically or symbiotically. Saprobic basidiomycetes occur in forests (in the soil, in leaf or twig litter, or as wood colonizers in standing trees or fallen stems), in open country (also in soil or decomposing litter), and in many other places. Basidiomycetous fungi, thereby serve an important ecological role as wood decomposers too. The species of basidiomycetes can be distinguished by the form and size of the basidium (including the number of sterigmata or appendages that bear the spores, presence or absence of clamp at the septum at the base), the presence and character of other structures, such as cystidia, metuloids (lamprocystidia) and cystidioles, and the appearance of the basidiospores, if present.

Lignin, a highly recalcitrant, heteropolymer substance comprising of phenylpropanoid units, present mostly in the wood part of the plant tissues. They contribute towards the rigidity of the plant tissue and resistance against biological attack on them (Higuchi, 1990). Paper and pulp industries, for an example, usually, uses chemicals for the breakdown of such lignin, which in the process releases numerous hazardous, toxigenic and carcinogenic chemical compounds to the environment (Harazono et al., 1996). The solution to the above problem was the usage of wood- rotting fungal strain

possessing the ability of biodegradation of lignin. The white rot fungi of Basidiomycetes strain possess an oxidative and an unspecific enzyme system that produces low molecular weight metabolites, extracellular enzymes and reactive oxygen species (Schoemaker, 1990; Shimada and Higuchi 1991; de Jong et al., 1992; Guillen et al., 1997).

As because the enzyme system shows unspecificity in depolymerization of lignin, such white rot basidiomycetous strains are studied for the exploration of their ability for the degradation of the recalcitrant aromatic pollutant degradation, that causes serious environmental pollution. This study circumscribes on the isolation of such efficient strain from the environment, possessing the potential of ligninolytic enzyme activity which could be used for an efficient degradation of serious environmental pollutants like dyes thereby exploring the importance of basidiomycetes strain in laccase enzyme production by solid-state fermentation on wheat bran, an agro-industrial waste.

2.2 Review of Literature

Some strains of white-rot fungi are capable of degrading lignin efficiently using a combination of extracellular ligninolytic enzymes, organic acids, some mediators, and accessory enzymes. These enzymes include phenol oxidase (laccase) and heme peroxidases like, lignin peroxidase (LiP), manganese peroxidase (MnP) and versatile peroxidase (VP) (Dashtban et al., 2010). White rot fungus are key regulators of the global carbon cycle. Their Lignin Modifying Enzymes, i.e., manganese peroxidases (MnP), E.C. 1.11.1.13; lignin peroxidases (LiP), E.C. 1.11.1.14 and laccases (Lac), E.C. 1.10.3.2, are directly involved in the degradation of lignin in their natural lignocellulosic substrates. The main lignin modifying enzymes are oxidoreductases, mainly of two major types of peroxidases, MnP (Manganese peroxidase) and LiP (Lignin peroxidase) and laccase (Toh et al., 2003). It has also been reported that in most of the case nitrogen limiting medium has shown an increase in the production of LiP and MnP, which thereby increased some of their very important characteristic like decolourisation (Banat et al., 1996; Singhal and Rathore 2001). They also help in the degradation of various xenobiotic compounds including dyes. Some white rot fungi

produce all the three lignin modifying enzymes while others produce only one or two of them. They are the most intensively studied dye decolorizing microorganisms (Wesenberg et al., 2003). Many white rot fungi e.g. *Phanerachaete chrysosporium, Ganoderma sp WR.1, Trametes trogii, Irpex lacteus, Dichomitus squalens, Pycnoporus* strains etc. have been intensively studied in connection with their ligninolytic enzyme production and their decolourisation ability (Dayaram et al., 2008). Studies have shown that higher penetrability and extensive organization of hyphae are the major reasons for the abundance of wood degrading fungi in the environment. Additionally, the higher laccase activity in the basidiomycete species, responsible for rotting wood depicts that the major role of such fungal laccase is depolymerization of the complex cell wall component of plant, i.e. lignin. Studies suggests that such a process of degradation is a resultant of synergistic reaction of certain non-enzymatic and enzymatic entities by the establishment of a balance between the enzyme dependant polymerization and depolymerization (Dwivedi et al., 2011). However, the use of white rot is not limited to dye degradation alone. It Has also been found that Decolorization ability of white rot fungi can be substantially increased by carefully optimizing the operational conditions such as nutrient content of the media, age of fungus and environmental and operational conditions (Kumaran et al., 2011).

The use of laccase in the textile industry is growing. It is used to bleach textiles, synthetic dyes and modify the surface of fabrics in the denim-washing process etc. (Rodríguez et al., 2006). Concerning their use in the area of biotechnology, fungal laccases have diverse applications, ranging from effluent decolouration and detoxification to pulp bleaching, removal of phenolics from wines, organic synthesis, biosensors, synthesis of complex medical compounds and dye transfer blocking functions in detergents and washing powders, many of which have been patented (Kunamneni et al., 2007). They have also successfully been introduced to the cotton textile industry, produce the aged look of denim and other garments, removal of wool fibres scales, resulting in improved anti-felting behaviour, hydrolysis of synthetic fibres surfaces, improving their hydrophilicity and aiding further finishing steps. Besides hydrolytic enzymes, oxidoreductases have also been used as powerful tools in

various textile-processing steps. Catalases have been used to remove H_2O_2 after bleaching, reducing water consumption. (Jo et al., 2008). Lignin peroxidases are monomeric homo proteins with molecular masses around 40 kDa, and their Fe^{3+} is penta coordinated to four heme tetrapyrrole nitrogen and a histidine residue. Lignin peroxidases are oxidized by H_2O_2 to give two electrons oxidized intermediate in which iron is present as Fe^{4+} and a free radical resides on the tetrapyrrole ring. (Isroi et al., 2011).

Laccases have been subject of serious research in the most recent decades since they have the accompanying properties: wide substrate particularity, need not bother with the expansion or union of a low sub-atomic weight cofactor, as their co-substrate – oxygen – is typically present in their condition, most laccases are extracellular proteins, making the purification methodology simple and they for the most part show an extensive dimension of strength in the extracellular condition. Such qualities make laccases very appropriate for their application to a few bioprocesses, for example, bio-pulping, bio-bleaching and the treatment of mechanical wastewater. The catalytic property of the fungal laccases can be better studied by the knowledge of the structure of the enzyme. As reported, fungal laccases (EC 1.10.3.2), structurally are multi copper oxidoreductases, exhibiting the ability to catalyze the oxidation of any substrate by one electron oxidation subsequently leading to the transference of four electrons to the catalytic copper atoms. These copper atoms on the other hand are used for the reduction of oxygen molecule to form two molecules of water in the reaction (Solomon et al., 1996; Hakulinen and Rouvinen, 2015; Jones and Solomon, 2015; Mehra et al., 2018).

The laccases produced by fungi are monomeric glycoprotein, produced extracellularly comprising of around 520-550 amino acids in their glycosylated form with a molecular weight ranging between 60-70 kDa. Their N-terminal contains sequence of signal peptides of around 20-22 amino acid residues. The intricate architecture of the enzyme shows that it comprises of three domains, each of which are like cupredoxin in nature, tightly arranged with each other, retaining a β- barrel like symmetry which contributes towards their efficient ability to act on their specific substrate for degradation (Giardina et al., 2010). The use of laccases to the previously mentioned procedures requires the generation of vast sums of catalyst requiring little to no effort.

Hence, investigation around there is arranged towards the look for effective generation frameworks.

Phaenerochaete chrysosporium, a basidiomycetous fungi has emerged as a model organism in textile and paper and pulp mill effluent remediation system. They have been reported to degrade starch, cellulose, pectin, lignin, lignocellulosic materials, thus are very useful in degradation and remediation of effluents generated by the industries (Assadi et al., 2001; Wesenberg et al., 2003; Fraco et al., 2009).

Solid state fermentation of agro industry wastes has gained much attention in biotechnology, e.g. production of enzymes, as its use offers higher productivities at low production costs (Shukla et al., 2010). Studies on fungal enzyme production in Solid State Fermentation have shown that Solid State Fermentation, in comparison with Submerged Fermentation, provides higher volumetric productivities, is less prone to problems with substrate inhibition and yields enzymes with a higher temperature or pH stability in comparison to liquid state fermentation. Also, the fermentation time is shorter and the degradation of the produced enzymes by undesirable proteases is minimized (Toca-Herrera et al., 2007) in case of SSF. Substrates used in SSF are generally insoluble in water. In practice, water is absorbed onto the substrate particles, which can then be used by microorganisms for growth and metabolic activities. Substrate for SSF can be divided into three major groups, starchy substrates, cellulose or lignocellulose and those with soluble sugars. Example of starchy substrate includes rice, cassava, wheat bran, rice bran, buckwheat seeds, corn meal, and sweet potato residue and banana meal. Lignocellulosic solid-substrate includes wheat straw, corn, rice straw, wheat bran, sugar-beet pulp and wood (Elisashvili and Kachlishvili 2009; Akpinar and Urek 2014). Substrates containing soluble sugars include grape pomace, sweet sorghum, sugar-beet, pineapple waste, carob pods and coffee pulp. Natural substrates are easily available and are cheaper than synthetic substrates. But they generally require pre-treatment to make their chemical constituents more accessible and their physical structure more susceptible to mycelial penetration. Physical treatment includes chopping or grinding to reduce size and cracking to make the interior of the particle more accessible (Sawraj et al., 2005). The process of enzyme harvesting includes adding of distilled water and mixing well in a rotatory shaker at 200 rpm at room temperature for 40 min, followed by filtration

and centrifugation. The cell free supernatant is used for the enzyme activity determination (Varalakshmi et al., 2008).

SSF is an appealing procedure for enzyme production since it presents numerous favourable circumstances, particularly for fungal development. The extracellular laccase is a secondary metabolite, thus are produced by different fungi at their stationary phase of growth which is influenced by various factors. AS produced by different types of fungi, the influence of such factors also exhibits variations during their cultivation. The carbon, nitrogen source availability, the concentration of the inducers are the crucial factors which draws the interest of many investigators (Majeau et al., 2010). In SSF, the profitability per reactor or fermenter volume is a lot higher contrasted to that of submerged culture. Likewise, the task cost is lower considering the utilization of the machines that utilizes less vitality. Various studies have been conducted so far for the establishment of effect of various factors for the production of laccase industrially by the process of solid-state fermentation by various organism. Studies have also revealed that the influence of parameters varies on the basis of substrates and organisms used, individually as well as synergistically, for laccase production. A study on laccase production by *Trametes hirsuta* (MTCC11397) has shown that the optimum pH for laccase production at an optimum growth temperature was around 5.5 and 7.5, whereas, fructose and ammonium sulphate to be the best source of carbon for the same. The same study has shown that if in the medium, copper sulphate was used at a concentration upto 1.0 mM, the production could witness around 2 fold increase in the laccase production at only 0.4 mM concentration of it, depicting the utilization of such studies for better formulation for laccase production, industrially (Dhakar and Pandey, 2013). Use of agro-modern deposits as substrates in SSF form gives an elective road and value expansion to these generally under-or non-used build ups. SSF forms have turned out to be especially reasonable for the creation of catalysts by filamentous organisms, because of the way that they imitate the regular living states of filamentous fungi. The determination of a fitting solid material for performing solid state fermentation is vital, as it has a sturdy impact on the procedure.

It has also been shown that enzyme production in solid-state fermentation (SSF) is higher than in submerged fermentation (SmF). They concluded that SSF culture is by all accounts working, normally, as a fed batch culture with quick oxygenation however moderate sugar supply. The procedure had the additional preferred standpoint of being a static procedure without mechanical vitality uses. Interestingly, SmF cultures fill in as homogeneous frameworks requiring huge vitality consumptions to supply oxygen at quick enough rates to adapt to high oxygen request. There is the need in such procedures for robotized sustained group supply of substrates to maintain a strategic distance from catabolite constraint. Further investigation of SSF frameworks may profit from the utilization of tiny procedures, for example, picture examination, microelectrodes, improvement of DNA tests with optical properties, for example, in situ hybridization of specific RNA messengers and the utilization of hued combination proteins utilized as labels of specific protein items. Maybe, heterogeneity of SSF frameworks will be changed further bolstering its good fortune to control microbial movement for enzyme generation when contrasted with the impediment of homogeneous frameworks present in SmF cultures.

2.3 Materials and Methods

2.3.1 Materials

The glassware used were of borosilicate procured from local vendor, Jalandhar. The chemicals, reagents and media used were of analytical grade from reputed companies like Potato Dextrose Agar (PDA) and Potato Dextrose Broth (PDB) was purchased from HIMEDA, Mumbai, India. The bacteriological Agar-Agar was purchased from Central Drug House (CDH), New Delhi, India. The antibiotic streptomycin was bought from CDH, New Delhi, India. Pure Crystal violet ($C_{25}N_3H_{30}Cl$), Malachite Green ($C_{23}H_{25}ClN_2$), Congo Red ($C_{32}H_{22}N_6Na_2O_6S_2$) were procured from Loba Chemi, Mumbai, India. Substrate like Guaiacol (0-methoxyphenol) Hi-LR (RM1118) and ABTS (2, 2'- Azino-bis- (3- ethylbenzothiazoline-6-sulfonic acid) diammonium salt (RM9270) were procured from HiMedia, Mumbai, India. Wheat bran (WB) was obtained from local market of Cantonment area, Jalandhar, Punjab, India.

2.3.2 Methods

2.3.2.1 Pre-processing of adsorbent

Wheat bran (WB) was obtained from local market of Cantonment area, Jalandhar, Punjab, India. The material was washed with distilled water, for removal of all dirt particles, followed by drying to constant weight, in hot air oven at 70 ºC for 8 hours/overnight. The dried material was screened through mesh no.30 (0.6 mm) and the sieved portion was transferred in sterile polybags /ziplock bags for further storage at room temperature in a cool and dry place (Alzeydien 2015).

2.3.2.2 Collection of samples for isolation of basidiomycetous strain from various samples

The samples were collected randomly from selected locations. 114 samples of basidiomycetes strain grown on pieces of wood from tree bark, wood scrapings from fallen stem, fruiting bodies grown on soil or on cow dung were collected from various places in Jalandhar (Jalandhar City, Jalandhar Cantt), Himachal Pradesh (Kangra, Palampur, Dalhousie), Jammu and Rajasthan. The samples were collected with the help of pre-sterilized scalpels and forceps, kept in pre-sterilized containers or autoclavable polybags and brought to the laboratory and refrigerated until used (Selvam et al., 2012).

2.3.3.3 Isolation of basidiomycetous strain collected from various samples

Within 24-48 hrs of sample collection, the samples were inoculated on to plates of WB agar medium, prepared by adding 2% WB (w/v) with 2% Agar Agar in 100ml of distilled water and autoclaved at 121ºC, under 15 lbs pressure for 15-20 mins to which 185 µg/ml, syringe filtered chloramphenicol was added as an antibacterial agent (Singh et al., 2013). If inoculation was from the fruiting bodies tissue culture technique (Revankar and Lele 2007) was followed for the inoculation of the samples, on either moistened wheat bran or on WB agar. The parts of the fruiting body either tissues of basidiocarp or the cap (upper region of the stem) were taken (Stamets and Chilton 1983), or part of underside of the cap, where the gill plate joints was excised off (Walting 1977). Sometimes after surface sterilization of the cuticle, obtained after peeling of skin, with 70% ethanol dipped swab, were inoculated. In case of tougher tissue part of the fruiting body, they were surface sterilized with 10% sodium hypochlorite for few seconds and the inoculated (Revankar and Lele 2007). If fungal samples were present on wood, parts of the wood along with the fungal specimen

were inoculated in autoclaved moistened WB in petri dishes. All the inoculated samples were incubated for a period of 7-10 days at 30°C for visibility of white mycelium along the surface of the medium (Lakkireddy and Kues 2017).

2.3.2.4 Purification and maintenance of fungal isolates

The fungal growth in the form of white, thread like mycelia and fruit bodies obtained were transferred onto wheat bran agar plates and further purified on slants and incubated at 30°C for 4 days and were then refrigerated at 4°C and stored for subsequent usage. For long term preservation the cultures were maintained as hyphal fragments in 15% (v/v) glycerol stock at -20°C (Singh et al., 2013; Paul et al., 2015).

2.3.2.5 Screening of isolates for laccase production by plate assay method

The ability of the isolates to produce laccase was screened by plate assay technique using ABTS (2-2'-Azino-bis-[3-ethylbenzthiazoline-6-sulfonic acid) and guaiacol. The WB agar plates were prepared by adding 3mM ABTS (0.05 % w/v) and 4mM guaiacol (0.01% w/v), individually. The ability of the isolates to grow and to decolorize crystal violet (CV), malachite green (MG) and congo red (CR), by adding at 0.003% concentration in the WB agar medium were also studied. 2mm diameter cork plug of actively growing mycelium from the periphery of fresh culture petri dish was taken and inoculated at 30°C for 7-15 days for growth and decolorization. The laccase activity was indicated based on the change in coloration around the inoculated plugs in ABTS (blue) and guaiacol plates (brown) and zone of discoloration at the base of the dye incorporated plates after incubation period (Ghebreslasie et al., 2016).

2.3.2.6 Secondary screening of selected isolates for laccase production under solid state fermentation (SSF)

5 grams of WB was taken in a 250-mL Erlenmeyer flask (borosilicate), to which 3.5 mL of moistening agent was added at pH 5. The moistening agent was prepared with 0.0004% $CuSO_4$, 0.005% Na_2HPO_4, 0.1% KH_2PO_4, 0.05% $MgSO_4$, 0.001% $CaCl_2$, 0.0001% $MnSO_4$, 0.0001% $ZnSO_4$, and 0.0001% $FeSO_4$ (w/v) in distilled water (Revankar and Lele 2007). The contents of the flask were autoclaved at 121°C for 20 minutes. The fermentation was carried out for a period of 7 days under a controlled environment at 30±5°C under a static condition in incubator (Revankar and Lele 2007). After the desired growth period of the isolates the content of the flasks was

crushed with the help of glass rod, to which 15 mL of distilled water was added and then shaken for 10 minutes in an orbital shaker at 100 rpm at room temperature. The contents were filtered through cheese cloth and the filtrate was centrifuged, in a cooling centrifuge (Remi, general purpose centrifuge, R-8C, 8X15 mL) at 5000 rpm for 10 minutes at 4°C (Singh et al., 2013). The supernatant obtained, considered as the crude enzyme, was collected for the measurement of laccase activity using guaiacol assay method (Kalra et al., 2013).

2.3.2.7 Study of morphological and microscopic characteristics of fungal isolates

Partial identification of the isolates was done by studying the colony morphology, staining by LPCB and by the determination of presence of clamp connection in the mycelium, thread like growth along the surface of the media, basidiospores attached on basidium and fruiting body development on the media. After 3-5 days of incubation period the isolates were examined for their mode of mycelia growth, color, and colony morphology (Rahman et al., 2011). The isolates were further examined by Wet Mount technique with Lacto Phenol Cotton Blue for the presence of clamp connections in the septa of the hyphae (Leck 1999).

2.3.2.8 Optimization of various parameters for laccase production by selected isolates under SSF

2.3.2.8.1 Optimization of days of incubation for laccase production by isolates

The optimization of the days of incubation for a period of 15days was performed. The experimental set up was done in the same as been discussed in the section 2.2.2.6 of this chapter, at an incubation temperature of 30 ± 5°C, pH 5, moistening agent at a concentration of 70%. The enzyme activity was evaluated at an interval of 24hrs for all the 3 isolates for a period of 15 days. Laccase activity was estimated by Guaiacol assay. Development of a reddish-brown colour because of the oxidation reaction by laccase of guaiacol was estimated spectrophotometrically at 450 nm. The reaction mixture was prepared by taking 1ml of Guaiacol (2mM), 3ml of sodium acetate buffer (10 mM) and 1 ml fungal supernatant. The blank was prepared with 1ml distilled water instead of the enzyme. The mixture was incubated for 15mins at 30 °C and the absorbance was measured spectrophotometrically. International Units (IU) is used to express enzyme activity, where to oxidize 1 µmol of guaiacol per min, the amount of

enzyme required is 1 IU. In IU/mL, laccase activity is calculated by the following formula (Kalra et al., 2013):

$$E.A = A \times (V/t) \times e \times v \quad \text{(Eq. 1)}$$

Where, E.A is enzyme activity; A, is absorbance; V, is total volume of the mixture (ml); t, is incubation time (mins); e, is the extinction coefficient of guaiacol (0.6740 µM/ cm); v, is the volume of the enzyme (mL).

2.3.2.8.2 Optimization of temperature for laccase production by isolates

The optimization of laccase activity under different temperature (25, 30, 35, 40 and 45°C) was done. The experimental set up was in accordance to that discussed before (section 2.2.2.6) for the optimized incubation for each isolate. After which the enzyme was harvested and calculated (Eq.1) in the same method as mentioned before (Kalra et al., 2013).

2.3.2.8.3 Optimization of pH for laccase production by isolates

The different pH selected were (3.5, 4, 4.5, 5, 5.5, 6, 6.5, 7, 7.5, 8, 8.5) , which under the optimized condition of days of incubation and temperature, as obtained from the previous experiments were used to perform the experiment in the same way, as discussed in 2.2.2.6. The pH was adjusted by 0.1M NaOH and 0.1M HCl and measured by using a pH meter (VLab) after autoclaving at 121°C for 15-20 mins under 15 lbs pressure. After the optimized days of incubation at temperature (30 °C) the enzyme was harvested and calculated by following the Eq.1 by the process mentioned above (Kalra et al., 2013).

2.3.2.8.4 Optimization of amount of substrate for laccase production by isolates

The amount of substrate was varied from 4, 5, 6, 7 to 8 gm. Under the optimized condition of days of incubation, temperature and pH the experiment was conducted. The laccase activity was calculated (Kalra et al., 2013) by following the process as same as above by SSF (Revankar and Lele 2007) by subsequent enzyme harvesting (Singh et al., 2013).

2.3.2.8.5 Optimization of moistening agent for laccase production by isolates

The optimized condition of days of incubation temperature, pH, substrate concentration was taken into consideration for the optimization of moistening agent (50, 60, 70, 80, 90 %) required for optimal production of laccase (Revankar and Lele 2007; Singh et al., 2013 and Kalra et al., 2013).

2.3.2.8.6 Optimization nitrogen source for laccase production by isolates

Under the optimized condition of above all parameters for all the 3 isolates, maximum laccase production was estimated, as above (Revankar and Lele 2007; Singh et al., 2013 and Kalra et al., 2013) by taking two types of nitrogen sources (Yeast extract and ammonium sulphate at a concentration of 0.5, 1, 1.5, 2, 2.5 %).

2.3.2.8.7 Optimization copper sulphate for laccase production by isolates

For optimization of copper sulphate concentration, the concentration was varied from 0.2mM, 0.4mM, 0.6 mM, 0.8mM to 1mM under the optimized condition of incubation period, temperature, substrate concentration, pH and nitrogen source. The experiment was conducted in the same manner as above (Revankar and Lele, 2007; Singh et al., 2013) and the enzyme activity was calculated following the Eq.1(Kalra et al., 2013).

2.3.2.9 Estimation of ligninolytic enzyme activities under optimized condition of SSF for laccase production

The laccase activity was estimated in the same process as above under the optimized condition of incubation period, temperature, pH, substrate concentration, moistening agent, yeast extract and mM copper sulphate. Under the same optimized conditions obtained for laccase production Manganese peroxidase and lignin peroxidase activity were also determined. The determination of Manganese Peroxidase activity was done using phenol red as substrate (Kuwahara et al.1984) by measuring optical density spectrophotometrically at 610 nm. The reaction mixture consists of enzyme extract (250µL), 0.1% phenol red (50µL), 250mM sodium lactate (100 µL), 2mM manganese sulphate (25 µL), 0.5% BSA (100µL), 0.2mM H_2O_2 (25 µL) in 0.1M citrate buffer pH 5 (0.5 mL). Lignin peroxidase activity was estimated by Tien and Kirk method (1983). The assay is based on the oxidation of veratryl alcohol (3, 4-dimethoxybenzyl alcohol) to veratraldehyde in the presence of H_2O_2; the increase in absorbance at 310 nm was checked. Reaction mixture contained 0.25 mL of enzyme solution, 0.25 mL of 1mM veratryl alcohol, 0.2 mM H_2O_2 and 0.5 mL of 0.1M citrate buffer.

2.3.2.10 Optimization of parameters for laccase production by response surface methodology (RSM)

Preliminary screening experiments were done with Plackett-Burman Design (PBD), one factor at a time approach was used to investigate effect of the parameters on laccase production. Based on the classical approach five independent variables, pH

(A) (3,3.5,4,4.5.5,5.5,6,6.5,7,7.5,8) temperature (B) (28-37^{o}C) copper sulphate (C) (0.2,0.4,0.6,0.8,1 mM), yeast extract (D) (0.5, 1,1.5, 2, 2.5%) and substrate concentration (E) (4, 5, 6, 7, 8 gm) were used for optimization of laccase production using RSM (Table 3.7.1), with α- values of the variable (± 1.415). RSM was applied to optimize the culture condition for laccase production and central composite rotational design (CCRD) was applied to optimize the selected variables. Each variable was studied at different levels and the variable ranged between [(-)1- (+)1]. The relationship between the response, i.e. laccase production, Y_c (IU/mL) and the factors A-E were mathematically given by the following equation (Eq. 2) Total 50 experiments were planned using Design Expert-9 to execute CCRD. The relationship between the variation in response, i.e. laccase production (Y_c) and the factors pH (A), temp. (B), copper sulphate (C), yeast extract (D) and substrate concentration (E) respectively, is represented mathematically by the second order model, by using the following equation (Vidya et al., 2014; Vijayaraghavan and Vincent 2014;) :

$$Y_c = \beta_0 + \beta_1 X_1 + \beta_2 X2 + \beta_3 X3 + \beta_4 X3 + \beta_5 X3 \quad \text{(main effects and intercept)}$$
$$+ \beta_{11} X_1{}^2 + \beta_{22} X_2{}^2 + \beta_{33} X_3{}^2 + \beta_{44} X_4{}^2 + \beta_{55} X_5{}^2 \quad \text{(interactions)}$$
$$+ \beta_{12}X_1X_2 + \beta_{13}X_1X_3 + \beta_{15}X_1X_5$$
$$+ \beta_{23}X_2X_3 + \beta_{24}X_2X_4 + \beta_{25}X_2X_5 + \beta_{34}X_3X_4 + \beta_{35}X_3X_5 + \beta_{45}X_4X_5 \quad \text{(Quadratic effect)}$$

(Eq. 2)

Where Y_c is the calculated response given by the model (with respect to enzyme activity) ; X1, X2, X3, X4, and X5 are the variables coded for each of the factors, respectively; β_0 , corresponds to the regression coefficient; β_1 β_{11} β_{12} β_{23} β_{34} and β_{45} are the model estimated coefficients representing effects like, linear, quadratic and interactive. They are the effects of factors (X1- X5) on response. The coding of the factors was done because each of the factors are expresses in different units.

In total 50 experimental runs were performed, and the mean of the triplicates were taken as the value of the dependent response.

The three-dimensional response surface plots were drawn based on the second order equation. They depict the effects of interaction between the independent and the dependent variables. The plot was prepared by taking into consideration of the centre

points of interval (constant values) to any two (at a time) of the independent variable of the CCRD (Neifar et al., 2011; Vijayaraghavan and Vincent 2014; Senthivelan et al., 2019).

2.3.2.11 Molecular Identification of the isolate

The whole genome analysis of the isolate was done by the *de novo* analysis technique by following the standard protocols by Chromous Biotech, Bangalore, India. The DNA samples were quality checked using Nanodrop and quantitated using Qubit dsDNA BR assay (Thermo Scientific, USA). The genomic library was prepared by taking the genomic DNA, fragmented using Covaris to generate 300-400 bp fragments. 100 ng of fragmented DNA was used to generate sequencing library using NEBNext® UltraTM II DNA Library Prep Kit for Illumina (#E7645S). the fragmented DNA was subjected to end repair followed by A – tailing and adapter ligation. Ampure bead-based size selection was performed to obtain the library of desired size. The size selected DNA were enriched by PCR amplification using illumina index adapter primers. The amplified product was purified using Ampure beads to remove unused primers. The Libraries were quantitated using Qubit DNA HS quantitation assay (Thermo Scientific) which specifically quantitates dsDNA assay and library quality was checked on Bioanalyzer 2100 using Agilent 7500 DNA kit. Bioinformatics analysis were done of the sequence read, their quality were also checked to understand some relevant properties of an ensemble of next generation sequencing reads such as length, quality scores and base distribution in order to assess the quality of the data and to discard low quality reads. The quality of raw reads sequenced was checked by using FASTQC and processed using Trim Galore (v: 0.5.0). The processed reads for the sample was assembled using SPAdes (v. 3.11.1) de novo assembler with default parameters for *denovo* Assembly of the isolate. GeneMark-ES has a special mode for analyzing fungal genomes, it uses eukaryotic ab initio gene finding algorithm. There were 6425 protein coding genes predicted through genemark of the isolate provided. The predicted proteins were annotated using uniprot database by Blastp. Gene ontology was studied of the annotated genes. The tool MISA was used for the identification and localization of perfect as well as compound microsatellites which are interrupted by a certain number of bases. Then with the help of NCBI Tree Viewer (TV), graphical display for phylogenetic trees

with two distance-based methods Minimum Evolution and Neighbour Joining were prepared.

2.3.2.12 Partial purification of laccase and its molecular weight determination by Sodium Dodecyl Sulphate-Polyacrylamide Gel Electrophoresis (SDS-PAGE) Technique

Crude laccase was partially purified by precipitation with ammonium sulphate at a concentration of 80% saturation and 70% ice cold ethanol from 8day old mycelial mat of isolate 4. The crude protein fraction was collected and centrifuged at 1000rpm for 10 mins. After discarding the supernatant, the pellet was dissolved in 0.1M sodium acetate buffer solution and the was dialysed with 10 KDa molecular weight cut off dialysis membrane (obtained from HiMedia, Bangalore, India). Dialysis was conducted against the same buffer in which the pellet has been dissolved, overnight at 4 ^{o}C. The molecular weight of the partially purified enzyme was determined by SDS-PAGE with 10% polyacrylamide gel, in comparison to a standard molecular marker/ molecular ladder (10-80 KDa) (El-Zayat 2008; Mishra et al., 2011).

2.3.2.13 Statistical Analysis

All the experiments have been performed in triplicates. The results have been expressed as mean ± standard deviation (SD). The software used was Microsoft Office (version 10), Excel 2010 to calculate the same. RSM was employed using the Design Expert version 8.0.

2.4 Result and Discussion

2.4.1 Collection of samples for isolation of basidiomycetous strain from various samples

Out of 114 samples collected from different zones of northern India (mostly) and few from western part of India, 26 samples were obtained which had shown growth of white mycelial growth on WB Agar. 2 isolates from Jalandhar City Model Town (J1, J2); 6 isolates from Jalandhar Cantt, Railway station area; 2 isolates were obtained from Lovely Professional University; 1 from Jalandhar Cantt. Paragpur Village; 1 from Jalandhar City, Devi Talab Mandir; 2 from Cheheru Railway station; 2 from Hamirpur, Bera, Himachal Pradesh; 3 from Kangra, Himachal Pradesh; 1 from Hamirpur, Saloni, Himachal Pradesh; 2 from Dalhousie, Himachal Pradesh; 1 from Jammu, Near Circuit house; 1 from Jammu, near IIIM and 1 from Ghana bird sanctuary, Rajasthan (Table 2.1), (Photograph 2.1). The prominent and distinct fungal mycelium were isolated from the plates and were then transferred to the same medium until pure colonies were obtained (Photograph 2.2, 2.3) (Fu et al., 2013).

2.4.2 Screening of isolates for laccase by plate assay method

4 out of 26 isolates had given distinguished results. S1 had given an average decolorization activity on CV in comparison to other dyes and ABTS, whereas on guaiacol it had given a prominent brown coloration around the colonies. C4 isolate had given a comparable result with average and good activity on dyes and guaiacol respectively. Whereas, S4 had given a good amount of decolorization on MG incorporated dye in comparison to other plates, on the contrary the discoloration zone and colored zone around the colony of K4 on dyes and guaiacol incorporated plates were poor but were comparable with that of S1, S4 and C4 with respect to other 22 isolates. Such plate assays were performed because it has already been reported that laccase (a ligninolytic enzyme) are non-specific towards substrates. They are divided into three types of substituted compounds, ortho-, meta-, and para, possessing one lone pair of electrons (Fu et al., 2013). In a review it has been stated that guaiacol and syringaldazine (both, ortho-substituted compounds) is the best substrate for most laccases (Thurston 1994). In another study, 2 isolates obtained were screened as laccase producers by using 2, 2´-azino-bis(3-ethylbenzthiazoline-6-sulfonic acid) (ABTS). Both isolates (TBB3 and EL2) were qualified as a high extracellular ABTS

oxidizing activity producer, thereby signifying the importance of such substrates for detection laccase production (Chan et al., 2016) It was also shown by a study by plate assay method that by day 4, the extent of mycelial growth on agar plates were comparable for all the cultures irrespective of they being able to decolorize dye present in the media (Table 2.2; Figure 2.1). It has been reported in the same research that *P. ostreatus* did not decolorize any of the test dye. On the contrary after 10 days of incubation *T. versicolor* decolorized the maximum number of dyes (Swamy and Ramsay, 1999).

2.4.3 Secondary screening of selected isolates for laccase production Solid State Fermentation (SSF)

On screening for laccase production by solid state fermentation under a culture condition at 30ºC, for seven days on wheat bran agar at a pH 5, S4 has been found to be the best isolate to produce laccase at a concentration of 3.21 IU/mL in comparison to other strains (S1, C4 and K4) (Table 2.3), (Figure 2.1) The result obtained was comparable with strain. In a study, for isolation of laccase from Pleurotus sp., the laccase activity, after 19^{th} day was found to be 83.83 U/ml at a pH 5.8 with tannic acid as an inducer and around 112.88 U/ml at a pH 6.5 without the inducer at room temperature (More et al., 2011). In most of the studies liquid medium have been used for describing ligninolytic system (Ardon et al., 1996; Picard et al., 1999) but many studies have emphasized the importance of solid-state fermentation. Studies have shown that at the beginning of lignin degradation there is a higher laccase activity which eventually decreases and remain constant. Laccase can act both as a detoxifier of substrates as well as an oxidizing agent of phenolic groups. It is the first enzyme in the series which is produced during the degradation which is involved in the cleavage of side chain and aromatic rings of lignin phenolic moieties (Higuchi, 1990). The eventual loss is attributed by LiP and MnP. In a study with *P. chrysosporium,* it has shown highest LiP and MnP but not that of laccase (Vyas et al., 1994). Whereas, *T. versicolor* showed the activities of all the three enzymes, exhibiting the synergistic mechanism for lignoinolysis (Valmaseda et al., 1991). Again, *I. lacteus* also has shown LiP and laccase activity but lacked MnP activity as earlier reported (Kasinath 2002) (Figure 2.1).

2.4.4 Study of morphological and microscopic characteristics of fungal isolates

Morphological and cultural characteristics of the isolates has shown that after 7days of growth on WB agar, the S4 has given the highest mycelial diameter of 8.18 cm in comparison to others. On microscopic examination by LPCB wet mount technique clamp connections were observed in case of S4 and S1, in case of S4 a basidium with 4 basidiospores were also observed but with only tuft of mycelia in case of C4 was seen. (Table 2.4) (Photograph 2.4, 2.5).

2.4.5 Optimization of various parameters for laccase production by selected isolates under SSF

Based on the above result, S1, S4 and C4 were found to be efficient enough for laccase (and/ ligninolytic enzymes). The further optimization experiment of various parameters for laccase production has shown a very different type of result.

2.4.5.1 Optimization of days of incubation for laccase production by isolates

On analysis it has been found out that for S4, best laccase production was seen on the 8th day, with 3.45 IU/mL laccase production, in comparison to 2.45 IU/mL for S1 (obtained on 7th day) whereas, in case of C4 it was only 1.57 IU/mL on the same day as that of S4. It has been observed that with the increase of days beyond 10th in case of S4 the enzyme activity decreased to 2.53 IU/mL till 15th day. Though S1's enzyme activity (1.53 IU/mL) till 15th day is comparable with S4 but C4 has exhibited a lot of reduction in the enzyme production beyond 8th day, which was the maximum for its enzyme production (Table 2.5; Figure 2.2).

2.4.5.2 Optimization of temperature for laccase production by isolates

All the three isolates (S1, S4 and C4) has exhibited the best laccase activity at 30 ºC under their respective optimal days of incubation period (7^{th} day for S1 and 8^{th} day for S4 and C4). The highest enzyme activity was shown by S4, 3.57 IU/mL, followed by S1, 2.39 IU/mL and C4, with 1.63 IU/mL laccase activity (Table 2.6, Figure 2.3). The enzyme activity result was obtained by guaiacol assay as mentioned above.

2.4.5.3 Optimization of pH for laccase production by isolates

Under the optimal condition of incubation period and temperature on variation of pH, the optimal pH at which S1, S4 and C4 had shown their best laccase activity was 8 in case of S1 with 3.14 IU/mL, 5.5 in case of S4 with 3.93 IU/mL and 5 in case of C4

with 2.06 IU/mL laccase activities (Table 2.7, Figure 2.4). From the result it is quite evident that amongst the three, S4 has shown the highest laccase activity under the prevailed conditions. Another significant result that had come in view was the pH tolerance by S1 strain and also by the laccase produced by the same. The result could be compared with that of *Perenniporia tephropora* KU-Alk4, another white rot fungus, which has shown the ability to produce both MnP and laccase at a pH 7.0 but only laccase at pH 8.0. The specific activity was also found to be higher of laccase at the pH 8.0, proving the enzyme to be resistant to alkalinity (Teerapatsakul and Chitradon, 2016).

2.4.5.4 Optimization of amount of substrate for laccase production by isolates

Under the optimized conditions of days of incubation, temperature and pH when the effect of substrate (WB) concentration was checked, it was found that 5 gm of substrate was optimum for 1 plug of diameter 2mm to produce maximum amount of laccase. The enzyme activity exhibited by S1, S4 and C4 were 3.16, 3.95, 2.10 IU/mL, respectively (Table 2.8; Figure 2.5). Showing S4 to be the best strain for laccase production. With 5% substrate, the enzyme activity was 3.95 IU/mL whereas, with 8%, there was a decrease in enzyme activity to 3.31 IU/mL. The difference is around 0.64, which is around 16.2%. A similar type of study has shown that the best laccase activity was shown with 2 gms of substrate concentration instead of 5 gms with a laccase activity around 9.95 IU/mL (Shafiq et al., 2016).

2.4.5.5 Optimization of moistening agent for laccase production by isolates

Moistening agent performs a very important role in the enzyme production under the solid-state fermentation. 70% moistening agent to the substrate volume of 5gm has found to the optimal for all the three strains to produce laccase the best. The laccase produced were 3.56, 4.27 and 2.49 IU/mL by S1, S4 and C4 respectively (Table 2.9, Figure 2.6). Again, the best strain found to be S4.

2.4.5.6 Optimization nitrogen source for laccase production by isolates

Two type of nitrogen sources has been evaluated, yeast extract and ammonium sulphate and it has been found that yeast extract at a concentration of 1% has shown the best result for all the strains to produce laccase around 6.65. 7.48 and 5.54 IU/mL

by S1, S4 and C4, respectively (Table 2.10, Figure 2.7). Whereas, ammonium sulphate has not shown any significant effect on the production by these strains.

2.4.5.7 Optimization copper sulphate for laccase production by isolates

Under all the above optimized state the last parameter which was evaluated for affecting the laccase production by the isolates were copper sulphate. It was chosen as it is a known fact that divalent ions especially Cu^{2+} shows positive effect on ligninolytic enzyme production, especially laccase. The best laccase activity was exhibited by S4 with 11.68 IU/mL, followed by S4, 8.46 and C4 6.51 IU/mL laccase production at a concentration of 0.4 mM of copper sulphate in the medium under the above optimized conditions (Table 2.11, Figure 2.8).

2.4.6 Estimation of ligninolytic enzyme activities under optimized condition of SSF for laccase production

On estimation of three different ligninolytic enzymes (laccase, LiP and MnP) under the above optimized state has given different results for the three different isolates. Isolate S1 has produced laccase to a concentration of 11.87 IU/mL which is comparable with its LiP production, around 10.12 IU/mL and lesser concentration of MnP, around, 9.72 IU/mL. A similar type of result been exhibited by the other two strains but the individual activities if considered, S4 has given the best result, producing around 15.84 IU/mL laccase, followed by 13.38 IU/mL LiP and then 12.56 IU/mL MnP. The least activity been shown by C4, with 9.46. 9.79 and 7.65 IU/mL of laccase, LiP and MnP activities, respectively (Table 2.12, Figure 2.9). Overall, S4 was the best isolate with the highest amount of laccase production was used for the further analysis and experimentation.

2.4.7 Optimization of parameters for laccase production by response surface methodology (RSM)

2.4.7.1 Combination of parameters

By using the Design Expert Software (version 11) the combination of parameters was obtained with 50 runs (Table 2.13; Figure 2.14).

2.4.7.2 RSM Table: Level of Significance

The model with sum square 597.80 with p-value 0.0004 was found to be significant (Table 2.14). While the residual with p - value 0.2874 was found to be insignificant.

The Model F-value of 3.99 implies the model is significant. There is only a 0.04% chance that an F-value this large could occur due to noise. P-values less than 0.0500 indicate model terms are significant. In this case B, C, AB, AE, BC, BE are significant model terms. Values greater than 0.1000 indicate the model terms are not significant. If there are many insignificant model terms (not counting those required to support hierarchy), model reduction may improve your model. The Lack of Fit F-value of 1.54 implies the Lack of Fit is not significant relative to the pure error. There is a 28.74% chance that a Lack of Fit F-value this large could occur due to noise. Non-significant lack of fit is good as requirement is to fit the model. When the F-values are taken into consideration in correspondence to the p-values of the respective factors, factor B (Temperature) has shown F-value to be 10.56, (higher the F-value significant is the factor for the enzyme production) and p - value was less (0.0004), thereby depicting that for the laccase production temperature plays the most significant role, next followed by Copper sulphate with a F- value 6.20 with corresponding p-value being 0.017.

2.4.7.3 Fit Statistics

A slight variation in the result was observed whereby, the predicted R^2 of 0.0695 was not as close to the adjusted R^2 of 0.4775 as one might normally expect; i.e. the difference is more than 0.2. This may indicate a large block effect or a possible problem with the model and/or data. Things suggested to be considered were model reduction, response transformation, outliers, etc. All empirical models were to be tested by doing confirmation runs. On the contrary the Adequate Precision measures the signal to noise ratio. In RSM study, a ratio greater than 4 is desirable. The present study ratio was 8.988 indicating an adequate signal. Thus, this model could be used to navigate the design space **(**Table 2.15**).**

2.4.7.4 Final Equation in terms of Actual Factors

The equation in terms of actual factors can be used to make predictions about the response for given levels of each factor. Here, the levels should be specified in the original units for each factor. This equation should not be used to determine the relative impact of each factor because the coefficients are scaled to accommodate the units of each factor and the intercept is not at the canter of the design space.

Response Equation:

-26.58074 +22.57012 (pH) +3.80537 (Temperature) -77.97826 ($CuSO_4$) -28.42229 (Yeast Extract) +4.54905 (substrate concentration) -0.815062 (pH * Temperature) -2.76601 (pH * CuSO4) -2.61738 (pH * Yeast extract) +1.99804 (pH * substrate conc.) +1.90504 (Temperature * CuSO4) +0.625791 (Temperature * Yeast extract) -0.725238 (Temperature * substrate conc.) +5.50438 (CuSO4 * Yeast extract) +3.13221 (CuSO4 * substrate conc.) +2.44455 (Yeast extract * substrate conc.)

2.4.7.5 The diagnostics

The diagnostics of the RSM was obtained and were given in normal plots, contour plots and 3D surfaces (Figure 2.15– 2.21)

2.4.7.6 Optimum Combination for laccase production

Under the optimum combination of all the factor the amount of laccase activity was given as 18.47 IU/mL (Table 2.16). The experimental validation of the RSM after the performing the experiment by following levels of factors, pH 5.15, temperature 32.53, $CuSO_4$ 0.76 mM, yeast extract 1.15, substrate concentration 5.62 gm the amount of laccase produced was 18.76 IU/mL, thereby abiding the mathematical explanation of the combination of the factors for the production of laccase. In a study conducted on extracellular laccase production by *Penicillium chrysogenum*, it was observed that, the optimum laccase activity, by the isolate, was 6.0 IU/mL, but on statistical optimization process of the medium at 32° C for a period of 5 days it was observed that the organism had an increased production to 7.9 IU/mL (Senthivelan et al., 2019). The model used had exhibited 98.9 % precision with only 1.05% variability. The result obtained in this study is thus comparable with the reference.

2.4.7.7 Run report comparison of Actual and predicted value

The run report on comparison between the actual and the predicted experimentation depicts that the design analysis has shown a high degree of fitting between the predicted and the actual or experimental data as the values are 17.61 and 17.52 IU/mL laccase activity (Table 2.16). In another study it was observed that *Pleurotus ostreatus* had shown an increased laccase activity from 3918 to 11985 IU/mL (Chiranjeevi et al., 2014). Based on the initial studies with various factors individually with wheat bran as a lignocellulosic substrate, at varied temperature, pH, substrate concentration,

nitrogen source, copper sulphate concentration, in reference to the literature has shown that pH of the culture medium should be considered as one of the most important parameter in case of fungus cultivation (Prasad, 2005; Janusz et al., 2007; Patel et al., 2009; Periyasamy and Palvanam, 2010, Chiranjeevi et al., 2014). It has also been reported that *P. ostreatus* has produced the highest amount of laccase at a pH 5.5 under a sub-merged fermentation process. The study abides by the present study, though the operation was under solid state fermentation, but the highest activity was shown at 5.5. Again, other study has also shown that *P. ostreatus* PVCRSP-7 with bran, 2.5-3.5 % (% w/v), supplemented with urea, as an inducer, has also led to production of laccase at an optimum concentration (Murugesan et al., 2007, Li et al., 2007). Various researchers have worked on various organisms and employed RSM for the optimization of various factors and their combinations for optimum laccase production by fungus, for example, on *Pichia pastoris* GS115-LCCA (Li, et al., 2007).The contour plots and the 3D plots has enabled in a pictorial representation of the relationship between different parameters for the enhanced laccase production by the isolate (S4). The relationship between the actual and predicted laccase activity is shown in Figure 2.14. The parity plot shows a good fit of the model with correct correlation between the actual and the predicted values to be satisfactory. This was depicted by the cluster of measurement in the plot in the vicinity to the diagonal line, depicting the fitness of the model and its applicability for the navigation of the design space. The contour and 3D plot (Figure 2.15) shows the relationship between pH and temperature, showing that with a F-value 5.38 (Table 2.16), the two factors affect each other with a maximum laccase activity 18.47 U/L. Plot (Figure 2.17) between pH and copper sulphate shows that they do not influence each other much with a F-value 3.06. The plot (Figure 2.18) between pH and Yeast extract, shows that there is not much influence on each other with a maximum F value 2.74 (the least F-value) for a combination of factors. Plot (Figure 2.19) shows the influence of pH on substrate concentration, which has shown a moderate effect on laccase production with a F-value of 6.39, depicting the pH and substrate jointly can affect the enhance laccase production by the isolate. Plot (Figure 2.20) between temperature and Copper sulphate on the other hand has shown a very good influence on each other with a F-value of 7.35. Plot (Figure 2.21) between Temperature and Yeast Extract has shown

on the other hand the least influence on each other with a F-value 0.79. In the next plot (Figure 2.22) the combination of temperature and substrate concentration has shown a below moderate influence on each other with a F-value of 4.26. In plot, the effect of copper sulphate on yeast extract has shown a lesser influence on each other with a F-value of 3.03. In plot between copper sulphate and substrate concentration the influence is quite less with a F-value 3.92. Lastly, the plot showing the relationship between yeast extract and substrate concentration has shown the least interaction between each other for laccase production. The 3D plots (Figure 2.19-2.22) were constructed for studying the interaction between different physiological parameters for the optimal production of laccase. The plots were created by plotting Z-axis to be the laccase production, the response against the two independent variables, while simultaneously placing the other independent variables at their O-level showing the acidic pH with increase in temperature showing positive effect on laccase production (Figure 2.19,M). Again, when the temperature was compared with copper sulphate, the 3D plot has not given an appropriate result, depicting that they do not show significant interaction between each other, thereby showing that temperature and a combination of temperature and copper sulphate plays a key role in laccase production by the isolate. The plots thereby concludes that as the experimental and the predicted values are quite close to each other, it can be said that the model was successfully validated.

2.4.8 Molecular Identification of the isolate

For whole genome analysis standard protocol was followed whereby, the initial DNA quality check was done, and the sample had passed the QC with a total DNA amount 132.8 ng (Table 2.17). The library quantity estimate was done using Qubit DNA HS kit had given 21.8 Qubit concentration (ng/µL) and the quality passed the test for further sequencing. The bioinformatics analysis has given the basic statistics of raw sequences providing the information of sample file name, total number of raw reads, read length, and percentage of GC content. Per base sequence quality, has shown the average and range of the quality scores across all bases. The graph divides the y-axis into very good quality calls (green), calls of reasonable quality (orange), and calls of poor quality (red). The x-axis represents the position in reads and the y-axis represents the per base Phred scores (Table 2.18)To be noted, the central red line is the median

value, the yellow box represents the inter-quartile range (25-75%), the upper and lower whiskers represent the 10% and 90% points and the blue line represents the mean quality.

The *denovo* Assembly was assembled with a total length of 20544164 bp before gap filling and 16312191 bp after gap filling. The assembly statistics before gap filling and after gap filling is available in (Table 2.19) A reference assisted genome finishing for all the assemblies was done using Chromosomer, a reference-based genome arrangement tool for producing draft chromosome sequences. Closely related well annotated reference genome ***Schizophyllum* commune H4-8 GCA_000143185, NW 003315672,** was chosen from the NCBI database.

Gene Prediction was done by GeneMark-ES. It has a special mode for analysing fungal genomes. It uses eukaryotic *ab initio* gene finding algorithm. There were 6425 protein coding genes which were predicted through genemark. Predicted proteins were annotated using uniprot database by Blastp. It was observed that in all most all the samples more than 80 % of predicted proteins showed greater than 50 % identity with annotated proteins in uniport.

For gene ontology analysis, 5295 genes were annotated, among them 2430, 1730 and 1544 genes were assigned to molecular function, cellular component and biological process respectively (Figure 2.12-2.13). In the molecular function a greater number of genes were assigned with catalytic activity and binding. Similarly, for cellular component, greater number of genes were assigned with membrane part and cell part. In case of biological process, a greater number of genes were assigned with cellular process, metabolic process and Biological regulation.

The identification and localization of perfect microsatellites as well as compound microsatellites which are interrupted by a certain number of bases. Microsatellites are di-, tri-, or tetra nucleotide tandem repeats in DNA sequences. The number of repeats is variable in populations of DNA and within the alleles of an individual. The SSR prediction of assembly scaffold shown in Table 2.20 depicts the distribution of different repeat type classes for mono, di, tri tandem repeats.

The NCBI Tree Viewer (TV) is the graphical display for phylogenetic trees with two distance-based methods Minimum Evolution and neighbour joining. The longest scaffold was given as a query in Blastn database, the highly identical strains was chosen and a distance-based Neighbour Joining tree was created. (Table 2.13) shows distance-based tree of the query and ***Schizophyllum*** commune H4-8 hypothetical protein, mRNA.

2.4.9 Partial purification of laccase and its molecular weight determination by Sodium Dodecyl Sulphate-Polyacrylamide Gel Electrophoresis (SDS-PAGE)

The molecular weight of the partially purified protein (laccase) was around 67 kDa, as observed after subsequent staining and de-staining on comparison with molecular ladder. The result obtained is like earlier result obtained by other researchers, molecular weight ranging between 60-70 kDa as earlier reported (Sadhasivam et al., 2008; Eggert et al., 1996) (Figure 2.6).

Thereby the Basidiomycetes strain isolated, nomenclature as, ***Schizophyllum*-S4** was a novel strain of white rot fungi showing 89% similarity with the *Schizophyllum* commune with ability to produce laccase was obtained.

2.5 References

1. Akpinar, M, Urek R. 2014. Extracellular ligninolytic enzymes production by *Pleurotus eryngii* on agro-industrial wastes. *Prep Biochem and Biotech* 44: 772–781.
2. Ardon O, Keven Z, Hadar Y. 1996. Enhancement of laccase activity in liquid cultures of ligninolytic fungus *Pleurotus ostreatus* by cotton stalk extract. *J of Biotech* 51:201-207.
3. Chan MY, Goh SM, Ong LGA. 2016. Isolation and Screening of Laccase Producing Basidiomycetes via Submerged Fermentations. *Int J of Agri and Biosys Eng* 10: 77-80.
4. Chiranjeevi PV, Pandian, MR, Satish, T. 2014. Enhancement of laccase production from *Pleurotus ostreatus* PVCRSP-7 by altering the nutritional conditions using response surface methodology. *Biores* 3: 4214-4225.
5. Coelho MA, Bakkeren G, Sun S, Hood M, Girand T. 2017. Fungal Sex: The Basidiomycota, Microbiology Spectrum. *Am Soc for Micro Press* :1-21.
6. Dashtban, M., Schraft, H., Syed, T.A., Qin, W., 2010. Fungal biodegradation and enzymatic modification of lignin, *Int J Biochem Mol Bio* 1: 36-50.
7. de Jong, E., Field, J.A., Dings, J.A.F.M., Wijnberg, J.B.P.A., de Bont. J.A.M., 1992. *De novo* biosynthesis of chlorinated aromatics by the white-rot fungus *Bjerkandera sp* BOS55. Formation of 3-chloro-anisaldehyde from glucose. *FEBS Let* 305: 220-224.
8. Dhakar K, Pandey A. 2013. Laccase production from temperature and pH tolerant fungal strain of *Trametes hirsuta* (MTCC11397). *Enz Res* : 1-9.
9. Dhakar, K. and Pandey, A., 2013. Laccase production from a temperature and pH tolerant fungal strain of *Trametes hirsuta* (MTCC 11397), *Hindawi Pub Corp*:1-9.
10. Dwivedi, U.N., Singh, P., Pandey, V.P., Kumar, A., 2011. Structure and function relationship among bacterial, fungal and plant laccases, *J Mol Cat B: Enz* 68:117-128.

11. Eggert, C., Temp, U., Errikson, K-El, 1996. The ligninolytic system of white rot fungus *Pycnoporus cinnabarinus*, purification and characterization of the laccase. *App Environ Micro* 62: 1151-1158.
12. El-Zayat, S.A., 2008. Preliminary studies on laccase production by *Chaetomium globossum* and endophytic fungus in *Glinus lotoides*, *Am- Eur J Agri and Environ Sc* 3: 86-90.
13. Fu Kai, Fu Shiyu, Zhan Huaiyu, Zhou Pandeng, Liu Mengru and Liu Hao, 2013. A newly isolated wood-rot fungus for laccase production in submerged cultures. *Biores* 8(1): 1385-1397
14. Ghebreslasie, Z., Premjet, D., Permjet S., 2016. Screening of fungi producing ligninolytic enzymes by plate test technique. *KKU Res J* 21: 200-209.
15. Giardina P, Faraco V, Pezzella C, Piscitelli A, Vanhulle S, Sannia G. 2010. Laccases: A never-ending story. *Cell Mol Life Sci* 67: 369–385.
16. Guillén, F., Martínez, M.J., Muñoz, C., Martínez, A.T., 1997. Quinone redox cycling in the ligninolytic fungus *Pleurotus eryngii* leading to extracellular production of superoxide anion radical. *Arch Biochem Biophys* 339: 190-199.
17. Hakulinen N, Rouvinen J. 2015. Three-dimensional structures of laccases. *Cell Mol Life Sci* 72: 857–868.
18. Higuchi T. 1990. Lignin biochemistry: Biosynthesis and biodegradation, *Wood Sc Tech* 24: 23-63.
19. Higuchi T. 1990. Lignin biochemistry: biosynthesis and biodegradation. *Wood Sc Tech* 24: 23-63.
20. Hood IA. 2006. The mycology of the basidiomycetes, heart rot and root rot in tropical *Acacia* plantations. Proceedings of a workshop held in Yogyakarta, Indonesia, 7–9 February 2006. *Canberra, ACIAR Proceedings* No. 124.
21. Janusz G, Rogalski J, Szczodrak J. 2007. Increased production of laccase by *Cerena unicolar* in sub-merged liquid cultures. *W J Micro Biotech* 23: 1459-1464.
22. Jones SM, Solomon EI. 2015. Electron transfer and reaction mechanism of laccases. *Cell Mol Life Sci* 72: 869–883.

23. Kasinath A. 2002. Studies on lignin degradation and bioremediation of textile dyes, Ph D Thesis, S P University, India.
24. Kuwahara M, Glenn JK, Morgan MA, Gold MH. 1984. Separation and characterization of two extracellular H_2O_2 dependent oxidases ligninolytic cultures of *Phanerochaete chrysosporium*. *FEBS Let* 169:247-250.
25. Lakkireddy K, Kues U. 2017. Bulk isolation of basidiospores from wild mushrooms by electrostatic attraction with low risk of microbial contaminations. *AMB Express* 7:1-22.
26. Leck A. 1999. Preparation of Lacto-Phenol Cotton Blue Slide Mounts. *Com Eye Health* 12: 24.
27. Li W, Picard DM, Beta T. 2007. Effect of thermal processing on antioxidant properties of purple wheat bran. *J Food Chem* 109:1080-1086.
28. Majeau JA, Brar SK, Tyagi RD. 2010. Laccases for removal of recalcitrant and emerging pollutants. Biores Tech 101:2331–2350.
29. Mehra R, Muschiol J, Meyer AS, Kepp KP. 2018. A structural- chemical explanation of fungal laccase activity. *Sci Rep* 8: 1-16.
30. Mishra A, Kumar S, Pandey AK. 2011. Laccase production and simultaneous decolorization of synthetic dyes in unique inexpensive medium by new isolates of white rot fungus. *Int Biodet Biodeg* 65: 487-493.
31. More SS, Renuka PS, Pruthvi K, Swetha M, Veena SM. 2011. Isolation, Purification, and Characterization of Fungal Laccase from *Pleurotus sp. SAGE, Hindawi, access to research, Enz Res* : 1-7.
32. Murugesa K, Nam I, Kim Y, Chang Y. 2007. Decolorization of reactive dyes by a thermostable laccase produced by *Ganoderma lucidum* in solid substrate culture. *Enz Micro Tech* 40: 1662-1672.
33. Neifar M, Kamoun A, Jaouani A, Ellouze-Ghorbel R, Ellouze- Chaabouni S. 2011. Application of asymmetrical and hoke designs for optimization of laccase production by white rot fungus *Fomes fomentarius* in solid state fermentation. *Enz Res*: 1-12.

34. Palvanam T, SatishKumar P. 2010. Production of laccase from *Pleurotus florida* NCIM1243 using Plackett-Burman design and response surface methodology. *J Basic Micro* 50: 325-335.
35. Patel H, Gupta A, Gupta S. 2009. Effect of different culture conditions and inducers on production of laccase by basidiomycetes fungal isolate *Pleurotus ostreatus* HP-1 under solid state fermentation. *Biores* 4: 268-284.
36. Paul JS, Tiwari KL, Jadhav SK. 2015. Long term preservation of commercial important fungi in glycerol at 4ºC. *Int J Bio Chem* 9: 79-85.
37. Periyasamy R, Palvannan T. 2010. optimization of laccase production by *Pleurotus ostreatus* IMI395545, using Taguchii DOE methodology. *J Basic Micro* 50: 548-556.
38. Picard MA, Vandertol H, Roman R, VazquezDuhalt R. 1999. High production of ligninolytic enzymes from white rot fungi in cereal bran liquid medium. *Can J Micro* 45: 627-631.
39. Prasad K, Mohana SV, Rao RS, Pati BR, Sarma PN. 2005. Laccase production by *Pleurotus ostreatus* 1804: Optimization of submerged culture conditionby Taguchi DOE methodology. *Bio Eng J* 24: 17-26.
40. Rahman A, Begum MF, Rahman Bari MA, Ilias GNM, FirozAlam M. 2011. Isolation and identification of *Trichoderma* species from different habitats and their use for bioconversion of solid waste. *Turk J Bio* 35: 183-194.
41. Revankar MS, Lele SS. 2007. Enhanced production of laccase using a new isolate of white rot fungus WR-1. *Pro Biochem* 41: 581-588.
42. Sadhasivam S, Savitha S, Swaminathan R, Lin FH. 2008. Production, purification, and characterization of mid redox potential laccase from newly isolated *Trichoderma harzianum* WL1. *Pro Biochem* 43: 736-742.
43. Schoemaker HE. 1990. On the chemistry of lignin degradation. *Recueil des Travaux Chimiques des Pays-Bas* 109: 255-272.
44. Selvam K, Priya MS, Sivaraj C, Arungandhi K. 2012. Identification and screening of wood rot fungi from western ghat area of south India. *Int J Chem Tech Res* 4: 379-388.

45. Senthivelan T, Kanagaraj J, Panda RC, Narayani T. 2019. Screening and production of a potential extracellular fungal laccase from Penicillium chrysogenum: Media optimization by response surface methodology (RSM) and central composite rotatable design (CCRD). *Biotech Rep* 23:1-15.
46. Shafiq A, Masood F. Naseer R, Naveed S, Rasool IG, Rahman A. 2016. Production, purification and characterization of laccase from white rot fungus. Pak J Sc 68(3):259-267.

47. Shimada M, Higuchi T. 1991. Microbial, enzymatic and biomimetic degradation of lignin. In: Hon DNS. *Shiraishi N (Eds.) Wood Cell Chem, NY, Marcel Dekker*: 557-619.
48. Smith M, Thurston CF, Wood DA. 1997. Fungal laccases: role in delignification and possible industrial applications. In Multi-cooper oxidases, ed. A. Messerschmidt. *Sing: W Sci Pub*: 201–224.
49. Solomon EI, Sundaram UM, Machonkin TE. 1996. Multicopper Oxidases and Oxygenases. *Chem Rev* 96: 2563–2606.
50. Stajic M, Persky L, Friesem D, Hadar Y, Wasser SP, Nevo E, Vukojevic J. 2006. Effect of different carbon and nitrogen sources on laccase and peroxidases production by selected *Pleurotus* species. *Enz Micro Tech* 38: 65–73.
51. Stamets P, Chilton JS. 1983. The mushroom cultivator, a practical guide to growing mushrooms at home. *Aga Press, Olympia, WA*: 415.
52. Teerapatsakul C, Chitradon L. 2016. Physiological regulation of an alkaline-resistant laccase produced by *Perennipora tephropora* and efficiency in biotreatment of pulp mill effluent. *Mycobio* 44(4): 260-268.
53. Thurston CF. 1994. The structure and function of fungal laccases. Micro 140: 19-26.
54. Tien M, Kirk TK. 1983. Lignin degrading enzyme from *Phanerochaete chrysosporium*: purification, characterization, and catalytic properties of unique H_2O_2-requiring oxygenase. *Proceed Nat Aca Sc USA* 81: 2280-2284.

55. Tripathi AK, Kumar NS, Gupta H, Gupta N. 2007. Treatment of industrial effluents: a mini-review. *Eco Environ Div, For Res Ins, Deh, Ind*.
56. Valmaseda M, Matinez M J, Martinez AT. 1991. Kinetics of wheat straw solid state fermentation with *Tramates versicolor* and *Pleurotus ostreatus* - lignin and polysaccharide alteration and production of related enzyme activities. *App Micro Biotech* 35: 817-823.
57. Vidya PK, Rao GR, Naik C, Sridhar M. 2014. A statistical approach for enhancing laccase yields from white rot fungi (WRF) using response surface methodology. J Enz Res 5(1): 55-65.
58. Vijayaraghavan P, Vincent SGP. 2014. Medium optimization for the production of fibrinolytic enzyme by *Paenibacillus* sp. IND8 using response surface methodology. *Hindawi Pub Corp, Sci W J* 14: 276942- 276949.
59. Vyas BRM, Volc J, Saesk V. 1994. Effect of temperature on production of manganese peroxidase and lignin peroxidase by *Phanerochaete chrysosporium*. *Fol Micro* 39: 19-22.
60. Watling R. 1977. How to identify mushrooms to genus V, cultural and developmental features. *Mad Riv Press, Eureka, CA*: 169.

Tables

Table 2.1 Collection of samples for isolation of basidiomycetous strain from various samples

S. No.	Sample Type	Place	No. of samples-No. of isolates obtained
1.	Pieces of wood, from bark of tree	Jalandhar City, New Model Town	**5 – 2 (J1-2)**
2.	Wood Scrapings, from stem of fallen tree	Jalandhar Cantt, Defence Colony	**7 - 0**
3.	Fruiting bodies in the soil	Jalandhar, Cantt, Railway Station	**21 – 6 (S1- 4, S11, S16)**
4.	Fruiting body in the soil	Jalandhar, Lovely Professional University	**8 – 2 (C2, C4)**
5.	Fruiting body on rotten wood	Jalandhar Cantt, Paragpur Village	**9 – 1 (JCB 1)**
6.	Fruiting body on cow dung	Jalandhar City, Devi Talab Mandir	**5 – 1 (JF 3)**
7.	Wood Scrapings, from stem of fallen tree	Jalandhar, Cheheru, near Railway Station	**11 – 2 (RS 9, 10)**
8.	Wood Scrapings, bark of pine tree	Hamirpur, Bhera Himachal Pradesh	**6 – 2 (SD1-2)**
9.	Pieces of wood, from bark of tree	Kangra, Palampur Himachal Pradesh	**7 – 3 (K 1, 4, 6)**
10.	Fruiting bodies from bark of tree	Hamirpur, Saloni Himachal Pradesh	**6 – 1 (HP 1)**
11.	Fully grown mushroom, from log of tree	Dalhousie, Air Force Area Himachal Pradesh	**5 – 2 (D 2, 3)**
12.	Wood Scrapings, from stem of fallen tree	Jammu, Near Circuit House, Jammu and Kashmir	**9 – 1 (JKC1)**
13.	Wood Scrapings, from stem of fallen tree	Jammu, near IIIM, Jammu and Kashmir	**8 – 2 (JK1-2)**
14.	Fruiting bodies from bark of tree	Sonipat, Haryana	**3 – 0**
15.	Fruiting bodies from bark of tree	Ghana bird sanctuary, Rajasthan	**4 – 1 (GH 1)**

Table 2.2 Screening of isolates for laccase by a plate assay method

S.No.	Name of isolate	Type of Indicator				
		CV	MG	CR	Guaiacol	ABTS
1.	J1	+	+	-	++	+
2.	J2	-	-	-	-	-
3.	S1	+++	++	++	++++	++
4.	S2	++	++	-	++	+
5.	S3	+	+	-	+	-
6.	S4	+++	+++++	++	+++++	+++
7.	S11	+	+	+	+	-
8.	S16	-	+	-	++	-
9.	C2	++	-	-	+	-
10.	C4	+++	+++	+++	+++++	+++
11.	JCB1	++	+	+	+	+
12.	JF3	+	+	+	+	+
13.	RS9	-	+	-	+	-
14.	RS10	-	-	+	++	+
15.	SD1	+	+	+	+	+
16.	SD2	++	+	-	+	-
17.	K1	+	++	-	+	+
18.	K4	++	++	+	+	+
19.	K6	+	+	+	+	+
20.	HP1	++	-	-	+	+
21.	D2	+	-	-	+	-
22.	D3	+	+	+	+	-
23.	JKC1	++	++	-	++	-
24.	JK1	+	-	-	+	-
25.	JK2	-	-	+	+	+
26.	GH1	++	+	-	+	-

+ Very poor activity
++ Poor activity
+++ Average activity
++++ Good activity
+++++ Very good activity

Table 2.3 Secondary screening of selected isolates for laccase production under solid state fermentation (SSF)

S.No.	Isolate	Day of Harvest	Laccase Activity (U/ml)
1.	S1	7	2.45 ± 0.5
2.	S4	7	**3.21 ± 0.7**
3.	C4	7	1.14 ± 0.2
4.	K4	7	1.02 ± 0.01

Culture Conditions:
Growth Medium: Wheat Bran Agar
Temperature, ºC: 30
Incubation time: 7 days
± Standard Deviation from the mean

Assay Condition:
Temperature, ºC: 30
pH: 6

Table 2.4 Study of morphological and microscopic characteristics of fungal isolates

S.No.	Isolate	Growth Media	Growth (cm)	Appearance	Microscopy
1.	S1	Wheat Bran Agar	7.5 ± 2.5	White mycelia along the surface of the media	Clamp connection was observed by LPCB wet mount
2.	S4	Wheat Bran Agar	8 ± 1.8	White mycelia along the surface of the media with fruiting bodies	Clamp connection was observed by LPCB wet mount
3.	C4	Wheat Bran Agar	8.5 ± 0.9	White mycelia along the surface of the media with orange pigmentation	Mycelia was observed under microscope by LPCB wet mount
Culture Conditions: Growth Medium : Wheat Bran Agar ; Temperature, ºC: 30 ; Incubation time: 7 days					

Table 2.5 Optimization of days of incubation for laccase production by isolates

S.No.	Days of incubation	Laccase Activity (IU/mL) of Test Isolates		
		S1	**S4**	**C4**
1.	**1**	0.42 ± 0.02	0.31 ± 0.09	1.11 ± 0.28
2.	**2**	0.53 ± 0.08	1.47± 0.08	1.42 ± 0.61
3.	**3**	0.80 ± 0.93	1.79 ± 0.76	1.47 ± 0.47
4.	**4**	1.30 ± 0.15	1.95 ± 0.69	1.49 ± 0.37
5.	**5**	1.58 ± 0.86	2.16 ± 0.16	1.51 ± 0.49
6.	**6**	1.68 ± 0.19	2.56 ± 0.47	1.53 ± 0.85
7.	**7**	**2.45 ± 0.11**	3.21 ± 0.53	1.14 ± 0.87
8.	**8**	2.37 ± 0.12	**3.45 ± 0.59**	**1.57 ± 0.91**
9.	**9**	2.28 ± 0.12	3.38 ± 0.54	1.43 ± 0.03
10.	**10**	2.07 ± 0.17	3.16 ± 0.06	1.31 ± 0.09
11.	**11**	1.98 ± 0.87	3.02 ±0.12	1.18 ± 0.02
12.	**12**	1.83 ± 0.14	2.87 ± 0.98	0.79 ± 0.05
13.	**13**	1.77 ± 0.05	2.71 ± 0.26	0.67 ± 0.03
14.	**14**	1.62 ± 0.79	2.68 ± 0.33	0.53 ± 0.01
15.	**15**	1.53 ± 0.91	2.53 ± 0.62	0.48 ± 0.05

Culture Conditions:
Growth Medium: Wheat Bran
Temperature, ºC: 30
Incubation time: 7 days
± Standard Deviation from the mean

Assay Condition:
Temperature, ºC: 30
pH: 5

Table 2.6 Optimization of temperature for laccase production by isolates

S.No.	Temperature (ºC)	Laccase Activity (IU/mL) of Test Isolates		
		S1	**S4**	**C4**
1.	25	2.13 ± 0.54	3.12 ± 0.06	1.55 ± 0.86
2.	30	**2.39** ± 0.32	**3.57 ± 0.89**	**1.63** ± 0.76
3.	35	2.21± 0.86	3.39 ± 0.47	1.55± 0.62
2.	40	2.02± 0.94	2.89 ± 0.66	1.21± 0.08
3.	45	1.75 ± 0.11	1.65 ± 0.56	0.78 ± 0.03

Culture Conditions: **Assay Condition:**
Growth Medium: Wheat Bran Temperature, ºC: 30
Incubation time: days: 7 (S1), 8 (S4, C4)
± Standard Deviation from the mean

Table 2.7 Optimization of pH for laccase production by isolates

S.No.	pH	Laccase Activity (IU/mL) of Test Isolates		
		S1	**S4**	**C4**
1.	3	1.75 ± 0.56	1.82 ± 0.43	0.89 ± 0.75
2.	3.5	1.81 ± 0.73	1.95 ± 0.87	1.24 ± 0.37
3.	4	1.88 ± 0.68	2.25 ± 0.06	1.49 ± 0.29
4.	4.5	1.97 ± 0.51	2.59 ± 0.01	1.72 ± 0.32
5.	5	2.41 ± 0.03	3.62 ± 0.29	**2.06 ± 0.53**
6.	**5.5**	2.49 ± 0.07	**3.93 ± 0.54**	1.99 ± 0.44
7.	6	2.52 ± 0.54	2.97 ± 0.67	1.56 ± 0.47
8.	6.5	2.64 ± 0.11	2.76 ± 0.46	1.40 ± 0.51
9.	7	2.76 ± 0.32	2.22 ± 0.54	1.35 ± 0.76
10.	7.5	2.87 ± 0.47	2.05 ± 0.07	1.20 ± 0.41
11.	8	**3.14 ± 0.98**	1.98 ± 0.03	1.08 ± 1.05
12.	8.5	3.01 ± 0.11	1.92 ± 0.02	0.879 ± 0.09

Culture Conditions: **Assay Condition:**
Growth Medium: Wheat Bran Temperature, ºC: 30
Incubation time: days: 7 (S1), 8 (S4, C4) pH: 5
Temperature, ºC: 30
± Standard Deviation from the mean

Table 2.8 Optimization of amount of substrate for laccase production by isolates

S.No.	Substrate conc. (gm)	Laccase Activity (IU/mL) of Test Isolates		
		S1	**S4**	**C4**
1.	4	2.87 ± 0.07	3.23 ± 0.11	1.67± 0.62
2.	5	**3.16 ± 0.61**	**3.95 ± 0.36**	**2.10 ± 0.86**
3.	6	2.46 ± 0.54	3.66 ± 0.89	1.70± 0.76
4.	7	2.15 ± 0.25	3.42 ± 0.27	1.54 ± 0.91
5.	8	2.02 ± 0.11	3.31 ± 0.56	1.27 ± 0.43

Culture Conditions: **Assay Condition:**
Growth Medium: Wheat Bran Temperature, ºC: 30
Incubation time: days: 7 (S1), 8 (S4, C4) pH: 5
pH: 8 (S1), 5.5 (S4), 5 (C4)
Temperature, ºC: 30
± Standard Deviation from the mean

Table 2.9 Optimization of moistening agent for laccase production by isolates

S.No.	Percentage (%)	Lacasse Activity (IU/mL) of Test Isolates		
		S1	**S4**	**C4**
1.	50	1.87 ± 0.76	2.23 ± 0.01	1.67± 0.62
2.	60	2.06 ± 1.01	2.86 ± 0.09	1.70± 0.76
3.	70	**3.56 ± 0.61**	**4.27 ± 0.16**	**2.49 ± 0.86**
4.	80	3.38 ± 0.25	3.42 ± 0.19	1.61 ± 0.90
5.	90	2.26 ± 0.11	2.87 ± 0.45	1.28 ± 0.03

Culture Conditions:
Growth Medium: Wheat Bran
Incubation time: days: 7 (S1), 8 (S4, C4)
pH: 8 (S1), 5.5 (S4), 5 (C4)
Temperature, ºC: 30
± Standard Deviation from the mean

Assay Condition:
Temperature, ºC: 30
pH: 5

Table 2.10 Optimization nitrogen source for laccase production by isolates

S.No.	Isolate	Nitrogen Source			
		Yeast Extract		**Ammonium Sulphate**	
		%	**Laccase Activity (IU/mL) of Test Isolates**	**%**	**Laccase Activity (IU/mL) of Test Isolates**
1.	**S1**	**0.5**	3.84 ± 0.58	**0.5**	1.57 ± 0.21
		1	**6.65 ± 0.64**	**1**	0.82 ± 0.98
		1.5	6.12 ± 0.87	**1.5**	0.71 ± 0.23
		2	4.56 ± 0.45	**2**	0.35 ± 0.07
		2.5	2.13 ± 0.87	**2.5**	0.11 ± 0.09
2.	**S4**	**0.5**	4.63 ± 0.54	**0.5**	0.62 ± 0.10
		1	**7.48 ± 0.85**	**1**	0.91 ± 0.89
		1.5	6.47 ± 0.03	**1.5**	1.18 ± 0.91
		2	5.28 ± 0.02	**2**	1.09 ± 0.17
		2.5	5.12 ± 0.11	**2.5**	0.06 ± 0.08
3.	**C4**	**0.5**	2.76 ± 0.75	**0.5**	1.21 ± 0.09
		1	**5.54 ± 0.47**	**1**	0.87 ± 0.17
		1.5	5.02 ± 0.53	**1.5**	0.37 ± 0.22
		2	5.12 ± 0.27	**2**	0.31 ± 0.18
		2.5	1.54 ± 0.48	**2.5**	0.22 ± 0.03

Culture Conditions:
Growth Medium: Wheat Bran
Incubation time: days: 7 (S1), 8 (S4, C4)
pH: 8 (S1), 5 (S4, C4)
Temperature, ºC: 30
Substrate concentration: 5 gm
± Standard Deviation from the mean

Assay Condition:
Temperature, ºC: 30
pH: 5

Table 2.11 Optimization copper sulphate for laccase production by isolates

S.No.	Isolate	Conc. of Copper Sulphate (mM)	Enzyme Activity (IU/mL) of test isolates
1.	**S1**	0.2	4.76 ± 0.72
		0.4	**8.46 ± 0.67**
		0.6	8.12 ± 0.54
		0.8	7.54 ± 0.36
		1.0	3.58 ± 0.21
2.	**S4**	0.2	7.78 ± 0.06
		0.4	**11.68 ± 0.49**
		0.6	11.12 ± 0.68
		0.8	9.43 ± 0.45
		1.0	4.52 ± 0.54
3.	**C4**	0.2	5.64 ± 0.09
		0.4	**6.51 ± 0.47**
		0.6	5.98 ± 0.65
		0.8	4.52 ± 0.38
		1.0	2.19 ± 0.72

Culture Conditions:
Growth Medium: Wheat Bran
Incubation time: days: 7 (S1), 8 (S4, C4)
pH: 8 (S1), 5 (S4, C4)
Temperature, ºC: 30
Substrate concentration: 5 gm
± Standard Deviation from the mean

Assay Condition:
Temperature, ºC: 30
pH: 5

Table 2.12 Estimation of ligninolytic enzyme activities under optimized condition of SSF for laccase production

S.No.	Isolates	Ligninolytic Enzyme Activity (IU/mL) of Test Isolates		
		Laccase[*1]	**MnP[*2]**	**LiP[*3]**
1.	**S1**	8.47 ± 0.19	6.72 ± 0.05	6.12 ± 0.75
2.	**S4**	**11.84 ± 0.67**	**9.56 ± 0.13**	**8.38 ± 0.01**
3.	**C4**	9.46 ± 0.16	6.65 ± 0.89	8.79 ± 0.98

Culture Conditions:
Growth Medium: Wheat Bran Agar
Incubation time: days: 7 (S1), 8 (S4, C4)
pH: 8 (S1), 5.5 (S4, C4)
Temperature, ºC: 30
Substrate concentration: 5 gm
Moistening agent, %: 70

± Standard Deviation from the mean

Assay Condition:
[*1]Temperature, ºC: 30
pH: 5
Incubation Time: 15mins
[*2 *3] Temperature: Room Temp.
Incubation Time: 30 secs
pH: 4.5

Table 2.13 Optimization of parameters for laccase production by response surface methodology (RSM): Combination of parameters

			Factor 1	Factor 2	Factor 3	Factor 4	Factor 5
Std	Run	Block	A:pH	B:Temperature	C:CuSO4	D:Yeast extract	E:substrate conc.
27	1	Block 1	4.2	34.4	1.1	1.9	6.8
49	2	Block 1	5.0	32.5	1.5	1.5	6.0
7	3	Block 1	4.2	34.4	1.9	1.1	5.2
33	4	Block 1	3.0	32.5	1.5	1.5	6.0
42	5	Block 1	5.0	32.5	1.5	1.5	8.0
19	6	Block 1	4.2	34.4	1.1	1.1	6.8
22	7	Block 1	5.8	30.6	1.9	1.1	6.8
20	8	Block 1	5.8	34.4	1.1	1.1	6.8
16	9	Block 1	5.8	34.4	1.9	1.9	5.2
41	10	Block 1	5.0	32.5	1.5	1.5	4.0
24	11	Block 1	5.8	34.4	1.9	1.1	6.8
45	12	Block 1	5.0	32.5	1.5	1.5	6.0
13	13	Block 1	4.2	30.6	1.9	1.9	5.2
17	14	Block 1	4.2	30.6	1.1	1.1	6.8
1	15	Block 1	4.2	30.6	1.1	1.1	5.2
28	16	Block 1	5.8	34.4	1.1	1.9	6.8
4	17	Block 1	5.8	34.4	1.1	1.1	5.2
31	18	Block 1	4.2	34.4	1.9	1.9	6.8
9	19	Block 1	4.2	30.6	1.1	1.9	5.2
11	20	Block 1	4.2	34.4	1.1	1.9	5.2
12	21	Block 1	5.8	34.4	1.1	1.9	5.2
30	22	Block 1	5.8	30.6	1.9	1.9	6.8
36	23	Block 1	5.0	37.0	1.5	1.5	6.0
10	24	Block 1	5.8	30.6	1.1	1.9	5.2
14	25	Block 1	5.8	30.6	1.9	1.9	5.2
37	26	Block 1	5.0	32.5	0.5	1.5	6.0
47	27	Block 1	5.0	32.5	1.5	1.5	6.0
15	28	Block 1	4.2	34.4	1.9	1.9	5.2
5	29	Block 1	4.2	30.6	1.9	1.1	5.2
6	30	Block 1	5.8	30.6	1.9	1.1	5.2
44	31	Block 1	5.0	32.5	1.5	1.5	6.0
35	32	Block 1	5.0	28.0	1.5	1.5	6.0
40	33	Block 1	5.0	32.5	1.5	2.5	6.0
8	34	Block 1	5.8	34.4	1.9	1.1	5.2
21	35	Block 1	4.2	30.6	1.9	1.1	6.8
3	36	Block 1	4.2	34.4	1.1	1.1	5.2
2	37	Block 1	5.8	30.6	1.1	1.1	5.2
38	38	Block 1	5.0	32.5	2.5	1.5	6.0
26	39	Block 1	5.8	30.6	1.1	1.9	6.8
25	40	Block 1	4.2	30.6	1.1	1.9	6.8
48	41	Block 1	5.0	32.5	1.5	1.5	6.0
34	42	Block 1	7.0	32.5	1.5	1.5	6.0
18	43	Block 1	5.8	30.6	1.1	1.1	6.8
46	44	Block 1	5.0	32.5	1.5	1.5	6.0
32	45	Block 1	5.8	34.4	1.9	1.9	6.8
50	46	Block 1	5.0	32.5	1.5	1.5	6.0
39	47	Block 1	5.0	32.5	1.5	0.5	6.0
23	48	Block 1	4.2	34.4	1.9	1.1	6.8
43	49	Block 1	5.0	32.5	1.5	1.5	6.0
29	50	Block 1	4.2	30.6	1.9	1.9	6.8

Table 2.14 RSM Table: Level of Significance

Source	Sum of Squares	df	Mean Square	F-value	p-value	
Model	597.80	15	39.85	3.99	0.0004	Significant
A-pH	0.0012	1	0.0012	0.0001	0.9914	
B-Temperature	105.56	1	105.56	10.56	0.0026	
C-CuSO4	61.97	1	61.97	6.20	0.0179	
D-Yeast extract	23.53	1	23.53	2.35	0.1343	
E-substrate conc.	13.58	1	13.58	1.36	0.2520	
AB	53.81	1	53.81	5.38	0.0265	
AC	30.60	1	30.60	3.06	0.0893	
AD	27.40	1	27.40	2.74	0.1071	
AE	63.87	1	63.87	6.39	0.0163	
BC	73.49	1	73.49	7.35	0.0104	
BD	7.93	1	7.93	0.7930	0.3795	
BE	42.60	1	42.60	4.26	0.0467	
CD	30.30	1	30.30	3.03	0.0908	
CE	39.24	1	39.24	3.92	0.0557	
DE	23.90	1	23.90	2.39	0.1314	
Residual	340.02	34	10.00			
Lack of Fit	291.10	27	10.78	1.54	0.2874	not significant
Pure Error	48.92	7	6.99			
Cor Total	937.82	49				

Table 2.15 Fit Statistics

Std. Dev.	3.16	**R^2**	0.6374
Mean	9.29	**Adjusted R^2**	0.4775
C.V. %	34.05	**Predicted R^2**	0.0695
		Adeq Precision	8.9878

Table 2.16 Optimum combination for laccase production

Run	pH	Temperature	CuSo4	Yeast Extract	Substrate Conc.	O.D	Enzymatic Activity	Predicted Value
1	4.2	34.4	0.2	1.9	6.8	0.257	5.02	5.55
2	5	32.5	1.0	1.5	6.0	0.304	5.94	9.29
3	4.2	34.4	0.4	1.1	5.2	0.651	12.72	10.08
4	3	32.5	1.0	1.5	6.0	0.281	5.49	9.30
5	5	32.5	1.5	1.5	8.0	0.349	6.82	7.96
6	4.2	34.4	1.1	1.1	6.8	0.157	3.07	1.45
7	5.8	30.6	1.9	1.1	6.8	0.254	4.96	10.41
8	5.8	34.4	1.1	1.1	6.8	0.279	5.45	5.47
9	5.8	34.4	1.9	1.9	5.2	0.318	6.22	5.38
10	5	32.5	1.5	1.5	4.0	0.364	7.11	10.62
11	5.8	34.4	1.9	1.1	6.8	0.189	3.69	4.43
12	5	32.5	1.5	1.5	6.0	0.489	9.56	9.29
13	4.2	30.6	1.9	1.9	5.2	0.571	11.16	8.81
14	4.2	30.6	1.1	1.1	6.8	0.349	6.82	8.31
15	4.2	30.6	1.1	1.1	5.2	0.781	15.27	13.89
16	5.8	34.4	1.1	1.9	6.8	0.284	5.55	5.88
17	5.8	34.4	1.1	1.1	5.2	0.549	10.73	10.02
18	4.2	34.4	1.9	1.9	6.8	0.457	8.93	12.30
19	4.2	30.6	1.1	1.9	5.2	0.681	13.31	12.55
20	4.2	34.4	1.1	1.9	5.2	0.905	17.69	12.29
21	5.8	34.4	1.1	1.9	5.2	0.178	3.48	6.96
22	5.8	30.6	1.9	1.9	6.8	0.641	12.53	12.72
23	5	37.0	1.5	1.5	6.0	0.197	3.85	5.58
24	5.8	30.6	1.1	1.9	5.2	0.548	10.71	12.41
25	5.8	30.6	1.9	1.9	5.2	0.193	3.77	4.76
26	5	32.5	0.5	1.5	6.0	0.65	12.70	12.13
27	5	32.5	1.5	1.5	6.0	0.498	9.73	9.29
28	4.2	34.4	1.9	1.9	5.2	0.84	16.42	14.61
29	4.2	30.6	1.9	1.1	5.2	0.159	3.11	6.26
30	5.8	30.6	1.9	1.1	5.2	0.571	11.16	5.91
31	5	32.5	1.5	1.5	6.0	0.249	4.87	9.29
32	5	28.0	1.5	1.5	6.0	0.637	12.45	13.00
33	5	32.5	1.5	2.5	6.0	0.49	9.58	11.04
34	5.8	34.4	1.9	1.1	5.2	0.197	3.85	4.54
35	4.2	30.6	1.9	1.1	6.8	0.594	11.61	5.11
36	4.2	34.4	1.1	1.1	5.2	0.549	10.73	11.64
37	**5.8**	**30.6**	**1.1**	**1.1**	**5.2**	**0.945**	**18.47**	17.45
38	5	32.5	2.5	1.5	6.0	0.149	2.91	6.44
39	5.8	30.6	1.1	1.9	6.8	0.857	16.75	15.93
40	4.2	30.6	1.1	1.9	6.8	0.543	10.61	10.42
41	5	32.5	1.5	1.5	6.0	0.681	13.31	9.29
42	7.0	32.5	1.5	1.5	6.0	0.681	13.31	9.28
43	5.8	30.6	1.1	1.1	6.8	0.901	17.61	17.52
44	5.0	32.5	1.5	1.5	6.0	0.518	10.12	9.29
45	5.8	34.4	1.9	1.9	6.8	0.648	12.67	8.72
46	5.0	32.5	1.5	1.5	6.0	0.498	9.73	9.29
47	5.0	32.5	1.5	0.5	6.0	0.257	5.02	7.54
48	4.2	34.4	1.9	1.1	6.8	0.369	7.21	4.31
49	5.0	32.5	1.5	1.5	6.0	0.401	7.84	9.29
50	4.2	30.6	1.9	1.9	6.8	0.652	12.74	11.11

Table 2.17 DNA QC: DNA quantity estimate using Nanodrop and Qubit dsDNA BR Kit

Sample ID	Nanodrop conc. (ng/ µl)	260/280	260/230	Qubit conc. (ng/ µl)	Vol of DNA Available (uL)	Total DNA Amount Available (ng)	Qubit conc. (ng/ µl) (for library construction)	QC status
S4	13.7	2.11	0.04	3.32	40	132.8	21.8	Passed

Table 2.18 Bioinformatics Analysis: Basic Statistics Summary of data

S.No.	Type of Data	Sample	Total Read	Read Length	% GC
1.	Raw	S4_R1.fastq	25482426	151	65
		S4_R2.fastq	25482426	151	65
2.	Processed	S4_R1.fastq	25013591	20-141	67
		S4_R2.fastq	25013591	20-141	67

Table 2.19 *Denovo* Assembly

S.No.	Assembly Statistics	Parameters	Sample
1.	Before Gap Filling	Total Number of Contigs	17789
		N50 (bp)	1061
		Longest Contig (bp)	160373
		%GC	61
		Total Length (bp)	20544164
2.	After Gap Filling	Total Number of Contigs	27
		N50 (bp)	1367385
		Longest Contig (bp)	3577230
		%GC	58
		Total Length (bp)	16312191

Table 2.20 SSR prediction of assembly scaffold and distribution of different repeat type classes of isolate S4

Description	Count
Total number of Scaffolds	27
Total Size of examined sequences (bp)	1972310
Total number of SSRs Identified	53
Number of SSR containing scaffolds	10
Number of scaffolds containing more than 1 SSR	9
Number of SSRs present in compound formation	3
Mono repeats	20
Di repeats	10
Tri repeats	23

Figures

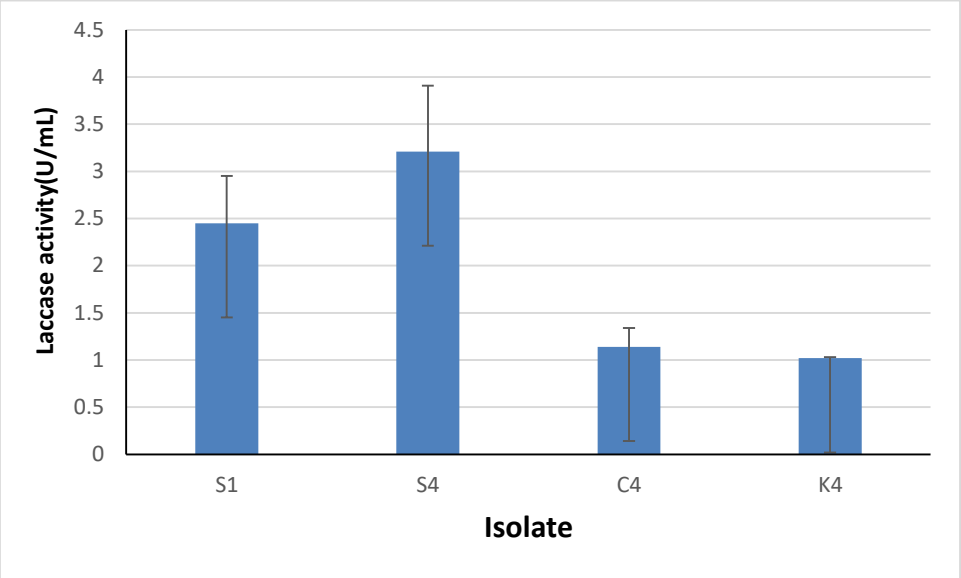

Figure 2.1: Secondary screening of selected isolates for laccase production Solid State Fermentation (SSF)

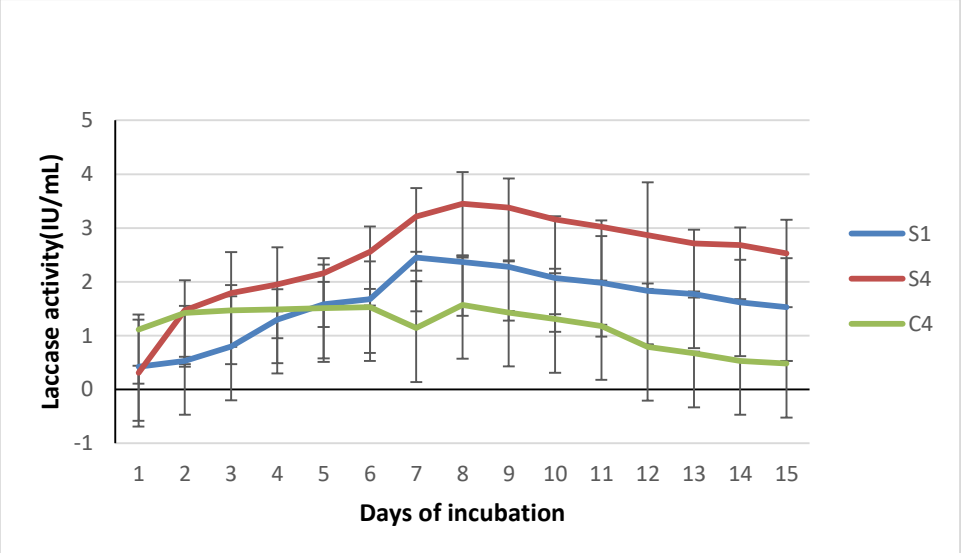

Figure 2.2: Effect of days of incubation on laccase activity by SSF

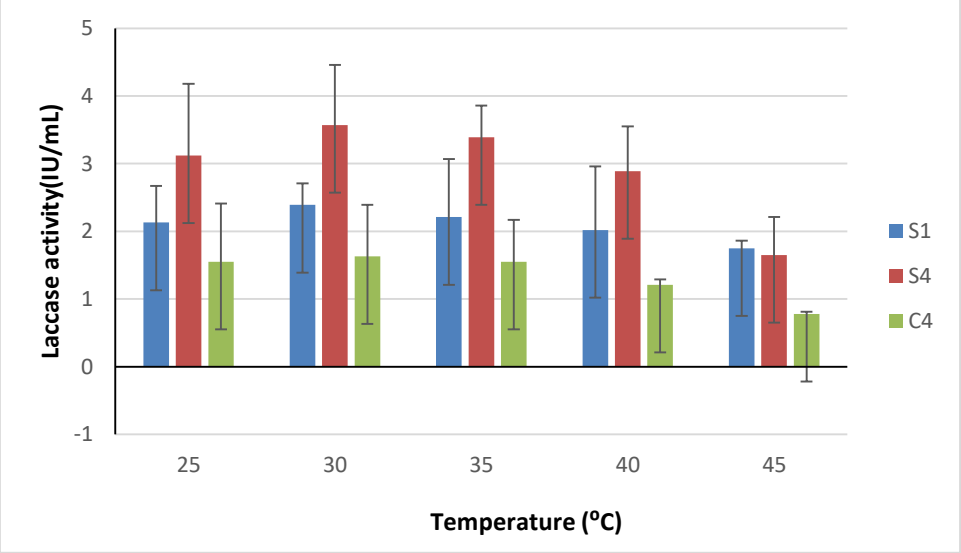

Figure 2.3: Effect of temperature on laccase activity by SSF

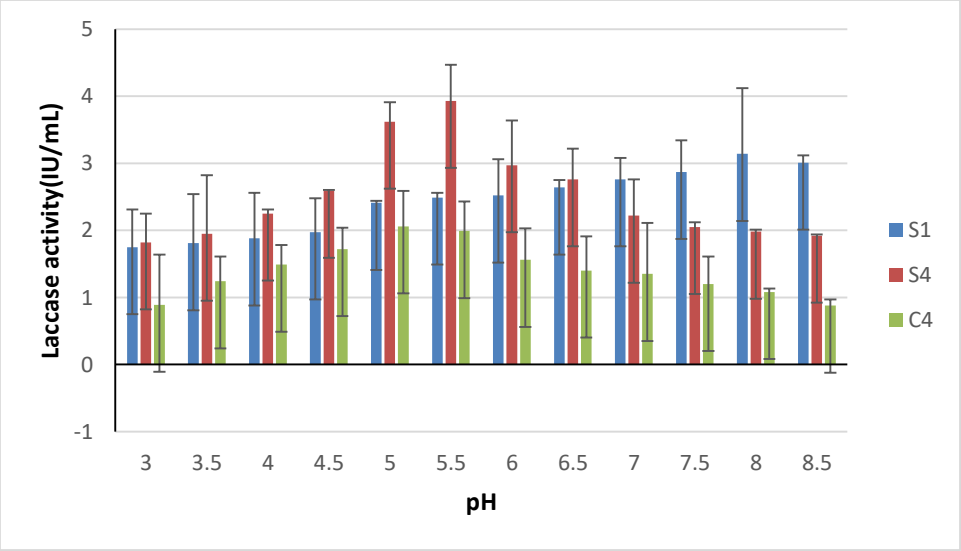

Figure 2.4: Effect of pH on laccase activity by SSF

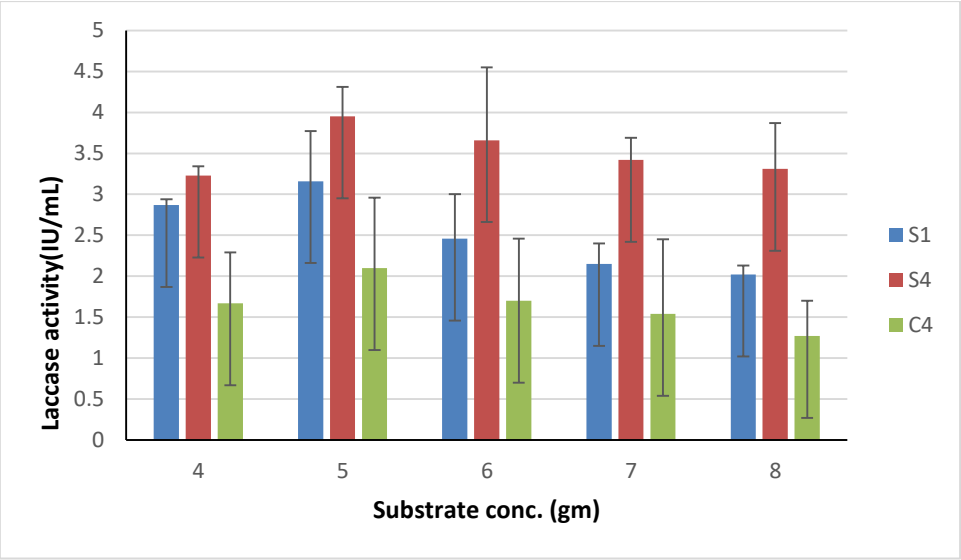

Figure 2.5: Effect of substrate concentration on laccase activity by SSF

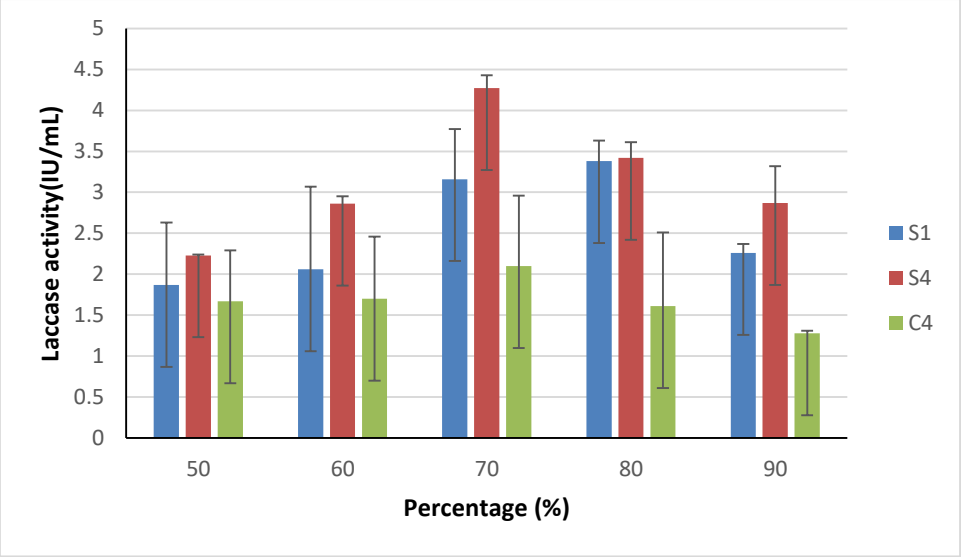

Figure 2.6: Effect of moistening agent on laccase activity by SSF

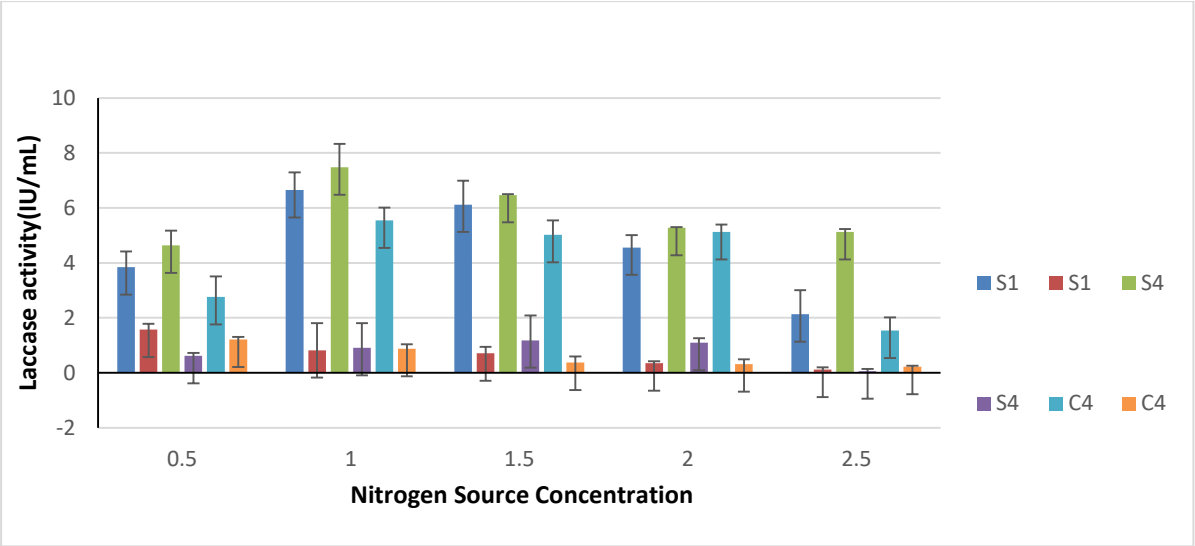

Figure 2.7: Effect of nitrogen source concentration on laccase activity by SSF

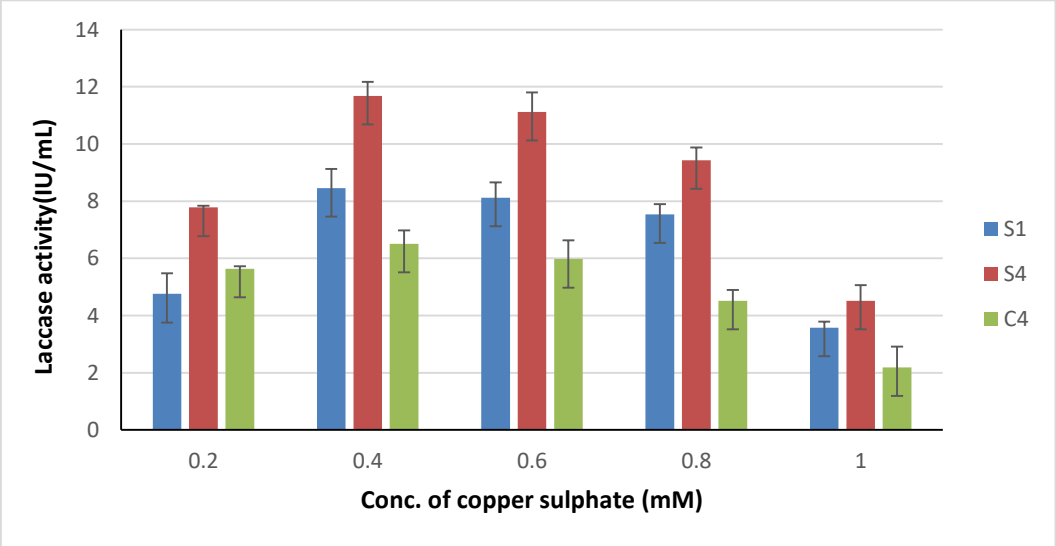

Figure 2.8: Effect of copper sulphate on laccase activity by SSF

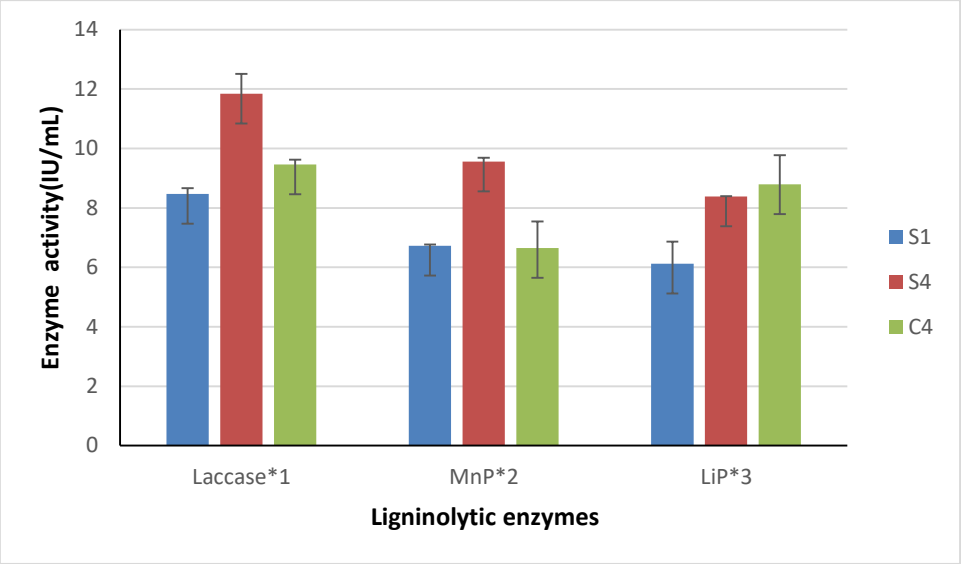

Figure 2.9: Estimation of laccase activity under optimized condition and determination of LiP (Lignin Peroxidase) and MnP (Manganese Peroxidase) activity under the same condition

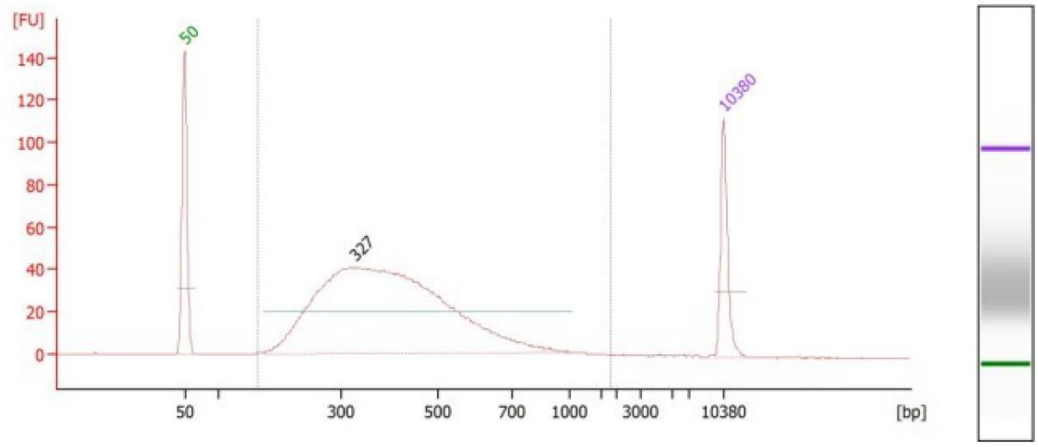

Figure 2.10: DNA QC: DNA quantity estimate using Nanodrop and Qubit dsDNA BR Kit

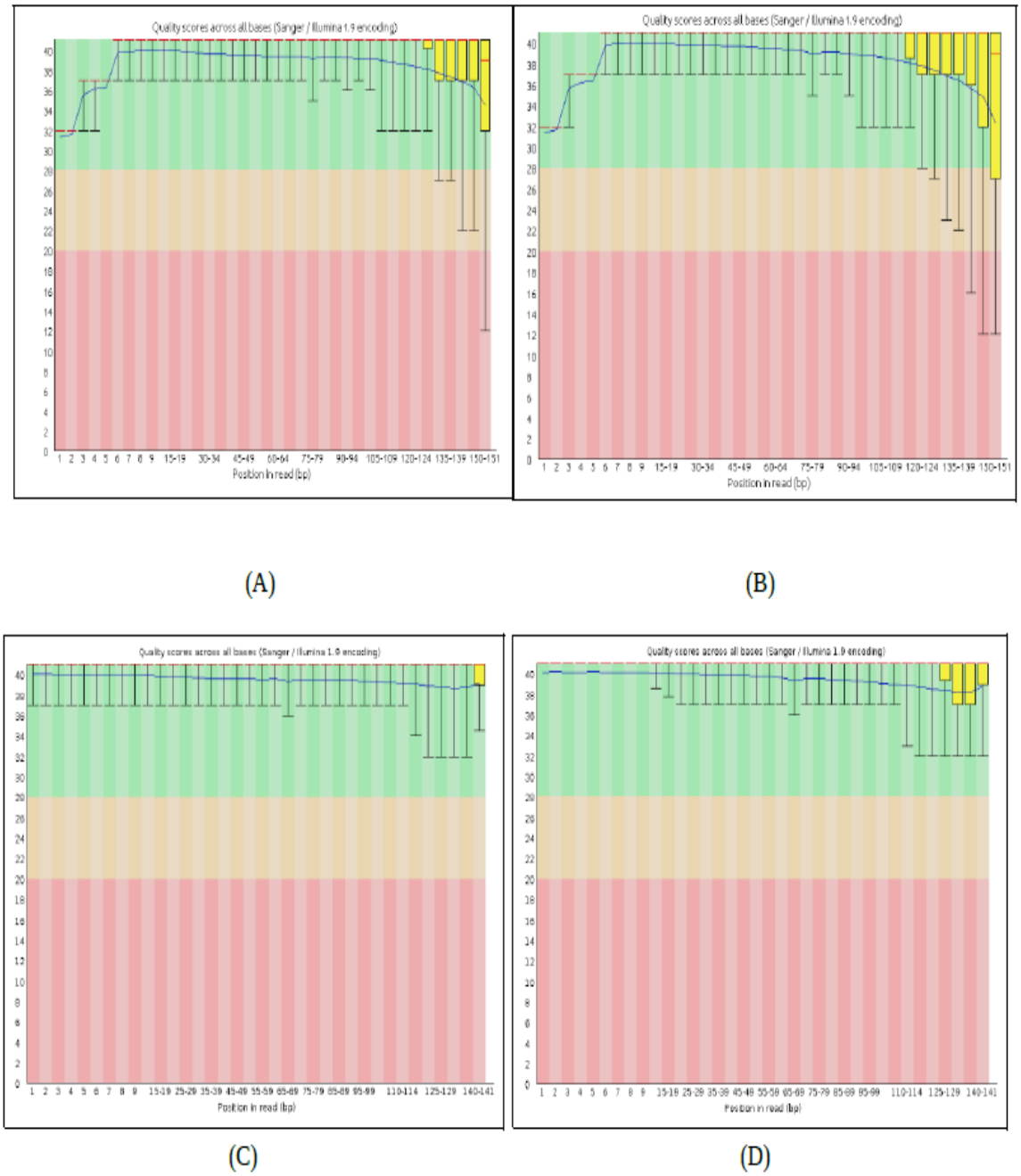

Figure 2.11: Bioinformatics Analysis: Basic Statistics Summary of data A and B depict the per base quantity of raw reads and C and D processed reads of the Sample ACT respectively. Note: 1. The central red line is the median value,2. The yellow box represents the inter-quartile range (25-75%),3. The upper and lower whiskers represent the 10% and 90% points, the blue line represents the mean quality.

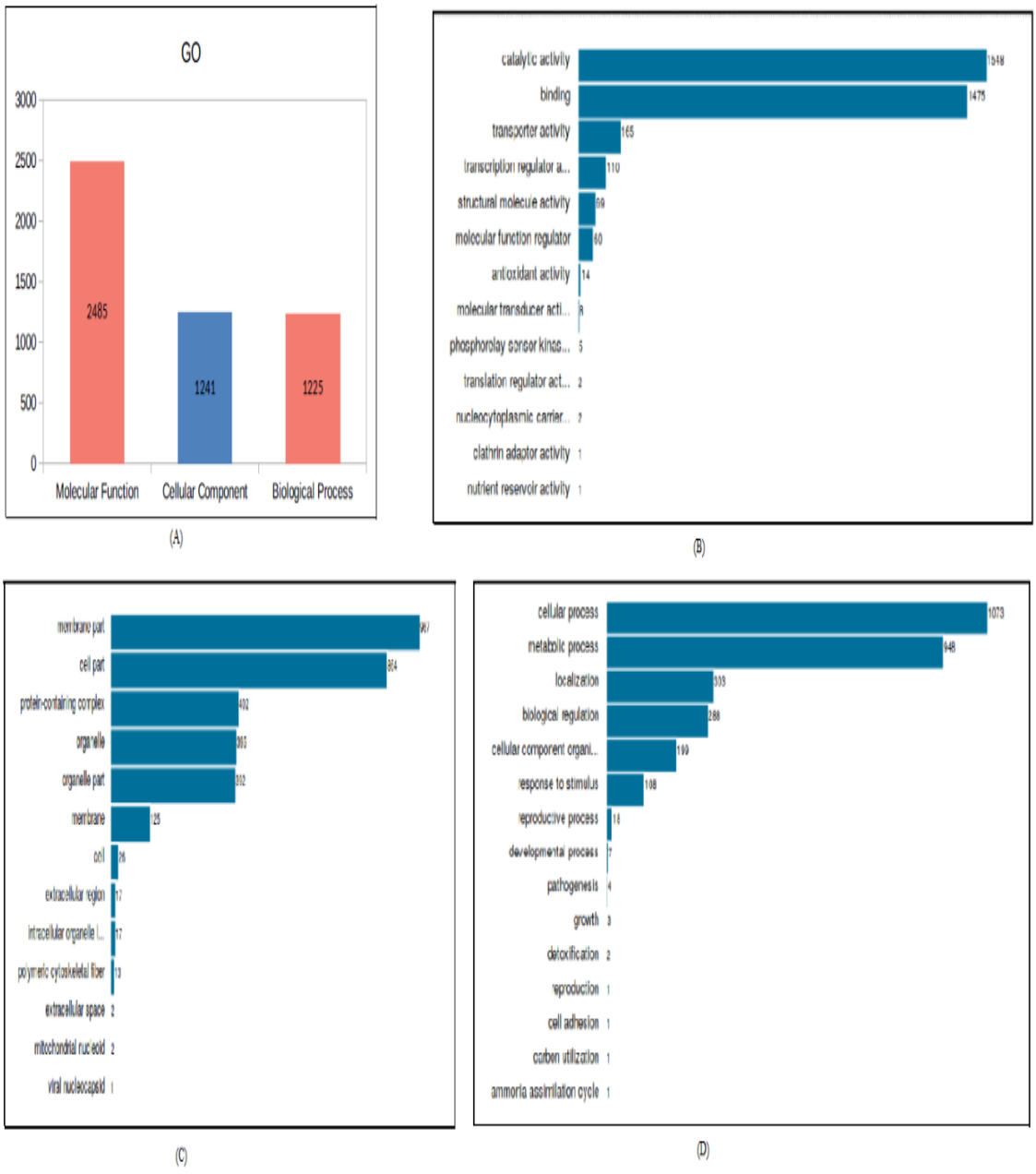

Figure 2.12: A- D Gene Ontology A: Gene Ontology Level, B: GO- Molecular Function, C: GO – Cellular Component, D: GO – Biological Process.

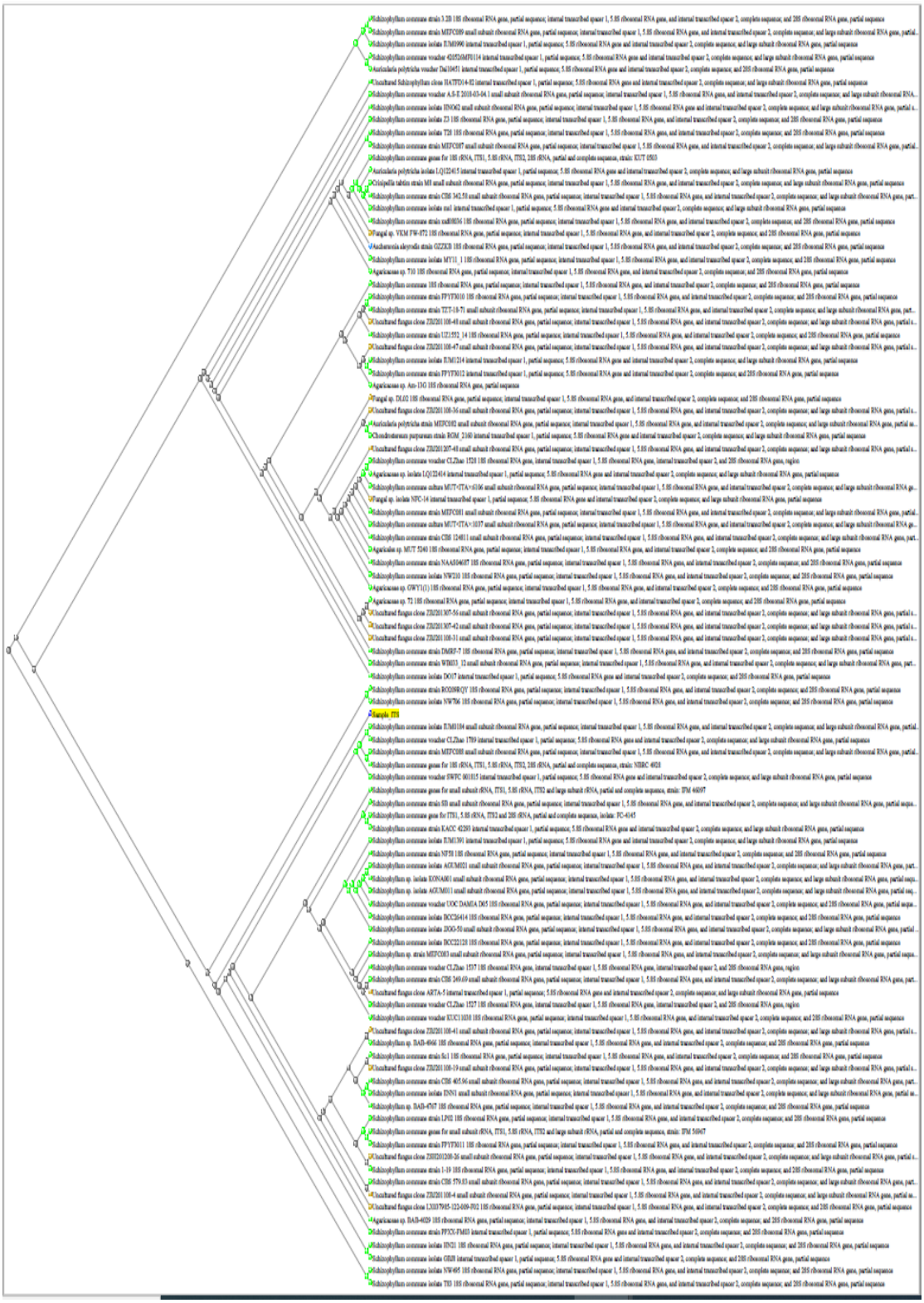

Figure 2.13: Molecular Identification of the isolate: NCBI Tree Viewer – Phylogenetic Tree Analysis

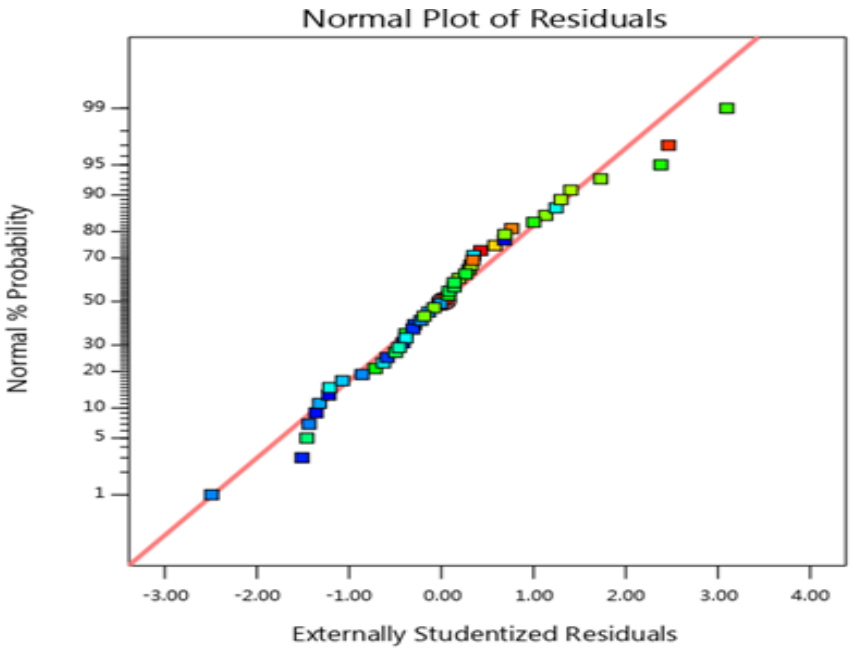

(A)

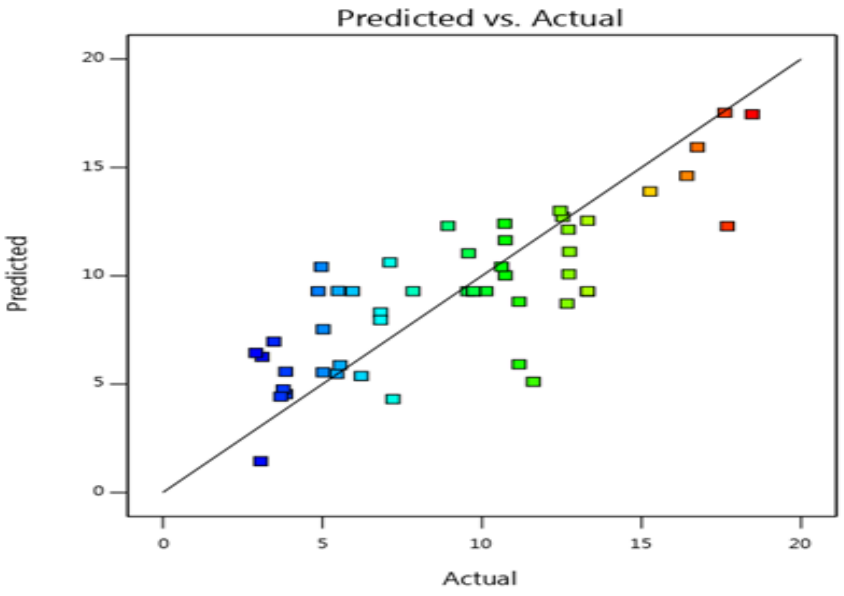

(B)

Figure 2.14: Response 1, (A) Normal Plot of Residuals; (B)Predicted Vs Actual Plot

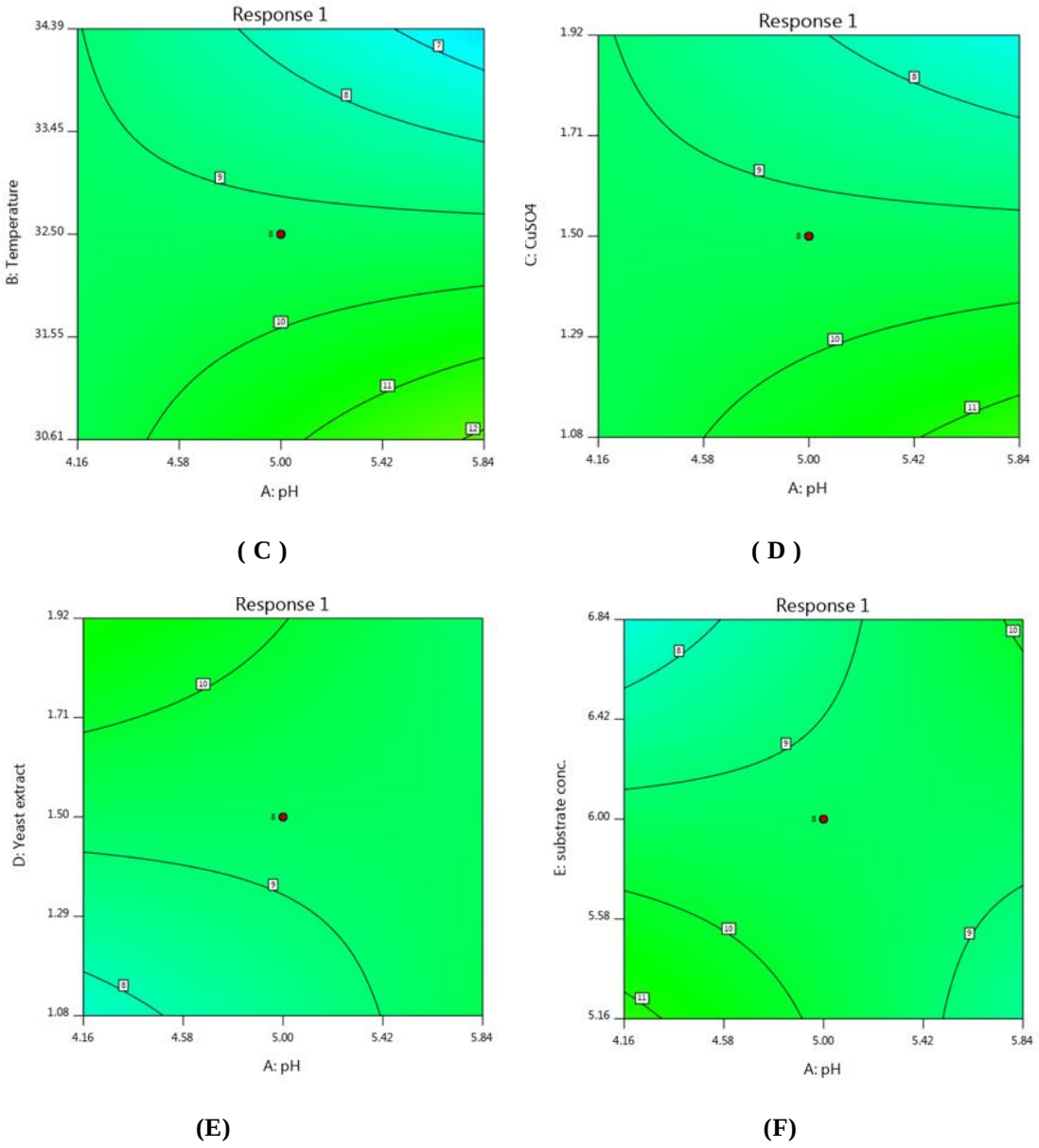

Figure 2.15: Response 1, Contour Plot (C) pH Vs Temp.; (D) pH Vs $CuSO_4$ (E) pH Vs Yeast Extract; (F) pH Vs Substrate Concentration

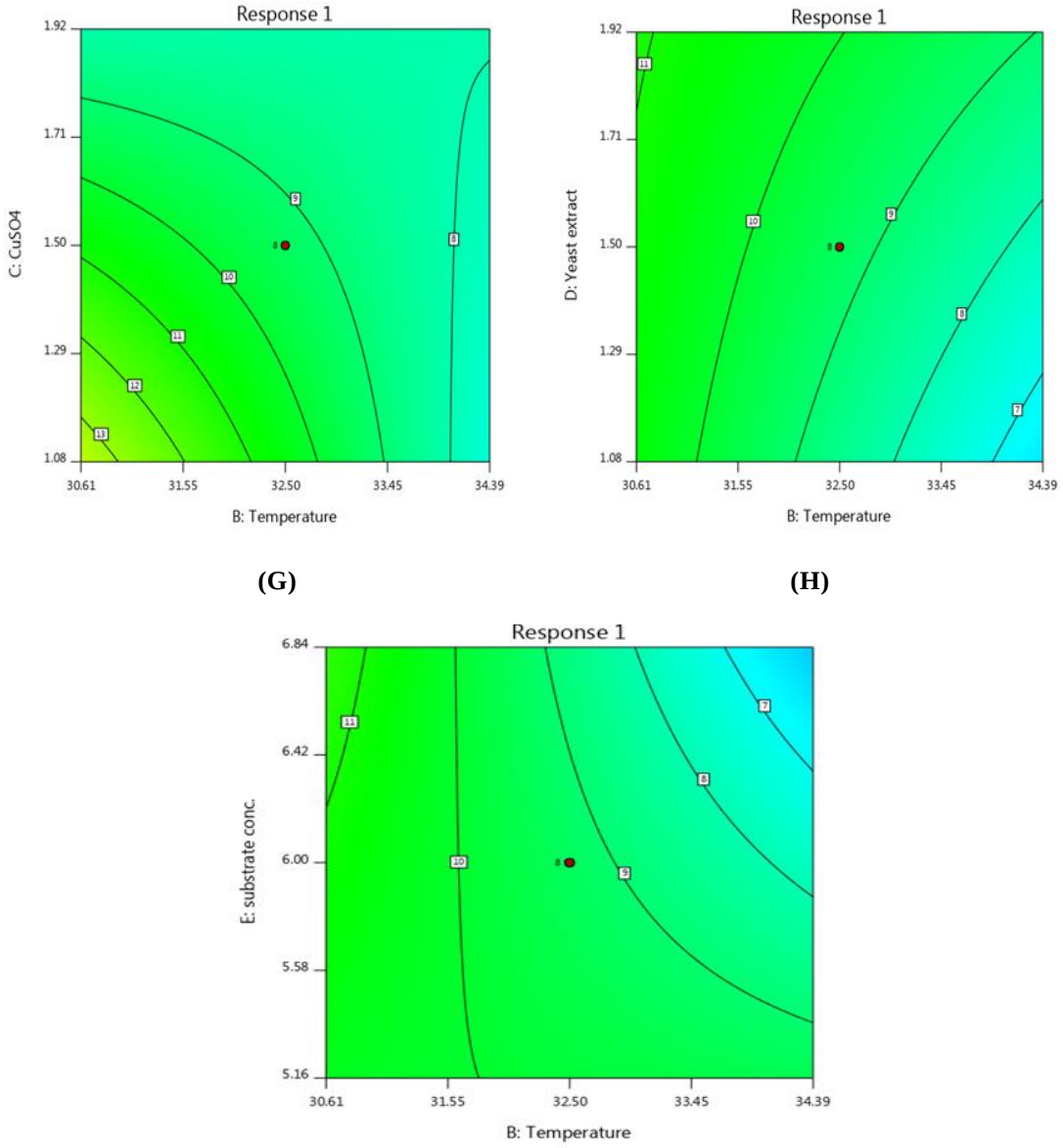

(G) **(H)**

(I)

Figure 2.16: Response 1, Contour Plot (G) Temp Vs $CuSO_4$.; (H) Temp Vs Yeast Extract (I) Temp Vs Substrate Concentration

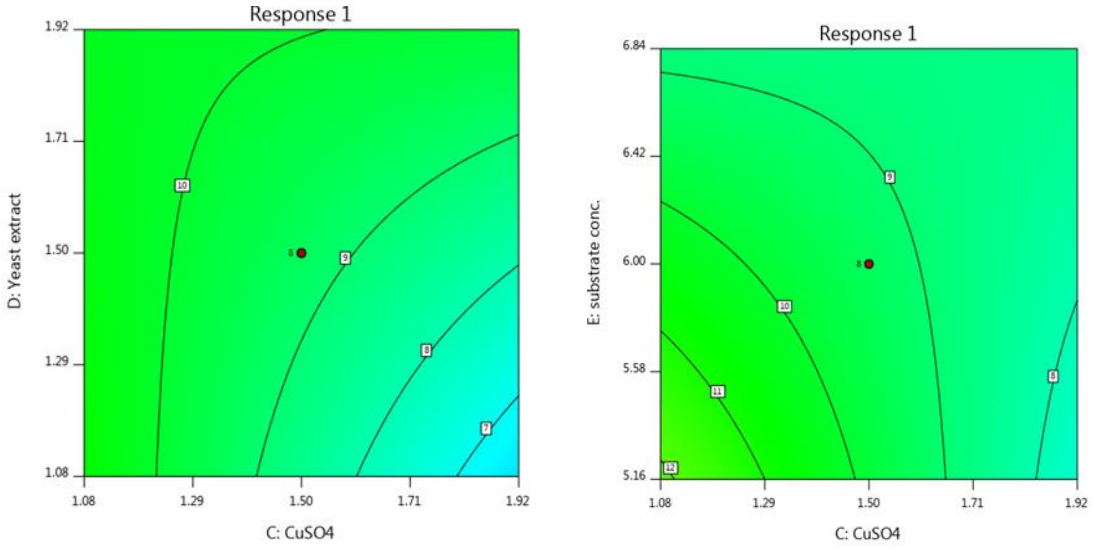

(J) **(K)**

Figure 2.17: Response 1, Contour Plot (J) $CuSO_4$.Vs Yeast Extract; (K) $CuSO_4$.Vs Substrate Concentration

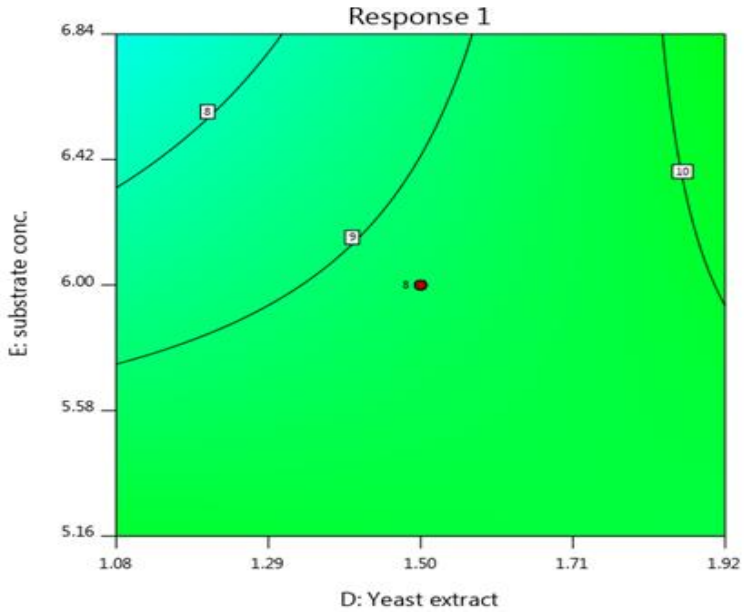

(L)

Figure 2.18: Response 1, Contour Plot (L) Yeast Extract Vs Substrate Concentration

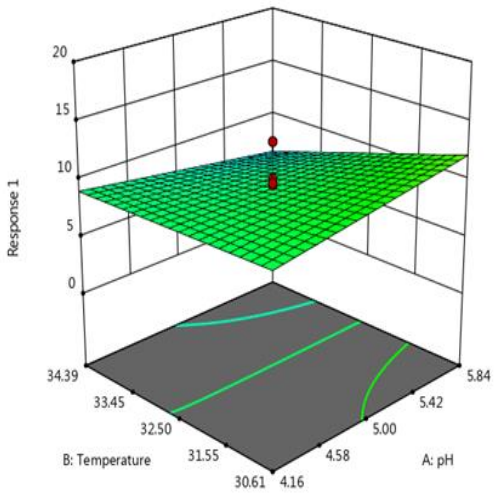

(M)

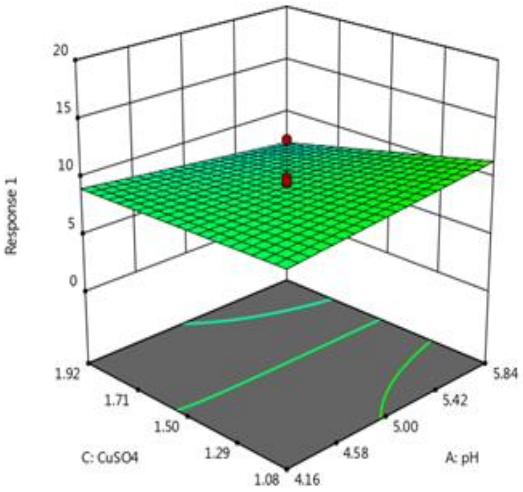

(N)

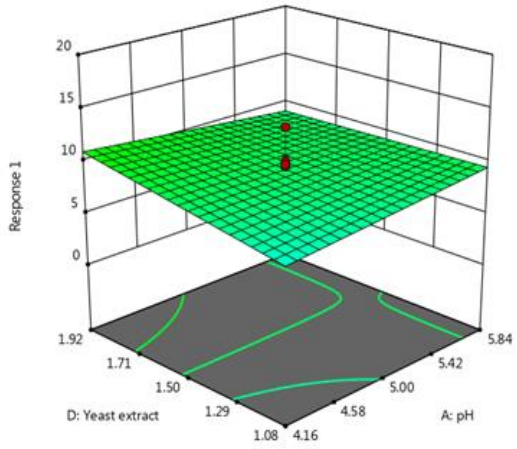

(O)

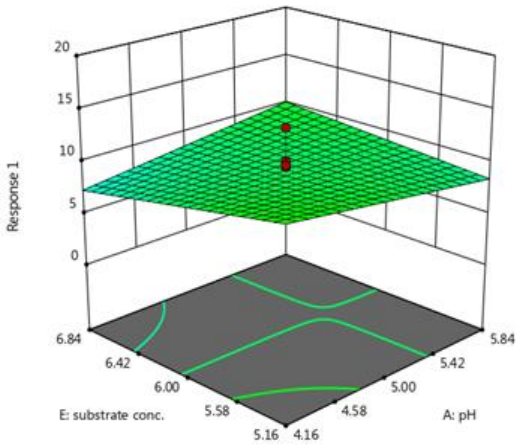

(P)

Figure 2.19: Response 1, 3D Plot (M) pH Vs Temp; (N) pH Vs $CuSO_4$; (O) pH Vs Yeast Extract ; (P) pH Vs Substrate Concentration

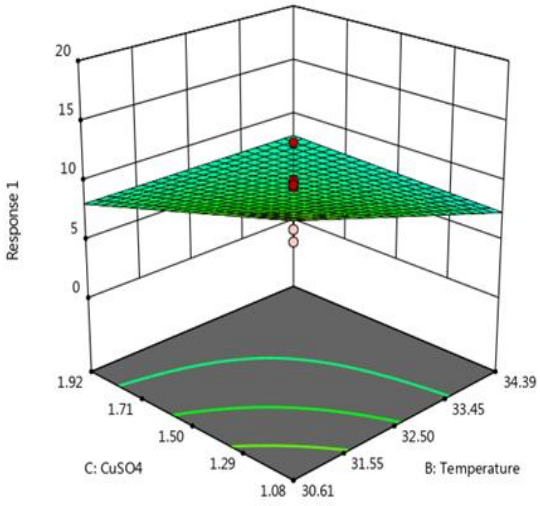

(Q)

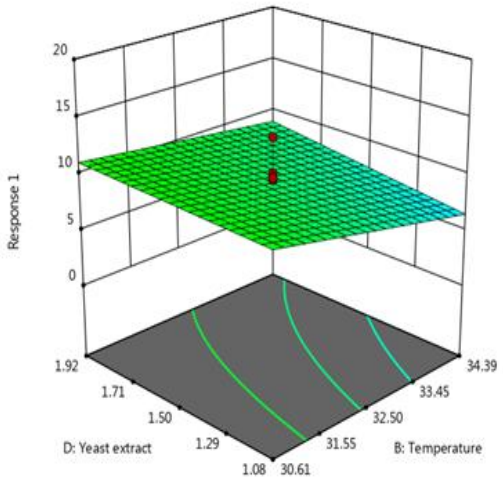

(R)

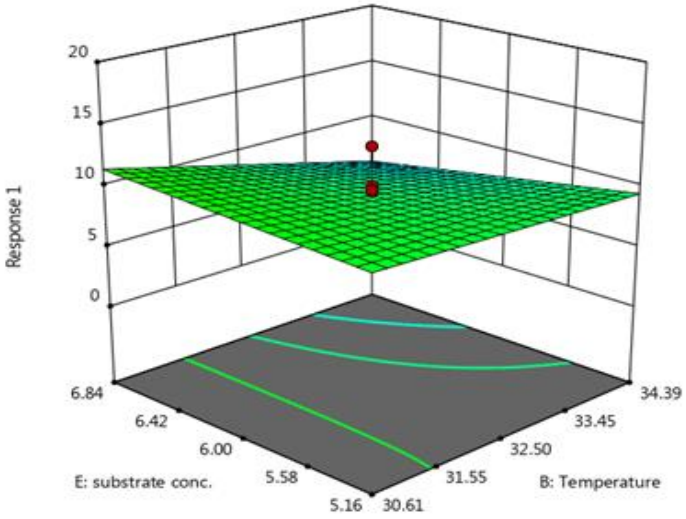

(S)

Figure 2.20: Response 1, 3D Plot (Q) Temp Vs $CuSO_4$; (R) Temp Vs Yeast Extract; (S) Temp Vs Substrate Concentration

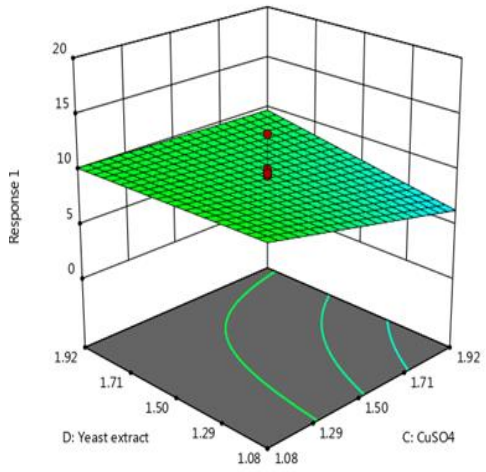

(T)

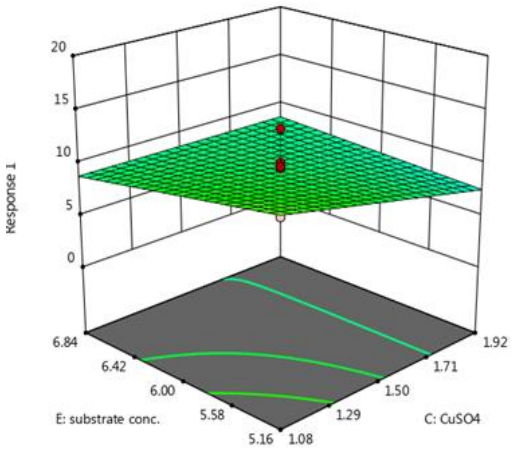

(U)

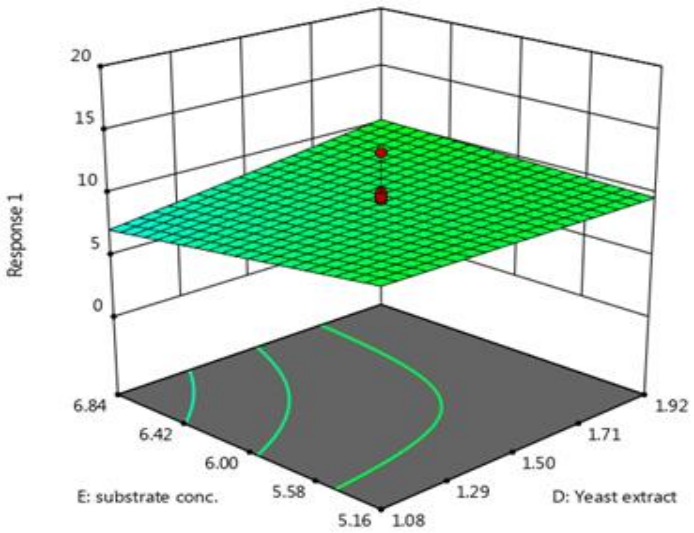

(V)

Figure 2.21: Response 1, 3D Plot (T) $CuSO_4$ Vs Yeast; (U) Copper Sulphate Vs Substrate Concentration; (V) Yeast Extract Vs Substrate Concentration

Photographs

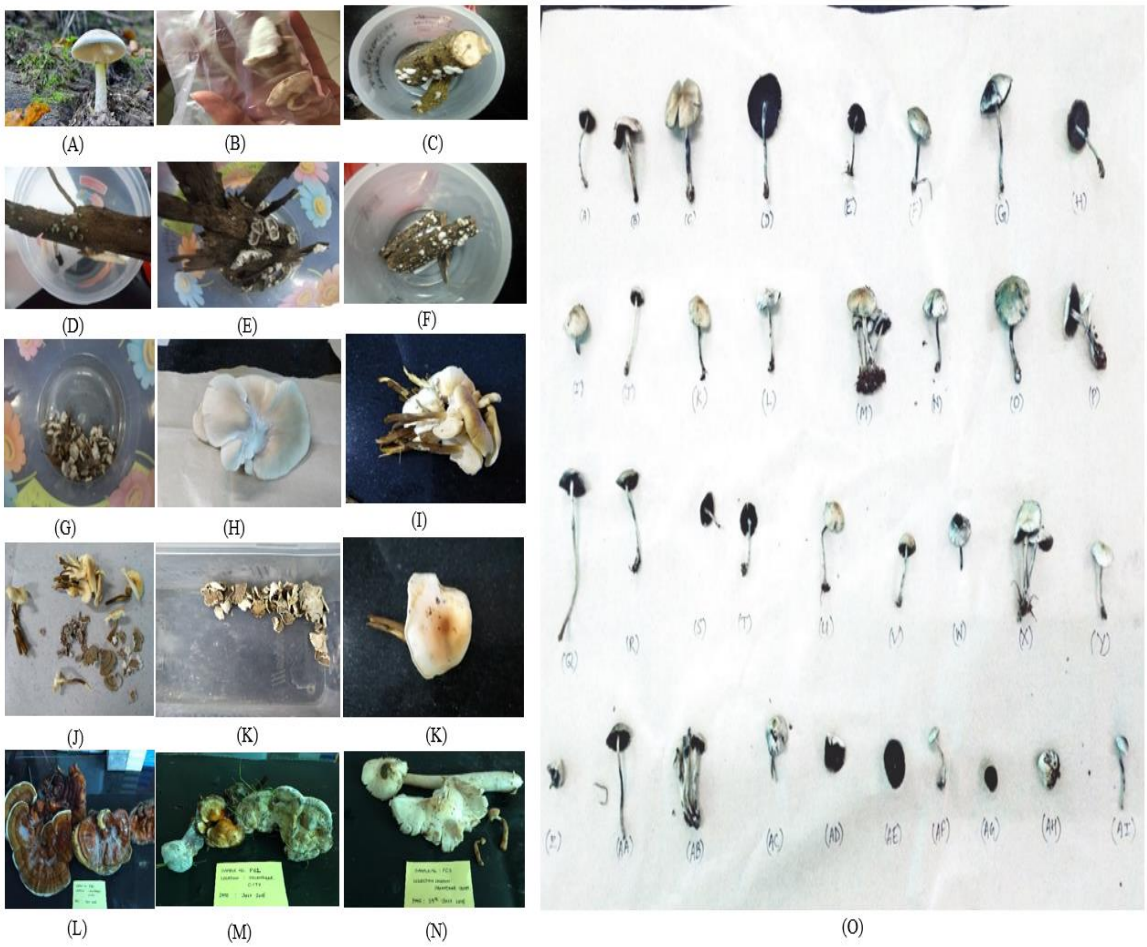

Photograph 2.1: Few of the samples collected from various places of Punjab: (A, B, H, L, M, N) and Himachal Pradesh (C, D, E, F, G, J, K, O); A, a fruiting body grown on soil; B,H,I,K, L,M,N are the uprooted fruiting bodies on wood logs; C,D,E and F are thick mycelium of Basidiomycetous strain on wood pieces; G,J and K are the caps of the Basidiomycetes fallen from the tree sides; O are the fruiting bodies uprooted from soil.

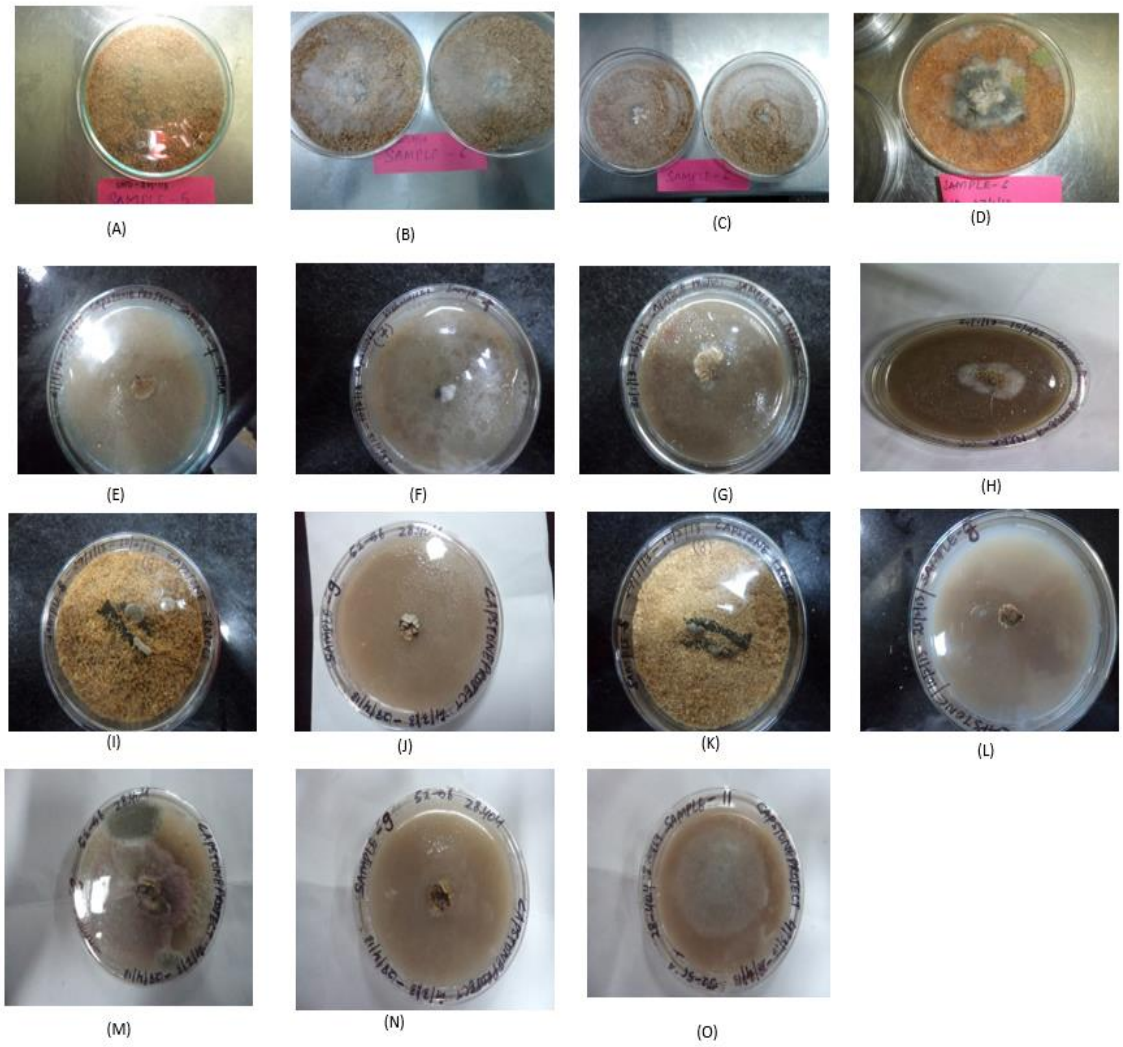

Photograph 2.2: Isolation of Basidiomycetous samples on wheat bran agar. A, B, C, D and J are the inoculation on moistened wheat bran in petri dishes; E, F, G, H,J,L,M,N,O are the inoculation on WB Agar plates. The plates are of different days of incubation, A (2 days); B, C (5 days); D(6 days); E (Day 0); F (2days); G (2 days), H(3 dyas); I and K (2 days); J, L,N,O (1 day), M, O(4 days)

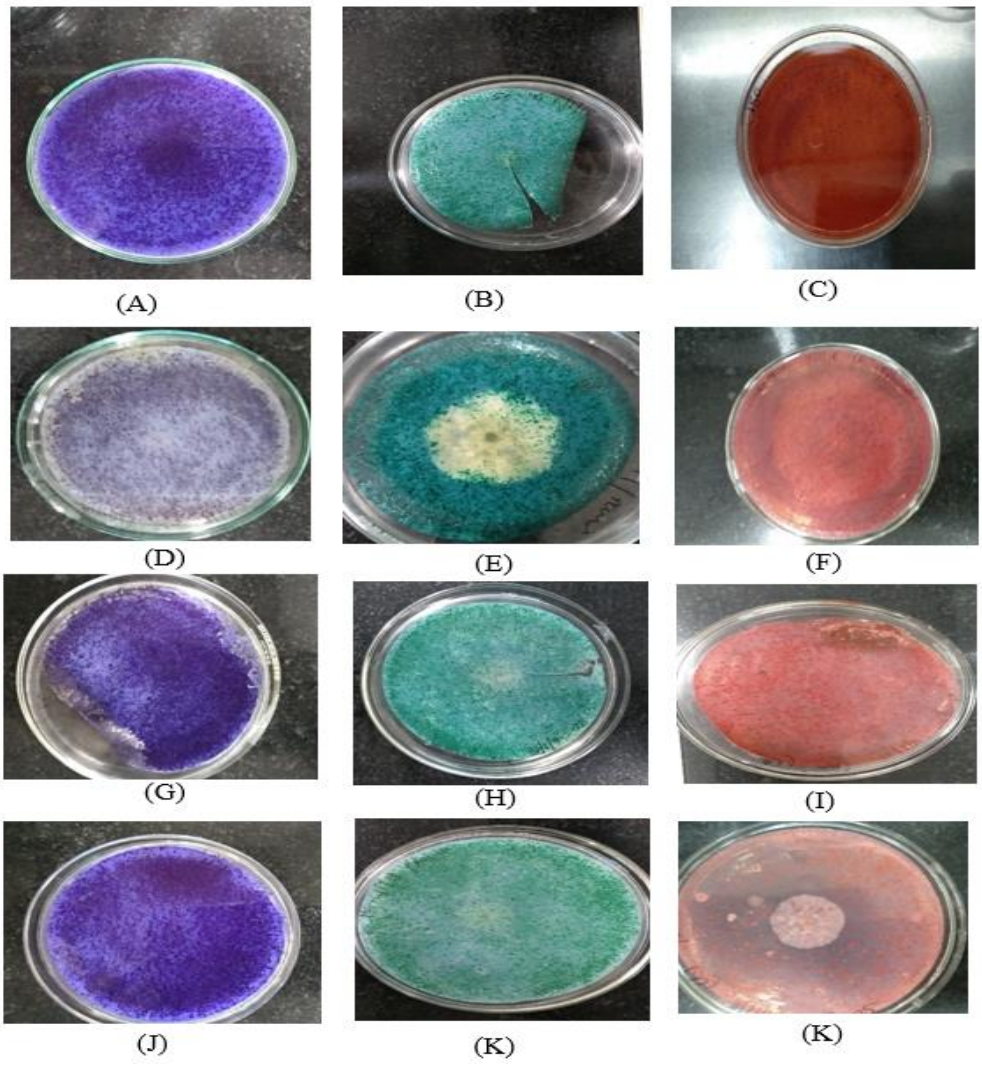

Photograph 2.3: Plate Assay results of the Basidiomycetes isolates obtained from various samples: Base of the plates of isolates for dye decolorization (A-C) of Isolate K4; (D-F) of isolate S4; (G-I) of C4 and (J-K) of S1; A,D,G,J are WB agar plate with Crystal Violet; B,E,H,K are WB with Malachite Green and C,F,I,K are WB agar plates with Congo Red.

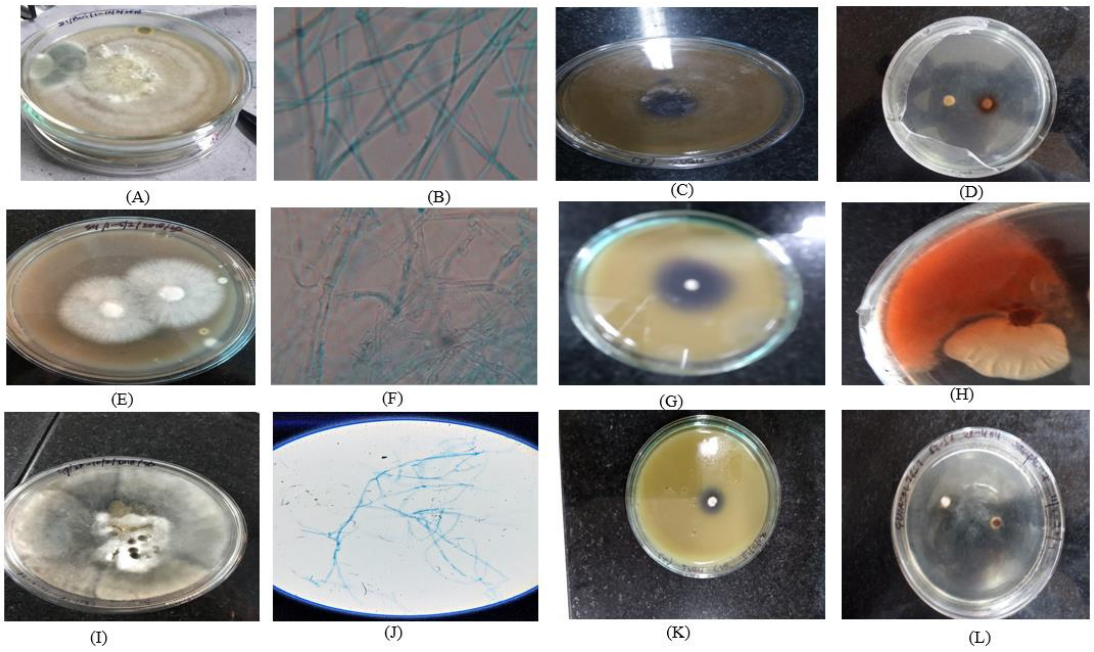

Photograph 2.4: Morphological and cultural characteristics of the isolates : laccase activity on ABTS plate of isolates: (A-D) of S1, (E-H) of isolate S4, (I-L) of isolate C4, A; A, D, F are the growth of isolates S1, S4 and C4; B,D,G are the microscopic view by LPCB staining; C,E,H are the presence of laccase by ABTS plate assay; D,H and L are laccase assay plate of strain S1, S4 and C4 respectively.

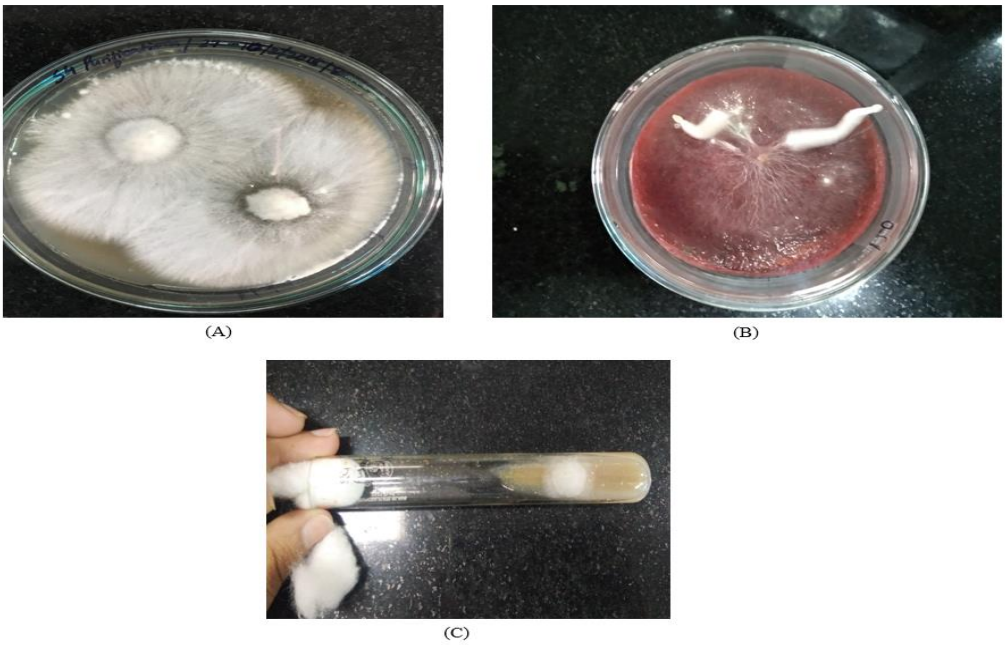

Photograph 2.5: Purification of S4, A-S4 Growth on WB Agar (after 8th day); B-Appearance of Fruiting body after 24days of incubation on dye (CR) incorporated plate; C-Agar slant of S4 isolate (4days).

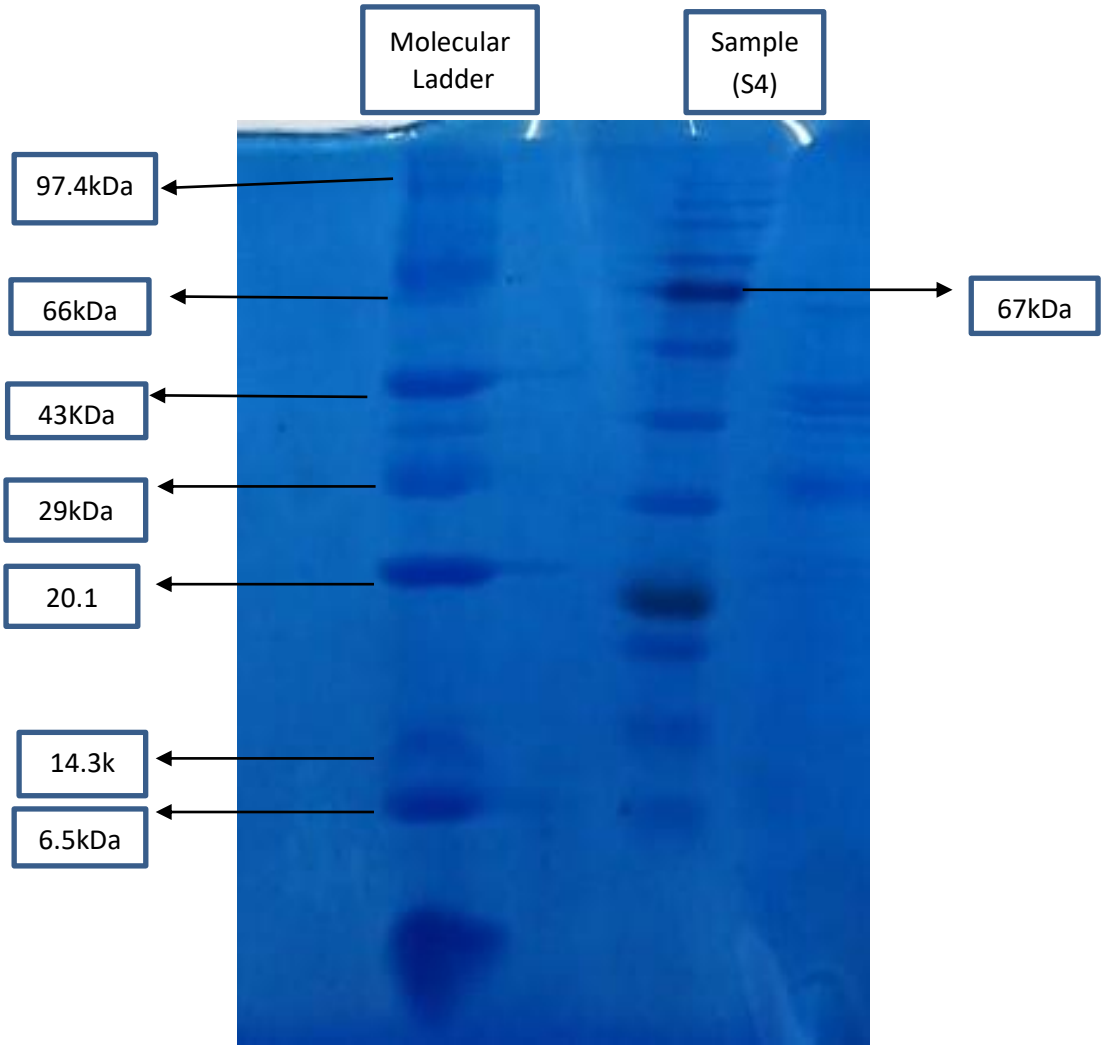

Photograph 2.6: Molecular weight analysis by Sodium Dodecyl Sulphate - Polyacrylamide Gel Electrophoresis (SDS-PAGE) of laccase produced by isolate S4

Chapter 3

Evaluation of wheat bran as a dye adsorbent

3.1 Introduction

Industrial pollution is affected by the scale of industrial activity, its sectoral composition and the technologies employed in the processes for production. The US Environmental Protection Act (EPA) maintains several databases at national level containing information on the environmental performance of regulated facilities across the US (Hettige et al., 1995). The pollution intensity indices were constructed by considering four major sectors, like, the Toxic Release Inventory (TRI), The Aerometric Information Retrieval System, National Pollutant Discharge Elimination System and The Human Health and Ecotoxicity Databases, where the information on the annual release of toxic chemicals to the environment is maintained by TRI (Anonymous 1, 2009). It has been well established the most intensive industrial sectors, in terms of toxic waste release to the output, are industrial chemicals, plastics, paper and metals. The middle-ranked industrial sectors, in the above category, are associated with consumer products such as electrical appliance, textiles and cleaning preparation, followed by high shipment value machine tool industries, with food and drink sectors, being the least intensive (Raymond et al., 1994). The process of establishing and maintaining similar databases in India has been slow. In response to a Writ Petition No. 657, 1995, in October 2003 (Anonymous 2, 2007), the Supreme Court of India passed an order for the preparation of toxic inventory for the generation of hazardous wastes by the state. These data were to be further compiled by the Central Pollution Control Board to pass National Toxic Inventory, ensuring that industries dealing with hazardous wastes prepare database based on the nature and the quantity of the hazardous chemicals being used in the plant, amount of solid wastes generated in the factory premises, and their emission in air and water were to be analyzed (Welch, 2009) to categorize the industries in accordance to the pollutants generated by them. The data was also used up for the development of inventory of each state hazardous waste generating unit produced by each state to quantify the total

amount of hazardous waste generation all over the country, so that necessary corrective measures could be employed to curb down the pollution.

Though industrialization is a key economic development, it is also recognized to be the root cause of environmental pollution. Environmental pollution is thus, a global threat (Paul et al., 2012) for obvious reasons. Conventional chemical-based industries like, printing, pharmaceutics, textiles, etc., are thus priority industries in India too, to bring down environment and health risks associated with them (Garcia et al., 2004). Wastewater from brewery, food and beverages, paper and pulp, palm oil industries, etc., provides a wider variety of industrial wastes, and thus, their disposal problems (Otokunefor et al., 2005; Ijeoma and Achi, 2011) are also more complex. The presence enormous turbidity, chemical oxygen demand (COD), biological oxygen demand (BOD), total suspended solids (TSS), high conductivity, hardness and very high amount microbial nutrients (promote growth of variety of coliforms and other types of microbes) are all important considerations to be made while managing the harmful waste waters (Emongor et al., 2005). These conditions are worsened by occasional discharge of raw sewage, containing heavy metals, polychlorinated biphenyls (PCBs), pesticides, poly aromatic hydrocarbons (PAHs), phenolic compounds and microorganisms (Davis and Gasse, 1988; Vesiland et al., 1990; Botkin and Kelly, 1998; Nubi et al., 2008) through storms, industrial effluent from refineries, petrochemical plants and oil refineries (Phiri et al., 2005), enhancing aquatic pollution. Contamination of air, soil, and water by effluents from the industries is associated with a heavy disease burden (WHO 2002) which could be part of the reasons for shorter life expectancy in the country, currently (WHO 2003) when compared to the developed nations (Yusuff and Sonibare 2004).

The overall aim of this chapter was to use a low cost agro-industrial waste material like wheat bran, for an efficient removal of dyes from their aqueous solution. The representative dyes used were lab grade crystal violet (CV), malachite green (MG), congo red (CR) and industrial grade disperse dark red (DDR) and disperse orange (DO). The physical method of dye removal, by means of adsorption was studied for the evaluation of the variation of the process on the substrate by usage of chemically variant types of dyes.

3.2 Review of Literature

Industrial dyes including, acid dyes like anthraquinone, triphenylmethane, azine, xanthene (Hunger 2003) and basic dyes like cyanine, hemicyanine, diphenylmethane, disperse dyes like azo, nitro, benzodifurane (Anonymous 3, 2019) are often used for acidic dyebaths on substrates like nylon, wool, silk, paper, inks, polyesters acrylic materials, plastic materials in industries like, textile, printing, paper and pulp, food and drug for giving them distinctive colour. In the year 1856, W.H. Perkins discovered the first synthetic dye, mauve. A wide range of colour fastness and bright hues were the characteristics of synthetic dyes (Kant 2012). Coal and tar were used for the preparation of mauve. The vibrant colour created, not only had a tremendous impact on the contemporary fashions but also spurred numerous other scientific discoveries. The advent had led to development of synthetic dyestuff industry leading to the introduction of another very important dye, magenta. That had led the subsequent development of water-soluble azo dyes representing a landmark in the synthetic dye industry (Axelsson et al., 2006). Though synthetic/chemical dyes are considered to be one of the major contributors to environment pollution as well associated with a number of health hazards, yet they offer advantages like, when applied they do not allow the shrinkage of the substrate on which applied, they dry quickly and lasts longer over natural dyes and have wide varieties, that are widely available and cost effective over the natural dyes owing to which, they are still used abundantly in a number of industrial applications.

Synthetic dyes majorly include direct dyes, acid dyes, vat dyes, azoic colour, basic dyes, reactive dyes, disperse dyes and Sulphur dyes (Anonymous 4, 2019). The different kinds of colours that are utilized in the textile business, for instance are, direct, dispersive, reactive, acid and basic dyes (Hunger, 2003). Direct dyes are monoazo, polyazo, benzidine and their derivatives and are used for dying cellulose fibres from aqueous liquor with sodium chloride. For colour fastness they are often mixed with sodium bicarbonate and copper sulphate for warm and cool colours respectively (Gohl and Vilensky 2005). Dispersive dyes are characterized by water insolubility with free ionizing group, with common usage in dying of cellulose diacetate, triacetate and polyester fibres (Chowdhury 2006), while reactive dyes, as per the name, their colourfastness is contributed by their ability to react with the

fibres. Most of their dyeing processes are carried out at boiling temperature. Chemically, they include mono-chlorotriazine, di-chlorotriazine etc. (Hunger 2003). Acid and basic dyes, mostly water-soluble dyes, applied under acidic conditions, as the name implies, mostly used for wool and silk and to a lesser extent on nylon. Whereas basic dyes cyanine, hemicyanine and employed on nylon, polyesters etc., respectively. Different chemical dyes exhibit different levels of environment as well as health hazards. Effluent with dyes flows in water and mix with soil leading to clogging ultimately affecting the soil productivity. They are toxic to aquatic life, may also inhibit the microorganisms existing there. They are also carcinogenic in nature leading to intestinal cancer, cerebral abnormalities, skin irritation, respiratory abnormalities, with various other types of complications (Doble and Kumar 2005)

Azo dye has a wide variety of application in textile materials, articles made of leather, and some may also find their applications in food and medical industries. They have more than one azo bond **[-N=N-]** associated with aromatic structure along with resistance towards the oxidizing agent. Due to mutagenic and carcinogenic effect of azo dye have a significant effect on human health and ecosystem (Yesilada et al., 2006). Anthraquinone dye has fused aromatic structure remain for a long time and wide range of colour (Fontenot et al., 2003). Acid dye is water soluble, and used for dyeing silk, wool and paper, etc. Chromophore of acid dyes includes, (anthraquinone, nitro, azine etc). Acid dye are utilized more in textile for processing and dyeing than in other industries for their colour fastness and can colour nylon and wool mostly (Hunger 2003). They are mainly anionic compound and bind to cationic ions of fibres (Christie 2007). Basic dyes are mainly used for dyeing of silk and wool. These water-soluble cationic dyes are commonly applied to paper, modified nylon, modified polyester and binds to acidic group (Hunger 2003 and Christie 2007). Reactive dyes are water soluble, anionic in nature and mainly used for imparting colour to silk, wool, nylon and leather (Khan and Malik 2014). Reactive dye shows narrow adsorption band and form covalent bonds with fibre. They are characterized by heterocyclic aromatic ring substituted with chlorine or fluoride (Yang et al., 2005). Dispersive dye is water insoluble, and third largest group of dyes mainly used on

polyester, cellulose, nylon and acrylic fibre. They generally contain azo, anthraquinone, nitro and styryl groups (Hunger 2003 and Christie 2007).

The industrial effluents containing synthetic colouring substances are very difficult to treat, as these chemical molecules are resistant to aerobic microbial digestion, breakdown by light, heat, or even oxidizing agents (Sun and Yang 2003; Kumar et al., 1998). Of textile dyes, azo dyes amount to around 60% (Hu and Wu 2001). Methanogenic bacteria help in biodegradation, but the azo functional group or the aryl amine derivatives generated during reductive biotransformation of the azo bond shows toxicity on the organism which inhibits their growth and resistance to biodegradation (Razo-Flores et al., 1997).

These toxicants prompt different medical issues in animals, while hindering the normal functioning of cells, leading to the alteration in physiological and biochemical functions. This results in the impairment in important functions like, respiration, kidney failure, osmoregulation, reproduction, skin allergic responses, prenatal birth defects and other immune & reproductive system related issues, and even mortality (Khan and Malik 2014). Dyes have carcinogenic and mutagenic effects on the human body with about 40 % of the globally used colorants contain organically bound chlorine, a known carcinogen (Acuner and Dilek 2004). Reports have shown that azo or nitro - dyes entering the body by ingestion can be acted upon by azo-reductases or nitro-reductases respectively, produced by the intestinal microorganisms or by the liver enzymes (Umbuzeiro et al., 2005). But, in either of the cases the production of n-hydroxyl amines by reductive cleavage has been reported to damage the DNA of the host exhibiting their carcinogenic property (Arlt et al., 2002; Umbuzeiro et al., 2005).

Consequently, it is necessary to develop vigorous, economically effective, and environment friendly strategies for the removal of these poisonous pollutants discharged in the environment. Various treatment strategies (like, switch assimilation, filtration, coagulation, adsorption, chemical precipitation, evaporation, electroplating, ion exchange, oxidation/reduction, activated sludge, aerobic and anaerobic treatment, electrolysis, magnetic separation, etc.) are being utilized for the removal of industrial pollutants including, dye waste (Bhatnagar and Sillanpaa 2010; Miretzky and Cirelli

2010; Crini 2006), but many of these methods are associated with the limitations of high reagent use & operational and maintenance cost, high voltage requirements and lethal auxiliary sludge development demands, call for evaluating more evolved and effective methods for waste treatment.

Adsorption is efficient for waste-water treatment where, the method is simply used to adsorb and subsequently remove the various toxic organic/inorganic pollutants present in the waste waters (Temesgen et al., 2018; Akar et al., 2018). Adsorption, as a method removal of synthetic dyes from the wastewater, offer a cost effective, at the same time, technologically simple, fast and highly efficient (Crini 2005; Liu et al., 2016; Santos et al., 2016; Zhang 2018) way to mitigate dye pollution.

Various low-cost adsorbents like, rice husk, wheat bran (Zhang et al., 1998; Kapoor et al., 1999) sugarcane bagasse (Aksu et al., 2001), corn cob, cactus leaves (Dakiky et al., 2002), tea waste (Amir et al., 2005), pine needle (Ahalya et al., 2005), saw dust (Yao et al., 2012), soyabean hulls (Abdolali et al., 2014), Sepiolite (Alkan et al., 2004), cross linked-chitosan beads (Chiou et al., 2004), vermiculite (Choi et al., 2004), cultivated clay (Juang et al., 1997), dolomite sorbent (Walker et al., 2003), baggase fly ash (Mall et al., 2006; Chiou et al., 2004), apple pomace and wheat straw (Robinson et al., 2002) and powdered peanut hull (Gong et al., 2005), have been proposed by several researchers to develop adsorption as a sustainable method for the removal of different pollutants from wastewater. The rough surfaces, variously sized pores, and presence of multiple active functional groups on their surfaces, significantly contribute towards their potential as adsorbents (Park et al., 2010) and subsequently as, agents for bioremediation.

It is these important characters of such natural adsorbents, because of which, these are now quickly replacing even other, already known adsorbents like, high cost commercially available activated carbon (Malik et al., 2016), as effective tools for bioremediation purposes. Activated carbon, though are very efficient in removal of taste, odour, micropollutants like, halides from wastewater, drinking water but has been reported to be ineffective for removal of metals nitrates, microorganisms (Amirault et al., 2003).

As highlighted above, lignocellulosic biomass offers a very attractive alternative to the search of efficient adsorbents for alleviating dye pollution. Biochemically, the lignocellulosic materials are the photo mass (Chandra and Madakka 2019) formed as a result of photosynthesis. These are mainly composed of Cellulose (30–50%), a linear polymer of β–D–glucopyranose sugar units, with an average polymer chain of 9,000 to 10,000 units. Around 65% of the cellulose is densely arranged with crystalline structure with no accessibility to water and other solvents, while the rest, consists of less oriented chains bound to the hemicellulose (20–40%) and lignin (15–25%) fractions of the biomass (Asadi et al., 2008). The sub- atomic structure of cellulose provides a range of characteristics like hydrophilicity, degradability and chirality subsequently, due to the fractional availability of polysaccharide to water and various solvents. The chemical reactivity is firmly a component of the high donor reactivity of the hydroxyl (-OH) group in cellulose particle (Acemioglu and Alma 2001). The hemicelluloses with lesser degree of polymerization, in comparison to cellulose, include non-crystalline polysaccharide polymers. They vary in their structure as well as in polymer organization depending on the source (Iqbal et al., 213). Lignin is an extremely branched non-crystalline polymer and is made up of 9 carbon units derived from substituted cinnamyl alcohol, derived from the source (Iqbal et al., 213). Additionally, water, cyclic hydrocarbons, organic and inorganic materials, ash and extractives, are also present in the lignocellulosic biomass, with their content variable in different plant sources (Cagnon et al., 2009; Connell et al., 2008). The chemical composition of some common lignocellulosic materials is given in Table 3.1.

Type	Cellulose	Hemi-cellulose	Lignin	Ash	Silica
Wheat straw	30–35	26–32	16–21	4.5–9	3–7
Barley straw	30–35	24-29	14-15	5-7	3-6
Rice straw	25–35	20-30	10-15	15-20	9-15
Sugarcane bagasse	32-44	25-35	19-24	1.5-5	<4
Corncob	35-45	5-15	35-45	1-2	<1
Cotton waste	80–95	5-20	-	<1	-
Olive stone	30-35	20-30	20–25	<1	5-9
Nut shell and stone	25–35	25-30	30-40	-	-

Table 3.1: Chemical composition of some common lignocellulosic materials (Adapted from Abdolali, et al, 2014).

Promising adsorption capacity (Table 3.2) are some important legitimate attributes of lignocellulosic waste materials that make them one of the ideal candidates to be used as sorbents in environment dye pollution control.

Furthermore, to enhance the adsorptive ability of such materials, functional group potential and number of active sites on their surfaces, can be improved by some pre-treatment methods. These include, usage of different kinds of modifying agents (Ngah and Hanafiah 2008; Bhatnagar and Sillanpaa 2010). These include, organic and mineral acids (HNO_3, HCl, H_2SO_4, acetic acid, citric acid and formic acid), bases and basic solutions (NaOH, Na_2CO_3, $CaCl_2$ and $Ca(OH)_2$), oxidizing agents (H_2O_2 and K_2MnO_4) and many other chemical compounds (formaldehyde, glutaraldehyde, CH_3OH and epichlorohydrin).

Adsorbent	**Dye**	**q_m (mg/g)**	**Sources**
Bagasse	Acid blue 25 Basic red 22	674 942	Juang, et al., 2002 Juang ,et al., 2002
Corncob	Acid blue 25	1060	Juang, et al., 2002
Pinewood	Acid blue 264	1176	Tseng, et al., 2003
Rice husk	Basic green 4	511	Guo, et al., 2003
Mahogany sawdust	Acid yellow 36	183.8	Malik, 2003
Straw	Basic blue 9	19.82	Kannan and Sundaram, 2001
Rice husk	Acid yellow 36	86.9	Malik, 2003
Sugarcane bagasse	Acid orange 10 Crystal violet	5.78 10.44	Tsai, et al., 2001 Parab, et al., 2009
Almond shell	Direct red 80	90.09	Ardejani, et al., 2008
Orange peel	Acid violet	19.88	Rajeswari, et al., 2001
Coir pith	Congo red	2.6	Namasivayam and Kavitha, 2002
Maize cob	Acid blue 25	41.4	Geundi and Aly, 1992
Hazelnut shell	Acid blue 25	60.2	Ferrero, 2007
Wheat bran	Crystal violet	80.37	Wang, et al., 2008
Coffee husk	Methylene blue	90.1	Oliviera, et al., 2008
Tree fern	Basic Red 13	408	Ho, et al., 2005
Japonica	Crystal violet	82.83	Wang, et al., 2008
Pineapple leaf powder	Crystal violet	78.22	Chakraborty, et al., 2012
Peanut hull	Methylene blue	68.06	Gong, et al., 2005
***q_m: Maximum adsorption capacity**			

Table 3.2: Adsorption capacities of some agro- industrial by-products (*Adapted from* Johnson et al., 2008)

Wheat bran is one of the most promising low-cost lignocellulosic biosorbents (Singh et al., 2011). It is being used in certain industrial applications like, in baking industry, because of its nutrient richness (Onipe et al., 2016) for dietary benefits, and hence, a

large amount of the same can be successfully made available for bioremediation processes with the help of microorganisms.

Wheat bran is the outer multi-layered shell of wheat seed and is a by-product of milling. Second to rice, as food crop, different varieties of wheat are cultivated worldwide, with *Triticum aestivum vulgare* and *Triticum turgidum durum* varieties as the most important, commercially (Macrae et al., 1993). The bran fraction consists of the pericarp, testa, hyaline and aleurone layers. The conventional milling of wheat grains separates the endosperm (which produces the white flour when milled) from the embryo and the bran layers (Figure 3.1). The bran fraction is formed after the removal of aleurone cells, along with the other bran layer, and the embryo (Stevenson et al., 2012). The hyaline layer is composed mainly of poorly cross-linked arabinoxylans (Barron et al., 2007). 50% bran is represented by aleurone layer and is composed of thick cell walls enclosing intracellular compounds which are rich in vitamins, minerals, and antioxidant compounds. Aleurone cell walls contain 29% β-glucans and 65% relatively linear arabinoxylan, with high amounts of esterified ferulic acid monomer (Rhodes et al., 2002). Wheat bran comprises of 12% H_2O, 13-18% protein, 3.5% fat, 56% carbohydrates and 59-60% phenolic acid and minor amount of minerals (Singer et al., 2013).

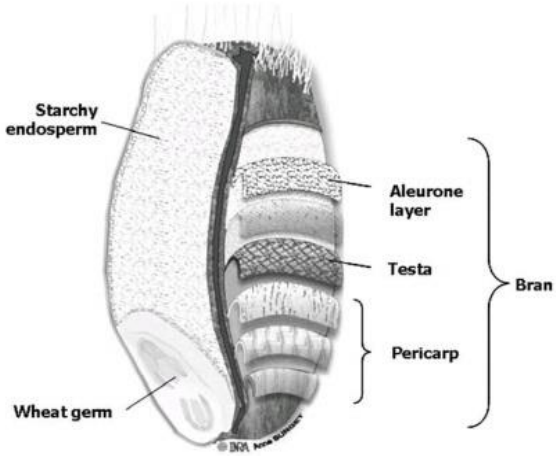

Photograph 3.1: Wheat kernel with constitutive layers of wheat bran (Adapted from Hemery et al., 2009).

Dielectric spectroscopy investigations (Antoine et al., 2004) have demonstrated that the structural and functional differences between the different bran layers correspond to different physical properties. However, the charge on the wheat bran depends on the cell wall i.e., branched or cross-linked versus linear. Pericarp is composed of negatively charged particles, while aleurone comprises of positively charged particles mainly due to the presence of ferulic acid (Hemery et al., 2009). Studies indicate high adsorption rate of wastewaters on wheat bran and the fact that it can be cheaply and locally made available for use in treatment of wastewaters, makes it an attractive biosorbent (Zhang et al., 2017).

The dyes used in this study are Crystal Violet (CV, basic dye), Malachite Green (MG, basic dye), Congo Red (CR, azo dye), Disperse Dark Red (DDR, reactive azo dye) disperse orange (DO, reactive azo dye), with variable chemical properties, as highlighted below (Table 3.3).

Crystal violet, or gentian violet, is used for dyeing of cotton and silk, staining biological specimens, and is also an active component in Gram stain (Anonymous 5, 2019)**.** CV is highly carcinogenic and mutagenic to mammalian cell, cause skin irritation and also can lead to kidney failure (Saha et al., 2013). Congo red is water soluble benzidine based azo dye and is mainly used for staining in amyloids and in textile, paper etc. (Hunger 2003) but has a complex structure and exhibit carcinogenicity (Li et al., 2016)**.** Malachite green is N–methylated di-aminotriphenyl methane dye, used for colouring, and as an antifungal agent in fish farming industry (Hunger 2003). Malachite green is highly toxic to humans affecting immune and reproductive system and is even banned in several countries (Youssef et al., 2008). Unfortunately, it is still used in India extensively for dying cotton, wool, leather, jute as well as an antiseptic (Anonymous 6, 2019). Disperse Orange is chemically either azo or anthraquinone dyes. In addition to colouring synthetic fibres, azo compounds have been used in hair dyes, fur dyes, leather processing, printer's ink and photographic products (Hunger 2003). At the same time, it is a well-known cause of allergic contact dermatitis which may be due to the dye itself, or because of its metabolic products (Goon et al., 2003). Disperse Dark Red is an azo dye, characterized by the presence of one or more azo groups (-=N-) and represent up to

70% of the amount of dyestuffs consumed in industrial applications (Hunger 2003). Their toxic properties are related to the nature and position of the substituents with respect to the aromatic rings and amino nitrogen atom (Ferraz et al., 2011).

Name of dye	**Characteristics**			**Reference**
	λ_{max} (nm)	**Solubility**	**Chemical structure**	
Congo red	497	In water	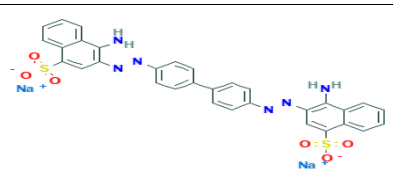	Lavanya et al., 2014
Crystal violet	590	In water	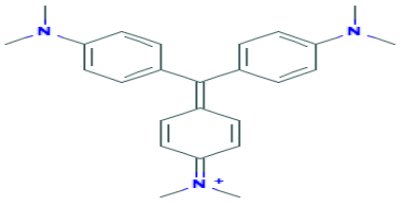	Selvapandi et al., 2015
Disperse orange	420	In water	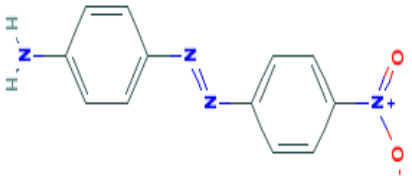	Sharma et al., 2013
Disperse dark red	520	In water	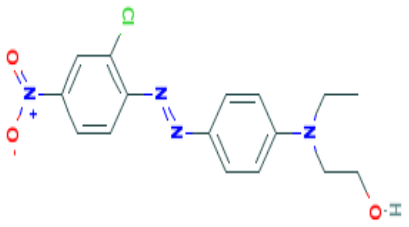	Sharma et al., 2013
Malachite green	**616**	In water	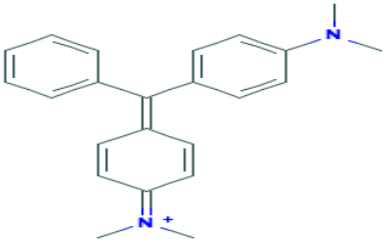	Ram et al., 2013

Table 3.3: Major chemicals characteristics of selected industrial dyes (Adapted from Anonymous 7, 2019*)*

3.3 Material and Methods

3.3.1 Materials

All the chemicals and reagents were of analytical grade and purchased from HiMedia, Bangalore, India and Genei, Delhi, India. Pure Crystal violet, CV ($C_{25}N_3H_{30}Cl$), Malachite Green, MG ($C_{23}H_{25}ClN_2$), Congo Red, CR ($C_{32}H_{22}N_6Na_2O_6S_2$), Disperse Dark Red, DDR ($C_{20}H_{13}NO_4$), Disperse Orange, DO ($C_{18}H_{14}N_4O_2$) was procured from Loba Chemi, Mumbai, India.

3.3.2 Methods

3.3.2.1 Pre-processing of adsorbent

Wheat bran (WB) was obtained from local market of Cantonment area, Jalandhar, Punjab, India. The bran was processed and preserved in the same manner as it has been described in chapter 2 (Alzeydien 2015).

3.3.2.2 Batch Adsorption Studies

3.3.2.2.1 Effect of pH on percent dye decolorization by test adsorbent

Batch adsorption experiment was carried out in 100 ml conical flask with 20 ml working volume of 100 mg/L of aqueous solution of CV, MG, CR, DDR and DO. A weighed amount (200 mg), at a concentration of 10 gm/L, of biosorbent was added to the solution. The flasks were kept under static condition, in the incubator at varying the initial pH (2, 3, 4, 5, 6, 7, 8, 9, 10, 11, 12) of the aqueous dye solution at temperature of 30 °C for 180 mins to study effect of pH on the adsorption capacity of wheat bran. The pH was adjusted by 0.1M NaOH and 0.1M HCl and measured by using a pH meter (VLab). After 3 hrs (180 mins), 2ml of samples were dispensed out in microcentrifuge tubes, centrifuged for 15 min at 5000 rpm. The supernatant was collected, residual concentration of test dye was spectrophotometrically determined at 582 nm (Akazdam et al., 2017) by using a UV/Vis double beamed spectrophotometer (Shimadzu- 1800). The standard curve for crystal violet, malachite green, congo red, disperse dark red, disperse orange was plotted using dilutions (10-130 mg/L) of a 1000 mg/L stock solution, at 582 nm, 616 nm, 497 nm, 520 nm, 420 nm wavelength. The curve was used to calculate change in dye concentration after the adsorption on adsorbent (Selvapandiyan 2015). The amount of dye adsorbed per unit WB (mg dye/gm adsorbent) was calculated according to a mass balance (state of equilibrium, a condition beyond which no further adsorption can take place on the provided adsorbent) on the dye concentration using Eq. (1) (Zhu et al., 2008):

$$\mathbf{q_e} = \frac{(\mathbf{C_0} - \mathbf{C_e})\,\mathbf{V}}{\mathbf{W}} \qquad \text{(Eq.1)}$$

Where C_0 and C_e (mg/L) are the concentrations of initial adsorbate and at equilibrium respectively. V is the volume of the sample (mL) and W is the mass of the adsorbent used. The % decolorization of the dye was calculated using the following Eq. (2.):

$$\textbf{\% decolorization} = [\mathbf{D_0} - \mathbf{De} \,/\, \mathbf{D_0}] \times \mathbf{100} \qquad \text{(Eq.2.)}$$

Whereby, D_o = Initial absorbance of dye solution and D_e = Final absorbance of dye solution

3.3.2.2.2 Effect of Adsorbate concentration and Incubation Time on percent dye decolorization

The influence of adsorbate concentration (10, 20, 30, 40, 50, 60, 70, 80, 90, 100, 110, 130 mg/L) and adsorbate-adsorbent contact time (30, 60, 90, 120,150, 180, 210, 240 mins) on adsorption equilibrium was investigated at temperature of 30 °C at under optimized pH for all the 5 dyes (CV, MG, CR, DDR and DO). The residual dye concentration was determined, spectrophotometrically at 582, 616, 497, 520, 420 (nm) wavelength (Akazdam et al., 2017) as already explained. The dyes adsorbed per unit WB and percent decolorization was calculated by using the above formulae respectively.

3.3.2.2.3 Effect of adsorbent dosage on percent dye decolorization

Variable concentration (2,4,6,8,10,12,14 gm/L) of adsorbent were suspended in optimized aqueous solution of adsorbate (CV, MG, CR, DDR and DO) at an optimized pH and incubation time, at 30 °C and the residual dye concentration was determined spectrophotometrically for the calculation of dye per unit WB and decolorization percent on the basis of the above mentioned formulae (Akazdam et al., 2017).

3.3.2.2.4 Effect of Temperature on percent dye decolorization

The effect of temperature (25°, 30°, 35°, 40°, 45°, 50°, 55°, 60°, 65°, 70 °C) on equilibrium was evaluated by suspending WB in aqueous solution of CV, MG, CR, DDR, DO maintained at optimum pH for optimized incubation time. The residual dye

concentration and percent decolorization were estimated by using above mentioned formulae (Akazdam et al., 2017).

3.3.2.2.5 Effect of Chemical Modification of WB on percent decolorization

25 gm of the bran was added to 250 mL of 0.4 mol/L Citric Acid and the mixture was dried for 2 hr at 50° C. The mixture was centrifuged (4000 rpm) and the leftover solid-phase material was dried at 70°C for 6 hrs before it was grounded. Next, the material was esterified in presence of ethanol at 120°C for 3 hrs. Further, the acid-functionalized wheat bran (AMWB) was washed repeatedly with 0.05 M $NaHCO_3$ (Hariharan and Nambisan 2012; Feng et al., 2017), followed by washing with deionized water before being grounded and finally stored in dark coloured glass containers for further usage.

Similarly, 25 gms of pre-processed bran was mixed with 5% NaOH solution and autoclaved at 15 psi for 15 minutes. Further, the bran was separated from the solution by filtration, and washed thoroughly with distilled water, until the pH of the filtered alkali solution was close to neutral. After drying at 70°C for 6 hrs, the treated WB (ALMWB) was stored in dark coloured bottles for its further usage (Chowdhury et al., 2013).

200 mg of adsorbent, each of acid-modified, alkali-modified and unmodified wheat bran was dispensed in 100 mg/L aqueous solution of test dyes (CV,MG,CR,DDR and DO), incubated under optimized conditions of incubation time, temperature, pH, adsorbent and adsorbate dosage (Alzeydien 2008). Subsequently, the residual dye concentration (of each dye) was determined spectrophotometrically for the determination of dye per unit WB and percent decolorization by applying the above formulae for each dye (Djilali 2012; Akazdam et al., 2017).

3.3.2.3 Adsorption Isotherm studies

Adsorption isotherms were plotted by fitting the equilibrium data to the Langmuir and Freundlich (Bulut et al., 2007) isotherms. It was done by a graphical representation showing the relationship between the amount adsorbed by unit weight of adsorbent (10 gm/L) and the amount of adsorbate remaining in a test medium at equilibrium, with different initial concentration (60-120 mg/L), at a temperature of 30°C for CV, MG and CR, respectively and 40 and 45 ºC for DDR and DO, respectively with initial

pH 8, 11, 4, 5, 5 for CV, MG, CR, DDR and DO respectively to show the distribution of adsorbate solute between the liquid and the solid phase.

The empirical model of adsorption is either given by Langmuir isotherm model, which assumes that the adsorption can occur only at definite localized sites and at a finite number. The non-linear expression of the model is given by the following equation (Eq.3) (Zhu et al., 2008).

$$q_e = q_m k_L \frac{C_e}{1+k_L C_e} \quad \text{(Eq.3)}$$

Where, C_e is the concentration of the dye solution at equilibrium (mg/L); q_e is the corresponding adsorption capacity (mg/g); q_m (mg/g) and k_l (l/mg) are constants related to adsorption capacity and energy or net enthalpy of adsorption, respectively.

Or given by the Freundlich isotherm model which describes the non-ideal and reversible adsorption, one of the most-earliest relationship known. Based on assumption, it can be applied to multilayer adsorption concerning surface energetic heterogeneity. The non-linear expression of this type of isotherm can be illustrated by the following equation (Eq.4) (Freundlich, 1906):

$$q_e = k_f C_e^{1/n} \quad \text{(Eq.4)}$$

where k_f and n are the constants, which measure the adsorption capacity and intensity; respectively. The sustainability and applicability of the isotherm equation to the equilibrium were compared by judging the values of the correlation coefficients, R^2 and normalized standard deviation. The non-linear graph was plotted using Microsoft excel for the determination of isotherm.

3.3.2.4 Batch Kinetic studies

This study is like that of the batch adsorption studies, the only difference being in this case the adsorbent - adsorbate solution was taken at predetermined time intervals to measure the concentration of the solutions. The amount of adsorption (q_t) at time 't' was calculated using the following formula, Eq. 5. (Zhou et al., 2012):

$$q_t = \frac{(C_0 - C_t)V}{W} \quad \text{(Eq.5)}$$

Where, C_0 and C_t (mg/L) are concentrations in liquid phase of the adsorbate at the initial and any time 't', respectively. V is the volume of the solution and W is the mass of the adsorbent used. By using pseudo- first and second order models the adsorption kinetics of crystal violet on the adsorbent (wheat bran) was investigated.

3.3.2.4.1 Pseudo First-order kinetic model

The pseudo first order kinetic model is generally expressed as follows (Ho and Mackay 1998):

$$l_n(q_e - q_t) = ln\, q_e - k_1 t \quad \text{(Eq.6)}$$

where the amount of adsorbed adsorbate is q_e, at equilibrium, (mg/g), q_t, is the amount of solute adsorbed per unit weight of the adsorbent at time, (mg/g), k_1 , is the rate constant of the pseudo first order sorption (1/h), a plot of ln ($q_e - q_t$) versus t gives a straight line with k_1 as slope and lnq_e as an intercept (Eq. 6).

3.3.2.4.2 Pseudo second- order kinetic model

The kinetic model of pseudo second order equation can be expressed as (Ho and Mackay 1998):

$$\frac{t}{q_t} = \frac{1}{k_2 q_e^2} + \frac{1}{q_e} t \quad \text{(Eq.7)}$$

$1/q_e$ and 1/h is obtained as the slope and intercept, respectively, of the linear plot of t/q_e versus t (Eq. 7).

3.3.2.5 Spectroscopic analysis of active functional groups

The structure and compositional information of the proximate functional groups present on WB, dye (CV, MG, CR, DDR and DO) adsorbed WB and chemically modified (Acid and alkali treated) wheat bran (AMWB and ALMWB, respectively) were analyzed by using Fourier Transfer Infrared (FTIR) spectra. The spectra were recorded by spectroscopy (FTIR model 8400S Shimadzu) in the range using potassium bromide (KBr) disc containing 1% of finely grounded samples (WB, AMWB, ALMWB, dye adsorbed WB, dye adsorbed AMWB and ALMWB). The

mixture was pressed into KBr wafer under vacuum condition and was used for IR studies in the range of 4000-500cm^{-1} (Fisal et al., 2013).

3.3.2.6 Statistical Analysis

All the experiments have been performed in triplicates. The mean values of the observed data have been presented and standard deviation (± SD) was calculated. The entire calculation was done by using Microsoft Office (version 10) Excel, 2010.

3.4 Result and Discussion

3.4.1 Batch Adsorption Studies

3.4.1.1 Effect of pH on percent dye decolorization by test adsorbent

The test adsorbent (WB) has shown the maximum percent of dye decolorization at a pH of 8 in case of CV; 11, in case of MG; 4 in case of CR and at 5, both for DDR and DO. The Table 3.4; Graph 3.1 reveals a gradual increase in removal of CV reaching to the maximum pH, 8 with a removal of 87.7%. In case of MG, the maximum percent of decolorization (95%), was shown at pH 11 (Table 3.4; Figure 3.1), the result is like that of removal of CV with respect to the alkalinity range of pH as in case of CV. At a pH 8 in case of MG, if compared, the adsorbent had led to the decolorization of around 90%, eventually with an increase of pH, it increases to the maximum of 94.98 % at 11 and then it goes down. In case of Congo Red (CR), a sodium salt of sulphonic acid, an azo dye, WB has shown 87% decolorization at a pH 4 (Table 3.4; Figure 3.1). DDR and DO, the other two industrial azo dyes were decolorized by WB by around 91 and 92% at a pH 5 respectively with the same initial concentration of dyes (100 mg/L) (Table 3.3; Figure 3.1). Thereby, showing that the azo-grouped dyes have decolorized at an acidic pH in comparison to basic dyes.

As pH affects both the degree of ionization of the dye as well as the surface properties of the adsorbent, hydrogen ions affect the surface charge of the adsorbents and the adsorbate species. The sorption is greatly affected by the variation of solution pH (Akazdam et al., 2017). The point of zero charge (pH pzc) is also an important factor for the determination of the linear range of pH sensitivity indicating the type of surface-active centres and the ability of the surface to adsorb (Silva et al., 2004). A decrease by 1% was observed in percent decolorization of CV on increase of pH from 8 to 9. Though contradictory to our study another study has reported, maximum percent decolorization of CV on a substrate at a pH 11.0 (Selvapandian et al., 2015). Similarly, another study has revealed that with an increase in pH from 3 to 9, the adsorptive capacity of a substrate increased for the removal of CV (Madhavakrishnan et al., 2009). With respect to MG, a study has revealed that the maximum adsorption of MG was attained at a pH range of 7-9 (i.e. an alkaline pH), with around 90% of dye removal on wheat bran, as an adsorbent. It has also been stated that pH greatly influences the adsorption capacity along with the colour intensity of a specific dye

(Papinutti et al., 2006). A study on evaluation of various parameters for adsorption of CR on palm, pine and olive, as different adsorbents, by using Taguchi method, has shown that at pH 6.2, 6.7 and 6.7 respectively, a good percentage of removal of CR on such adsorbents were observed, with olive to be the best out of the three with around 95 % of dye removal (Berkane et al., 2019). In a similar study, the effect of pH on adsorption of reactive dyes like RB19 (Reactive Blue), RR195 (Reactive Red), RY145 (Reactive Yellow), on wheat bran has shown a decrease in adsorption with increase in pH, with an optimum pH to be 1.0 (Cicek et al., 2006; Malik 2004). Reactive and acidic dyes have anionic characters, with a higher uptake values under lower pH by the adsorbents, which may be due to electrostatic attractions between negatively charged dye anions and positively charged wheat bran surface. A negatively charged surface site on the adsorbent on the other hand does not favour the adsorption of dye anions due to electrostatic repulsion (Cicek et al., 2006; Malik 2004).

3.4.1.2 Effect of Adsorbate concentration and Incubation Time on percent dye decolorization

The effect of initial adsorbate concentration (Table 3.5; Figure 3.2) was determined, where the highest (87.9%) decolorization of CV occurred on 100 mg/L adsorbate concentration after an incubation period of 180 mins at 10 gm/L concentration of wheat bran at a temperature of 30 ºC. This may be due availability of larger surface area at the beginning for the adsorption (Alzaydien 2015). With increase in contact time, the percentage removal increases, and it remains constant after 180mins, showing reaching of equilibrium for different initial concentrations of CV, with 100 mg/L concentration showing 88% dye removal. The adsorption and desorption occur simultaneously for which equilibrium reaches after an appropriate time, which may be attributed by the composition of the wheat bran (Ata et al., 2012). A concentration of 2 gm/L for pearl millet, lead to a decrease in removal of CV from 80% to 71%, dye concentration increased from 15-50 mg/L, with equilibrium within 3 hr 30 mins (Selvapandiyan et al., 2015), as also similar to the current investigation where, 10% decrease in the CV removal percentage with increase in dye concentration from 100 to 110 mg/L. Another study highlights equilibrium of CV adsorption on tamarind seed powder at around 50 mins with 75.4% removal of the dye (Karthik et al., 2019).

In case of MG, the maximum of 95% removal was observed of 110 mg/L concentration of dye at a pH 10 after 210 mins on 10 gm/L of adsorbent. If compared with CR, its maximum adsorption or percent removal of dye (97%) was obtained after 210 mins of exposure at a pH 4 with 100 mg/L of dye on 10 gm/L of adsorbent while as mentioned above, exhibiting a decrease in the percent removal with increase in the dye concentration and remaining constant with the increase of time with same concentration of dye.

On the other hand, DDR, inspite of being an azo dye, has shown a maximum percent of dye removal (91%) after 180 mins of 100 mg/L initial dye concentration on the same, 10 gm/L concentration of adsorbent (WB). Though a decrease in the percent decolorization of dye was observed with increase in dye concentration but with higher concentration of adsorbate, a very slow increase in the dye decolorization was observed with increase in time which may be contributed by the fact that increase in adsorption of dyes with increase in dye concentration is observed. It has been shown that when the initial dye concentration is increased, the dye adsorption per unit mass of the adsorbent has also increased, demonstrating increase or decrease of dye adsorption depends upon initial dye concentration (Namasivayam et al., 1996; Markandeya and Mohan 2017). The next, industrial grade, azo dye, DO, has given the maximum percent of dye removal (92%) on 10 gm/L concentration of adsorbate, at an initial pH and dye concentration of 5 and 100 mg/L respectively for an incubation period of 180 mins. DO has exhibited a sharp decrease in percent removal with increase in dye concentration and a very slow progress of dye removal with increase in concentration as well as with an increase in time, which may be a consequence of accumulation of dye ions which decreases the total surface area of the adsorbent particles available for adsorption of dyes (Gong et al., 2007; Markandeya and Mohan 2017).

In another study conducted with RB19 (Reactive Blue19), RB195 (Reactive Blue195) and RY145 (Reactive Yellow145), on the other hand has exhibited establishment of equilibrium within 300 mins. The study concluded that the duration for reaching equilibrium was independent of initial dye concentration, as well as of the dye species. The contact time is very significant for wastewater treatment by adsorption

(Mall et al., 2006). For strong chemical bonding of adsorbate with adsorbent requires a longer contact time for the attainment of equilibrium. Our study has also shown that with the increase of dye concentration from 100-150 mg/L the adsorption capacity (mg/gm) had increased on a 1gm/L concentration of adsorbent but beyond which saturation of adsorption was observed (Cicek et al., 2006).

3.4.1.3 Effect of adsorbent dosage on percent dye decolorization

The effect of adsorbent dose (Table 3.6; Figure 3.3) was studied at 30 ºC with the initial dye concentration of 100 mg/L. As the adsorbent dose increased from 2-4 mg/L, an abrupt increase in dye removal was observed from 28-64%, followed by a gradual increase upto of 88% dye removal with adsorbent dose of 12 mg/L in case of CV. Beyond this, no significant change in the adsorption occurred. In case of MG, CR, DDR and DO, maximum adsorption has been exhibited with 12 gm/L, with dye decolorization percentage 96, 97, 93 and 93 % respectively, the adsorbent beyond which has shown a saturation. This might be because of over-crowding by the adsorbent particles which had led to the overlapping of the sites for adsorption (Namasivayam et al., 1998). The initial rapid increase in the percent dye removal with an increase in the adsorbent dose might be attributed to the availability of surface area with higher concentration of the adsorbent. Though the adsorbent best adsorbed all the test dyes (CV,MG,CR,DDR and DO) at a concentration of 12 gm/L at 30ºC, respectively, yet, the adsorptive ability at 12 gm/L was only marginally better with lesser adsorbent dose of 10 gm/L, which was only 0.18, 1.41, 0.3, 1.9 and 0.74 % of variation for CV, MG, CR, DDR and DO respectively. Thus, for further experimentation 10 gm/L and not 12 gm/L of adsorbent dose was taken into consideration. Thereby to reduce the cost of adsorbent and to propose a cost-effective concentration, 10 gm/L was taken as an optimum concentration for getting maximum percent of decolorization. A study has revealed similar type of observations where, CV on *Lysiloma latisiliquum* seed powder, showed an increase in dye removal from 60-85% with an increasing adsorbent dose (0.5- 2.5 gm/L) (Karthik et al., 2019). The Figure 3.3 depicts that the maximum removal of dye was obtained in 12 gm/L dose of adsorbent showing the fluctuation to be a consequence of an increase in the no. of possible active sites and surface region of the adsorbent. One finding indicates that percentage of CV adsorption on WB, determined by adsorption capacity, is within a

specific range of initial concentration of CV. Similar study has revealed that the adsorption yield of WB of few reactive dyes (RB 19, RR 195, RY145) increased with increasing adsorbent dosage while the adsorbed dye amount per unit adsorbent weight decreased by increasing adsorbent dosage from 0.5 to 3 gm. At higher WB to solute concentration ratios, a very fast superficial sorption onto the adsorbent surface takes place that produces a lower concentration of solute in the solution than during the lower concentration of adsorbent to solute. Increase in adsorption yield at low dosage of adsorbent can be explained by the availability of more adsorption sites. The decrease in the amount may be due to the splitting effect of concentration gradient (flux) between the adsorbate and the adsorbent with an increase in adsorbent dosage causing a decrease in the amount of dye adsorbed onto unit weight of the adsorbent (Vadivellan and Kumar 2005). Again, the adsorption capacity comes from the increase in number of available adsorption sites that allows the binding of a greater number of dye molecules onto the surface of adsorbent (Gong et al., 2007). Again with respect to time the rate of adsorption is high due to the adsorption of dye molecules on the upper surface, which decrease as the dye penetrates into the inner porous structure of the palm ash (Ahmad et al., 2007) could justify the result obtained in present study.

3.4.1.4 Effect of Temperature on percent dye decolorization

Under specific incubation conditions, temperature was found to influence dye adsorption as well, when 87.9% CV removal by WB was seen at 30°C incubation temperature. Interestingly, the adsorptive ability was similar even at higher temperatures of 35°C (87.12% dye removal) and 40°C (86% dye removal), with a sharp drop beyond 40°C incubation temperature (Table 3.7; Figure 3.4). MG, 30 ºC, 95.10%; CR, 35 ºC, 97.08%; DDR, 40 ºC, 93.45 %; DO, 35 ºC, 92.49%. A previous study has revealed that with an increase in the temperature from 20-50ºC an increase in adsorption has been observed of reactive dyes (RB 19, RR 195, RY145), exhibiting an endothermic process to have occurred. In general, with an increase in temperature, diffusivity of dye ions increases consequently resulting in the increase of adsorption rate, if diffusion is the rate controlling step (Benguella and Benaissa 2002).

3.4.2 Effect of Chemical Modification of WB on its dye adsorptive ability

Influence of acid and alkali modification of WB was studied to compare the effect of chemical modification of wheat bran with the unmodified sorbent (Table 3.8; Figure 3.5). Under static conditions, at a temperature of 30°C, initial pH of 8 for a period of 180 mins, alkali-modified wheat bran (ALMBW) yielded 92% of CV removal in comparison to unmodified WB (88%). In contrast, acid-modified WB (AMBW) (83%) did not perform better than unmodified WB. In case of MG, alkali modification (ALMWB) also has shown a better result with 98% removal in comparison to acid modified bran (AMWB) (90%) but, unmodified wheat bran, in comparison to AMWB has also shown a better result with 95% removal in contrast to a behaviour of acid modified adsorbent in case of CV. Generally, both the basic dyes (CV and MG) have exhibited better result on ALMWB in comparison to AMWB. All azo dyes, CR, DDR and DO, on the other hand were better removed with a dye removal percentage around 99, 95 and 96 % respectively, on AMWB in comparison to ALMWB. But the study has shown a comparable result with unmodified WB which exhibited a decrease by 1.56, 1.92 and 2.93 % compared to AMWB. The percentage of DO removal on AMWB and MG removal on ALMWB has thereby shown the best results, in comparison to unmodified WB. The carboxyl groups in acid modified WB is believed to be primarily responsible for the adsorption of the basic dyes (Hashemian et al., 2008). Inferior performance of acid-modified bran, in comparison to both alkali-modified as well as unmodified bran, is inherently expected to be contributed to proton, which most importantly influences at low pH, and can consequently compete with cationic dyes for surface sites. Adsorption of methylene blue on papaya seeds has shown that adsorption was minimum at pH 3.0, with increase in dye removal up to a pH of 4.0, after which, it remained constant (Hameeda and Khaiary 2008; Djilali et al., 2012) showing a difference of 1 unit of pH has increased an increase in dye removal, though the maximum removal had taken place in an acidic pH. The observation might be due to specific physical forces responsible for decrease in adsorption (Akazdam et al., 2017). Adsorption studies of coomassie brilliant blue on wheat bran on the other hand, has shown an increase in the percent dye removal up to a temperature of 60º C beyond which, the absorptive efficiency decreased (Ata et al., 2012). Studies have shown that dye removal progressively

increases with increasing solution pH. It has been shown that at pH 2, the sorption whether of Methylene Blue or of Malachite Green onto timber sawdust is less efficient with only 44% and 50.43% removal. The low adsorption at a lower pH is undoubtedly contributed by proton, which are predominantly present at such pH consequently competing with the cationic dyes for the surface sites (Djilali et al., 2012). On the contrary, in another study, removal of Acid Red 111 was analyzed over a pH range of 2-5 over different contact time and had given a reduction in the amount of adsorption with increasing pH. This behaviour was explained based on the change in the surface charges of lignocellulosic materials. By increasing the pH, the surface of the adsorbent gets more negatively charged, which does not favour the adsorption of anionic dyes due to electrostatic repulsion (Djilali et al., 2012). The Acid Red111 had exhibited different time range of reaching of equilibrium, 8 and 4 hrs in case of both modified oak cups pulp and pine cone, respectively but at the same pH, 2. This revealed that the not only the electrostatic forces which were important for the adsorption of dye molecules on the adsorbent but also covalent co-ordination bonds between dye molecules and surface functional groups were important for the same (Berraksu et al., 2012).

3.4.3 Adsorption Isotherm

The adsorption of CV, MG, CR, DDR, DO on WB were studied as a function of different concentration (mg/L) of all the dyes individually, while keeping all other parameters, pH (8,10,4,5,5) for CV, MG, CR, DDR and DO respectively, sorbent concentration (10 gm/L) and temperature 30ºC, constant for all dyes for a period of 180 mins for CV, DDR and DO and 210 mins for MG and CR. The findings reveal (Table 3.9; Figure 3.7, Figure 3.8, Figure 3.9, Figure 3.10) the relation between concentrations of the dye at equilibrium and their corresponding adsorption capacity respectively, showing at 100 mg/L CV, CR, DDR and DO, respectively and 110 mg/L in case of MG, the adsorption capacity of WB has shown an increase till 180 mins for CV, DDR and DO and 210 mins for MG and CR, respectively. After which it remains constant showing that the equilibrium was reached. Such equilibrium study models describe the distribution of adsorbate species among liquid and adsorbent based on the set of assumptions related to homogeneity and heterogeneity of adsorbents (Kumar and Krithika 2009). The graphs show Langmuir and Freundlich isotherm of WB by

non-linear and linear analysis. Table 3.9 (Figure 3.6, 3.7, 3.8, 3.9, 3.10) shows the corresponding values of the isotherm parameters, their correlation coefficients (R^2) and related standard errors for each parameter. RL between 0 and 1 indicates favourable adsorption (McKay et al., 1982).

Table 3.9 depicts the parameters for Langmuir and Freundlich isotherm for the bioadsorption of the five different test dyes (CV, MG, CR, DDR, DO) on WB. The Table 3.10 and Figure 3.6 suggests that non-linear Langmuir model, with R^2 value generates a satisfactory fit to the experimental data, while the Freundlich model does not with R^2 value 0.9503 in case of CV. Table 3.10 and Figure 3.7 depicts that with R^2 value 0.9992 and maximum adsorption capacity 11.142 mg/g in case of MG showing fit for non-Linear Langmuir model of adsorption. Table 3.10 and Figure 3.8 with R^2 value 0.9986 and maximum adsorption capacity 15.172 mg/g in case of CR showing fit for Linear Langmuir model of adsorption. Table 3.10 and Figure 3.9 with R^2 value 0.9977 and maximum adsorption capacity 12.347 mg/g in case of DDR showing fit for Linear Langmuir model of adsorption. Table 3.10 and Figure 3.10 with R^2 value 0.9932 and maximum adsorption capacity 15.982 mg/g in case of DO showing fit for Linear Langmuir model of adsorption model.

3.4.4 Batch Kinetics

The adsorption kinetic study was important for the optimization of the process condition for dye adsorption onto adsorbents. The adsorption kinetics of CV, MG, CR, DDR and DO on WB were analyzed by using two models, pseudo first order and pseudo second order thermodynamics model. Table 3.8 reports the kinetic model parameters and their constant values, calculated from various plots at 30º C in case of CV, MG and CR respectively and 40°C and 45°C for DDR and DO respectively. q_e values (12.07, 13.46, 12.26, 11.88 and 13.28 mg/g) with R^2 values (0.9665, 0.9814, 0.9627 and 0.9503) for CV, MG, CR, DDR and DO, respectively. The values depict that they are more matching with pseudo second order kinetic model. Monolayer coverage capacities of WB for Reactive Blue 19, 195 and 145 dyes , in another study, were obtained as117.6, 119.1 and 196.1 mg/gm at 60°C respectively, with a

regression coefficient (R^2) for pseudo second order kinetic model higher than 0.99 (Cicek et al., 2007), in contrast to that of the present study.

3.4.5 Spectroscopic analysis of active functional groups

Three major changes along with minor ones were observed in the FT-IR spectrum of CV adsorbed WB in comparison to that for unadsorbed WB. Figure 3.11 (A) and Graph 3.12 (A). reveal the reduction in amide (-NH) group by the stretching band at 459 cm^{-1} and 522 cm^{-1} and stretching of hydroxyl (-OH) group at 3308 cm^{-1} peak, this broad adsorption corresponds to alcohols, phenols and carboxylic acids as in pectin, cellulose and lignin, showing the presence of "free" hydroxyl groups on the adsorbent surface (Li et al, 2007 and Liang et al., 2010). The changes in the absorption peaks of two spectrum, therefore, clearly indicates the adsorption of CV dye onto the surface of WB. Figure 3.11 (B) on comparison with Figure 3.12 (B) shows that there is change in the surface with the presence of ester bonds on acid treatment at 1730 cm^{-1}, depicting the changes of functional groups on the surface of the WB on acid modification and above that on dye adsorption on them. Figure 3.12 (C) in comparison to Figure 3.11 (C) also shows changes on the surface of the WB after alkali treatment with medium and strong intensity, 1,3,5 substitutions. However, the regeneration capacity of such materials often poses a serious drawback, which may limit their practical application (Djilali et al., 2012).

Figure 3.13 on comparison with Figure 3.11, FTIR spectra of MG depicts a strong stretch of -C-O of vinyl ether at 1031 cm^{-1} with medium stretch at 2924 cm^{-1} indicating presence of alkane (-C-H). Figure 3.13 (C). depicts the presence of strong -S=O a strong sulfoxide stretches, indicating the presence of halo group at 1035 and 520 cm^{-1}, respectively. In Figure 3.14, FTIR spectrum of CR on WB shows a strong broadband at around 1026 cm^{-1} indicates the presence of stretch of -C-O of vinyl ether as that observed in MG on WB. The stretch at 3296 cm^{-1} indicates the presence of strong bond of -OH stretching indicating the presence of carboxylic group, along with a strong stretching of alkene group (-C=C). In Figure 3.14. stretch at 3288 cm^{-1} indicates a strong bond of carboxylic acid group with -OH stretching with a strong stretch of -S=O, a sulfonamide group at 1369 cm^{-1} with a strong alkene (-C=C) group at 896 cm^{-1}. In a similar study of adsorption of CV on pearl millet it has been shown

that there was an intense absorption band at 3423 cm^{-1} assigned to O–H bond stretching. The two CH_2 stretching bands at 2924 and 2856 cm^{-1} were observed depicting asymmetric and symmetric stretching of CH_2 groups showing the same wave numbers before and after the adsorption, indicating that these groups did not participate in the adsorption process. Sharp intense peaks were observed at 1645 cm^{-1}, before and after absorption assigned to the aromatic C–C ring stretching. The wave numbers of these bands were not different before and after the adsorption of CV. Bands ranging from 1116 to 1022 and 1122 to 1024 cm^{-1} before and after adsorption, respectively, assigned to C–O stretching vibrations (Selvapandian et al., 2015).

Figure 3.15, FTIR spectra of DDR on WB depicts the common vinyl ether bond like that of CV and MG at 1026 cm^{-1}, with a sharp stretching at 3282 cm^{-1} showing the presence alkyne group with strong -OH group depicting carboxylic group on Figure 3.15 (B) (DDR on acid modified WB) with a strong C-Cl stretching at 538 cm^{-1} , depicting the attachment of -Cl group reaction of DDR with the substrate. With similar type of functional group presence in case of DO as depicted in Figure 3.16 (A, B, C), in that of CR. A similar result has been observed in a study of adsorption of azo dye on WB, wave number of 3420 cm^{-1} indicates the possible presence of -OH, -NH groups on the adsorbent surface. The bands that are observed at 2930 and 1420 cm^{-1} suggest the presence of C-H group. The peak at 1645 cm^{-1} band is caused by the C=O stretching band of the carboxyl group. The absorption peak at 1540 cm^{-1} corresponding to the C-O bending vibration of the carboxylate ions (Wang and Chen 2009). In a study, FTIR analysis of natural and modified biosorbent (pinecone and oak cup pulps) did not differ significantly from the spectrum obtained of unmodified sorbent (Berakksu et al., 2012). A similar result was also obtained in another study, where sorption capability of modified and unmodified wood for removal of methylene blue was done (Janos et al., 2009).

Thus, this study reveals that the dyes belonging to similar chemical groups though different, chemical formula and molecular structure tend show adsorption capacity on surface of the test adsorbent in a similar fashion.

3.5 References

1. Acemioglu B, Alma HM. 2001. Equilibrium studies on adsorption of Cu (II) from aqueous solution onto cellulose. *J Col Interface Sc* 243: 81-84.
2. Acuner E, Dilek FB. 2004. Treatment of tectilon yellow 2G by *Chlorella vulgaris*. *Pro Biochem* 39: 623–631.
3. Ahalya N, Kanamadi RD, Ramachandra TV. 2005. Biosorption of chromium (VI) from aqueous solutions by the husk of Bengal gram (*Cicerari entinum*). *Elec J Biotech* 3: 258–264.
4. Ahmad A, Hameed BH, Aziz N. 2007. Adsorption of direct dye on palm ash: kinetic and equilibrium modelling. *J Haz Mat* 141: 70-76.
5. Akar ST, Aslan S, Akar T. 2018. Conversion of natural mineral to effective geosorbent by coating MnO_2 and its application potential for dye contaminated wastewaters. *J Cleaner Pro* 189: 887-897.
6. Akazdam S, Chafi M, Yassine W, Gourich B. 2017. Removal of Acid Orange 7 Dye from Aqueous Solution Using the Exchange Resin Amberlite FPA-98 as an Efficient Adsorbent: Kinetics, Isotherms, and Thermodynamics Study, *J. Mat Env Sc* 8: 2993-3012.
7. Aksu Z. 2001. Equilibrium and kinetic modelling of cadmium (II) biosorption by *C. vulgaris* in a batch system: effect of temperature. *Sep Pur Tech* 21: 285–294.
8. Altundogan HS. 2005. Cr(VI) removal from aqueous solution by iron (III)hydroxide-loaded sugar beet pulp. *Proc Biochem* 40: 1443–1452.
9. Alzaydien AS. 2015. Adsorption Behaviour of Methyl Orange onto Wheat Bran: Role of Surface and pH. *Ori J Chem* 31: 643-651.
10. Amir HM, Dariush N, Forugh V, Shahrokh N.2005. Tea waste as an adsorbent for heavy metal removal from industrial wastewaters. *Am J App Sc*: 372–375.
11. Anonymous 3, http://vipulorganics.com/blog/tag/basic-dyes/, Use of Dyes and Pigments in Paper and Pulp industries accessed on 20/08/2019.
12. Anonymous 5, Gram Staining Procedure, available at https://serc.carleton.edu/microbelife/research_methods/microscopy/gramstain.html, accessed on 17/10/2019.

13. Anonymous 6, Malachite Green a carcinogen, Inida Environmental Portal, Knowledge for changing, available at http://indiaenvironmentportal.org.in/node/27860/ , accessed on 17/10/2019
14. Anonymous 7, Dyes and Dyeing, available at https://www.flinnsci.com/api/library/Download/c46ad9cfbff64e9cae7caf3aed645692 , accessed on 17/10/2019.
15. Anonymous1,http://web.worldbank.org/archive/website01004/WEB/IMAGES/MULTI_-2.PDF, Industrial Pollution Projection System, accessed on 23/02/2019.
16. Anonymous2,http://www.indiatogether.org/uploads/document/document_upload/2132/env-bluelady-sc11sep.pdf, Supreme court of India, Writ Petition, 2007,accessed on 27/08/2019.
17. Anonymous4,http://apsacwestridge.edu.pk/assets/admin/upload/notes/ClassificationOfDyes.pdf, Lesson 2: Introduction to dyes , accessed on 16/10/2018.
18. Arlt VM, Glatt H, Muckel E, Pabel U, Sorg BL, Schmeiser HH, Phillips DH. 2002. Metabolic activation of the environmental contaminant 3-nitrobenzanthrone by human acetyltransferases and sulfotransferase. *Carcino* 23:1937–1945.
19. Ata S, Din MI, Rasool A, Qasim I, Mohsin Ul. 2012. Equilibrium, thermodynamics and kinetics sorption studies for the removal of coomasie brilliant blue on wheat bran as a low-cost adsorbent. *J Ana Met Chem*: 1-8.
20. Axelsson J, Nilsson U, Terrazas E, Aliaga TA, Welander U. 2006. Decolorization of the textile dyes Reactive Red 2 and Reactive Blue 4 using *Bjerkandera* sp. Strain BOL 13 in a continuous rotating biological contactor reactor. *Enz Micro Tech* 39: 32–37.
21. Benguella B, Benaissa H. 2002. Cadmium removal from aqueous solutions by chitin: kinetic and equilibrium studies. *Wat Res* 36: 2463-2474.
22. Berkane N, Meziane S, Aziri S. 2019. Optimization of Congo red removal from aqueous solution using Taguchi experimental design. *Sep Sc Tech*: 1-11.
23. Berraksu N, Ayan EM, Yanik J. 2012. Use of forestry wastes for biosorption of dyes and Cr (VI), Hindawi Publishing Corporation. *J Chem*: 1-10.

24. Bharathi KS, Ramesh SPT. 2013. Fixed-bed column studies on biosorption of crystal violet from aqueous solution by *Citrullus lanatus* rind and *Cyperus rotundus*. *App Wat Sc* 3: 673-687.
25. Botkin DB and Kelly EA. 1998. Environmental Science, Earth as a Living Planet. *John Wiley Sons* USA 2: 420-424.
26. Chandra MRGS, Madakka M. 2019. Comparative Biochemistry and kinetics of microbial lignocellulolytic enzymes. *Rec Dev App Micro Biochem*: 147-159.
27. Choudhary AKR. 2006. Textile Preparation and Dyeing. *Sc Pub* New Delhi.
28. Chowdhury S, Chakraborty S, Saha PD. 2013. Response surface optimization of a dynamic dye adsorption process: a case study of crystal violet adsorption onto NaOH-modified rice husk. *Env Sc Pol Res* 20: 1698-1705.
29. Cicek F, Ozer D, Ozer A, Ozer A. 2007. Low cost removal of reactive dyes using wheat bran. *J Haz Mat* 146: 408-416.
30. Dakiky M, Khamis M, Manassra A, Mer'eb M. 2002. Selective adsorption of chromium (VI) in industrial wastewater using low-cost abundantly available adsorbents. *Adv Env Res* 6: 533–540.
31. Davies B and Gasse F. 1988. African wetlands and shallow water bodies/Zones humides et lacs peu profonds d'Afrique, Bibliography/Bibliographie, Trav.Doc. *Inst Fr Rech Sci Dév Coop* : 211-502.
32. Djilali Y, Elandaloussi EH, Aziz A, Menorval LC. 2012. Alkaline treatment of timber sawdust: A straightforward route toward effective low-cost adsorbent for the enhanced removal of basic dyes from the aqueous solution. *J Saudi Chem Soc*: 241-249.
33. Doble M, Kumar A. 2005. Biotreatment of industrial effluents, 1st Edition, Elsevier Butterworth–Heinemann, Burlington, **ISBN:** 9780750678384.
34. Emongor V, Nkegbe E, Kealotswe B, Koorapetse I, Sankwase S, Keikanetswe S. 2005. Pollution indicators in Gaborone industrial effluent. *J App Sc* 5: 147-150.
35. Fakayode SO. 2005. Impact assessment of industrial effluent on water quality of the receiving Alaro river in Ibadan Nigeria *AJEAM-RAGEE* 10: 1-13.

36. Feng Y, Liu Y, Xue L, Sun H, Guo Z, Zhang Y, Yang L. 2017. Carboxylic acid functionalized sesame straw: a sustainable cost-effective bioadsorbent with superior dye adsorption capacity. *Bio Res Tech* 238: 675-683.
37. Freundlich HMF.1906. Over the adsorption in solution. *J Phy Chem* 57: 385–471.
38. Garg VK, Kaushik P. 2007. Influence of textile mill wastewater irrigation on the growth of sorghum cultivars. *App Eco Env Res* 6: 1–12.
39. Gohl EP and Vilensky LD. 2005. Textile Science, CBS Publishers and Distributors, New Delhi.
40. Gong R, Zhang X, Liu YS, Liu B. 2007. Uptake of cationic dyes from aqueous solution by biosorption onto granular kohlrabi peel. *Biores Tech* 98: 1319-1323.
41. Hariharan S, Nambisan P.2012. Optimization of lignin peroxidase, manganese peroxidase, and Lac production from Ganoderma lucidum under solid state fermentation of pineapple leaf. *Bio Res Tech* 8: 250-271.
42. Hashemian S, Dadfarnia S, Nateghi MR, Gafoori F. 2008. Sorption of acid red 138 from aqueous solutions onto rice bran. *Afr J Biotech* 7: 600–605.
43. Hettige H, Martin P, Singh M, Wheeler D.1995.The Industrial Pollution Projection System, The World Bank Policy Research Department Environment, Infrastructure, and Agriculture Division.
44. Ho YS, Mackay G. 1998. The sorption of lead (II) ions on peat. *W Res J* 33: 578-584.
45. Hunger K. 2003. Industrial Dyes, Chemistry, Properties, Application, *Wiley-VCH*, ISBN 3-527-30426-6.
46. Ijeoma K and Achi OK. 2011. Industrial effluents and their impact on water quality of receiving rivers in Nigeria. *J App Tech Env Sani*. 1: 75-86.
47. Iqbal HM, Kyazee NI, Keshavaraz T. 2013. Advances in the valorization of lignocellulosic materials by biotechnology: an overview. *Biores Tech* 8: 3157-3176.
48. Janos P, Coskun Pilarova SV, Rejnek J. 2009. Removal of basic (Methylene Blue) and acid (Egacid Orange) dyes from waters by sorption on chemically treated wood shavings. *Biores Tech* 100:1450–1453.

49. Johnson TA, Jain N, Joshi HC, Prasad S. 2008. Agricultural and agro-processing wastes as low cost adsorbents for metal removal from wastewater: a review. *J Sc Ind Res* 67: 647-658.
50. Kant R. 2012. Textile dyeing industry an environmental hazard. *Nat Sc* 4: 22–26.
51. Kapoor T, Viraraghavan DR, Cullimore. 1999. Removal of heavy metals using the fungus *Aspergillus niger*. *Biores Tech* 70: 95–104.
52. Khan S, Malik A. 2013. Environmental deterioration and human health: Natural and anthropogenic determinants. *Env Health Eff Tex Ind Wastewater*: 55-71.
53. Kumar PS, Krithika K. 2009. Equilibrium and kinetic study of adsorption of nickel from aqueous solution onto bael tree leaf powder. *J Eng Sc Tech* 4: 351-363.
54. Maclachalam S, Zalik S. 1963. Plastid structure, chlorophyll concentration and free amino acid composition of a chlorophyll mutant of barley. *Can J Bot* 41: 1053–1062
55. Macrae R, Robinson RK, Sadler MJ. 1993. Encyclopaedia of food science, food technology and nutrition. *Lon Aca Press*.
56. Madhavakrishnan S, Manickavasagam K, Vasanthakumar R, Rasappan K, Mohaviraj R, Pattabhi S. 2009. Crystal violet dye from aqueous solution using *Rincus communis* pericarp carbon as an adsorbent. *e-J Chem* :1109-1116.
57. Malik DS, Jain CK, Anuj KY. 2016. Removal of heavy metals from emerging cellulosic low-cost adsorbents: a review. *App Wat Sc* 7: 2113-2136.
58. Malik P. 2004. Dye removal from wastewater using activated carbon developed from sawdust: adsorption equilibrium and kinetics. *J Haz Mat* 113: 81-88.
59. Mall ID, Srivastava VC, Agarwal NK. 2006. Removal of Orange-G and Methyl Violet Dyes by Adsorption onto Bagasse Fly Ash—Kinetic Study and Equilibrium Isotherm Analyses. *Dyes Pig* 69: 210-223.
60. McKay G, Blair HS, Gardner JR. 1982. Adsorption of dyes on chitin. I. Equilibrium studies. *J App Pol Sc* 27: 3043–3057.

61. Mondal NB, Kar S. 2017. Potentiality of banana peel for removal of Congo red dye from aqueous solution: isotherm, kinetics and thermodynamics studies. *App Wat Sc* 8: 157-169.
62. Namasivayam C, Prabha D, Kumutha M. 1998. Removal of direct red and acid brilliant blue by adsorption on to banana pith. *Biores Tech* 64: 77–79.
63. Namsivayam CN, Muniasamy K, Gayatri MR, Ranganathan. 1996. Removal of dyes from aqueous solutions by cellulosic waste orange peel. *Biores Tech* 57: 37-43.
64. Nubi OA, Osibanjo O, Nubi AT. 2008. Impact assessment of dumpsite leachate on the qualities of surface water and sediment of river Eku, Ona-Ara local government, Oyo State, Nigeria. *Sc World J* 3: 17-20.
65. Oleszczuk, P. 2008. Phytotoxicity of municipal sewage sludge composts related to physico-chemical properties, PAHs and heavy metals. *Ecotox Env Saf* 69(3): 496-505.
66. Otokunefor TV and Obiukwu C. 2005. Impact of refinery effluent on the physicochemical properties of a water body in the Niger Delta. *App Eco Env Res* 3: 61-72.
67. Papinutti L, Mouso N, Forchiassin F. 2006. Removal and degradation of fungicide dye malachite green from the aqueous solution using the system wheat bran -Fomes sclerodermeus. *Enz Micro Tech* 39: 848-853.
68. Paul SA, Chavan SK, Khambe SD, 2012, Studies on characterization of textile industrial waste-water in solapur city. *Int J Chem Sc* 10: 635–642.
69. Phiri O, Mumba P, Moyo BHZ, Kadewa W. 2005. Assessment of the impact of industrial effluents on water quality of receiving rivers in urban areas of Malawi. *Int J Env Sc and Tech* 2: 237-244.
70. Rajeswari K, Subashkumar R, Vijayaraman K. 2014. Degradation of Textile dyes by isolated *Lysinibacillus sphaericus* strain RSV-1 and *Stenotrophomonas maltophilia* strain RSV-2 and toxicity assessment of degraded product. *J Env and Ana Tox* 4(4): 1-10.
71. Razo-Flores E, Donlon B, Lettinga G, Field JA. 1997. Biotransformation and biodegradation of N- substituted aromatics in methanogenic granular sludge. *FEMS Micro Rev* 20: 525–538.

72. Selvapandian P, Ananthakumar. K, Cyril A. 2015. Biosorption of crystal violet from aqueous solution by pearl millet powder: Isotherm modelling and kinetic studies. *J App Res Wat Was Wat* 2: 143-149.
73. Stevenson L, Phillips F., O' Sullivan K, Walton J. 2012. Wheat bran: its composition and benefits to health, a European perspective. *Int J Food Sc Nut* 63: 1001-1013.
74. Temesgen F, Gabbiye N, Sahu O. 2018. Biosorption of reactive red dye (RRD) on activated surface of banana and orange peels: economical alternative for textile effluent. *Sur Inter* 12: 151-159.
75. Umbuzeiro GA, Freeman H, Warren SH, Kummrow F, Claxton LD. 2005. Mutagenicity evaluation of the commercial product CI Disperse Blue 291 using different protocols of the Salmonella assay. *Food Chem Tox* 43: 49–56.
76. Vadivelan V, Kumar KV. 2005. Equilibrium, kinetics, mechanism, and process design for the sorption of methylene blue onto rice husk. *J Col Int Sc* 286: 90-100
77. Verma AK, Dash RR, Bhunia P. 2012. A review on chemical coagulation/flocculation technologies for removal of color from textile wastewaters. *J Env Mgt* 93:154–168.
78. Verma AK, Dash RR, Bhunia P. 2012. A review on chemical coagulation/flocculation technologies for removal of color from textile wastewaters. *J Env Mgt* 93: 154–168.
79. Vesiland PA, Peirce JJ, Weiner RF.1990. Environmental Pollution and Control, *Burtonworth Heinemann Publishers*, USA: 389.
80. Welch CG. 2009. Toxic Release Inventory for India: A discussion paper, Institute for Financial Management and Research. *Centre Dev Fin, Working Paper series.*
81. WHO. 2002. Water pollutants: biological agents, dissolved chemicals, non-dissolved chemicals, sediments, heat, WHO CEHA, Amman.
82. WHO.2003. The world health report 2003: shaping the future, World Health Organization, 1211 Geneva 27.
83. Yusuff RO, Sonibare JA. 2004. Characterization of textile industries effluents in Kaduna, Nigeria and pollution implications. Global Nest: *Int J* 6: 212–221.

84. Zhang L, Zhao L, Yu Y, Chen C.1998. Removal of lead from aqueous solution by non-living *Rhizopus nigricans*. *Wat Res* 32:1437– 1444.
85. Zhou Q, Wang X, Liu J, Zhang L. 2012. Phosphorus removal from wastewater using nano-particulates of hydrated ferric oxide doped activated carbon fiber prepared by Sol-Gel method. *Chem Eng J* 200: 619–626.
86. Zhu B, Fan T, Zhang D. 2008. Adsorption of Copper ions from aqueous solution by citric acid modified soyabean straw. *J Haz Mat* 152: 300-308.

Tables

Table 3.4 Effect of pH on percent dye decolorization by test adsorbent

S.No.	pH	Industrial Dye				
		CV*[1]	**MG*[2]**	**CR*[3]**	**DDR*[4]**	**DO*[5]**
1.	**2**	71.27±0.6	66.69±0.4	86.10±0.3	43.65±0.1	42.46±0.2
2.	**3**	74.48±0.5	58.52±0.1	90.88±0.3	75.96±0.4	74.26±0.1
3.	**4**	75.22±0.7	56.69±0.1	**96.76±0.1**	77.88±0.3	81.39±0.2
4.	**5**	81.13±0.6	74.48±0.3	85.57±0.2	**91.15±0.2**	**92.34±0.1**
5.	**6**	83.18±0.1	81.91±0.8	81.88±0.6	89.23±0.2	86.48±0.3
6.	**7**	85.21±0.5	89.48±0.2	56.23±0.7	84.81±0.2	81.24±0.2
7.	**8**	**87.71±0.8**	90.07±0.1	37.79±0.1	75.58±0.3	76.41±0.2
8.	**9**	86.69±0.8	91.32±0.5	36.43±0.2	58.08±0.4	68.21±0.2
9.	**10**	86.23±0.8	**94.98±0.1**	36.17±0.1	55.96±0.2	53.34±0.1
10.	**11**	85.13±0.1	93.35±0.3	35.23±0.2	35.96±0.2	34.24±0.4
11.	**12**	85.02±0.1	91.12±0.1	35.02±0.2	33.96±0.2	29.45±0.4

Crystal Violet*[1]; Malachite Green*[2]; Congo Red*[3]; Disperse Dark Red*[4]; Disperse Orange*[5]

Incubation Conditions:

Adsorbate concentration, mg/L: 100 Incubation time, mins: 180

Adsorbent dose, gm/L:10 Temperature, °C: 30

Table 3.5 Effect of adsorbate concentration & incubation time on percent dye decolorization

S.No.	Dye	Adsorbate conc. (mg/L)	Time (mins)							
			30	60	90	120	150	180	210	240
1	CV[*1]	60	55.96±0.7	65.56±0.7	78.95±0.4	85.51±0.6	87.12±0.4	88.17±0.9	88.73±0.3	88.64±0.7
		70	51.77±0.3	58.80±0.2	67.78±0.3	78.30±0.3	85.96±0.5	88.08±0.6	88.51±0.4	88.57±0.6
		80	46.05±0.1	58.18±0.3	66.09±0.9	76.41±0.6	84.20±0.2	88.03±0.4	88.05±0.9	88.01±0.1
		90	43.97±0.1	54.78±0.1	65.84±0.1	74.67±0.1	82.80±0.5	87.98±0.6	87.95±0.7	87.92±0.4
		100	38.39±0.7	49.57±0.1	58.87±0.9	71.69±0.8	81.99±0.2	**87.93±0.7**	87.85±0.3	87.86±0.1
		110	31.00±0.2	43.64±0.2	50.46±0.9	68.24±0.4	70.71±0.3	77.65±0.2	78.30±0.7	78.93±0.2
		120	24.00±0.3	34.00±0.1	45.45±0.5	49.17±0.2	52.76±0.4	54.58±0.1	56.24±0.2	56.19±0.3
2	MG[*2]	60	60.07±0.5	68.82±0.6	82.20±0.1	87.72±0.2	94.55±0.3	97.72±0.4	98.16±0.1	98.10±0.3
		70	57.50±03	72.86±0.2	81.02±0.7	82.13±0.8	91.10±0.4	96.80±0.2	97.98±0.1	97.18±0.3
		80	56.42±0.3	71.12±0.2	80.66±0.2	81.47±0.2	88.21±0.2	95.59±0.2	96.82±0.5	96.76±0.4
		90	48.67±0.1	70.07±0.2	79.77±0.2	80.51±0.2	88.11±0.4	94.57±0.2	95.69±0.6	95.64±0.6
		100	47.60±0.1	67.57±0.1	76.44±0.1	79.92±0.1	87.98±0.5	94.46±0.4	95.51±0.2	95.19±0.2
		110	37.27±0.1	63.23±0.1	72.27±0.1	77.20±0.1	85.20±0.5	94.10±0.1	**95.05±0.2**	94.88±0.2
		120	24.23±0.2	52.56±0.2	57.23±0.8	64.96±0.1	75.21±0.5	85.32±0.1	87.21±0.2	87.02±0.1
3	CR[*3]	60	76.68±0.4	83.27±0.2	84.78±0.1	93.98±0.5	95.28±0.3	97.67±0.3	98.23±0.3	98.07±0.1
		70	73.01±0.1	76.16±0.6	83.78±0.1	88.54±0.2	92.67±0.4	94.78±0.3	97.12±0.3	97.08±0.1
		80	71.08±0.3	73.24±0.5	78.57±0.3	86.17±0.2	85.37±0.2	93.98±0.8	96.87±0.3	96.35±0.7
		90	71.93±0.3	74.06±0.2	76.94±0.2	83.96±0.1	89.84±0.1	92.56±0.1	96.36±0.2	96.02±0.1
		100	58.31±0.2	66.91±0.2	68.83±0.2	71.70±0.1	79.25±0.3	86.49±0.1	**96.99±0.8**	96.12±0.1
		110	36.51±0.1	47.81±0.1	54.27±0.1	59.71±0.1	67.44±0.7	72.57±0.2	72.12±0.1	72.06±0.2
		120	23.26±0.4	28.12±0.3	35.54±0.3	37.67±0.5	40.23±0.3	42.12±0.1	42.45±0.2	42.15±0.2
4	DDR[*4]	60	65.12±0.5	71.08±0.4	82.32±0.3	84.78±0.1	89.38±0.3	94.58±0.4	96.56±0.1	96.50±0.2
		70	56.28±0.2	65.74±0.1	75.48±0.1	78.91±0.1	84.89±0.2	94.45±0.6	95.32±0.5	95.18±0.4
		80	53.32±0.1	61.35±0.1	63.59±0.3	77.69±0.1	84.45±0.2	92.78±0.3	94.38±0.4	94.01±0.1
		90	47.61±0.2	55.36±0.3	62.68±0.4	75.93±0.2	84.58±0.1	91.20±0.2	91.15±0.3	91.05±0.1
		100	43.34±0.1	53.82±0.4	61.36±0.2	74.21±0.3	83.37±0.1	**91.20±0.2**	91.19±0.4	91.17±0.3
		110	32.35±0.3	48.45±0.2	52.78±0.1	65.18±0.5	75.26±0.6	79.86±0.2	81.65±0.3	81.98±0.3
		120	28.34±0.2	46.65±0.2	56.65±0.4	64.87±0.3	74.37±0.1	76.38±0.1	76.98±0.1	78.28±0.1
5	DO[*5]	60	67.23±0.3	73.15±0.3	83.26±0.3	86.47±0.2	88.97±0.5	94.76±0.2	95.54±0.2	95.69±0.2
		70	57.48±0.2	66.26±0.2	74.82±0.5	78.65±0.2	87.73±0.1	94.52±0.3	94.78±0.1	94.70±0.1
		80	52.13±0.1	67.34±0.3	73.68±0.2	77.53±0.1	86.61±0.2	93.63±0.2	93.45±0.1	93.22±0.2
		90	45.62±0.1	54.53±0.1	61.38±0.2	76.45±0.1	85.34±0.2	92.99±0.2	92.67±0.2	92.57±0.2
		100	38.25±0.3	48.74±0.1	59.39±0.1	73.42±0.3	84.65±0.1	**92.42±0.2**	92.26±0.3	92.33±0.4
		110	35.38±0.3	47.41±0.1	51.58±0.4	63.49±0.4	74.68±0.1	78.56±0.1	83.26±0.4	83.11±0.1
		120	27.87±0.3	45.81±0.1	50.56±0.1	58.84±0.3	63.38±0.2	72.03±0.1	72.39±0.1	72.46±0.1

Crystal Violet*[1]; Malachite Green*[2]; Congo Red*[3]; Disperse Dark Red*[4]; Disperse Orange*[5]
Incubation Conditions:
*[1]: pH 8; Adsorbent dose, gm/L:10; Temperature, º C: 30
*[2]: pH 10; Adsorbent dose, gm/L:10; Temperature, º C: 30
*[3]: pH 4; Adsorbent dose, gm/L:10; Temperature, º C: 30
*[4]: pH 5; Adsorbent dose, gm/L:10; Temperature, º C: 30
*[5]: pH 5; Adsorbent dose, gm/L:10; Temperature, º C: 30

Table 3.6 Effect of adsorbent dosage on percent dye decolorization

S. No.	Dye	Adsorbent dose (gm/L)						
		2	4	6	8	10	12	14
1	CV[*1]	27.73±0.1	63.97±0.3	75.66±0.8	78.23±0.1	87.95±0.4	**88.11±0.3**	88.03±0.8
2	MG[*2]	80.84±0.2	83.10±0.4	84.37±0.7	86.80±0.1	95.01±0.1	**96.37±0.1**	96.43±0.2
3	CR[*3]	57.97±0.2	64.53±0.2	78.84±0.1	88.12±0.1	96.78±0.3	**97.08±0.3**	97.06±0.2
4	DDR[*4]	54.29±0.1	63.27±0.3	76.48±0.1	89.65±0.2	91.24±0.1	**93.02±0.5**	93.03±0.3
5	DO[*5]	57.21±0.3	65.87±0.2	77.49±0.3	87.21±0.3	92.47±0.3	**93.16±0.2**	93.09±0.1

Crystal Violet*[1]; Malachite Green*[2]; Congo Red*[3]; Disperse Dark Red*[4]; Disperse Orange*[5]
Incubation Conditions:
*[1]: pH 8; Adsorbate conc., mg/L:100; Incubation Time, mins: 180; Temperature, º C: 30
*[2]: pH 10; Adsorbate conc., mg/L:110; Incubation Time, mins: 210; Temperature, º C: 30
*[3]: pH 4; Adsorbate conc., mg/L:100; Incubation Time, mins: 210; Temperature, º C: 30
*[4]: pH 5; Adsorbate conc., mg/L:100; Incubation Time, mins: 180; Temperature, º C: 30
*[5]: pH 5; Adsorbate conc., mg/L:100; Incubation Time, mins: 180 Temperature, º C: 30

Table 3.7 Effect of Temperature on percent dye decolorization

S. No.	Dye	Temp (ºC)									
		25	**30**	**35**	**40**	**45**	**50**	**55**	**60**	**65**	**70**
1.	**CV**[*1]	75.50± 0.3	**87.98± 0.1**	87.12± 0.8	86.80± 0.1	78.61± 0.8	65.43± 0.8	63.70± 0.6	56.55± 0.9	46.55± 0.9	42.55±0. 9
2.	**MG**[*2]	78.05± 0.2	**95.10± 0.5**	89.45± 0.1	88.98± 0.3	85.08± 0.3	79.33± 0.1	68.57± 0.1	65.78± 0.7	55.55± 0.9	35.55±0. 9
3.	**CR**[*3]	89.95± 0.5	96.73± 0.2	**97.08± 0.1**	88.70± 0.1	75.25± 0.4	62.49± 0.5	51.75± 0.2	49.12± 0.2	42.55± 0.9	42.05±0. 9
4.	**DDR**[*4]	85.83± 0.3	91.22± 0.2	91.89± 0.2	**93.45± 0.4**	91.12± 0.1	81.23± 0.1	76.41± 0.2	60.23± 0.1	50.27± 0.2	41.23±0. 1
5.	**DO**[*5]	86.28± 0.4	92.37± 0.3	**92.49± 0.1**	92.55± 0.1	93.33± 0.2	89.46± 0.1	81.15± 0.1	72.57± 0.3	58.58± 0.2	39.28±0. 2

Crystal Violet*[1]; Malachite Green*[2]; Congo Red*[3]; Disperse Dark Red*[4]; Disperse Orange*[5]
Incubation Conditions:
*1: pH 8, Incubation time: mins: 180; Adsorbate dose, mg/L: 100; Adsorbent dose, gm/L: 10
*2: pH 10; Incubation time, min: 210; Adsorbate dose, mg/L: 110; Adsorbent dose, gm/L: 12
*3: pH 4; Incubation time, min: 210; Adsorbate dose, mg/L: 100; Adsorbent dose, gm/L: 12
*4: pH 5; Incubation time, min: 180; Adsorbate dose, mg/L: 100; Adsorbent dose, gm/L: 12
*5: pH 5; Incubation time, min: 180; Adsorbate dose, mg/L: 100; Adsorbent dose, gm/L: 12

Table 3.8 Effect of Chemical Modification of WB on its dye adsorptive ability

S. No.	Dye	WB[#1]	Modified WB	
			AMWB[#2]	**ALMWB**[#3]
1	**CV**[*1]	88.06±0.2	82.65±0.1	92.45±0.5
2	**MG**[*2]	95.25±0.1	89.87±0.1	98.39±0.4
3	**CR**[*3]	97.02±0.8	98.58±0.3	74.56±0.1
4	**DDR**[*4]	93.55±0.1	95.47±0.4	72.36±0.1
5	**DO**[*5]	93.48±0.2	96.41±0.1	70.24±0.2

Wheat Bran[#1]; Acid Modified Wheat Bran[#2]; Alkali Modified Wheat Bran[#3]
Crystal Violet*[1]; Malachite Green*[2]; Congo Red*[3]; Disperse Dark Red*[4]; Disperse Orange*[5]
Incubation Conditions:
*1: pH 8, Incubation time: mins: 180; Adsorbate dose, mg/L: 100; Adsorbent dose, gm/L: 10; Temperature, ºC: 30
*2: pH 10; Incubation time, min: 210; Adsorbate dose, mg/L: 110; Adsorbent dose, gm/L: 12; Temperature, ºC: 30
*3: pH 4; Incubation time, min: 210; Adsorbate dose, mg/L: 100; Adsorbent dose, gm/L: 12; Temperature, ºC: 30
*4: pH 5; Incubation time, min: 180; Adsorbate dose, mg/L: 100; Adsorbent dose, gm/L: 12; Temperature, ºC: 40
*5: pH 5; Incubation time, min: 180; Adsorbate dose, mg/L: 100; Adsorbent dose, gm/L: 12; Temperature, ºC: 45

Table 3.9 Adsorption Isotherm: Parameters for Langmuir and Freundlich

S. No.	Dye	C_e (mg/L)	q_e (mg/gm)	C_e/q_e	ln C_e	ln q_e
1.	**CV**[*1]	7.10	5.29	1.342	1.960	1.665
		8.34	6.17	1.353	2.121	1.819
		9.58	7.04	1.360	2.260	1.952
		10.38	7.92	1.366	2.381	2.069
		12.07	8.79	1.372	2.490	2.174
		15.64	9.44	1.658	2.750	2.244
		19.62	10.04	1.954	2.980	2.306
2.	**MG**[*2]	1.10	5.9	0.187	0.098	1.674
		1.41	6.9	0.206	0.346	1.579
		2.54	7.7	0.328	0.933	1.113
		3.88	8.6	0.450	1.355	0.797
		4.49	9.6	0.470	1.502	0.754
		15.35	10.5	1.466	2.730	0.382
3.	**CR**[*3]	2.02	6.80	0.296	0.701	1.917
		2.50	7.75	0.323	0.917	2.047
		3.28	8.67	0.378	1.186	2.160
		5.15	10.49	0.490	1.639	2.350
		7.22	11.28	0.640	1.977	2.422
4.	**DDR**[*4]	3.25	5.67	0.573	1.178	1.735
		3.89	6.61	0.588	1.358	1.888
		5.78	7.42	0.778	1.754	2.004
		7.96	8.20	0.970	2.074	2.104
		8.46	9.15	0.924	2.135	2.213
		12.83	9.72	1.319	2.551	2.274
		17.68	10.23	1.728	2.872	2.325
5.	**DO**[*5]	3.14	5.69	0.551	1.144	1.738
		3.84	6.62	0.580	1.345	1.890
		5.10	7.49	0.680	1.629	2.013
		6.31	8.37	0.753	1.842	2.124
		7.58	9.24	0.820	2.025	2.223
		11.85	9.82	1.206	2.472	2.284
		20.08	9.99	2.010	2.999	2.301

Crystal Violet*[1]; Malachite Green*[2]; Congo Red*[3]; Disperse Dark Red*[4]; Disperse Orange*[5]

C_e : Equilibrium concentration of dye, q_e = adsorbed amount of dye

Incubation conditions:

[*1]: pH 8, Incubation time: mins: 180; Adsorbate dose, mg/L: 100; Adsorbent dose, gm/L: 10; Temperature, ºC: 30

[*2]: pH 10; Incubation time, min: 210; Adsorbate dose, mg/L: 110; Adsorbent dose, gm/L: 12; Temperature, ºC: 30

[*3]: pH 4; Incubation time, min: 210; Adsorbate dose, mg/L: 100; Adsorbent dose, gm/L: 12; Temperature, ºC: 30

[*4]: pH 5; Incubation time, min: 180; Adsorbate dose, mg/L: 100; Adsorbent dose, gm/L: 12; Temperature, ºC: 40

[*5]: pH 5; Incubation time, min: 180; Adsorbate dose, mg/L: 100; Adsorbent dose, gm/L: 12; Temperature, ºC: 45

Table 3.10 Adsorption Isotherm: Constant values for Langmuir and Freundlich

S. No.	Dye	Types of Isotherm	Parameters	Values
1.	CV[*1]	Non-Linear Langmuir	q_m	**19.790**
			K_L	0.056
			R^2	**0.9713**
		Linear Freundlich	K_F	1.664
			N	1.963
			R^2	0.9503
2.	MG[*2]	Non-Linear Langmuir	q_m	11.142
			K_L	1.021
			R^2	**0.9992**
		Linear Freundlich	K_F	6.271
			N	4.675
			R^2	0.8978
3.	CR[*3]	Non-Linear Langmuir	q_m	15.172
			K_L	0.412
			R_2	**0.9986**
		Linear Freundlich	K_F	1.173
			N	2.519
			R^2	0.9803
4.	DDR[*4]	Non-Linear Langmuir	q_m	12.347
			K_L	0.270
			R^2	**0.9977**
		Linear Freundlich	K_F	4.410
			N	3.337
			R^2	0.9922
5.	DO[*5]	Non-Linear Langmuir	q_m	15.982
			K_L	0.1775
			R^2	**0.9932**
		Linear Freundlich	K_F	3.884
			N	2.850
			R^2	0.9792

Crystal Violet*[1]; Malachite Green*[2]; Congo Red*[3]; Disperse Dark Red*[4]; Disperse Orange*[5]
q_m : maximum adsorption capacity; KL: constant for adsorption capacity
KF: constant for energy or net enthalpy of adsorption
n: constant for measuring the intensity of adsorption

Table 3.11 Batch Kinetics: Constant values for Kinetic model

S. No.	Dye	Model	Kinetic Parameters	Concentration of dye (mg/L)
1.	CV[*1]	Pseudo- first-order	k_1	0.01318
			qe (mg/g)	9.329
			R^2	0.9578
		Pseudo-second-order	qe (mg/g)	12.07
			k_2 (/min)	0.00105
			R^2	**0.9665**
2.	MG[*2]	Pseudo- first-order	k_1	0.01579
			qe (mg/g)	10.66
			R^2	0.9757
		Pseudo-second-order	qe (mg/g)	13.46
			k_2 (/min)	0.001185
			R^2	**0.9814**
3.	CR[*3]	Pseudo- first-order	k_1	0.014
			qe cal (mg/g)	9.666
			R^2	0.9302
		Pseudo-second-order	qe cal(mg/g)	12.26
			k_2 (/min)	0.001157
			R^2	**0.9627**
4.	DDR[*4]	Pseudo- first-order	k_1	0.01434
			qe (mg/g)	9.418
			R^2	0.9260
		Pseudo-second-order	qe (mg/g)	11.88
			k_2 (/min)	0.00124
			R^2	**0.9503**
5.	DO[*5]	Pseudo- first-order	k_1	0.01168
			qe (mg/g)	10.01
			R^2	0.9557
		Pseudo-second-order	qe (mg/g)	13.28
			k_2 (/min)	0.0007985
			R^2	**0.9611**

Crystal Violet*[1]; Malachite Green*[2]; Congo Red*[3]; Disperse Dark Red*[4]; Disperse Orange*[5]
Incubation conditions:
[*1]: pH 8, Incubation time, mins: 180; Adsorbate dose, mg/L: 100; Adsorbent dose, gm/L: 10; Temperature, ^oC: 30
[*2]: pH 10; Incubation time, min: 210; Adsorbate dose, mg/L: 110; Adsorbent dose, gm/L: 12; Temperature, ^oC: 30
[*3]: pH 4; Incubation time, min: 210; Adsorbate dose, mg/L: 100; Adsorbent dose, gm/L: 12; Temperature, ^oC: 30
[*4]: pH 5; Incubation time, min: 180; Adsorbate dose, mg/L: 100; Adsorbent dose, gm/L: 12; Temperature, ^oC: 40
[*5]: pH 5; Incubation time, min: 180; Adsorbate dose, mg/L: 100; Adsorbent dose, gm/L: 12; Temperature, ^oC: 45

Figures

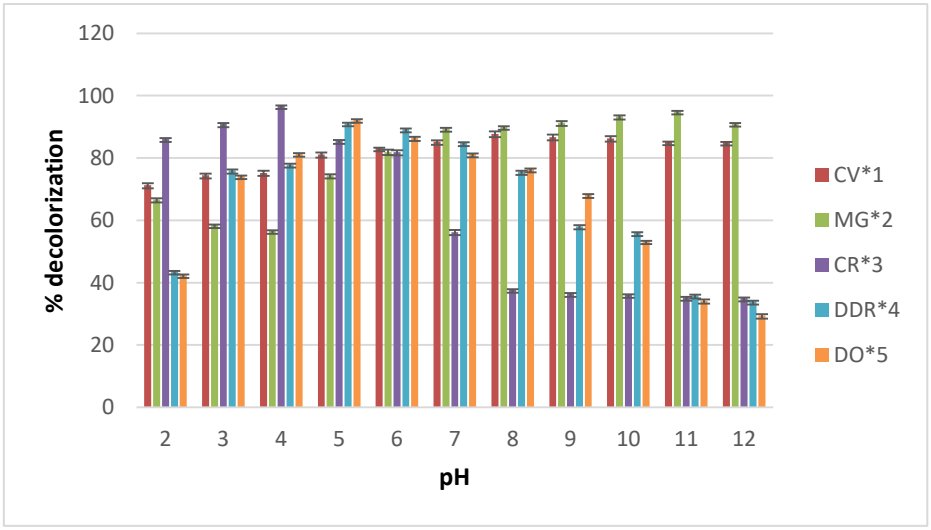

Figure 3.1: Effect of pH on percent dye decolorization by test adsorbent

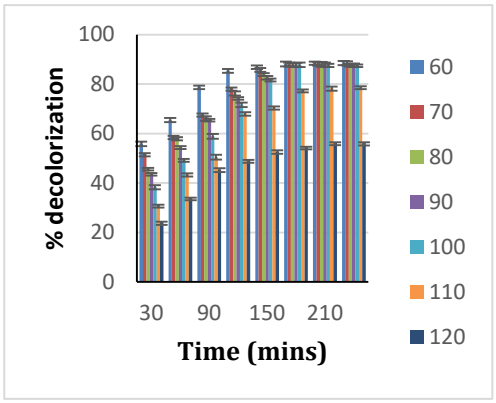

(A)

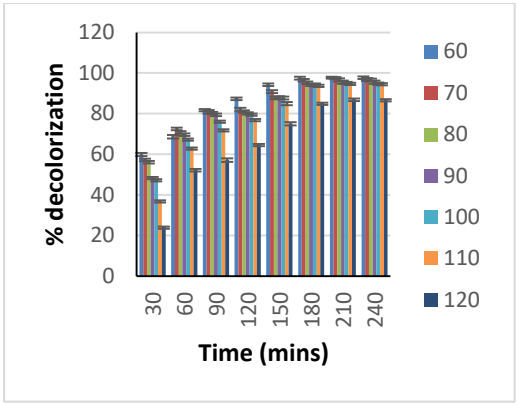

(B)

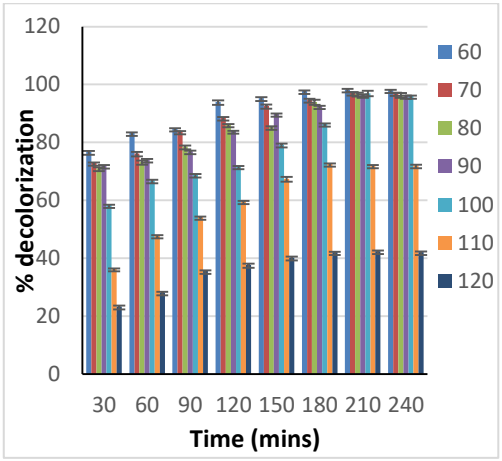

(C)

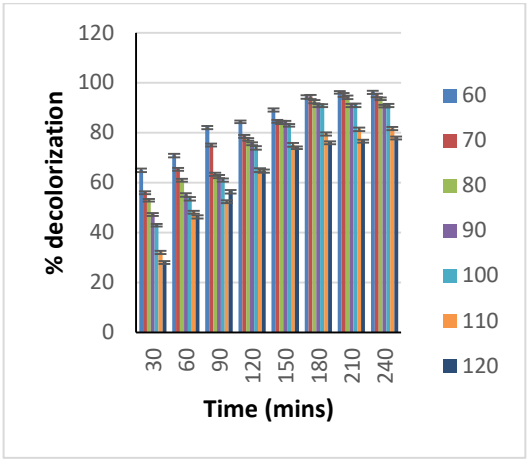

(D)

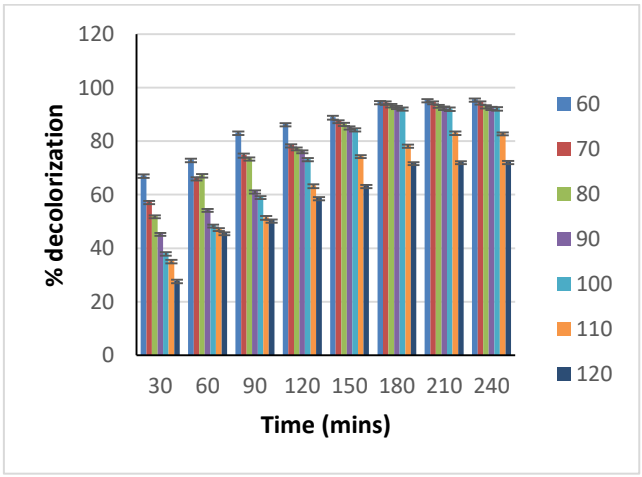

(E)

Figure 3.2: Effect of adsorbate concentration & incubation time on percent dye decolorization. A: (CV*1), B: (MG*2), C: (CR*3), D: (DDR*4), E: (DO*5)

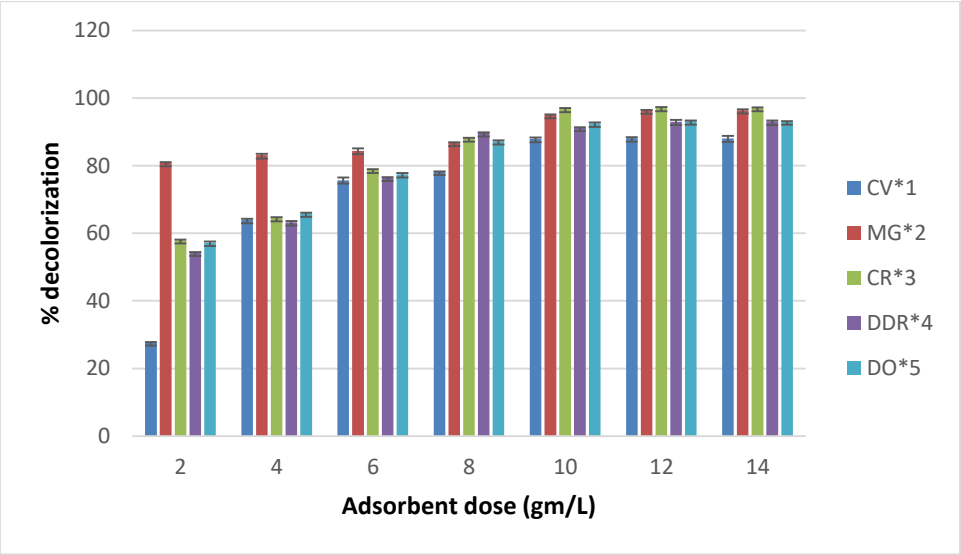

Figure 3.3: Effect of adsorbent dosage on percent dye decolorization

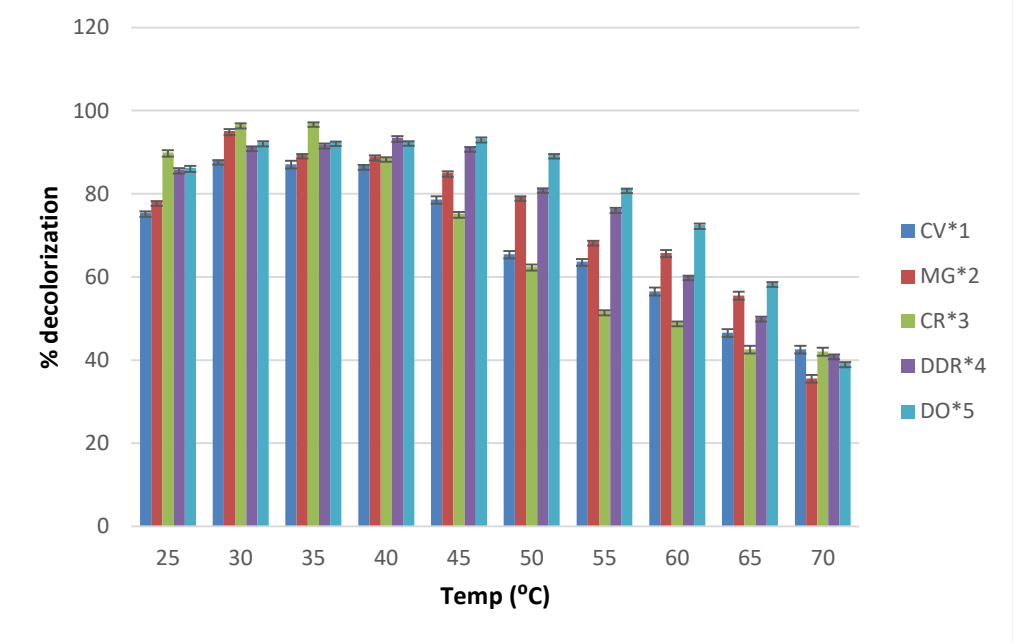

Figure 3.4: Effect of Temperature on percent dye decolorization.

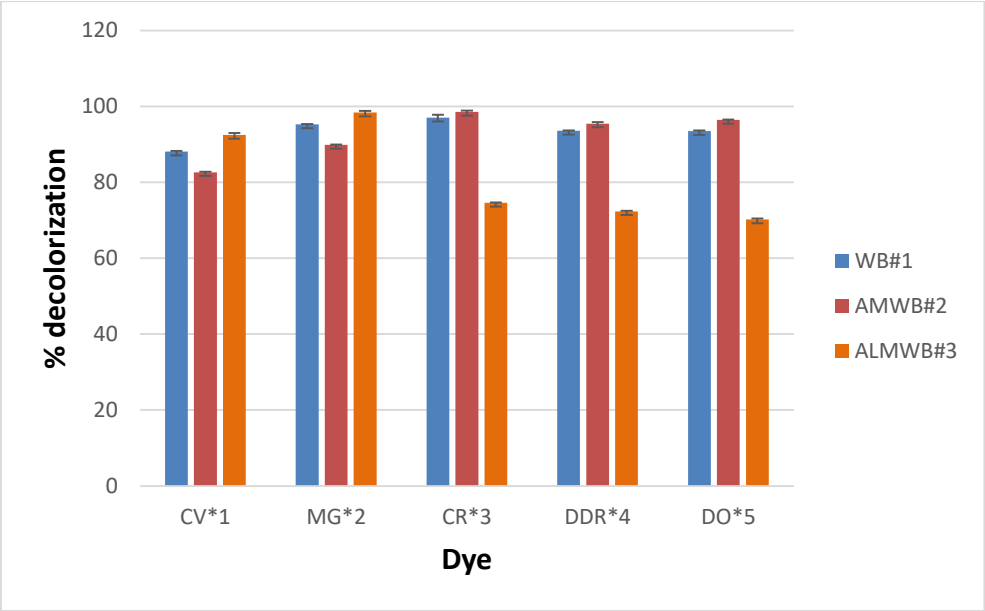

Figure 3.5: Effect of Chemical Modification of WB on its dye adsorptive ability

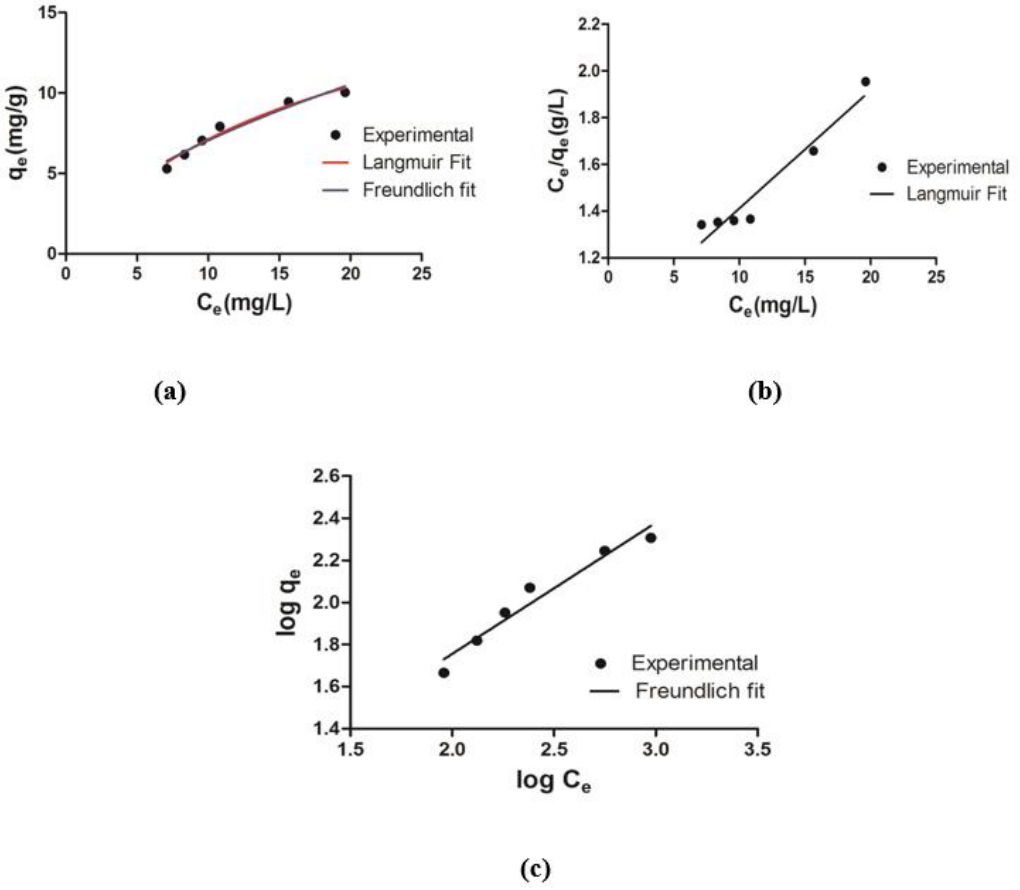

Figure 3.6: Adsorption Isotherm: (a) Non-Linear Langmuir Isotherm plot for CV (b) Linear Langmuir Isotherm plot for CV (c) Linear Freundlich Isotherm plot for CV

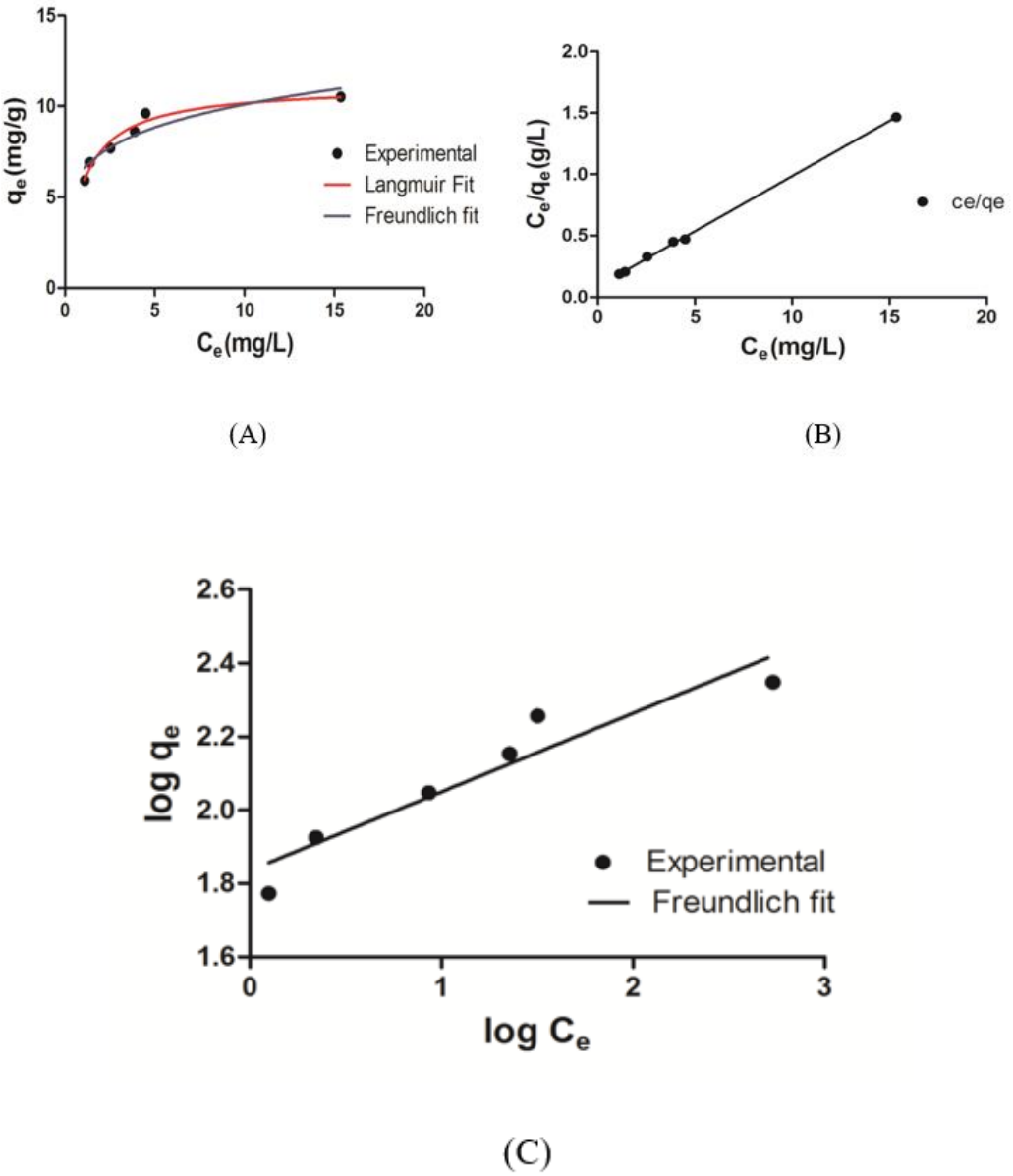

Figure 3.7: Adsorption Isotherm: (A) Non-Linear Langmuir Isotherm plot for MG (B) Linear Langmuir Isotherm plot for MG (C) Linear Freundlich Isotherm plot for MG

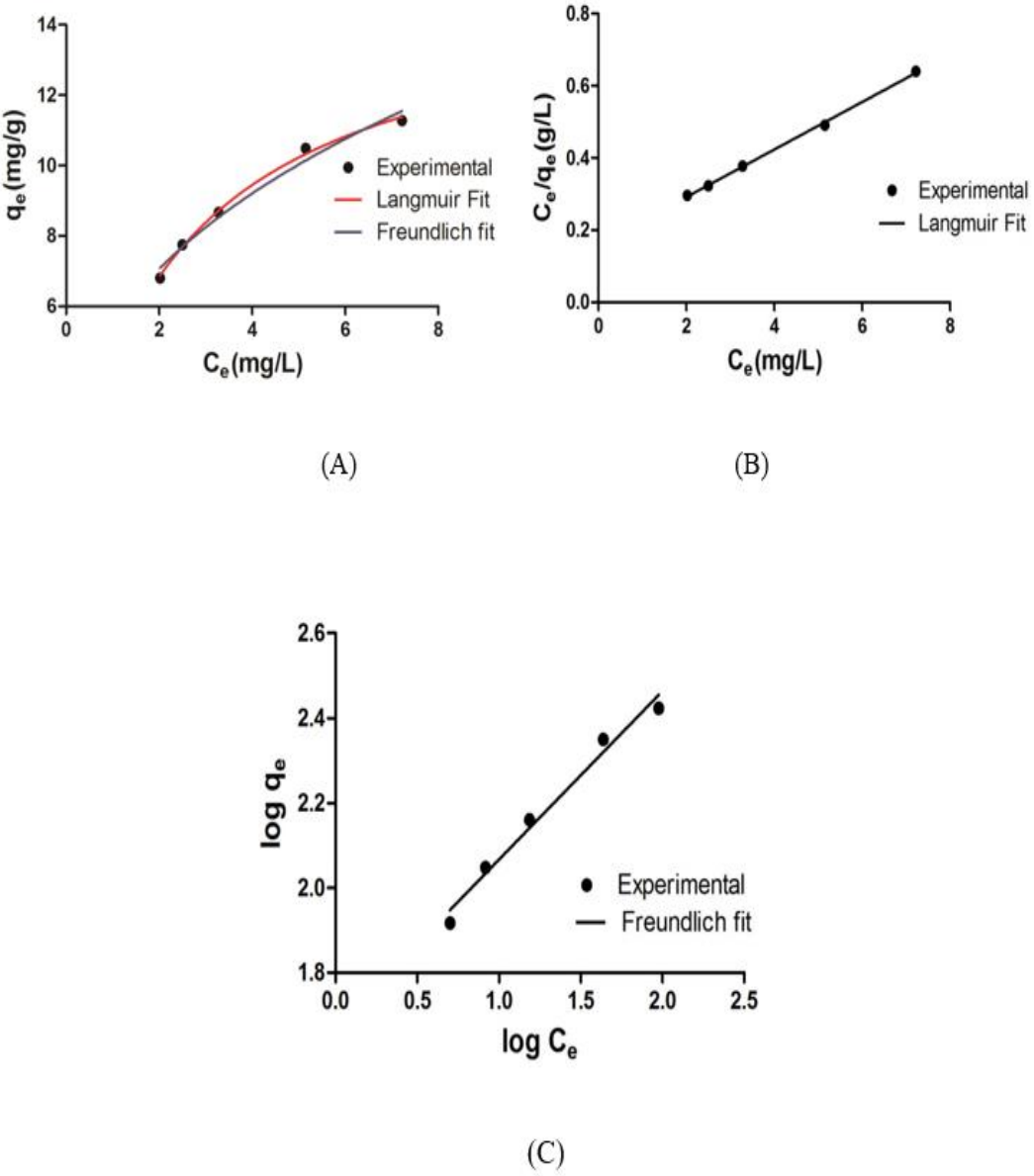

Figure 3.8: Adsorption Isotherm: (A) Non-Linear Langmuir Isotherm plot for CR (B) Linear Langmuir Isotherm plot for CR (C) Linear Freundlich Isotherm plot for CR

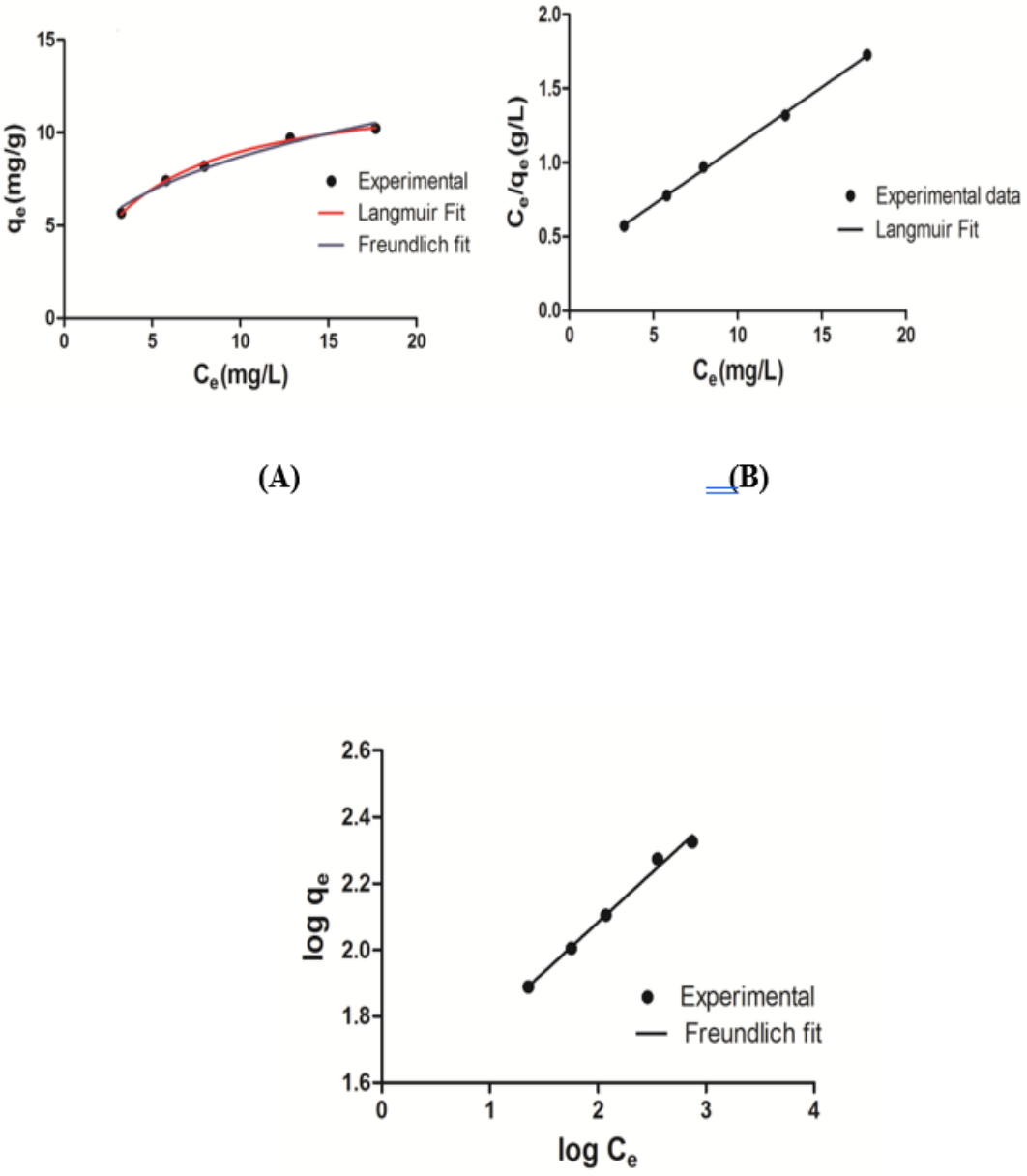

Figure 3.9: Adsorption Isotherm: (A) Non-Linear Langmuir Isotherm plot for DDR (B) Linear Langmuir Isotherm plot for DDR (C) Linear Freundlich Isotherm plot for DDR

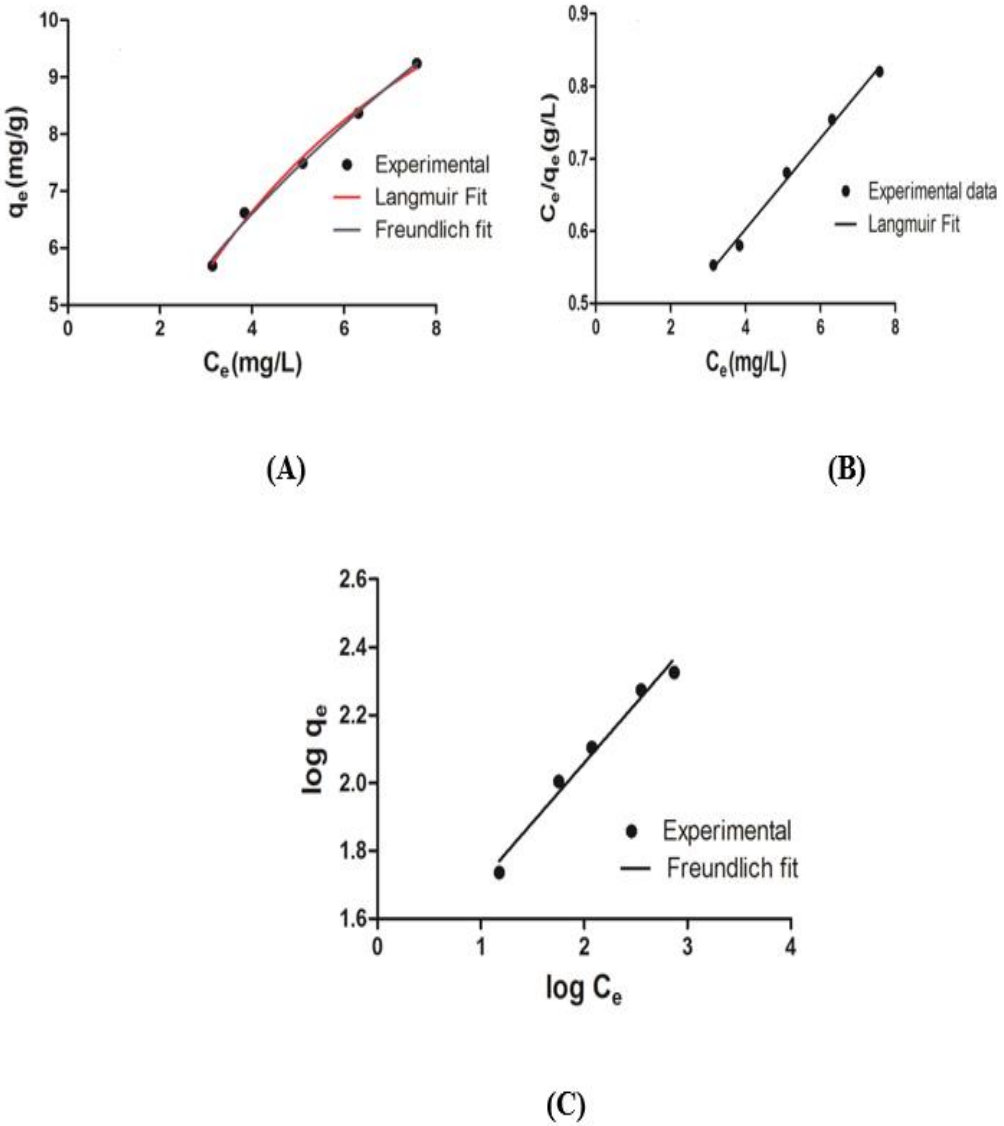

Figure 3.10: Adsorption Isotherm: (A) Non-Linear Langmuir Isotherm plot for DO (b) Linear Langmuir Isotherm plot for DO (c) Linear Freundlich Isotherm plot for DO

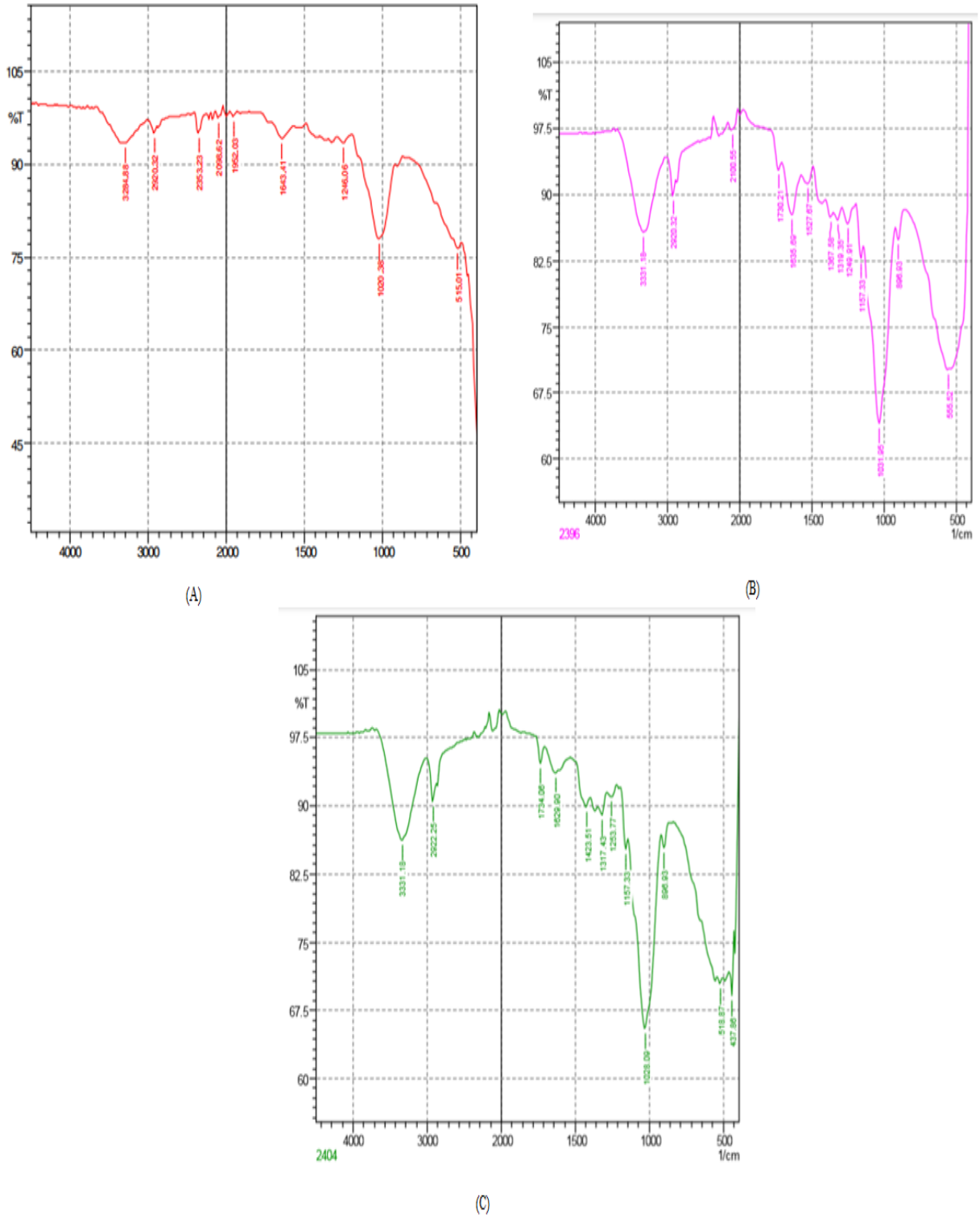

Figure 3.11: Spectroscopic Analysis: (A) FTIR of unadsorbed WB (B) FTIR of Acid Modified WB (C) FTIR of Alkali Modified WB

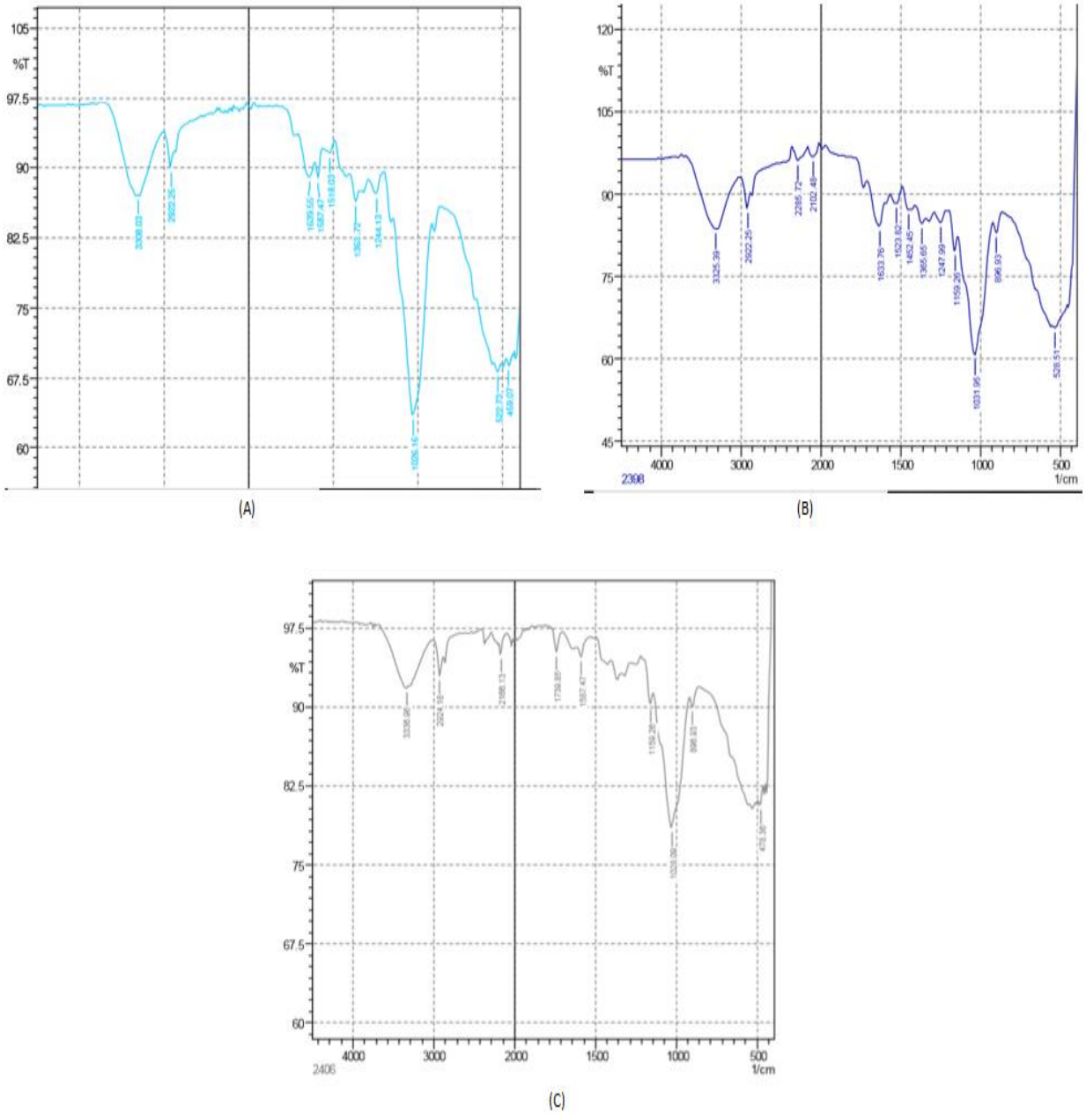

Figure 3.12: Spectroscopic Analysis: (A) FTIR of CV adsorbed on unmodified WB (B) FTIR of CV adsorbed on acid modified WB (C) FTIR of CV adsorbed on alkali modified WB

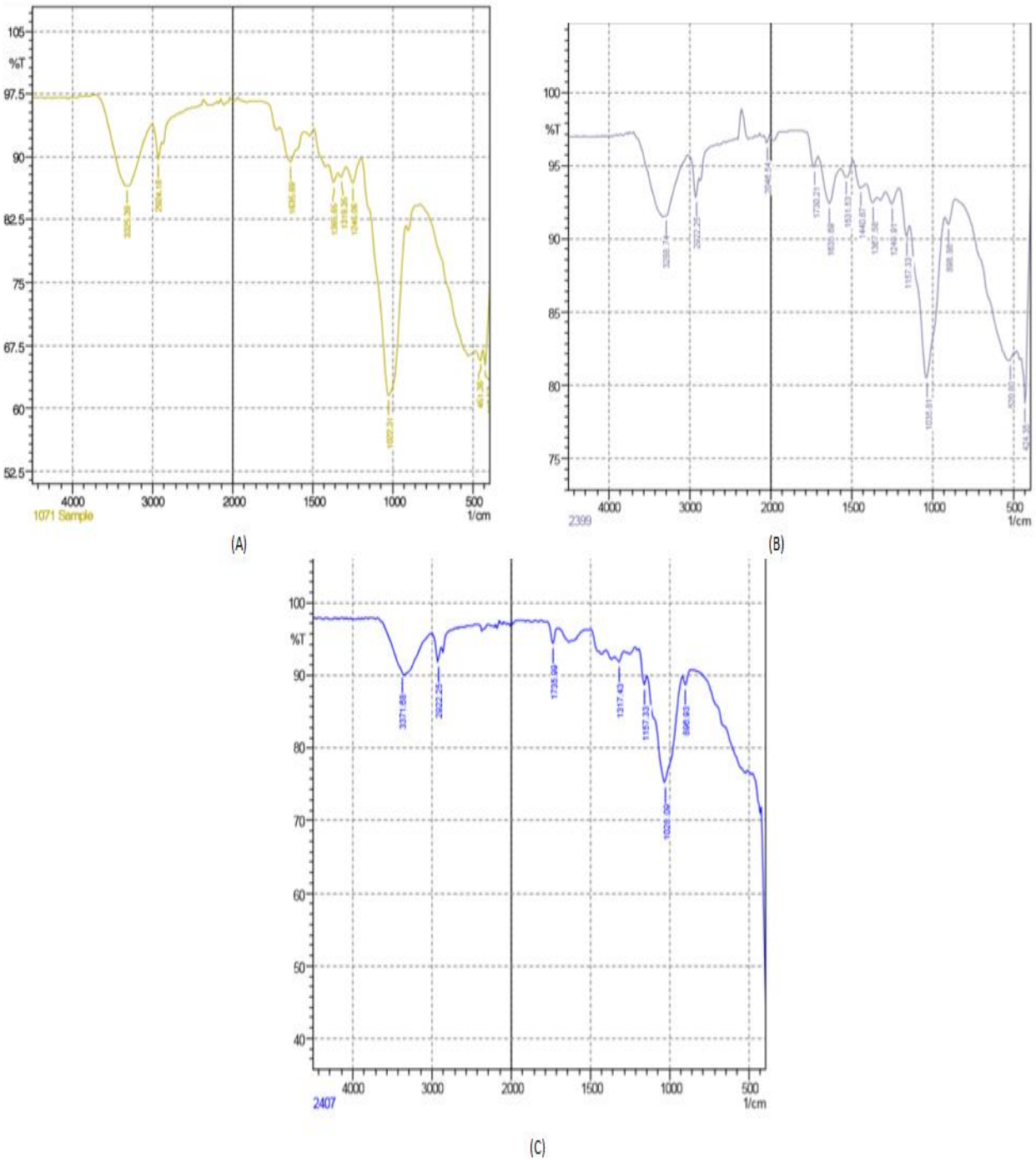

Figure 3.13: Spectroscopic Analysis: (A) FTIR of MG adsorbed on unmodified WB (B) FTIR of MG adsorbed on acid modified WB (C) FTIR of MG adsorbed on alkali modified WB

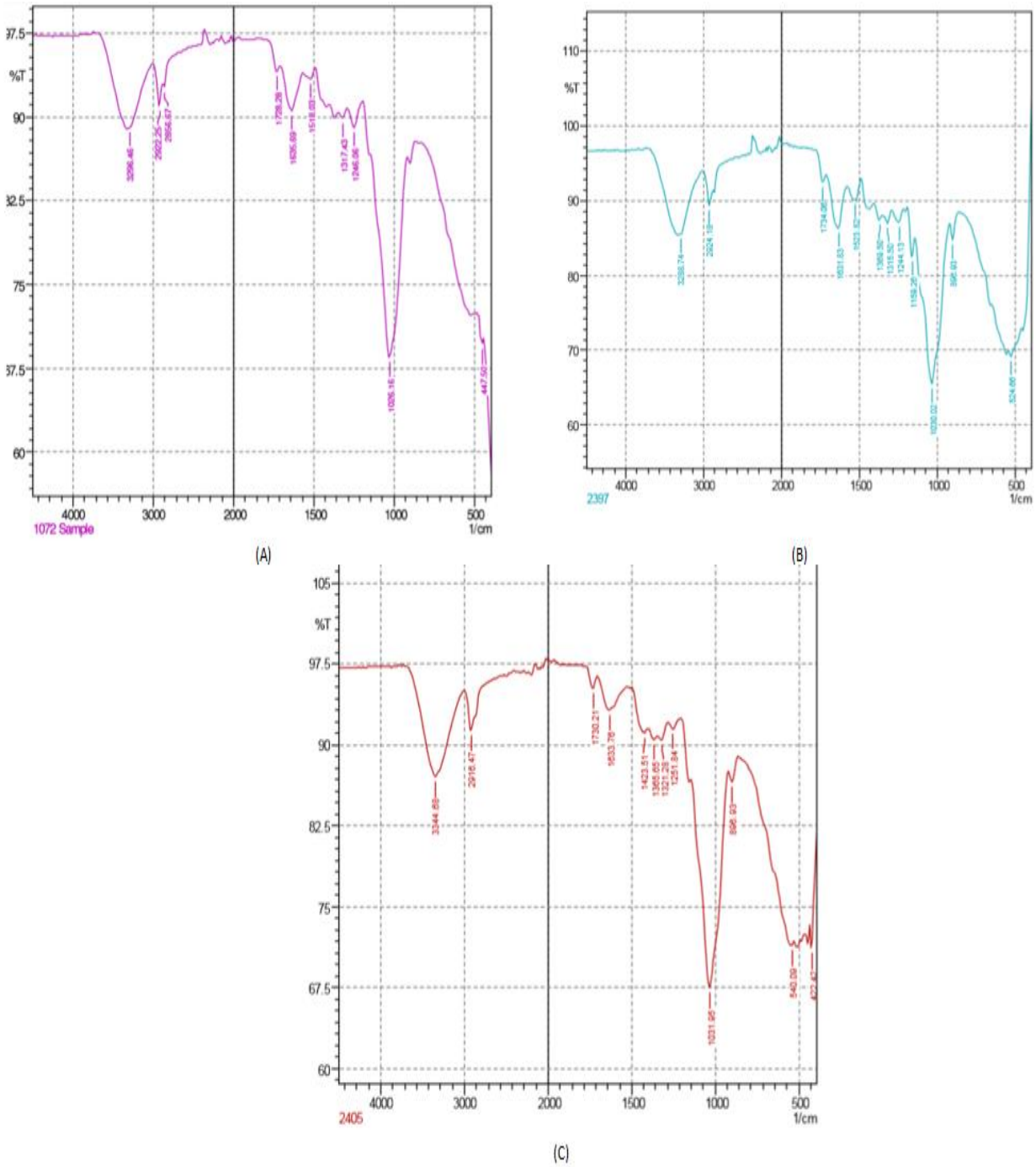

Figure 3.14: Spectroscopic Analysis: (A) FTIR of CR adsorbed on unmodified WB (B) FTIR of CR adsorbed on acid modified WB (C) FTIR of CR adsorbed on alkali modified WB

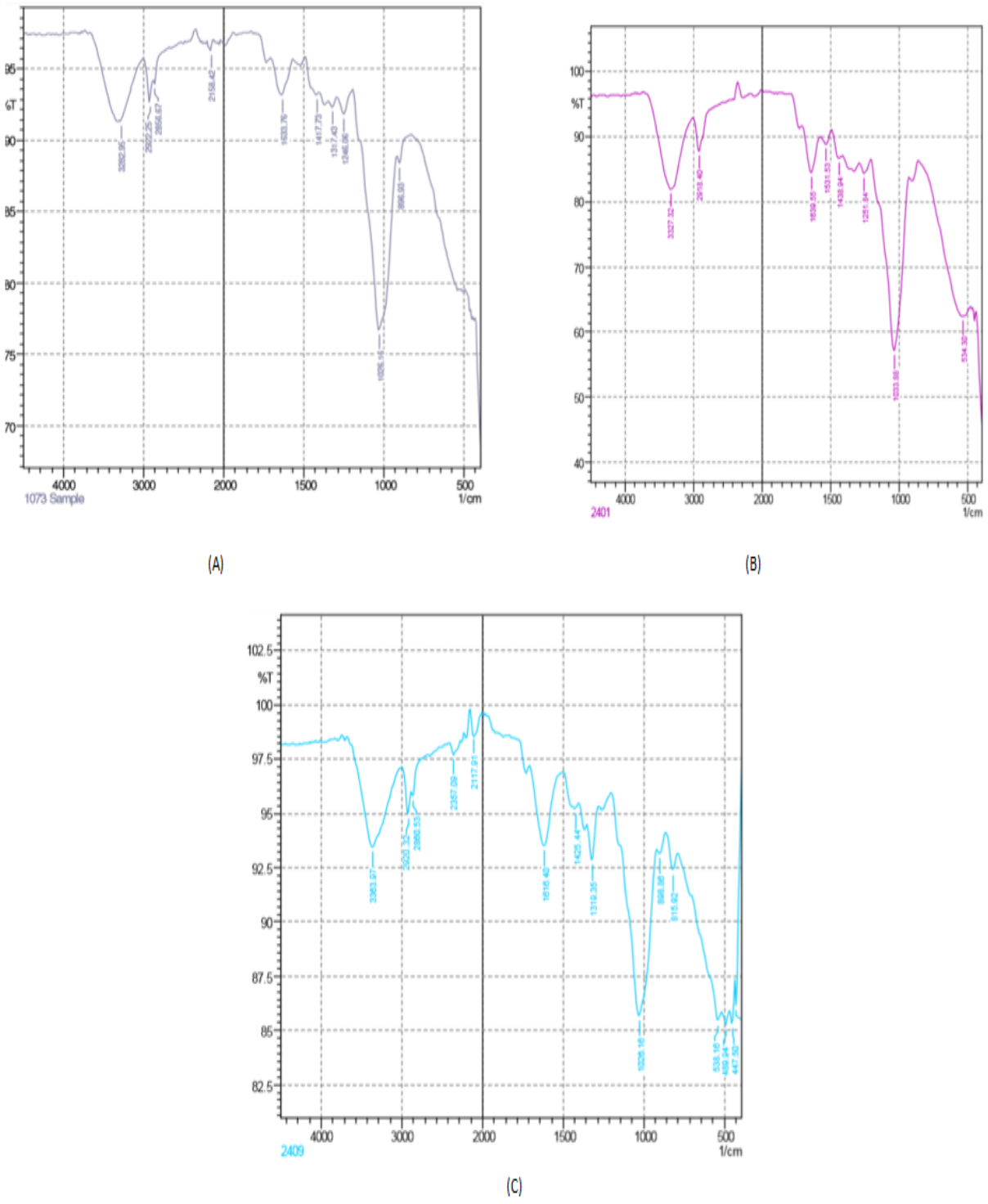

Figure 3.15: Spectroscopic Analysis: (A) FTIR of DDR adsorbed on unmodified WB (B) FTIR of DDR adsorbed on acid modified WB (C) FTIR of DDR adsorbed on alkali modified WB

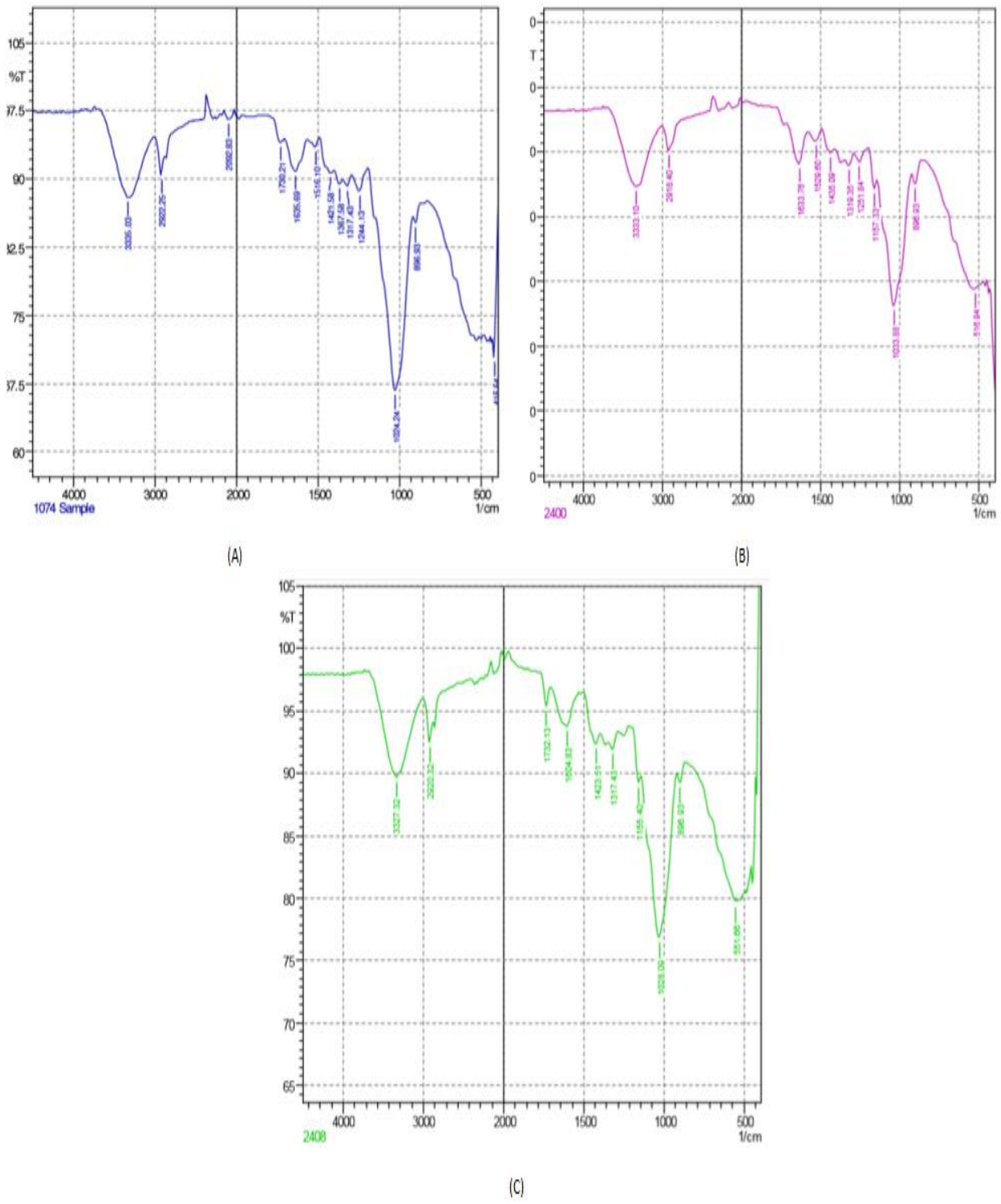

Figure 3.16: Spectroscopic Analysis: (A) FTIR of DO adsorbed on unmodified WB (B) FTIR of DO adsorbed on acid modified WB (C) FTIR of DO adsorbed on alkali modified WB

Chapter 4

Recycling potential of spent dye adsorbed substrate-fungal biomass for dye removal

4.1 Introduction

The white rot fungi at present, are known to be the most efficient microorganisms capable of widespread lignin degradation, and laccases has emerged as an important enzyme in delignification of lignin rich substrates (Sharma et al. 2005). Laccases have been playing a crucial role in bioremediation of toxic chemical wastes (Mayer and Staples 2002), dye degradation (Mendoza et al. 2011). They are also used in pre-treatment of lignocellulosic biomass to produce biofuels (Placido and Capareda 2015); in food processing industries (Minussi et al., 2002), detoxification of effluents from paper and pulp industries (Rodriguez-couto et al., 2005; Sadhasivam et al., 2010), petrochemical industries. They have also been reported to be used as a tool in biomedical industries, bioremediating agents to clean up herbicides (Crecchio et al., 1995; Dura and Esposito 2000; Bastos and Magan 2009) etc. It has even been exploited for the development of biosensors for detection of the presence of xenobiotics in the environment (Duran et al., 2002). The extracellular laccases are usually produced by different fungi during the stationary phase of their growth. It is affected by various cultivation factors (Rivera-Hoyos et al., 2013) amongst which the availability of carbon, nitrogen source, and concentration of inducer are very crucial factors that affects the enzyme production (Majeau et al., 2010).

Biosorption (adsorption) by agro-industrial lignocellulosic materials may be an alternative method for removal dyes from effluents. There are innumerable studies on biosorption potential of various lignocellulosic biomass (Kahraman and Yalcin 2005; Tunc et al., 2009; Wang and Chen 2009; Sen et al., 2011). Dye-adsorbed lignocelluloses interestingly create another source of pollution, might as such dye adsorbed lignocellulosic may persist in nature with dyes still bound to them. Thus, dye adsorption of lignocellulosic biomass might not completely solve the problem of dye pollution. Use of a combination of biosorption followed by solid-state fermentation (SSF) by some dye degrading strain of microorganism may be a good

alternative. It is already known that lignocellulosic substrates could be utilized as solid substrate during solid state fermentation (SSF) (Moldes et al., 2003; Rodriguez and Sanroman 2005; Shah et al., 2005; Stajic et al., 2006; Pant and Adholeya 2007; Boran and Yesilada 2011). Additionally, in a simultaneous manner it can be used as biosorbent. White rot fungi, the most important class of laccase producing organisms, can be cultured on such solid substrates. Therefore, these two methods, biosorption on lignocellulosic substrate and growth of microorganism on the dye adsorbed substrate for bio-decolorization by solid state fermentation, could be an integrated methodology for an effective bio-decolorization.

The aim of this study was thereby to use an isolated novel strain of Schizophyllum commune (Scizophyllum-S4) for the potential decolorization and degradation of the dye adsorbed agricultural waste material, wheat bran, which would not only provide a substratum for the growth but also for the enzyme production by the isolate, which could help in the mineralization of the dyes. The other important aspect of this study was the regeneration of the adsorbent after their usage and saturation, as most of the adsorbents are disposed off in the nature after usage, which poses potential threat to the environment being secondary pollutants. Thus, the reusability of the adsorbent was also evaluated in this study.

4.2 Review of Literature

Laccases, a benezenediol: oxygen oxidoreductase, E.C. 1.10.3.2 is a member of multicopper oxidase family. They could oxidize various aromatic amines and phenolic compounds by reduction of four electron of molecular oxygen to water (Piontek et al., 2002). Bacterial laccases have also been investigated and are well characterized (Martins et al., 2002), however, laccases are widely distributed in fungal groups like, Ascomycetes, Deuteromycetes and Basidiomycetes. They are particularly found abundantly in many of the lignin metabolising white rot fungi (Thurston 1994; Bourbonnais et al., 1995; Leontievsky 1997; Mayor and Staples 2002). Much rigorous research has been done on *Tremetes versicolor*, belonging to the group of basidiomycetes as it has been reported that the laccase produced by them exerts the highest redox potential among other laccases (Xin and Geng 2011). It has been shown that laccase produced by *Tremetes versicolor* is particularly promising for industrial applications for environmental remediation due to its high catalytic activity on various types of contaminants (Johannes and Majcherczyk 2000; Kim and Nicell 2006). But economically, high production and purification cost of laccase has turned out to be a limitation for their industrial application, thereby drawing the interest among the researchers for the development of a cost-effective enzyme production system through either discovery or isolation of potentially better microbial producers or through genetic modification of already known strains.

Laccase production by basidiomycetes using submerged fermentation has been reported extensively, though in nature these organisms mostly grows under solid-state conditions (El-Batal et al., 2015). SSF has thus emerged as a major thrust area to produce enzymes, and other economically important products. This may be a result of their high volume of production, low cost of production, reduced energy requirement, as a simple and natural fermentation substrate/media (Kapoor et al., 2000), lower waste output and higher product recovery. Solid state fermentation (SSF), is a type of fermentation process that occurs in absence or near absence of free liquids, whereby the microorganisms can grow on solid substrates (Pandey et al., 2002). Successful exploitation of SSF has been seen for food production (Hesseltine, 1983), animal feed production (Nigam and Singh 1996; Sandhu and Joshi 1997), biofuel production (Hinman et al., 1992; Ingram et al., 1998; Lapadatescu and Bonname 1999) and for

biological synthesis of different types of microbial enzymes (Gombart et al., 1999). SSF has been exploited presently in environmental biotechnology by various researchers for the remediation of industrial dyes for the purpose of decolorization (Nigam et al., 2000; Robinson et al., 2001). SSF has in fact enhanced the valuation of different types of agro-industrial residues for production of required enzymes as well to serve the purpose as an adsorbent (Sharma and Arora 2010; Kumar et al., 2013) for industrial pollutants, as, such residues are found to be greatly adapted to the fermentation conditions prevailing in solid state fermentation.

Although there are lots of studies on dye decolorization activity of white rot fungi during liquid fermentation; however, there have been limited studies on dye bio-decolorization and laccase production using of two-step method (Nigam et al., 2000; Robinson and Nigam 2008; Rodriguez et al., 2009; Kadam et al., 2011). A research has already shown *Funalia trogii* ATCC 200800 and *Trametes versicolor* ATCC200801 have already been shown to be effective in dye decolorization under liquid fermentation conditions (Yesilada et al., 2003). But there have been very few studies on dye decolorization activity of these such strains of white rot fungi by solid state fermentation of already dye adsorbed substrates.

Theoretically it has been seen that metal ions possesses the ability to stabilize and destabilize protein via which they can change the activity of the enzymes. Industrial wastewater on the other hand carries different types of metal ions. Researches has been done to determine the effect of metal ions in the process of biodegradation. It has been shown that metal ions like Cu^{2+}, Mo^{2+}, Zn^{2+} has positive effect on the enzyme system and changes the degradation rate of pollutants whereas presence of Fe^{2+}, Fe^{3+} has shown inhibition of the process. Whereby the inhibition of substrate conversion may be a consequence of hindrance of the electron transport system of the laccase enzyme by Fe-ions (Torres et al., 2003). Thus, optimization of various physiological parameters enables in the evaluation of the effect of different factors on the enzyme production by the isolated strain of microorganism under suitable or adverse environmental condition.

Researches are ongoing to evaluate the influence of various parameters like type of agricultural wastes, course of time, effect of pH, metal ions, mediators etc. on simultaneous production of laccase and dye degradation (Dassi et al., 2016). In one such study, it has been shown that a combination of wheat bran and corn straw has exhibited significant laccase production by *Trametes sp.* (32.09 U/ g ds), exhibiting the microbial product yield can get affected by a combination of different lignocellulosic substrates (Prakasham et al., 2006; Mahalaxmi et al., 2010).

Again, degradation of biphenyls, was exhibited around 10% on 4^{th} day of incubation, but around 90% on 10^{th} day of fermentation with *Tremetes sp*. showing the influence of time of incubation or fermentation for simultaneous degradation and laccase production (Zeng et al., 2017). The study of degradation of biphenyls is significant for the present study because, different varieties of benzidine derivative of biphenyls are used in dyes. In previous studies, it has also been shown that lignin modifying enzyme activities were stimulated by BPA (biphenyls) at a concentration till 300 mg/L (Shin et al., 2007) supporting the fact that pollutants on the other hand induces the production of the specific enzyme that can lead to their own degradation (Zeng et al., 2017). It has previously been reported that dye adsorbed lignocelluloses could also be used to produce ligninolytic enzymes (Rodrıguez et al., 2009).

Few previous researches have shown there are possibilities to use dye adsorbed lignocelluloses to produce ligninolytic enzymes by solid state fermentation process. But at the same time, it is worth mentioning that the production efficiency depends on the type of microbial strain as well on the substrate used (Tychanowicz et al., 2004). In a study for determination of an efficient substrate for ligninolytic substrate between wheat bran and rice husk, it was shown that wheat bran was efficient between the two, in enzyme production (480 U/mL) under solid state fermentation process probably because of their high content of carbohydrates, which can be used as carbon source, thereby proving to be an efficient substrate, for fungal growth (Tychanowicz et al., 2009). In another study it has been reported that malachite green adsorbed wheat bran was used for LiP (Lignin peroxidase) production under solid state fermentation by fungus, *Fomes sclerodermeus* (Papinutti et al., 2006).

As reported in chapter 2, *Schizophyllum*-S4 was found to be a potential laccase producer. Simultaneously efficiently removing dye in a plate assay. Wheat bran already been established to be an efficient dye adsorbent, as discussed in chapter 3, the current investigation was done to check the efficiency of the combination of Wb-F (Wheat Bran -Fungal) biomass for an efficient dye removal and degradation. The white rot fungi, *Schizophyllum*-S4, has shown a potential of laccase activity, 18.47 IU/mL on wheat bran. Again, wheat bran was also proven to be an efficient substrate for the efficient adsorption of different types of dyes of around dye removal efficiency of around 88% (Crystal Violet), 95% (Malachite Green), 97% (Congo Red), 93.5% (Disperse Dark Red) and 93.4% (Disperse Orange). Thereby, the next purpose of the present research was to explore the combination of wheat bran-fungal biomass (Wb-F) as an alternative substratum for laccase production with a simultaneous ability of the laccase produced to decolorize and degrade the dye been present on the bran already as well as reusage of the same biomass for the subsequent cycles for evaluation of the dye removal capacity of the combination produced.

4.3 Material and Methods

4.3.1 Materials

The reagents and chemicals used in this study were of analytical grade, purchased from Genei, New Delhi, India and HiMedia, Bangalore, India. Pure dyes of, Crystal Violet, Malachite Green, Congo Red were purchased from Loba Chemi, Mumbai, India. Two industrial grade dyes (Disperse Dark red and Disperse Orange) were procured from reputed textile industry in Ludhiana (name withheld), Punjab, India. Plastic and glasswares used were of polyvinyl chloride and borosilicate, purchased from local vendors. Culture media were purchased from HIMEDA, Mumbai, India.

4.3.2 Methods

4.3.2.1. Sub-culturing of *Schizophyllum*-S4

A 2mm disc of fungal mycelium was cut with the help of a sterile cork borer and aseptically transferred into a 2mm diameter well, cut onto the surface of a sterile wheat bran agar plate. Sub-culturing of Schizophyllum- S4 was performed by picking up the white mycelium with a cork borer and inoculated on wheat bran (WB) agar (Shafiq et al., 2015). After 4-5 days of their growth in the medium, producing white coloured mycelium, the culture was used for further experimentation for enzyme production on dye adsorbed wheat bran.

4.3.2.2 Preparation of substrate for evaluation of dye adsorbed, Wb-F biomass

Wheat bran purchased and processed as explained previously in chapter 2 (section 2.2.2.1) (Alzeydien 2015) was mixed with the dyes (CV, MG, CR, DDR and DO) under respective optimized conditions, as discussed in chapter 3. Under optimized pH of 8, 10, 4 and 5, 5 for CV, MG, CR, DDR and DO, respectively; incubation time of 180 mins for CV, DDR and DO and 210 mins for MG and CR; adsorbent dosage 100 mg/L for CV,CR, DDR and DO and 110 mg/L for MG; adsorbate dosage of 10 gm/L for CV, MG, CR, DDR and DO and incubated at optimized temperature of 30°C for CV, MG, CR and 40 and 45°C for DDR and DO respectively. After the respective optimized period of incubation for adsorption of each dye, 2 plugs of 2mm diameter of the isolate (Schizophyllum-S4) was inoculated and incubated at 30°C for the period to during which the assessment has to be made for enzyme production under the SSF condition.

4.3.2.3 Optimization for laccase production by Solid State Fermentation on dye adsorbed wheat bran by *Schizophyllum*-S4

4.3.2.3.1 Effect of days of incubation on laccase production by *Schizophyllum*-S4 under SSF using dye adsorbed wheat bran

The effect of days of incubation on laccase production by Schizophyllum-S4 was done for a period of 15 days. 5 gm of dye adsorbed wheat bran (of each dye, CV, MG, CR, DDR and DO) were taken to which 3.5 mL of moistening agent (preparation, as in chapter 2, section 2.2.2.6) was added to the bran and autoclaved at 121°C for 20 mins under 15 lbs pressure. After autoclaving 2, 2 mm plugs were cut with sterile cork borer and inoculated under a sterile condition under the static condition (Revankar and Lele 2007). After the desired growth period, the content of each flasks was crushed with the help of a glass rod by addition of 15 mL of distilled water and shaken for 10 mins in an orbital shaker at 200 rpm at a temperature of 55°C. The slurry obtained were squeezed through cheese cloth and filtered through Whatman filter paper 1. The filtrate obtained was centrifuged, in a cooling centrifuge (Remi, general purpose centrifuge, R-8C, 8X15 mL) at 5000 rpm for 10 minutes at 4°C (Singh et al., 2013). The supernatant obtained, considered as the crude enzyme, was collected for the measurement of extracellular laccase enzyme activity using the guaiacol assay method (Kalra et al., 2013). The control for the experiment was only wheat bran with organism with which a comparison was made base on the enzyme production. The maximum percent decolorization was done in 180 mins in case of CV and CR, DDR and Do whereas 210 mins in case of MG, which was also compared.

The laccase activity was enumerated spectrophotometrically (Shimadzu) by guaiacol assay method (as discussed in Chapter 2) by using the following formula (Kalra et al., 2013):

$$E.A = A \times (V/t) \times e \times v \qquad \text{(Eq.1)}$$

E.A being enzyme activity; A, absorbance; V, total volume of the mixture (mL); t, incubation time (mins); e, the extinction coefficient of guaiacol (0.6740 µM/ cm); v, the volume of the enzyme (mL).

Estimation of laccase produced under the above conditions and dye decolorization percentage was also determined, simultaneously, by monitoring the absorbance at the

maximum wavelength (CV, 582; MG, 616; CR, 497; DDR, 520; DO, 420) for each dye solution after the stipulated days of fungal cultivation by Solid State Fermentation. For calculation of the amount of dye decolorized from the dye adsorbed wheat bran a modified method was employed for the desorption of dyes from the pellets obtained after SSF (Yesilada et al., 2003). 50% methanol (solvent) was used as a solvent for the desorption of dye from the substrate. 5ml of solvent was added to 0.5gm of the dried dye saturated white rot fungus (S4) grown substrate. It was shaken rigorously for 12hrs in shaking incubator (at 200 rpm). Dye extract solvent was then obtained in test tubes after filtration. The solvent-dye mixture was then left for 1hr at 65 ºC to evaporate the solvent. After which the volume in the test tube was made upto 5ml with distilled water and concentration of the desorbed dye was then measured spectrophotometrically to calculate the percent decolorization (Robinson et al., 2002). All the experiments were executed in triplicates and standard deviation was applied to reduce the error (Ozmen and Yesilada 2012). The % decolorization of the dye was calculated using the following Eq.2 :

$$\% \text{ decolorization} = [\mathbf{D_0 - De} / \mathbf{D_0}] \times \mathbf{100} \quad \text{(Eq.2.)}$$

Whereby, D_o = Initial absorbance of dye solution and D_e = Final absorbance of dye solution

4.3.2.3.2 Effect of pH on laccase production by *Schizophyllum*-S4 under SSF using dye adsorbed wheat bran

The effect of pH was determined by performing the experiment at a pH range of 5, 5.5, 6, 6.5, 7, 7.5, 8, 8.5, 9 and 9.5 under the desired pH for each dye. After predetermined duration of incubation the sample was collected and enzyme activity was calculated in the same process as mentioned above (Revankar and Lele 2007; Singh et al., 2013 and Kalra et al., 2013).

4.3.2.3.3 Effect of temperature on laccase production by *Schizophyllum*-S4 under SSF using dye adsorbed wheat bran

The temperature range at which the experiment was conducted was from 25, 30, 35, 40, 45 to 50 ºC to evaluate the effect under new experimental condition. The optimized value obtained with days of incubation and pH were taken into consideration here and the experiment for enzyme activity calculation was done in the

same manner as above by taking growth of organism on wheat bran as a control for the estimation of enzyme activity in the above manner (Revankar and Lele 2007, Singh et al., 2013 and Kalra et al., 2013).

4.3.2.3.4 Effect of nitrogen source on laccase production by *Schizophyllum*-S4 under SSF using dye adsorbed wheat bran

The optimized temperature obtained, along with the other optimized values of incubation period and pH from the above experiments the effect of nitrogen sources (0.5, 1, 1.5, 2, 2.5 %) on the enzyme production on the dye adsorbed bran by Schizophyllum-S4 was conducted, with only wheat bran and organism as a control (Revankar and Lele 2007, Singh et al., 2013. After the optimized incubation period as obtained from above the enzyme was harvested and the enzyme activity was calculated by following the above-mentioned formula (Kalra et al., 2013).

4.3.2.3.5 Effect of copper sulphate on laccase production by *Schizophyllum*-S4 under SSF using dye adsorbed wheat bran

The optimal value obtained of nitrogen sources obtained from the above experimental set up, the next optimization of copper sulphate concentration was evaluated at a range of 0.2 mM, 0.4 mM, 0.6 mM, 0.8 mM and 1 mM with only wheat bran and organism as a control. The enzyme activity was calculated by following the above formula and the evaluation was done of the effect (Revankar and Lele 2007; Singh et al., 2013 and Kalra et al., 2013).

4.3.2.4 Chromatographic Analysis

An Agilent 1200 series HPLC system with DAD (Diode Array Detector) was used for the analysis of the samples obtained after 8 days of culturing of *Schizophylum*-S4 on the dye adsorbed wheat bran. 254 nm, stainless steel, Ultracarb, ODS column was used, with 5 µm, packing from Phenomenex (150x4.6 mm, I.D.) was used. RP-C18 guard pre-column was installed, to protect the analytical column. The injection volume 100 µL was introduced initially. Flow rate 1 mL/min at a temperature of 25 ^{o}C for separation column was maintained. The sample analysis was done using liquid chromatograph coupled to mass spectrometer operated by Turbolonspray ionization technique under a positive mode (Leite et al., 2016). The same experimentation was performed with 98% pure dye samples individually for comparison and calculation of

percent degradation of the dyes (CV, MG, CR, DDR and DO). The following formula was used for the calculation of percent degradation:

$$\text{Degradation \%} = 100 - \text{Purity of sample} \times \frac{\text{Area of sample}}{\text{Area of Standard}} \quad \text{(Eq.3)}$$

4.3.2.5 Comparison of recyclability of only bran and bran with *Schizophyllum*-S4 as an adsorbent for decolorization

For comparison of dye adsorption and percent decolorization by only bran and bran with S4 by solid state fermentation, 2 sets of experiments were done, one bran with dye (under their optimized condition as was performed in chapter 3) another with bran, dye and organism for simultaneous production of laccase and degradation of dyes under the optimized condition for laccase production on dye adsorbed bran by *Schizophylum* S4 (Zeng et al., 2017). After the cultivation by solid state fermentation for 14 days for CV and 15 days for MG, CR, DDR and 16 days for DO, the residual dye was extracted from each set up with 50% methanol as stated above (Robinson et al., 2002) and the filtrate was analysed spectrophotometrically. For reusability of the adsorbed bran obtained after the desorption studies the filtered loaded sorbent was collected and mixed with 10 ml of 0.5M HCl at 25 °C for 30 mins. Then the regenerated sorbent was washed with distilled water for reusage in the next run. For four cycles the process was repeated. In accordance to the following equation the regeneration efficiency (RE) was calculated (Elgarahy et al., 2019):

$$\text{RE (\%)} = \frac{\text{Amount of adsorbed dye (mg) at run } (n+1)}{\text{Amount of adsorbed dye (mg) at run (1)}} \times 100 \quad \text{(Eq.4)}$$

Where, n is number of regeneration cycle.

4.3.2.6 Statistical Analysis

All the experiments have been performed in triplicates. The mean values of the observed data have been presented and standard deviation (± SD) was calculated. The entire calculation was done by using Microsoft Office (version 10) Excel, 2010.

4.4 Result and Discussion

4.4.1 Optimization for laccase production by Solid State Fermentation on dye adsorbed wheat bran by *Schizophyllum*-S4

4.4.1.1 Effect of days of incubation on laccase production by *Schizophyllum*-S4 under SSF using dye adsorbed wheat bran

It has already been reported that lignocellulosic substrates with adsorbed dye could be used as a substrate for growth and laccase production by fungus (Nigam et al., 2000; Robinson and Nigam 2008; Rodriguez et al., 2009). As in chapter 3, the maximum % decolorization of dyes (CV, MG, CR, DDR and DO) on wheat bran under an optimized condition were 88, 96, 97, 93.7 and 93.4 % respectively. After the same experimental set up of adsorption, the dye adsorbed WB was used to conduct experiment for laccase production by Schizophyllum-S4 (the best isolate). The experiment conducted has revealed that there was a variation in laccase production with respect to days of incubation on dye adsorbed bran in comparison to bran without dye. As shown in chapter 2, while executing the effect of days of incubation on laccase production on wheat bran, on 8th day, Schzophyllum-S4 has produced 3.45 IU/mL laccase (maximum), which is comparable to 15th (3.42 IU/mL) , 13th (3.23 IU/mL) , 13th (3.58 IU/mL) , 15th (3.17 IU/mL) and 16th day (3.12 IU/mL) when grown on CV, MG, CR, DDR and DO respectively. However, the maximum enzyme production on dye adsorbed bran was shown on, 14th day in case of CV (3.69 IU/mL) with dye decolorization of 87.25%, 15th day for MG (3.84 IU/mL) with 91.31%, 15th day for CR (3.93 IU/mL) with 91.66 %, 15th day for DDR (3.16 IU/mL) with 76.94 % and 16th day for DO (3.12 IU/mL) with 78.38 % decolorization. Though, if enzyme activity and percent dye decolorization is compared with respect to days of incubation it was not like the day with maximum decolorization has shown an increased enzyme activity too. On the contrary in case of MG, 93% decolorization was shown on 14th day (3.72 IU/mL enzyme production) but maximum enzyme production of 3.84 IU/mL was shown on 15th day (91.31% decolorization). CR has also shown variation with 91.78% decolorization on 16th day (3.86 IU/mL) while with maximum enzyme production 3.93 IU/mL on 15th day. DDR and DO has not shown as such variation but both the enzyme production and dye decolorization percentage were less in comparison to other dyes.

In a study with *Funalia trogii*, it was found that it had shown a maximum laccase activity of 2.78 U/mL on the 10th day in wheat bran adsorbed with Astrazon Black dye, which had also shown a decrease in laccase activity after this day. Again, when the same medium was used for laccase production by T. versicolor, it had produced 2.74 U/mL of laccase on the 10th day and highest was shown on the 20th day with 3.17 U/ml laccase production (Ozmen and Yesilada 2012).

4.4.1.2 Effect of pH for laccase production by *Schizophyllum*-S4 by SSF on dye adsorbed wheat bran

The effect of pH on laccase production on dye adsorbed wheat bran has shown the maximum laccase production, 8.14, 7.46, 8.98, 5.38 and 5.35 IU/mL at a pH of 8.5 for CV, MG, CR, DDR and at 8 for DO respectively on 14^{th} day of incubation for CV, 15^{th} day for MG, CR and DDR and 16^{th} day for DO. Whereas, when *Schizophyllum*-S4 was grown on wheat bran alone, the optimum pH for laccase production was 5.5 with a maximum laccase activity of 3.93 IU/mL (Chapter 2). It has been reported that at an acidic pH the fungal laccases have shown higher stability (Leonowicz et al., 1884), however, it has also been said that exceptions are also available (Meyer 1986). If laccase shows stability at an elevated pH (8-8.5), they are of special importance in pulp bleaching etc. (Sharma et al., 2014).

4.4.1.3 Effect of temperature for laccase production by *Schizophyllum*- S4 by SSF on dye adsorbed wheat bran

The effect of temperature on evaluation has shown 35 ºC to be optimum for the maximum laccase activity on the dye adsorbed bran by the isolate. The respective enzyme activity on dye adsorbed bran with CV, MG, CR, DDR, DO being 8.79, 8.25, 9.58, 6.87, 6.48 IU/mL, exhibiting an increase in the laccase activity in comparison to 30 ºC by about 7.3, 9.5, 6, 21.6 and 17 % respectively. The respective dye decolorization percentage being 94.91, 96.85, 98.76, 87.69 and 87.97 % with an overall increase in % decolorization with an increase in temperature. Review suggests that temperature profiles for laccase activity shows an optimum temperature range between 50 and 70ºC, like other extracellular ligninolytic enzymes (Baldrian 2005). Though, few enzymes with optima below 35 ºC have also been described like that of Ganoderma lucidum, its highest enzyme activity has been shown at 25ºC (Ko, et al., 2005).

4.4.1.4 Effect of yeast extract for laccase production by *Schizophyllum*-S4 by SSF on dye adsorbed wheat bran

Yeast Extract was used as a nitrogen source, as while optimization for laccase production (Chapter 2), between the two nitrogen sources, yeast extract had given a better result in comparison to ammonium sulphate for laccase production by *Schizophyllum*-S4 strain. While optimization, in a similar manner on dye adsorbed wheat bran 1% yeast extract has given a better result with enzyme production around 9.15, 8.97, 9.52, 7.89 and 7.93 IU/mL laccase production on CV, MG, CR, DDR and DO adsorbed bran respectively. Though not a very significant increase was observed with respect to dye decolorization, with 95.36, 96.99, 98.78, 87.75 and 87.98 % with respect to CV, MG, CR, DDR and DO. A study has shown 1% yeast extract to be its optimum concentration amongst other organic nitrogen source for the decolorization of amaranth with around 75% decolorization (Revankar and Lele 2007).

4.4.1.5 Effect of copper sulphate for laccase production by *Schizophyllum*-S4 by SSF on dye adsorbed wheat bran

The optimum copper sulphate concentration was found to be 0.4mM with laccase activity 9.57, 9.24, 10.59, 8.31 and 8.42 IU/mL with corresponding percent decolorization 95.48, 97.01, 98.99, 88.26 and 88.18 on CV, MG, CR, DDR and DO adsorbed bran respectively. The study also reveals that with increase of copper sulphate ion concentration the laccase activity reduces but the dye decolorization reduction does not reduce proportionately i.e. the dye decolorization percentage reduction is slow in comparison to reduction in laccase activity. Heavy metals can be toxic for white rot fungi, but they do affect the growth and production of extracellular enzymes by them (Akpinar and Urek 2017). Copper sulphate is an efficient inducer for laccase production though not much is known about the essential role played by them in lignocellulose degradation (Baldrian, 2003). Laccase, as already been stated that is a blue copper oxidase, containing four copper atoms per molecule at the catalytic centre, helps in the catalysis of four electron reduction of oxygen to form water molecule. Additionally, it has also been reported that copper also has effect at the transcriptional level of the laccase synthesis. This metal, thereby, has the capacity to regulate the mRNA levels of laccase encoding genes in different fungi (Vrsanka et al., 2016). Though it is known that copper atoms serve as a cofactor in the catalytic

core of laccase. Thus, a very less concentration (in millimolar range) can affect the production of active enzyme positively (Patel et al., 2009; Bertrand et al., 2013). A study conducted on *P. eryngii* has revealed that the maximum laccase production was observed with 70 µM of copper sulphate but decreased when the concentration was increased beyond that. The maximum laccase activity shown by the same organism with the said copper sulphate concentration was 2193. 056 ± 50.4 U/mL (Akpinar and Urek 2017). Another study has revealed that copper sulphate supplementation at a concentration of 1 mM to defined basal medium could induce laccase production by *Tremetes versicolor* under SSF condition (Xin and Geng 2011). Different studies proposed that copper ions regulate the laccase activity by induction of gene expression or by regulation of translational or post translational activity (Fonseca et al., 2010). The result obtained in our study can be supported by the findings obtained in another experiment which shows a reduction of laccase production with copper sulphate concentration beyond 100 µM by *P. ostreatus* (Elsayed et al., 2012). Another study has shown that metal ions (Cu^{2+}, Zn^{2+} and Mo^{2+}) at a concentration 1mM did not exert a significant effect on degradation of bisphenol A by organism (Zeng et al., 2017), the result of which concurs with the present study.

It has been reported that laccase has an immense potential for azo-dye reduction (Chivulula et al., 1995; Kirby et al., 2000; Peralta et al., 2003; Blanquez et al., 2004; Novotny et al., 2004). These enzymes are phenol oxidases with multicopper molecules. They possess the ability to decolorize and degrade dyes by following an extensive non-specific free radical mechanism leading to the formation of phenolic compounds, which thereby avoids the formation of toxic aromatic amines (Chivukula et al., 1995; Wong and Yu, 1999).

In another study of decolorization of azo dyes like Direct Blue 71 and Reactive Black 5 by *T.hirsuta*, it had been shown that decolorization of such dyes were mainly attributed by the extracellular enzymes, like laccase produced by it. This study was also in agreement with another previous study with *T. hispida* (Rodriquez et al., 1999). It has been reported that 1-amino-substituted anthraquinoid dyes have shown to be good substrates for T. hirsute laccase production. In comparison to Reactive Black 5, Direct Blue 71 was shown to be a better substrate for laccase production by

T.hirsuta (Abadulla et al., 2000). The study thereby supported this study that the dye adsorbed substrate though slowed down the laccase production but did not hinder the enzyme and could support the enzyme production also, though at a slower rate.

4.4.2 Chromatographic Analysis

The HPLC-DAD chromatograms obtained of the desorbed CV, MG, CR, DDR and DO after treatment with *Schizophylum*-S4 under SSF condition was compared with the chromatogram of each of the dyes respectively, of 98% purity, for the determination of percent degradation. The result has revealed that in case of CV the peak obtained for pure sample at a retention time between 5.7 to 6.8 mins shows a decrease in the peak area (retention time 6.215 mins) when compared with its corresponding treated sample. This reduction in peak area depicts the degradation of the dye by 60.94% with the formation of few degraded products. Whereas, for MG at a retention time between 3.141 min, the peak shows a sharp decrease, exhibiting around 62.47% degradation. CR has shown 48.26% degradation at a retention time of 3.9846 mins. Whereas, DDR and DO has shown 51.57% and 44.01% degradation at a retention time of 3.918 min and 6.411 min respectively. It has been shown in another study that a less intense peak of m/e 374, was may be few to the formation of an ion by the rearrangement of neutral crystal violet, depicting the protonation of a tertiary nitrogen to form a leuco crystal violet cation having a molecular weight around 374 (Bumpus and Brock 1988). The study revealed that the major fragment ion of m/e 104 (typical of N-methylamine) and none of the fragment of m/e 121 (that of N,N-dimethylaniline) was shown confirming the structural assignment of N,N',N"-trimethyl pararosaniline. In another study of degradation of malachite green (MG) by *P.coccineus* IUM0032 species, the HPLC analysis has shown that, the untreated sample had shown a sharp peak after 20 mins, whereas, the treated sample did not show the same, depicting it to be free from UV absorbing compound along with high degrading ability by the organism. The incubation period given in the study was of 3 days, thus, the study also depicted that there was an increase in the laccase activity gradually reaching to 38 U/mL during the 3 days of incubation and decrease in lignin peroxidase enzyme which was initially more, proving that laccase was responsible for the degradation to take place (Kang et al., 2014). The above study thereby has supported the present study which also has shown that laccase activity was around

1.38 IU/mL of the isolate, which was in a gradual increasing mode. In regard to the other ligninolytic enzymes produced by the organism, it has also been shown in chapter 2 that in comparison laccase, the other ligninolytic enzymes produced by *Scizophyllum*-S4 was always less, thereby proving that laccase was the enzyme responsible for the degradation of the dye.

4.4.3 Comparison of recyclability of only bran and bran with *Schizophyllum*-S4 as an adsorbent for decolorization

The concept behind this experimentation was to reuse the dye adsorbed wheat bran for laccase production by white rot fungi. The fungi during the process would degrade the dye adsorbed on the bran before been disposed of to the environment, as the dye adsorbed lignocellulosic material may pose an environmental pollution problem, if discarded untreated. The result obtained was, the dye removal capacity of bran with microorganism was more in comparison to only bran. In case of CV in the first cycle, the percent removal was 87.85 on bran but 95.38 on bran with S4, as in Table 4.7, showing around 7.89 % increase in dye removal percentage. In case of MG in the first cycle, though not much difference was observed with around 1% increase, whereas in case of CR, it has shown around 2% increase in dye removal in case of bran with S4 in comparison to only bran. Though with DDR and DO it has shown decrease by 1.4% in dye decolorization percentage which may be because the culture in presence of the dye has gone for producing laccase very slowly as depicted in the Table 4.4.1, on 15^{th} and 16^{th} day , DDR and DO respectively was producing laccase 3.15 and 3.12 IU/mL which may go for slow increase with prolong duration of incubation. The next subsequent usage of the dye adsorbed bran with organism has shown a very significant result with removal percentage of 61.89, 66.28, 68.79, 61.77 and 64.38 % removal till 5^{th} cycle, depicting the involvement of the fungal mycelium as an adsorbent along with the wheat bran in the process of decolorization.

4.5 Reference

1. Abadulla E, Tznanov T, Costa S, Robra KH, Paulo AC, Gubitz GM. 2000 Decolorization and detoxification of textile dyes with a laccase from *Tremetes hirsute*. *App Env Micro* 66: 3357-3362.
2. Akazdam S, Chafi M, Yassine W, Gourich B. 2017. Removal of Acid Orange 7 Dye from Aqueous Solution Using the Exchange Resin Amberlite FPA-98 as an Efficient Adsorbent: Kinetics, Isotherms, and Thermodynamics Study. *J. Mat Env Sc* 8: 2993-3012.
3. Alzaydien AS. 2015. Adsorption Behavior of Methyl Orange onto Wheat Bran: Role of Surface and pH. *Ori J Chem* 31: 643-651.
4. Baldrian P. 2005. Fungal laccases - occurrence and properties. *FEMS Micro Rev* 30: 215–242.
5. Bastos AC, Magan N. 2009. *Trametes versicolor*: potential for atrazine bioremediation in calcareous clay soil, under low water availability conditions. *Int Biodet Biodeg* 63: 389–394.
6. Blanquez P, Casas N, Font X, Gabarrell X, Sarra M, Caminal G, Vicent T.2004. Mechanism of textile metal dye biotransformation by *Trametes versicolour*. *J Wat Res* 38: 2166–2172.
7. Boran F and Yesilada O. 2011. Enhanced production of laccase by fungi under solid substrate fermentation condition. *Biores* 6: 4404-4416.
8. Bourbonnais R, Paice MG, Reid ID, Lanthier P, Yaguchi M. 1995. Lignin oxidation by laccase isozymes from *Trametes versicolor* and role of the mediator 2,2'-azinobis(3ethylbenzthiazoline-6-sulfonate) in kraft lignin depolymerization. *App Env Micro* 61: 1876–1880.
9. Bumpus JA and Brock BJ. 1988. Biodegradation of crystal violet by white rot fungus, *Phaenerochaete chrysosporium*. *App Env Micro* 54: 1143-1150.
10. Chivukula M, Renganathan V. 1995. Phenolic azo dye oxidation by laccase from *Pyricularia oryzae*. *App Env Micro* 61: 4347–4377.
11. Crecchio C, Ruggiero P, Pizzigallo MDR. 1995. Polyphenoloxidases immobilized in organic gels: properties and applications in the detoxification of aromatic compounds. *Biotech Bioeng* 48: 585–591.

12. Dassi D, Mechichi HZ, Frikha F, Rodriguez-Couto S, Nasri M, Mechichi T. 2016. Sawdust waste as a low-cost support -substrate for laccases production and adsorbent for azo dyes decolorization. *J Env Health Sc Eng* 14: 1-12.
13. Dura ´n N, Esposito E. 2000. Potential applications of oxidative enzymes and phenoloxidase-like compounds in wastewater and soil treatment: a review. *App Cat B: Environ* 28: 83–99.
14. Duran N, Rosa MA, D'Annibale A, Gianfreda L. 2002. Applications of laccases and tyrosinases (phenoloxidases) immobilized on different supports. *Enz Micro Tech* 31: 907–931.
15. El-Batal, AI, El-Kenawy NM, Yassin AS, Amin MA. 2015. Laccase production by *Pleurotus ostreatus* and its application in synthesis of gold nanoparticles, *Biotech Rep* 5: 31–39.
16. Elgarahy AM, Elwakeel KZ, Elshoubaky GA, Mohammad SH. 2019. Microwave accelerated sorption of cationic dyes onto green marine algal biomass. *Env Sc Pol Res* 26: 22704-22722.
17. Elsayed MA, Mohamed MH, Ali M, Bakry MHE, Abdelmageed MO. 2012. Optimization of cultural and nutritional parameters for the production of laccase by *Pleurotus ostreatus* ARC280. *Bra Biotech J* 2: 115–132.
18. Fonseca MI, Shimizu E, Zapata PD, Villalba LL. 2010. Copper inducing effect on laccase production of white rot fungi native from Misiones (Argentina). *Enz Micro Tech* 46: 534–539.
19. Gombert AK, Pinto AL, Castilho LR, Freire DMG. 1999. High yield Bacillus subtilis protease production by solid state fermentation. *Pro Biochem* 35: 85 – 90.
20. Hesseltine CW. 1983. Microbiology of oriental fermented food. *Ann Rev Micro* 37: 575–601.
21. Hinman ND, Schell DJ, Riley CJ, Bergeron PW, Walter PJ. 1992. Preliminary estimate of the cost of ethanol production for SSF technology. *App Biochem Biotech* 34(5): 639–649.
22. Ingram LO, Gomez PF, Lai X, Moniruzzaman M, Wood BE, Yomano LP, York SW. 1998. Metabolic engineering of bacteria for ethanol production. *Biotech Bioeng* 58: 204–214.

23. Johannes C, Majcherczyk A. 2000. Natural mediators in the oxidation of polycyclic aromatic hydrocarbons by laccase mediator systems. *App Env Micro* 66: 524–528.
24. Kadam AA, Telke AA, Jagtap SS, Govindwar SP. 2011. Decolorization of adsorbed textile dyes by developed consortium of Pseudomonas sp. SUK1 and *Aspergillus ochraceus* NCIM-1146 under solid state fermentation. *J Haz Mat* 189: 486-494.
25. Kahraman S and Yalcin P. 2005. Removal of dyes from aqueous solution using various agricultural wastes as biosorbent. *Fres Env Bull* 14: 1196-1201.
26. Kang HW, Yang YH, Kim SW, Kim S, Ro HS. 2014. Decolorization of triphenyl methane dyes by wild mushroom. *Biotech Biopro Eng* 19: 519-525.
27. Kapoor M, Beg QK, Bhushan B, Dadhich KS, Hoondal GS. 2000. Production and partial purification and characterization of a thermo-alkali stable poly-galacturonase from *Bacillus sp*. MG-cp-2. *Pro Biochem* 36: 467–473.
28. Kim YJ, Nicell JA. 2006. Impact of reaction conditions on the laccase-catalyzed conversion of bisphenol A. *Biores Tech* 97: 1431–1442.
29. Kirby N, Marchan R, McMullan G. 2000. Decolourization of synthetic textile dyes by *Phlebia tremellosa*. *FEMS Micro Let* 188: 93–96.
30. Ko EM, Leem YE, Choi H. 2001. Purification and characterization of laccase isozymes from the white-rot basidiomycete *Ganoderma lucidum. App Micro Biotech* 57: 98–102.
31. Kumar NSM, Ramasamy R, Manonmani, HK. 2013. Production and optimization of L- asparaginase from *Cladosporium* sp. using agricultural residues in solid state fermentation. *Indus Crops Pdts* 43: 150–8.
32. Lapadatescu C and Bonnarme P. 1999. Production of aryl metabolites in solid state fermentation of white rot fungus *Bjerkandera adusta*. *Biotech Let* 21: 763 –769.
33. Leite LS, Maselli BS, Umbuzeiro GA, Nogueiro RPF. 2016. Monitoring ecotoxicity of disperse red 1 dye during photo-fenton degradation. *Chem Elsevier* 148: 511-517.

34. Leonowicz A, Edgehill RU, Bollag JM. 1884. The effect of pH on the transformation of syringic and vanillic acids by the laccases of Rhizoctonia praticola and Trametes versicolor. *Arch Micro*137: 89–96.
35. Leontievsky A, Myasoedova N, Pozdnyakova N, Golovleva L.1997. Yellow laccase of *Panus tigrinus* oxidizes nonphenolic substrates without electron-transfer mediators. *FEBS Let* 413: 446–448.
36. Mahalaxmi Y, Sathish T, SubbaRao C, Prakasham, RS. 2010. Corn husk as a novel substrate for the production of rifamycin B by isolated *Amycolatopsis sp*. RSP 3 under SSF. *Pro Biochem* 45: 47–53.
37. Majeau JA, Brar SK, Tyagi RD. 2010. Laccases for removal of recalcitrant and emerging pollutants. *Biores Tech* 101: 2331–2350.
38. Martins LO, Soares CM, Pereira MM, Teixeira M, Costa T, Jones GH, Henriques AO. 2002. Molecular and biochemical characterization of a highly stable bacterial laccase that occurs as a structural component of the *Bacillus subtilis* endospore coat. *J Bio Chem* 277: 18849–18859.
39. Mayer AM, Staples RC. 2002. Laccase: new functions for an old enzyme. *Phytochem* 60: 551–565.
40. Mayer AM. 1986. Polyphenol oxidases in plants-recent progress, *Phytochem* 26: 11–20.
41. Mendoza L, Jonstrup M, Hatti- Kaul R, Mattiasson B. 2011. Azo dye decolorization by a laccase/mediator system in a membrane reactor: enzyme and mediator reusability. *Enz Micro Tech* 49: 478–484.
42. Minussi RC, Pastore GM, Dura ´n, N. 2002. Potential applications of laccase in the food industry. *Trends Food Sc Tech* 13: 205–216.
43. Moldes D, Gallego PP, Couto SR, Sanroman A. 2003. Grape seeds: The best lignocellulosic waste to produce laccase by solid state cultures of *Trametes hirsute*. *Biotech Let* 25: 491-495.
44. Nigam P and Singh D. 1996. Processing of agricultural wastes in solid state fermentation of microbial protein production. *J Sc Ind Res* 55: 373–380.
45. Nigam P, Armour G, Banat IM, Singh D, Marchant R. 2000. Physical removal of textile dyes from effluents and solid-state fermentation of dye-adsorbed agricultural residues. *Biores Tech* 72: 219-226.

46. Novotny C, Svobodova K, Kasinath A, Erbanova P. 2004. Biodegradation of synthetic dyes by *Irpex lacteus* under various growth conditions. *Int J Biodet Biodeg* 54: 215–223.
47. Ozmen N and Yesilada O. 2012. Valorization and biodecolorization of dye adsorbed on lignocellulosics using white rot fungi. Biores Tech 7: 1656-1665.
48. Palmieri G, Cennamo G, Faraco V, Amoresano A, Sannia G, Giardina P. 2003. Atypical laccase isoenzymes from copper supplemented *Pleurotus ostreatus* cultures. *Enz Micro Tech* 33: 220–230.
49. Pandey A, Soccol CR, Mitchell D. 2000. New developments in solid fermentation: I-bioprocesses and products. *Pro Biochem* 35: 1153–1169.
50. Pant D and Adholeya A. 2007. Enhanced production of ligninolytic enzymes and decolorization of molasses distillery wastewater by fungi under solid state fermentation. *Biodeg* 18: 747-659.
51. Papinutti L, Mouso N, Forchiassin F. 2006. Removal and degradation of the fungicide dye malachite green from aqueous solution using the system wheat bran—*Fomes sclerodermeus*. *Enz Micro Tech* 39: 848–853.
52. Peralta-Zamora P, Pereira CM, Tiburtius ERL, Moraes SG, Rosa MA, Minussi RC, Duran N. 2003. Decolourization of reactive dyes by immobilized laccase. *App Cat B: Env* 42: 131–144.
53. Piontek K, Antorini M, Choinowski T. 2002. Crystal structure of a laccase from the fungus *Trametes versicolor* at 1.90-A resolution containing a full complement of coppers. *J Bio Chem* 277: 37663–37669.
54. Placido J and Capareda S. 2015. Ligninolytic enzymes: a biotechnological alternative for bioethanol production. *Biores Bio* 2: 1–12.
55. Prakasham RS, Rao S, Sarma PN. 2006. Green gram husk–an inexpensive substrate for alkaline protease production by *Bacillus sp*. in solid-state fermentation. *Biores Tech* 97: 1449–1454.
56. Revankar MS, Lele SS. 2007. Synthetic dye decolorization by white rot fungus, Ganoderma sp. WR-1. *Biores Tech* 98: 775-780.
57. Rivera-Hoyos CM, Morales-Alvarez ED, Poutou-Pinales RA, Pedroza-Rodriguez AM, Rodriguez-Vazquez R, Delgado-Boada JM. 2013. Fungal laccases. *Fun Bio Rev* 27: 67–82.

58. Robinson T and Nigam P. 2008. Remediation of textile dye wastewater using a white-rot fungus *Bjerkandera adusta* through solid-state fermentation (SSF). *App Biochem Biotech* 151: 618-628.
59. Robinson T, Chandran B, Nigam P. 2002. Studies on desorption of individual textile dyes and a synthetic dye effluent from dye-adsorbed agricultural residues using solvents. *Biores Tech* 84: 299-301.
60. Robinson T, McMullan G, Marchant R, Nigam P. 2001. Remediation of dyes in textile effluent: a critical review on current treatment technologies with a proposed alternative. *Biores Tech* 77: 247–255.
61. Rodriguez E, Pickard MA, Vazquez-Duhalt R. 1999. Industrial dye decolorization by laccases from ligninolytic fungi. *Curr Micro* 38:27–32.
62. Rodrıguez-Couto S, Osma JF, Toca-Herrera JL. 2009. Removal of synthetic dyes by an eco-friendly strategy. *Eng LifeSc* 9:116–123.
63. Rodriquez-Couto S and Sanroman MA. 2005. Coconut flesh: A novel raw material for laccase production by *Trametes hirsuta* under solid-state conditions. Application to Lissamine Green B decolourization. *J Food Eng* 71: 208-213.
64. Sadhasivam S, Savitha S, Swaminathan K. 2010. Deployment of *Trichoderma harzianum* WL1 laccase in pulp bleaching and paper industry effluent treatment. *J Cleaner Pro* 18: 799–806.
65. Sandhu DK and Joshi VK. 1997. Solid State Fermentation of apple pomace for concomitant production of ethanol and animal feed. *J Sc Ind Res* 56: 86 –90.
66. Sen TK, Afroze S, Ang HM. 2011. Equilibrium, kinetics and mechanism of removal of Methylene Blue from aqueous solution by adsorption onto pine-cone biomass of Pinus radiata. *Wat Air Soil Pol* 218: 499-515.
67. Shafiq A, Masood R, Naseer R, Naveed S, Rasool LG, Rahman A. 2016. Production, Purification and Characterization of laccase from white rot fungus, *Pak J Sc* 68: 259-267.
68. Shah MP, Reddy GV, Banerjee R, Babu PR, Kothari IL. 2005. Microbial degradation of banana waste under solid state bioprocessing using two lignocellulolytic fungi (Phylosticta spp. MPS-001 and Aspergillus spp. MPS-002). *Pro Biochem* 40: 45-451.

69. Sharma A, Thakur VV, Shrivastava A, Jain RK, Mathur RM, Gupta R, Kuhad, RC. 2014. Xylanase and laccase based enzymatic kraft pulp bleaching reduces adsorbable organic halogen (AOX) in bleach effluents: a pilot scale study. *Biores Tech* 69: 96–102.
70. Sharma KK, Kapoor M, Kuhad RC. 2005. In vivo enzymatic digestion, in vitro xylanase digestion, metabolic analogues, surfactants and polyethylene glycol ameliorate laccase production from Ganoderma sp. Kk-02. *Let App Micro* 41: 24–31.
71. Sharma RK, Arora DS. 2010. Production of lignocellulolytic enzymes and enhancement of in vitro digestibility during solid state fermentation of wheat straw by *Phlebia floridensis*. *Biores Tech* 3: 9248–53.
72. Shin EH, Choi HT, Song HG. 2007. Biodegradation of endocrine-disrupting bisphenol A by white rot fungus *Irpex lacteus*. *J Micro Biotec* 17: 1147–1151.
73. Stajic M, Persky L, Friesem D, Hadar Y, Wasser PS, Nevo E, Vukojevic J. 2006. Effect of different carbon and nitrogen sources on laccase and peroxidase production by selected Pleurotus species. *Enz Micro Tech* 38: 65-73.
74. Strong PJ and Claus H. 2011. Laccase: A review of the past and future in bioremediation. *Cri Rev Env Sc Tech* 41: 373-434.
75. Thurston CF. 1994. The structure and function of fungal laccases. *Micro* 140: 19–26.
76. Torres E, Bustos-Jaimes I, Borgne SL. 2003. Potential use of oxidative enzymes for the detoxification of organic pollutants. *App Cata B: Env* 46: 1–15.
77. Tunc O, Tanac H, Aksu Z. 2009. Potential use of cotton plant wastes for the removal of Remazol Black B reactive dye. *J Haz Mat* 163: 187-198.
78. Tychanowicz GK, Zilly A, de Souza CGM, Peralta RM. 2004. Decolourisation of industrial dyes by solid-state cultures of *Pleurotus pulmonarius*. *Pro Biochem* 39: 855–859.
79. Vrsanka M, Voberkova S, Langer V, Palovcikova D, Moulick A, Adam V, Kopel P. 2016. Induction of laccase, lignin peroxidase and manganese

peroxidase activities in white-rot fungi using copper complexes. *MDPI Mols* 21: 1-15.

80. Wang XS and Chen JP. 2009. Biosortion of Congo Red from aqueous solution using wheat bran and rice bran: Batch studies. *Sep Sc and Tech* 44: 1452-1466.
81. Wong Y, Yu J. 1999. Laccase-catalyzed decolourization of synthetic dyes. *Wat Res* 33: 3512–3520.
82. Xin F and Geng AL. 2011. Utilization of horticultural waste for laccase production by *Trametes versicolor* under solid-state fermentation. *App Biochem Biotech* 163: 235–246.
83. Xin F, Geng A. 2011. Utilization of horticultural waste for laccase production by *Trametes versicolor* under solid-state fermentation. *App Biochem Biotech* 163: 235–246.
84. Yesilada O, Asma D and Cing S. 2003. Decolorisation of the textile dye by fungal pellets. *Pro Biochem* 38: 933-938.
85. Zeng S, Zhao J, Xia L. 2017. Simultaneous production of laccase and degradation of bisphenol A with *Tremetes versicolor* cultivate don agricultural wastes. *Biopro Biosys Eng* 40: 1237-1245.

Tables

Table 4.1 Effect of days of incubation on laccase production by *Schizophyllum*-S4 under SSF using dye adsorbed wheat bran

S. No.	Days of Incubation	%D / E.A. (U/L)	Industrial Dye					$C^{1\#}$ (IU/mL)
			CV^{*1}	MG^{*2}	CR^{*3}	DDR^{*4}	DO^{*5}	
1.	**1**	**%D**	6.89 ± 0.34	5.62 ± 0.67	8.86 ± 0.54	14.37 ± 0.69	13.53 ± 0.71	0.32 ± 0.09
		E.A.	0.07 ± 0.31	0.06 ± 0.56	0.07 ± 0.11	0.11 ± 0.99	0.02 ± 0.11	
2.	**2**	**%D**	22.56 ± 0.06	7.49 ± 1.03	17.98 ± 1.02	26.01 ± 0.08	29.14 ± 0.04	1. 38± 0.11
		E.A.	0.08 ± 0.76	0.07 ± 0.61	0.07 ± 0.06	0.06 ± 0.23	0.06 ± 0.56	
3.	**3**	**%D**	33.04 ±0.44	24.10 ± 0.32	29.80 ± 0.46	35.03 ± 0.36	40.59 ± 0.34	1.76 ± 0.16
		E.A.	0.12 ± 0.35	0.11 ± 0.21	0.09 ± 0.42	0.09 ± 0.46	0.12 ± 0.09	
4.	**4**	**%D**	44.47 ± 0.27	45.93 ± 0.61	37.11 ± 0.52	42.91 ± 0.43	44.26 ± 0.32	2.02 ± 0.19
		E.A.	0.47 ± 0.36	0.21 ± 0.01	0.39 ± 0.43	0.18 ± 0.32	0.21 ± 0.02	
5.	**5**	**%D**	55.53 ± 0.98	50.38 ± 0.52	49.67 ± 0.68	48.20 ± 0.53	46.74 ± 0.48	2.18 ± 0.12
		E.A.	0.75 ± 0.13	0.59 ± 0.07	0.72 ± 0.71	0.38 ± 0.17	0.47 ± 0.22	
6.	**6**	**%D**	57.07 ± 0.29	51.36 ± 0.25	58.46 ± 0.32	50.98 ± 0.65	57.21 ± 0.02	2.61 ± 0.27
		E.A.	0.87 ± 0.01	0.81 ± 0.45	0.89 ± 0.57	0.65 ± 0.38	0.51 ± 0.08	
7.	**7**	**%D**	60.07 ± 0.08	56.89 ± 0.51	64.98 ± 0.23	51.61 ± 0.45	58.86 ± 0.77	3.18 ± 0.43
		E.A.	1.27 ± 0.01	1.38 ± 0.06	1.39 ± 0.76	0.89 ± 0.27	0.62 ± 0.49	
8.	**8**	**%D**	84.10 ± 1.02	66.56 ± 0.08	73.46 ± 0.17	58.35 ± 0.65	60.79 ± 0.37	**3.52 ± 0.19**
		E.A.	1.79 ± 0.76	1.83 ± 0.03	1.81 ± 0.41	1.13 ± 0.54	0.87 ± 0.32	
9.	**9**	**%D**	85.05 ± 0.21	87.95 ± 0.02	76.46 ± 0.18	68.49 ± 0.21	62.90 ± 0.33	3.27 ± 0.54
		E.A.	2.18 ± 0.09	2.13 ± 0.01	2.21 ± 0.33	1.48 ± 0.46	1.31 ± 0.37	
10.	**10**	**%D**	85.49 ± 0.51	89.36 ± 0.57	81.16 ± 0.28	67.11 ± 0.42	63.36 ± 0.33	3.13 ± 0.03
		E.A.	2.76 ± 0.65	2.69 ± 0.27	2.78 ± 0.65	1.93 ± 0.45	1.56 ± 0.38	
11.	**11**	**%D**	86.45 ± 0.98	89.36 ± 0.06	85.73 ± 0.28	71.90 ± 0.29	65.64 ± 0.01	2.96 ±0.27
		E.A.	2.89 ± 0.88	2.95 ±0.35	2.94 ± 0.43	2.18 ± 0.49	1.94 ± 0.36	
12.	**12**	**%D**	86.37 ± 0.37	90.23 ± 0.55	88.51 ± 0.01	75.36 ± 0.32	65.91 ± 0.01	2.81 ± 0.38
		E.A.	2.94 ± 0.32	3.10 ± 0.21	3.28 ± 0.45	2.48 ± 0.54	2.27 ± 0.76	
13.	**13**	**%D**	86.15 ± 0.65	90.88 ± 0.41	90.17 ± 0.35	75.80 ± 0.37	67.46 ± 0.64	2.69 ± 0.16
		E.A.	3.13 ± 0.44	3.23 ± 0.47	3.58 ± 0.86	2.89 ± 0.43	2.63 ± 0.47	
14.	**14**	**%D**	**87.25 ± 0.55**	93.05 ± 0.26	91.43 ± 0.31	76.18 ± 0.42	68.65 ± 0.01	2.61 ± 0.03
		E.A.	**3.69 ± 0.91**	3.72 ± 0.35	3.92 ± 0.33	3.17 ± 0.54	2.89 ± 0.01	
15.	**15**	**%D**	86.74 ± 0.31	**91.31 ± 0.21**	**91.66 ± 0.07**	**76.94 ± 0.87**	74.92 ± 0.35	2.49 ± 0.52
		E.A.	3.42 ± 0.43	**3.84 ± 0.55**	**3.93 ± 0.75**	**3.16 ± 0.65**	3.08 ± 0.54	
16.	**16**	**%D**	86.74 ± 0.02	91.31 ± 0.44	91.78 ± 0.62	77.32 ± 0.46	**78.38 ± 0.33**	**2.38** ± 0.12
		E.A.	3.23 ± 0.53	3.80 ± 0.67	3.86 ± 0.09	3.15 ± 0.04	**3.12 ± 0.47**	

Crystal Violet*[1]; Malachite Green*[2]; Congo Red*[3]; Disperse Dark Red*[4]; Disperse Orange*[5] ; Control[1#]

Culture Conditions:
Growth Medium: Dye adsorbed WB
pH: 5.5
Temperature, ºC: 30
Substrate concentration, gm: 5
Moistening agent, %: 70

Assay Condition:
*[1]Temperature, ºC: 30
pH: 5

± Standard Deviation from the mean

Table 4.2 Effect of pH on production by *Schizophyllum*-S4 under SSF using dye adsorbed wheat bran

S.No.	pH	%D / E.A.	Industrial Dyes					$C^{2\#}$ (IU/mL)
			CV[*1]	MG[*2]	CR[*3]	DDR[*4]	DO[*5]	
1.	5	%D	88.32 ± 0.36	93.53 ± 0.41	92.18 ± 0.27	75.19 ± 0.02	83.49 ± 0.01	3.65 ± 0.19
		E.A.	3.87 ± 0.21	4.13 ± 0.32	4.21 ± 0.70	2.98 ± 0.21	3.33 ± 0.09	
2.	5.5	%D	91.67 ± 0.32	93.67 ± 0.22	95.39 ± 0.01	77.27 ± 0.31	82.88 ± 0.34	**3.99± 0.33**
		E.A.	4.09 ± 0.26	3.98 ± 0.61	6.38 ± 0.53	3.01 ± 0.29	3.21 ± 0.87	
3.	6	%D	92.61 ± 0.61	93.87 ± 0.67	94.98 ± 0.32	75.56 ± 0.02	88.32 ± 0.47	2.91± 0.22
		E.A.	4.89 ± 0.27	3.88 ± 0.05	6.24 ± 0.32	3.05 ± 0.18	3.78 ± 0.87	
4.	6.5	%D	91.67 ± 0.47	93.28 ± 0.46	94.47 ± 0.22	74.65 ± 0.07	78.67 ± 0.08	2.72 ± 0.36
		E.A.	5.87 ± 0.27	4.01 ± 0.23	6.25 ± 0.37	2.25 ± 0.02	3.17 ± 0.47	
5.	7	%D	78.24 ± 0.48	85.38 ± 0.43	91.53 ± 0.38	72.38 ± 0.02	75.46 ± 0.32	2.31 ± 0.63
		E.A.	2.64 ± 0.46	3.46 ± 0.53	4.03 ± 0.58	1.89 ± 0.27	3.12 ± 0.98	
6.	7.5	%D	78.95 ± 1.05	81.25 ± 0.07	88.28 ± 0.32	73.98 ± 0.45	72.38 ± 0.29	2.11 ± 0.17
		E.A.	2.05 ± 0.27	2.67 ± 0.48	2.34 ± 0.43	1.86 ± 0.38	2.83 ± 0.22	
7.	8	%D	89.87 ± 0.19	88.89 ± 0.23	96.56 ± 0.28	84.26 ± 0.27	**86.86 ± 0.47**	1.94± 0.03
		E.A.	4.11 ± 0.98	2.11 ± 0.21	7.54 ± 0.78	4.87 ± 0.75	**5.35 ± 0.38**	
8.	8.5	%D	**93.45 ± 0.49**	**95.63 ± 0.39**	**97.37 ± 0.88**	**85.68 ± 0.26**	85.65 ± 0.37	1.83 ± 0.17
		E.A.	**8.14 ± 0.32**	**7.46 ± 0.37**	**8.98 ± 0.22**	**5.38 ± 0.29**	4.78 ± 0.38	
9.	9	%D	89.57 ± 0.67	86.43 ± 0.48	92.37 ± 0.83	76.31 ± 0.58	82.31 ± 0.57	1.76 ± 0.23
		E.A.	4.27 ± 0.77	2.87 ± 0.39	4.11 ± 0.76	3.14 ± 0.38	3.25 ± 0.78	
10.	9.5	%D	88.03 ± 0.28	86.87 ± 0.47	90.48 ± 0.48	74.64 ± 0.46	76.43 ± 0.43	1.60 ± 0.40
		E.A.	3.25 ± 0.43	2.77 ± 0.21	2.82 ± 0.76	2.75 ± 0.43	3.02 ± 0.32	

Crystal Violet*[1]; Malachite Green*[2]; Congo Red*[3]; Disperse Dark Red*[4]; Disperse Orange*[5] ; Control[2#]

Culture Conditions:
Growth Medium: Dye adsorbed WB
Incubation time: days: 14(CV), 15(MG, CR, DDR),16 (DO)
Temperature, ºC: 30
Substrate concentration, gm: 5
Moistening agent, %: 70
± Standard Deviation from the mean

Assay Condition:
[*1]Temperature, ºC: 30
pH: 5

Table 4.3 Effect of temperature on laccase production by *Schizophyllum*-S4 under SSF using dye adsorbed wheat bran

S. No.	Temperature (ºC)	%D / E.A.	Industrial Dyes					$C^{3\#}$
			CV[*1]	MG[*2]	CR[*3]	DDR[*4]	DO[*5]	
1.	25	%D	65.23 ± 0.87	67.25 ± 0.38	69.83±0.45	62.18 ± 0.01	71.06 ± 0.21	3.23 ± 0.12
		E.A.	1.56 ± 0.06	1.89 ± 0.02	2.45 ± 0.22	1.03 ± 0.04	1.54 ± 0.20	
2.	30	%D	93.99 ± 0.37	96.17 ± 0.05	97.87 ± 0.43	84.98 ± 0.31	85.98 ± 0.25	**3.69 ± 0.21**
		E.A.	8.16 ± 0.42	8.27 ± 0.11	9.13 ± 0.32	5.02 ± 0.37	5.29 ± 0.22	
3.	35	%D	**94.91 ± 0.97**	**96.85 ±0.29**	**98.76 ± 0.39**	**87.69 ± 0.33**	**87.97± 0.46**	3.42 ± 0.54
		E.A.	**8.79 ± 0.78**	**8.25 ± 0.37**	**9.58 ± 0.08**	**6.87 ± 0.25**	**6.48 ± 0.17**	
4.	40	%D	86.75 ± 0.46	85.48 ± 0.43	91.38 ± 0.38	82.67 ± 0.55	83.21 ± 0.08	2.85 ± 0.43
		E.A.	7.84 ± 0.54	6.57 ± 0.21	8.67 ± 0.29	5.89 ± 0.37	5.98 ± 0.05	
5.	45	%D	81.27 ± 0.67	83.21 ± 0.42	85.46 ± 0.51	79.98 ± 0.62	82.05 ± 0.47	1.68 ± 0.16
		E.A.	4.63 ± 0.01	5.71 ± 0.06	3.21 ± 0.45	1.87 ± 0.63	2.09 ± 0.22	
6.	50	%D	75.60 ± 0.77	72.47 ± 0.32	79.84 ± 0.19	86.21 ± 0.55	76.89 ± 0.17	1.53 ± 0.11
		E.A.	2.53 ± 0.57	2.48 ± 0.43	3.65 ± 0.49	1.61 ± 0.56	1.25 ± 0.31	

Crystal Violet*[1]; Malachite Green*[2]; Congo Red*[3]; Disperse Dark Red*[4]; Disperse Orange*[5] ; Control[3#]

Culture Conditions:
Growth Medium: Dye adsorbed WB
Incubation time: days: 14(CV), 15(MG, CR, DDR), 16(DO)
pH: 8.5 (CV,MG,CR,DDR); 8 (DO)
Substrate concentration, gm: 5
Moistening agent, % : 70
± Standard Deviation from the mean

Assay Condition:
[*1]Temperature, ºC: 30
pH: 5

4.4 Effect of yeast extract on laccase production by *Schizophyllum*-S4 under SSF using dye adsorbed wheat bran

S. No.	Nitrogen Source Yeast Extract (%)	%D / E.A.	Industrial Dyes CV[*1]	MG[*2]	CR[*3]	DDR[*4]	DO[*5]	C[4#]
1.	0.5	%D	90.04 ±0.78	86.98 ± 0.26	86.91 ± 0.37	86.27 ± 0.77	86.89 ± 0.09	0.67 ± 0.11
		E.A.	7.67 ± 0.65	7.21 ± 0.11	7.18 ± 0.28	6.12 ± 0.74	6.58 ± 0.02	
2.	1	%D	**95.36 ± 0.14**	**96.99 ± 0.35**	**98.78± 0.32**	**87.75 ± 0.29**	**87.98 ± 0.51**	1.03± 0.89
		E.A.	**9.15 ± 0.11**	**8.97 ± 0.42**	**9.52 ± 0.18**	**7.89 ± 0.37**	**7.93 ± 0.31**	
3.	1.5	%D	91.26 ± 0.25	86.78 ± 0.21	86.59 ± 0.27	84.36 ± 0.21	84.28 ± 0.29	1.22 ± 0.41
		E.A.	8.01 ± 0.27	7.21 ± 0.10	7.98 ± 0.36	5.29 ± 0.08	5.20 ± 0.81	
4.	2	%D	72.26 ± 0.38	72.04 ± 0.32	72.77 ± 0.23	68.32 ± 0.28	68.02 ± 0.42	1.02 ± 0.15
		E.A.	2.32 ± 0.32	2.21 ± 0.77	2.65 ± 0.21	1.68 ± 0.49	1.76 ± 0.27	
5.	2.5	%D	68.12 ± 0.33	68.03 ± 0.12	68.29 ± 0.42	67.89 ± 0.33	67.21 ± 0.68	0.10 ± 0.01
		E.A.	1.56 ± 0.08	1.45 ± 0.16	1.65 ± 0.89	1.55 ± 0.42	1.45 ± 0.77	

Crystal Violet*[1]; Malachite Green*[2]; Congo Red*[3]; Disperse Dark Red*[4]; Disperse Orange*[5] ; Control[4#]

Culture Conditions:
Growth Medium: Dye adsorbed WB
Incubation time: days: 14(CV), 15(MG, CR, DDR), 16(DO)
pH: 8.5 (CV,MG,CR,DDR); 8 (DO)
Temperature, º C : 35
Substrate concentration, gm: 5
Moistening agent, % : 70
± Standard Deviation from the mean

Assay Condition:
[*1]Temperature, ºC: 30
pH: 5

4.5 Effect of copper sulphate on laccase production by *Schizophyllum*-S4 under SSF using dye adsorbed wheat bran

S. No.	Copper Sulphate (mM)	%D / E.A.	Industrial Dyes CV[*1]	MG[*2]	CR[*3]	DDR[*4]	DO[*5]	C[5#]
1.	0.2	%D	95.21 ± 0.87	95.59 ± 0.99	96.11± 0.21	86.72 ± 0.62	87.01 ± 0.97	7.83 ± 0.16
		E.A.	7.31 ± 0.28	7.99 ± 0.19	8.02 ± 0.17	6.11 ± 0.29	6.17 ± 0.08	
2.	0.4	%D	**95.48 ± 0.31**	**97.01 ± 0.22**	**98.99 ± 0.22**	**88.26 ± 1.01**	**88.18 ± 0.01**	**11.87 ± 0.32**
		E.A.	**9.57 ± 0.08**	**9.24 ± 0.32**	**10.59 ± 0.41**	**8.31 ± 0.12**	**8.42 ± 0.34**	
3.	0.6	%D	95.38 ± 0.66	96.26 ± 0.68	95.39 ± 0.90	85.46 ± 0.42	85.88 ± 0.29	11.15 ± 0.28
		E.A.	8.01 ± 0.22	7.24 ± 0.09	7.59 ± 0.31	5.48 ± 0.31	5.98 ± 0.36	
4.	0.8	%D	93.93 ± 0.36	95.47 ± 0.64	93.65 ± 0.07	82.37 ± 0.36	81.23 ± 0.71	9.38± 0.25
		E.A.	5.22 ± 0.41	5.98 ± 1.01	4.35 ± 0.23	4.68 ± 0.02	3.32 ± 0.17	
5.	1	%D	86.34 ± 0.18	86.79 ± 0.15	88.32 ± 0.33	74.62 ± 0.05	73.29 ± 0.23	4.47 ± 0.27
		E.A.	3.28 ± 0.71	3.38 ± 0.57	3.65 ± 0.98	2.87 ± 0.34	2.69 ± 0.51	

Crystal Violet*[1]; Malachite Green*[2]; Congo Red*[3]; Disperse Dark Red*[4]; Disperse Orange*[5] ; Control[5#]

Culture Conditions:
Growth Medium: Dye adsorbed WB
Incubation time: days: 14(CV), 15(MG, CR, DDR), 16 (DO)
pH: 8.5 (CV, MG, CR, DDR); 8 (DO)
Temperature, º C: 35
Substrate concentration, gm: 5; Yeast Extract, %: 1
Moistening agent, %: 70
± Standard Deviation from the mean

Assay Condition:
[*1]Temperature, ºC: 30
pH: 5

Table 4.6 Chromatographic Analysis

S.No.	Dyes	Purity of standard (%)	Peak of standard	Peak of sample	Degradation Percentage
1.	**Crystal Violet**	**98**	2.650123e4	1.05612e4	**60.94%**
2.	**Malachite Green**	**98**	588886.35	225468.27	**62.47%**
3.	**Congo Red**	**98**	1.56199e4	0.82465e4	**48.26%**
4.	**Disperse Dark Red**	**98**	9867589.22	4876359.78	**51.57%**
5.	**Disperse Orange**	**98**	324586.72	185468.23	**44.01%**

Table 4.7 Comparison of recyclability of dye adsorbed WB-fungal (Wb-F) biomass as an adsorbent for decolorization

S.No.	Industrial Dye	WB / Wb-F	Reusability Cycles				
			Cycle 1	Cycle 2	Cycle 3	Cycle 4	Cycle 5
1.	**CV**[*1]	**WB**	87.85 ±0.45	74.48 ± 0.08	38.25 ± 0.97	27.45 ± 0.44	26.38 ± 0.24
		Wb-F	95.38 ± 0.28	87.69 ± 0.23	75.66 ± 0.16	65.49 ± 0.31	61.89 ± 0.76
2.	**MG**[*2]	**WB**	96.07 ± 0.67	86.28 ± 0.07	57.87 ± 0.98	38.93 ± 0.47	23.78 ± 0.87
		Wb-F	97.07 ± 0.09	91.79 ± 0.33	87.65 ± 0.20	76.46 ± 0.76	66.28 ± 0.61
3.	**CR**[*3]	**WB**	96.89 ± 0.01	88.37 ± 0.06	58.38 ± 0.77	41.28 ± 0.31	34.69 ± 0.38
		Wb-F	99.02 ± 0.06	92.36 ± 0.28	86.59 ± 0.87	73.56 ± 0.87	68.79 ± 0.98
4.	**DDR**[*4]	**WB**	92.95 ± 0.19	81.37 ± 0.45	49.98 ± 0.45	40.69 ± 0.06	42.39 ± 0.28
		Wb-F	91.46 ± 0.56	93.36 ± 0.38	85.52 ± 0.55	70.89 ± 0.43	61.77 ± 0.79
5.	**DO**[*5]	**WB**	92.89 ± 0.92	85.48 ± 0.22	42.66 ± 0.81	38.91 ± 0.78	29.78 ± 0.58
		Wb-F	91.12 ± 0.11	93.77 ± 0.03	82.07 ± 0.72	76.48 ± 0.21	64.38 ± 0.76

Crystal Violet*[1]; Malachite Green*[2]; Congo Red*[3]; Disperse Dark Red*[4]; Disperse Orange*[5]

Incubation conditions for adsorption on WB:

[*1]: pH 8, Incubation time, mins: 180; Adsorbate dose, mg/L: 100; Adsorbent dose, gm/L: 10; Temperature, ºC: 30

[*2]: pH 11; Incubation time, min: 210; Adsorbate dose, mg/L: 110; Adsorbent dose, gm/L: 12; Temperature, ºC: 30

[*3]: pH 4; Incubation time, min: 210; Adsorbate dose, mg/L: 100; Adsorbent dose, gm/L: 12; Temperature, ºC: 30

[*4]: pH 5; Incubation time, min: 180; Adsorbate dose, mg/L: 100; Adsorbent dose, gm/L: 12; Temperature, ºC: 40

[*5]: pH 5; Incubation time, min: 180; Adsorbate dose, mg/L: 100; Adsorbent dose, gm/L: 12; Temperature, ºC: 45

Culture Conditions for decolorization by WB+S4

Incubation time: days: 14(CV), 15(MG, CR, DDR), 16(DO)

pH: 8.5 (CV, MG, CR, DDR); 8 (DO)

Temperature, ºC: 35

Substrate concentration, gm: 5; Yeast Extract, %: 1; Copper Sulphate (mM): 0.4

Moistening agent, %: 70

± Standard Deviation from the mean

Figures

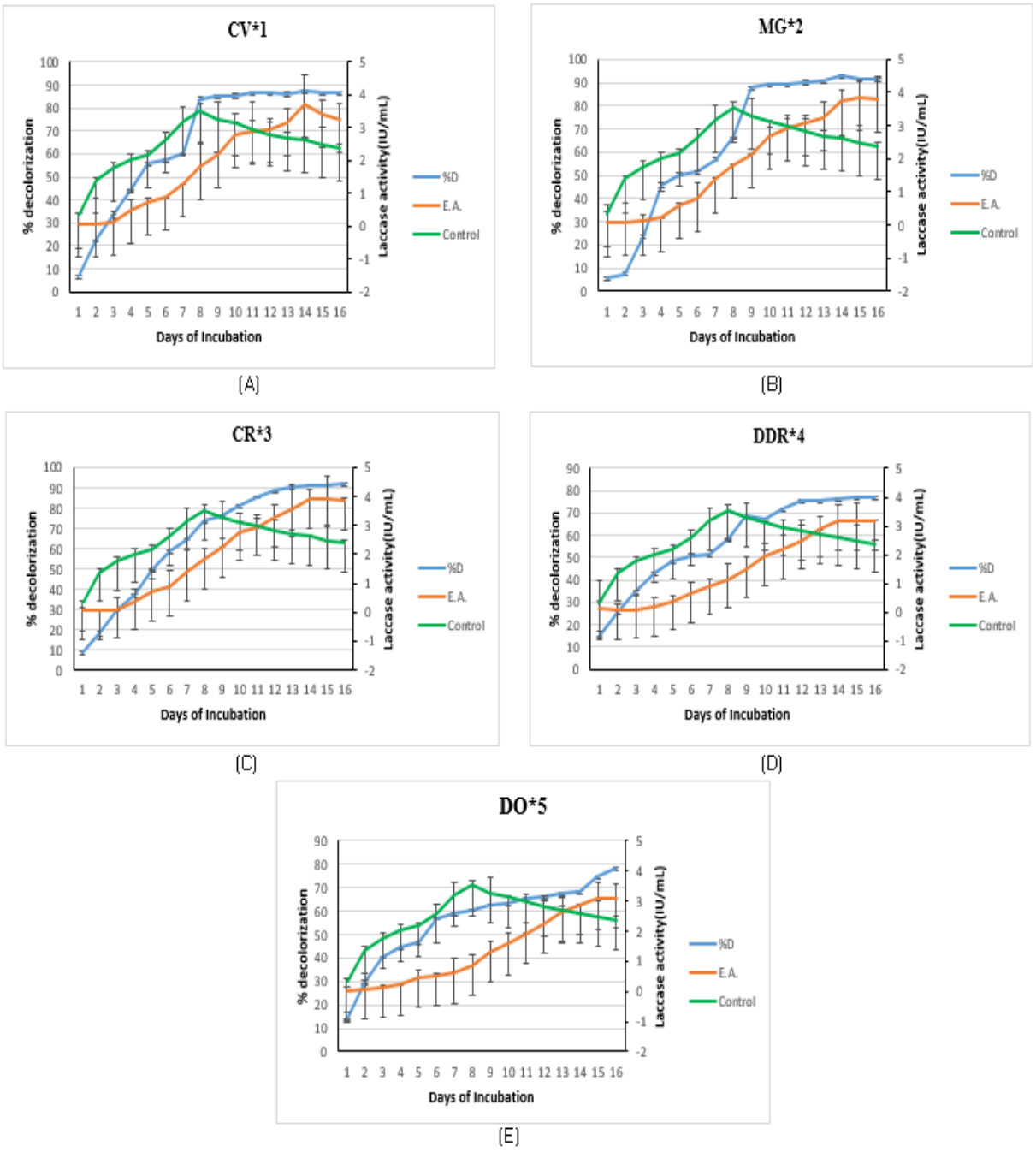

Figure 4.1: Effect of days of incubation on laccase production by *Schizophyllum*-S4 under SSF using dye adsorbed wheat bran. A: (CV*1), B: (MG*2), C: (CR*3), D: (DDR*4), E: (DO*5)

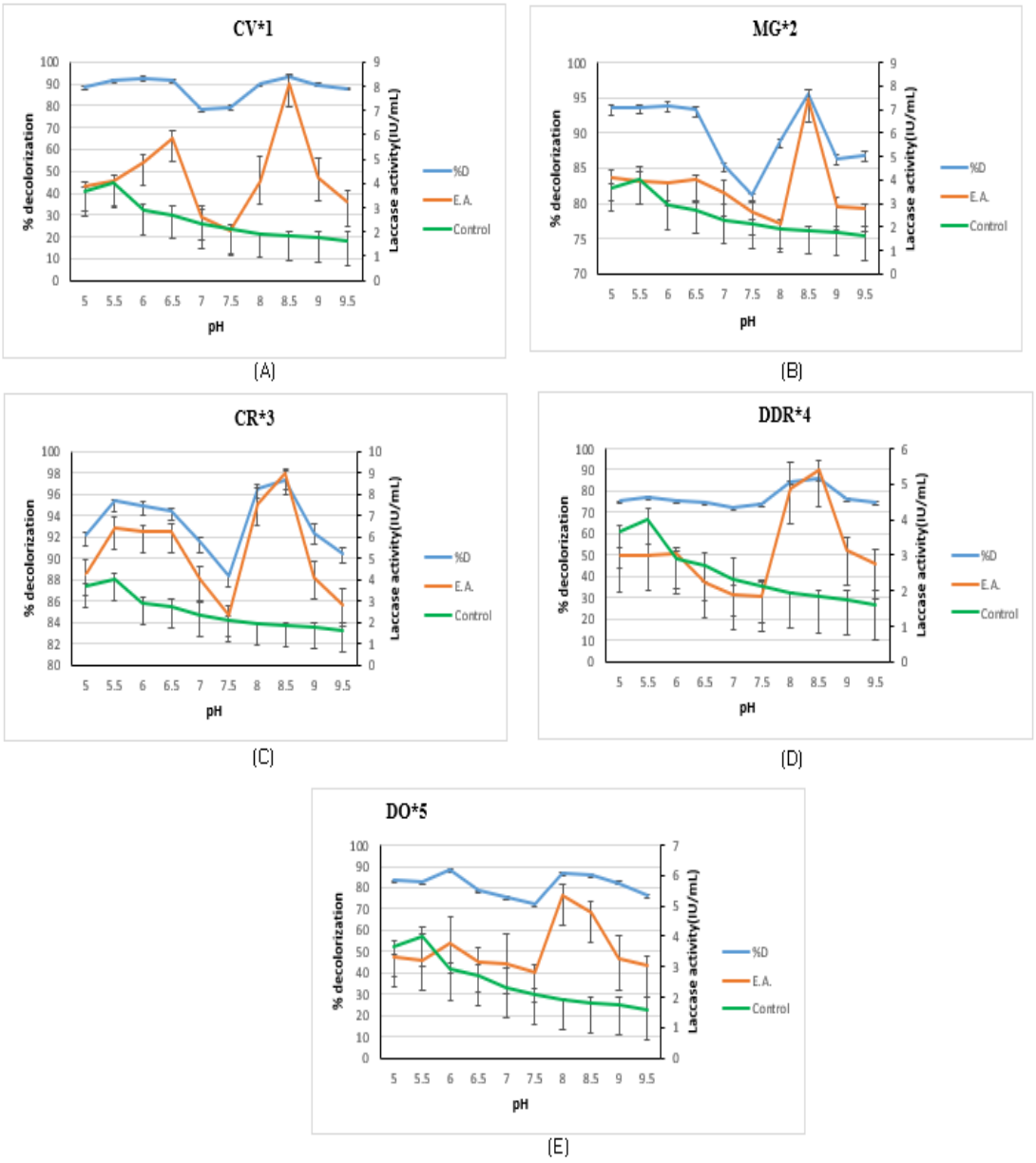

Figure 4.2: Effect of pH on production by *Schizophyllum*-S4 under SSF using dye adsorbed wheat bran. A: (CV*1), B: (MG*2) , C: (CR*3), D: (DDR*4), E: (DO*5).

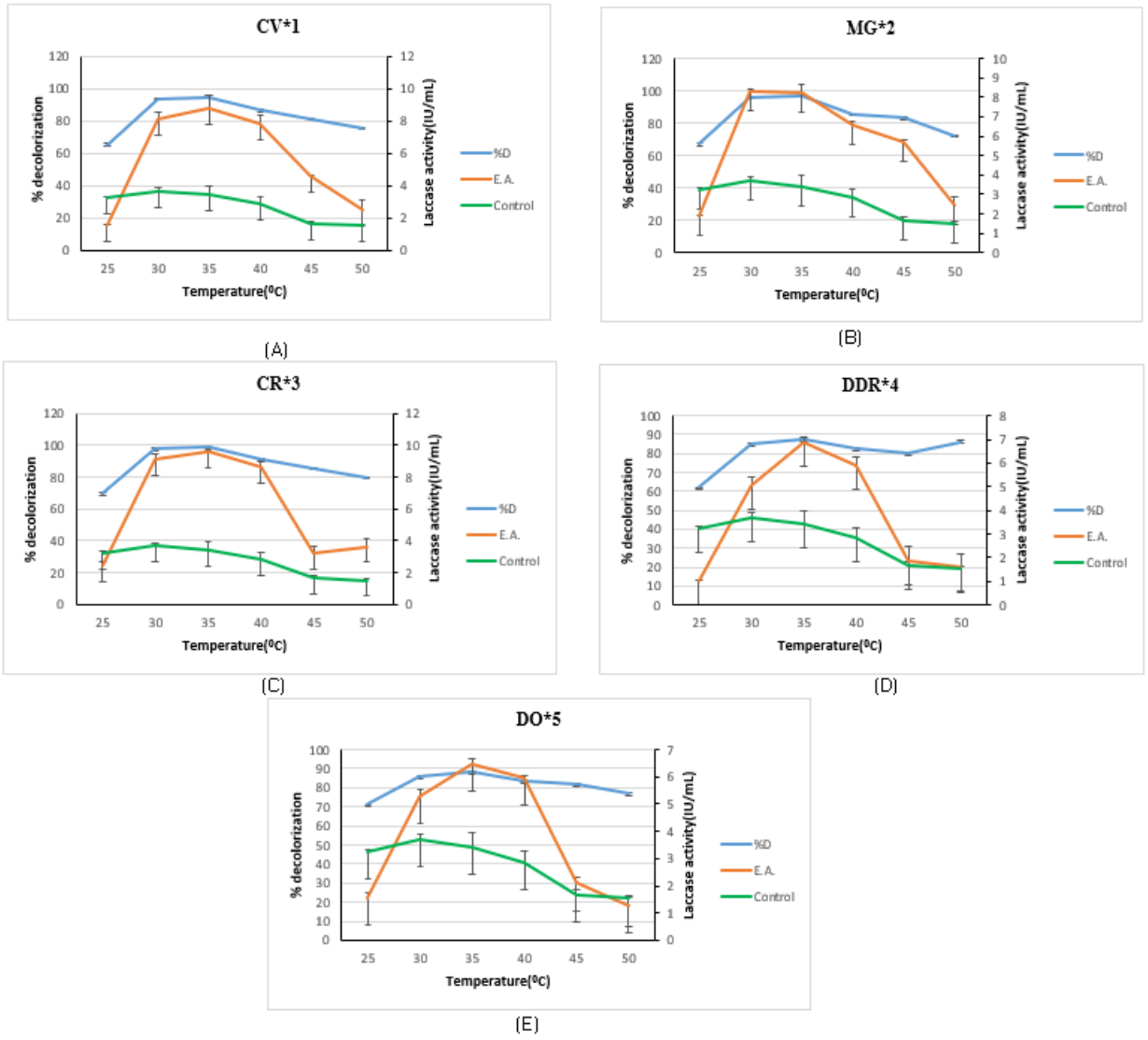

Figure 4.3: Effect of temperature on laccase production by *Schizophyllum*-S4 under SSF using dye adsorbed wheat bran. A: (CV*1), B: (MG*2), C:(CR*3), D: (DDR*4), E: (DO*5).

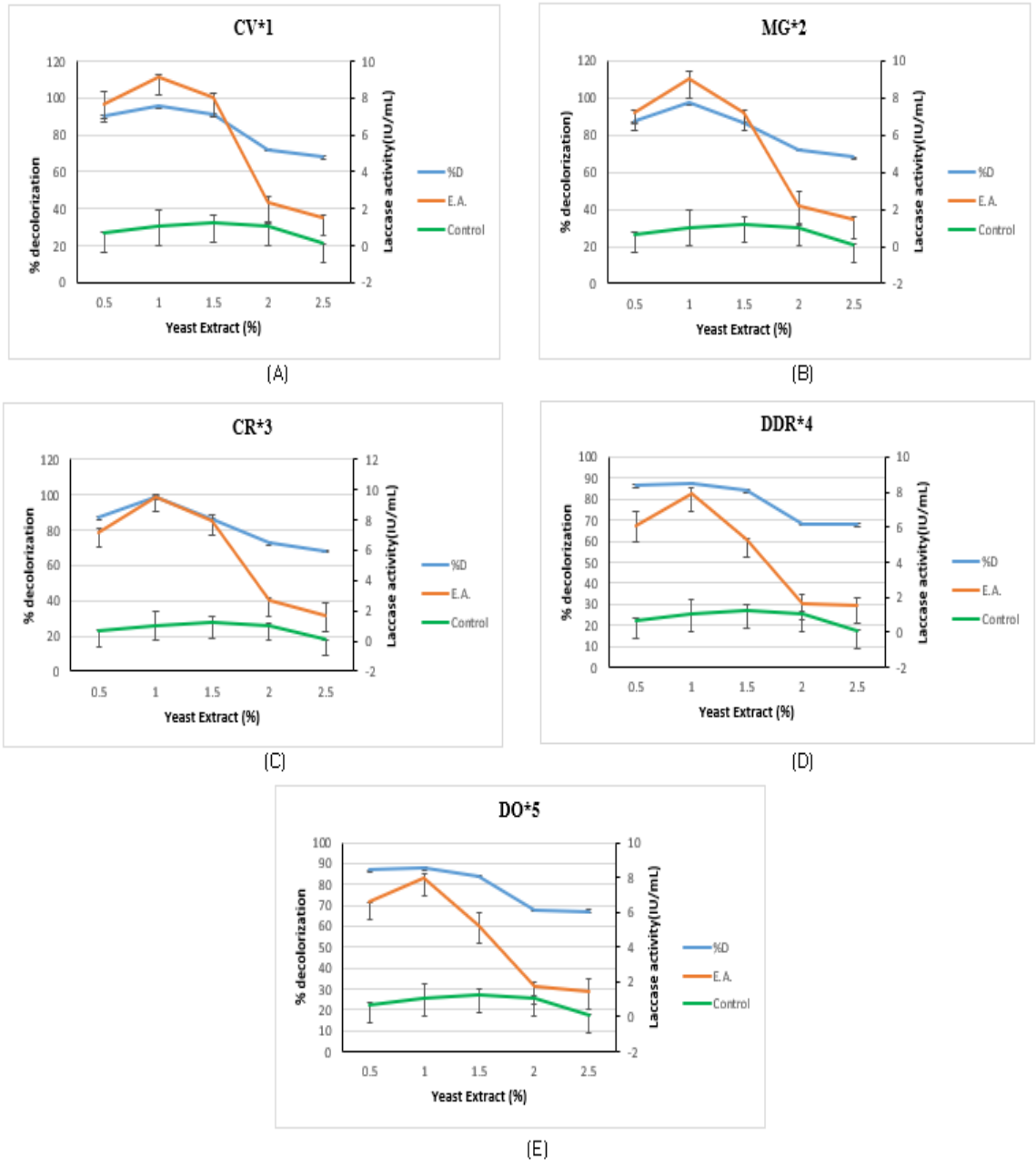

Figure 4.4: Effect of yeast extract on laccase production by *Schizophyllum*-S4 under SSF using dye adsorbed wheat bran.A: (CV*1), B: (MG*2), C:(CR*3), D: (DDR*4), E: (DO*5).

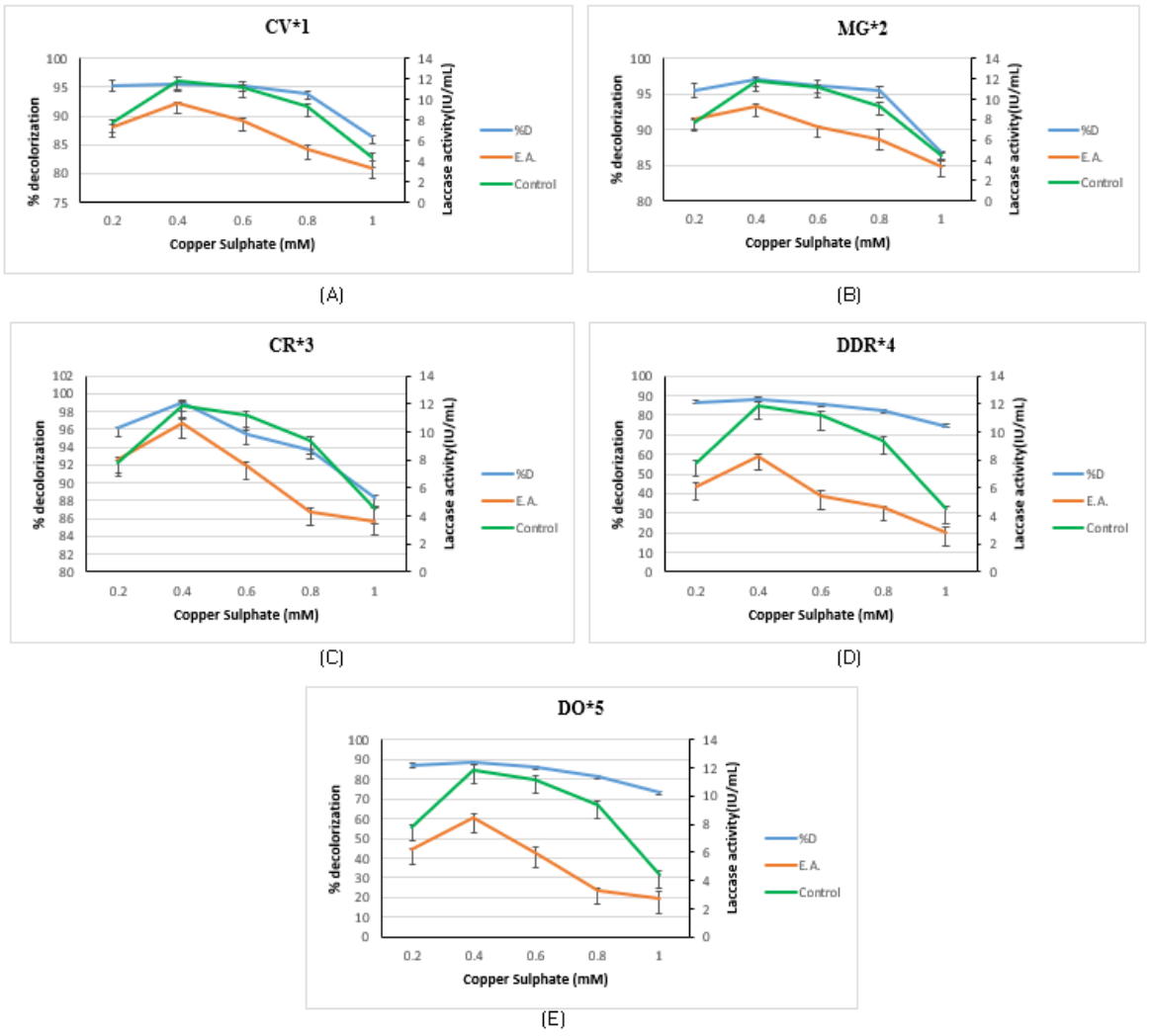

Figure 4.5: Effect of copper sulphate on laccase production by *Schizophyllum*-S4 under SSF using dye adsorbed wheat bran. A: (CV*1), B: (MG*2), C:(CR*3), D: (DDR*4), E: (DO*5).

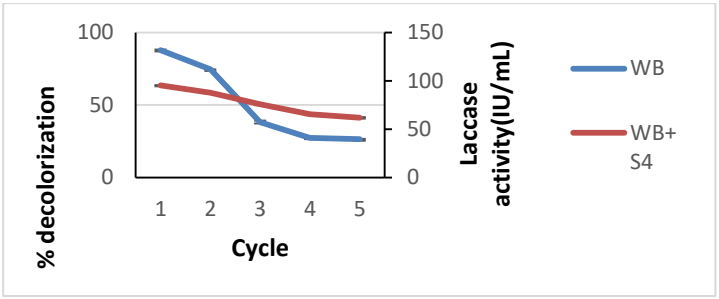

(A)

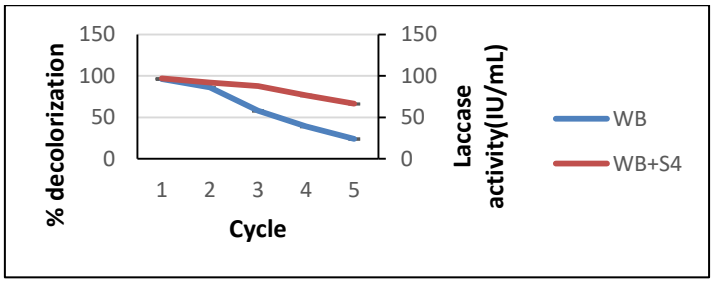

(B)

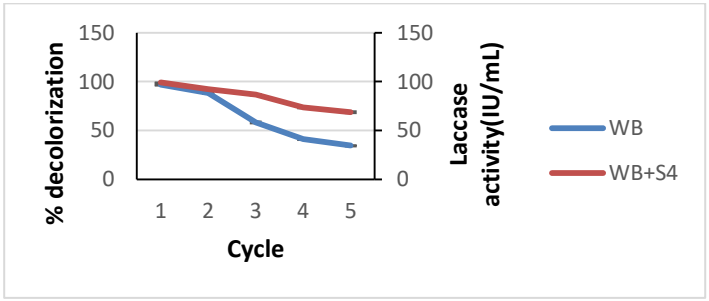

(C)

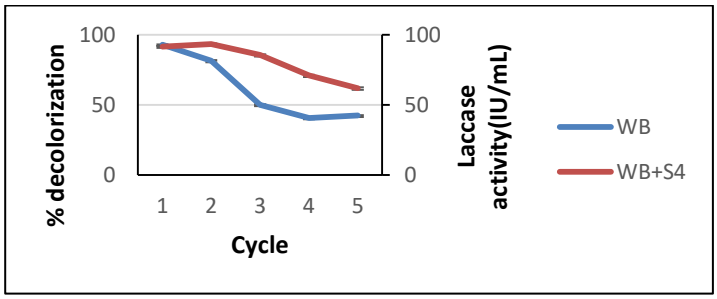

(D)

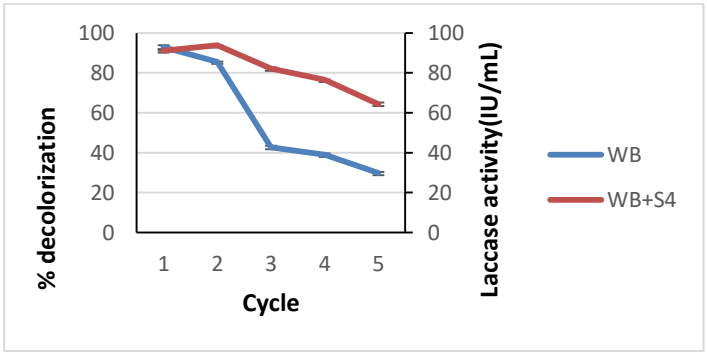

(E)

Figure 4.6: Comparison of recyclability of dye adsorbed WB-fungal (Wb-F) biomass as an adsorbent for decolorization. A: (CV*1), B: (MG*2), C:(CR*3), D: (DDR*4), E: (DO*5).

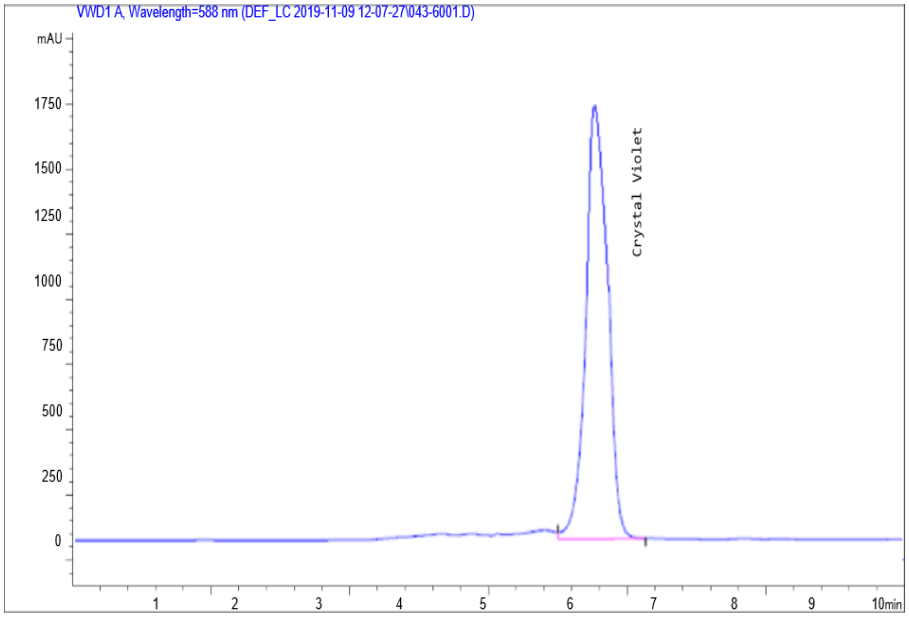

(A)

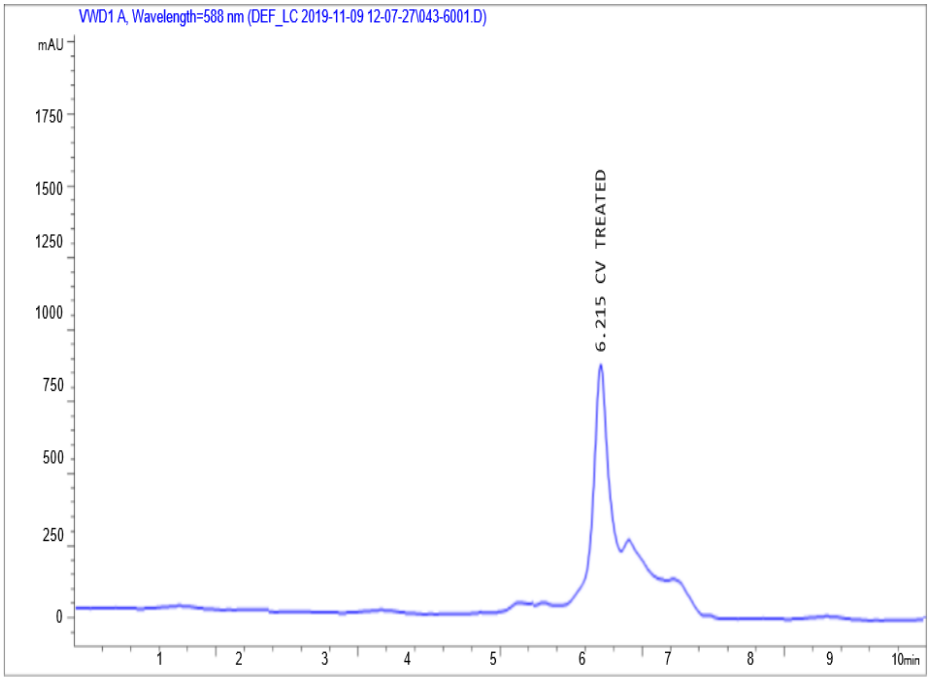

(B)

Figure 4.7 Chromatographic Analysis : Comparison of HPLC-DAD chromatogram of crystal violet (CV): (A) Control (98% pure CV) (B) Treated (bran adsorbed, *Schizophylum*-S4 treated)

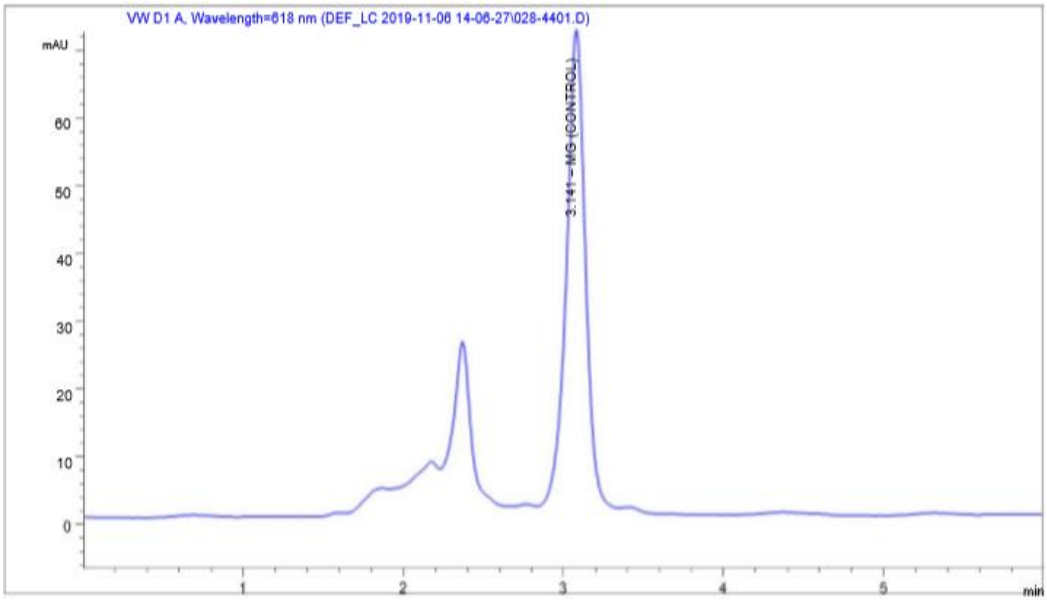

(C)

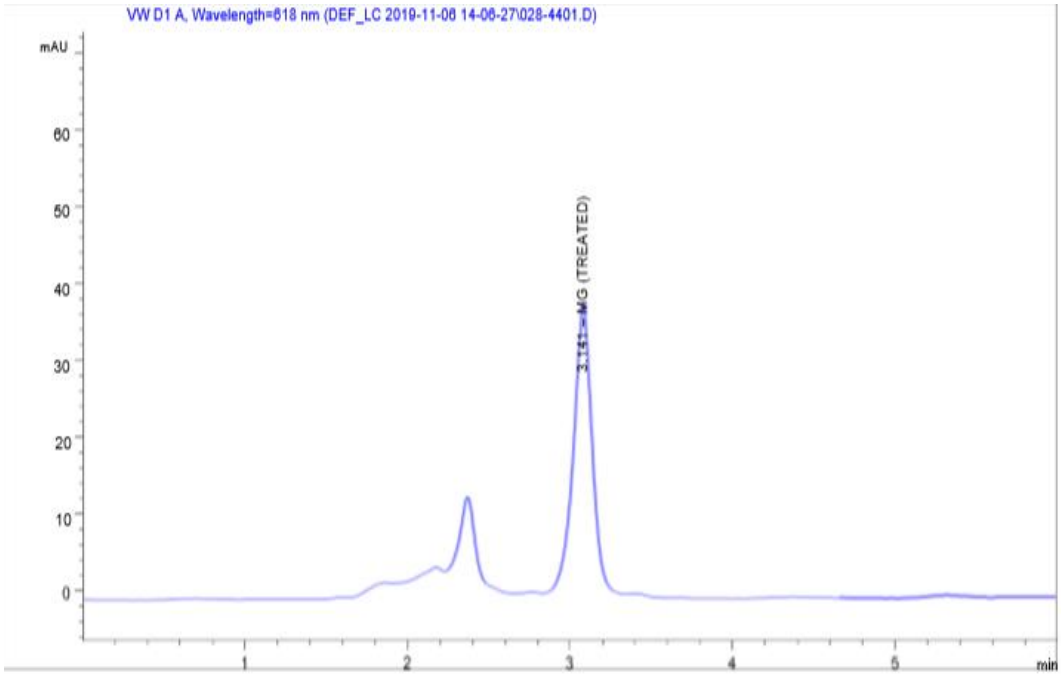

(D)

Figure 4.8 Chromatographic Analysis: Comparison of HPLC-DAD chromatogram of Malachite Green (MG): (C) Control (98% pure MG) (D) Treated (bran adsorbed, *Schizophylum*-S4 treated)

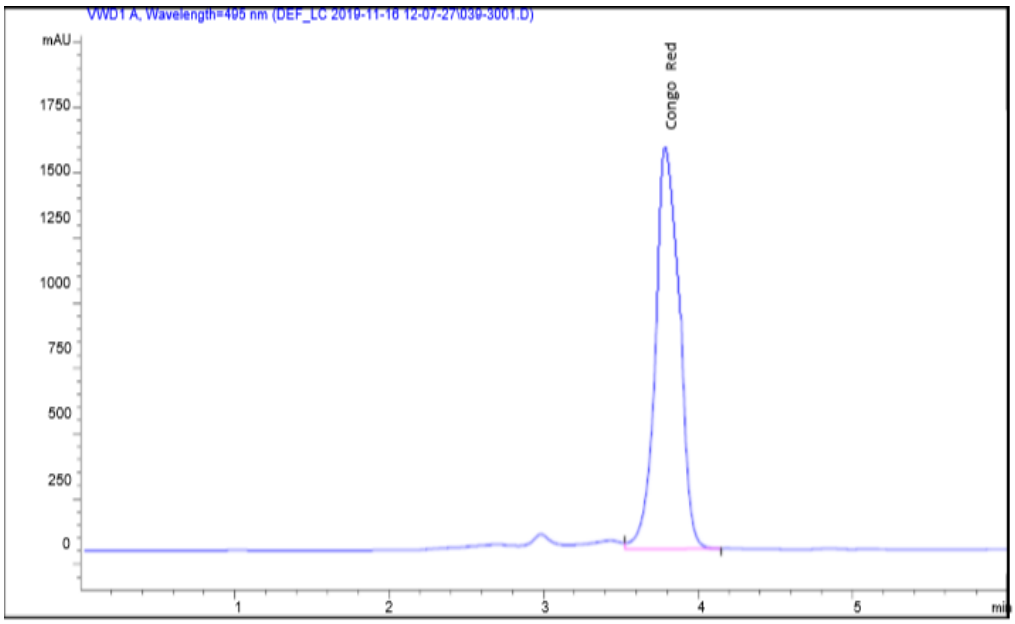

(E)

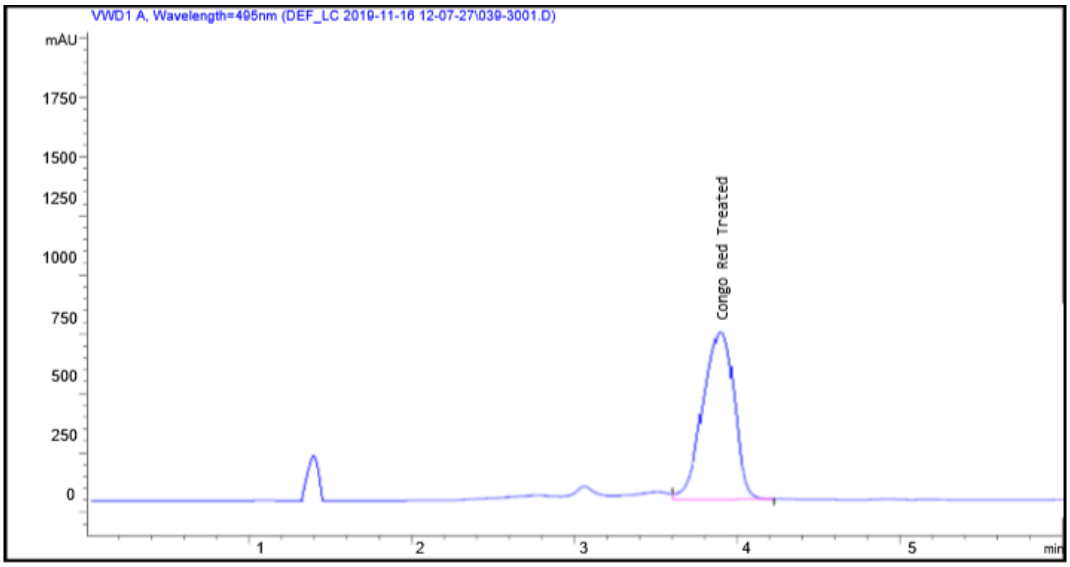

(F)

Figure 4.9 Chromatographic Analysis: Comparison of HPLC-DAD chromatogram of Congo Red (CR): (E) Control (98% pure MG) (F) Treated (bran adsorbed, *Schizophylum*-S4 treated)

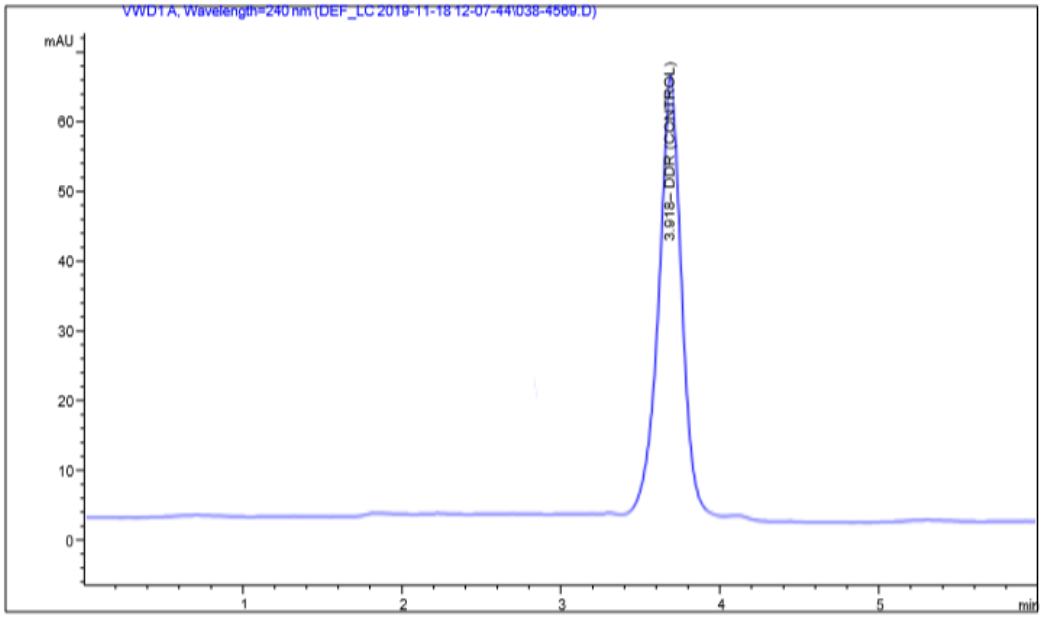

(G)

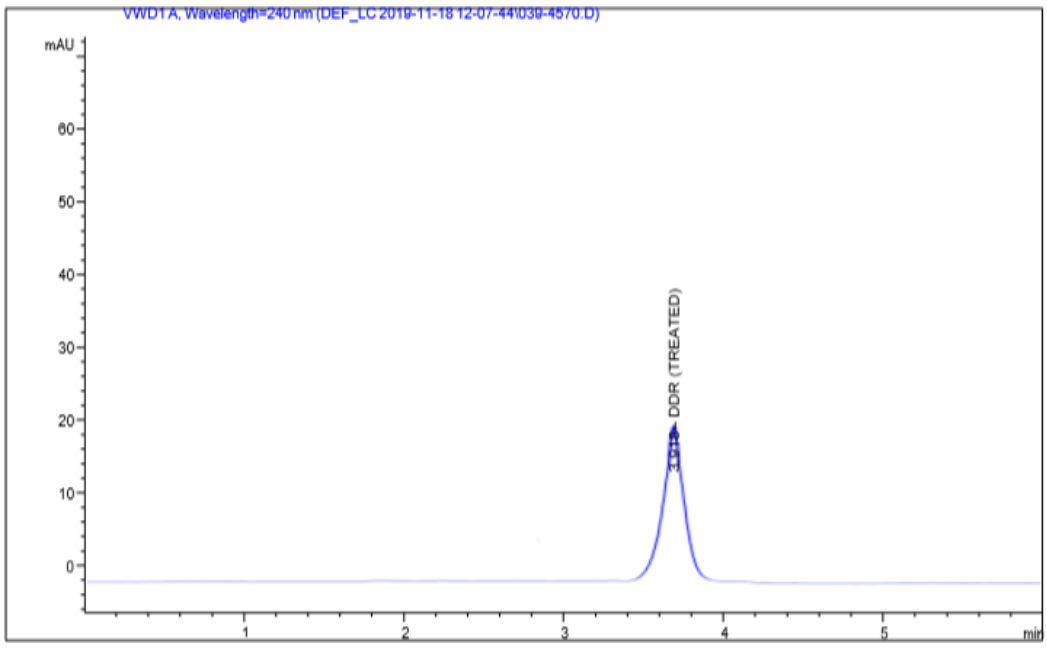

(H)

Figure 4.10 Chromatographic Analysis: Comparison of HPLC-DAD chromatogram of Disperse Dark Red (DDR): (G) Control (98% pure MG) (H) Treated (bran adsorbed, *Schizophylum*-S4 treated)

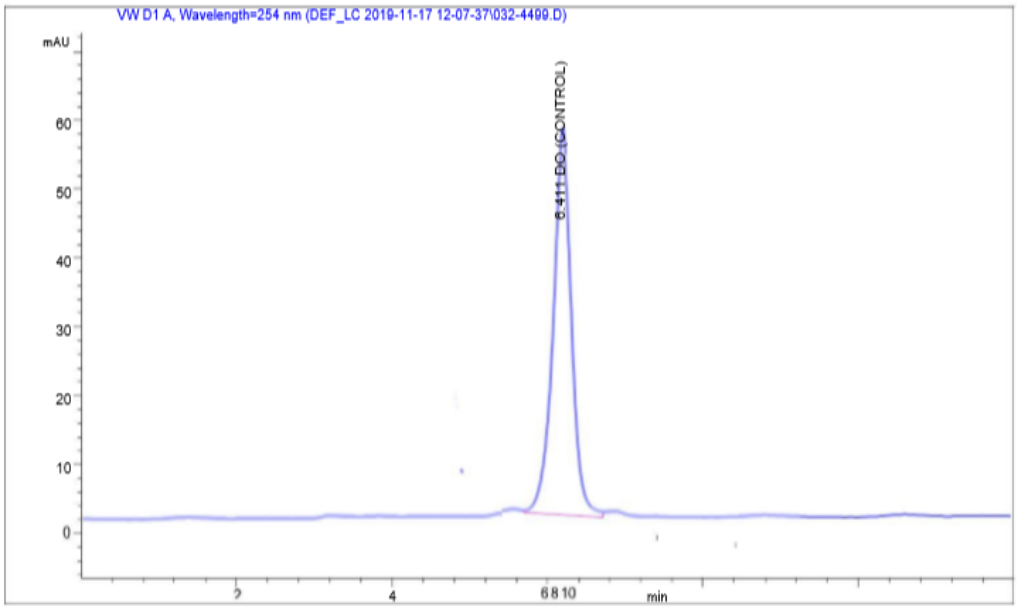

(I)

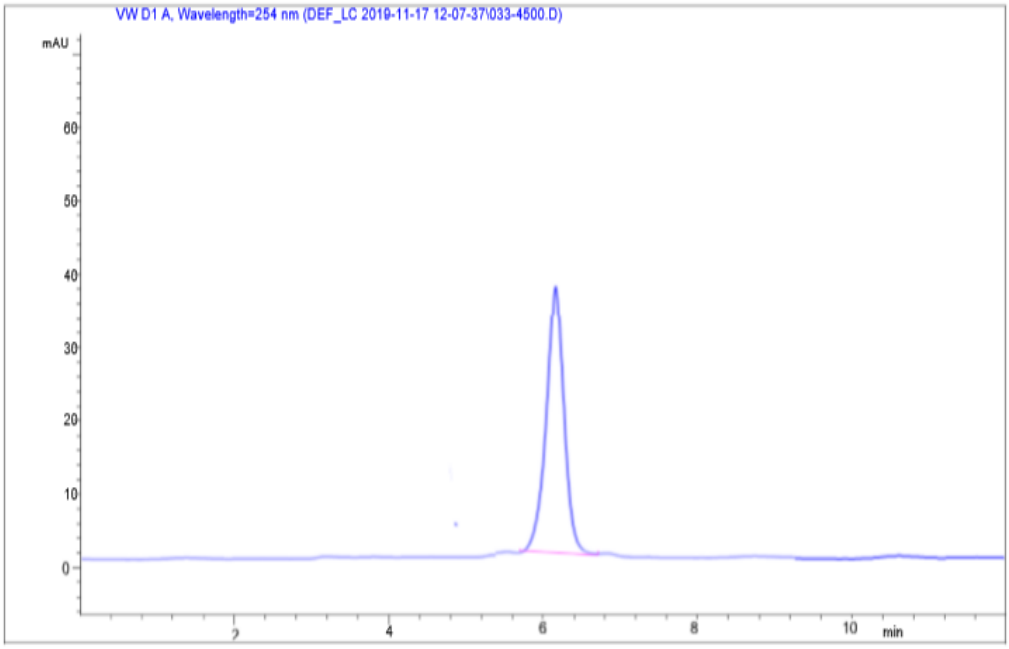

(J)

Figure 4.11 Chromatographic Analysis: Comparison of HPLC-DAD chromatogram of Disperse Orange (DO): (I) Control (98% pure MG) (J) Treated (bran adsorbed, *Schizophylum*-S4 treated)

Chapter 5

Designing of a cost-effective bioreactor for efficient industrial dye removal

5.1 Introduction

Environment pollution is presently the major thrust are around which most of the researches are being conducted. Dyes released by the various industries has always intrigued researchers to come out with some effective remediation process via which the environment and its components can be saved from their mal effects. In this present study, thus, by keeping that as the central issue, in a stepwise manner, endeavoured to seek out few feasible, cost effective robust and technologically sound solutions to ultimately serve the purpose of environment remediation in a sustainable way. If referred to the previous chapters of this research, initially a microbial system has been explored which could provide a rich enzyme system, which are / is, plays the key role in the process. Then proposed a cost-effective substratum which could be used by the isolated strain to produce more amount of the such an enzyme by means of fermentation technology. Then conjugative effect of the microorganism and the substratum was checked for effective dye (industrial) removal system. In this entire process the major aspects which were kept on priority were, the strain isolated should be a stable strain, the industrial waste of another industry could be utilized for some good and effective cause and ultimately provide a solution to a burning problem without much monetary investment. Thereby in the last part of the study, instead of designing a bioreactor, where lots of investments are already there and conventional systems are already running in large scale, in the industries, the research has tried to propose and design a IoT based effluent treatment plant prototype which could operate amalgamating with the other two key findings of this research, i.e. the novel isolate and the agro-industrial waste. The aim was to propose a novel process technology which could elevate the processing of the existing system without much investment. The scale up of the batch study was done by taking Congo Red as a representative dye and the representative industry which was taken into consideration

was textile industry (from Ludhiana), whose effluent samples were processed to validate the proper execution of the proposed process.

Amongst the various challenges faced by the textile industries, effluent treatment process is a major zone of concern, as the conventional treatment system does not effectively remove all the water pollutants. Amongst these, colour in waters have an immense negative impact on the environment as they are recalcitrant, which produces carcinogenic amines as their reaction products. The removal of such compounds before their disposal is thus, of significant environmental and economic importance. Thus, a smart and secured platform for a real-time effluent treatment plant management system by using a platform independent lose coupled cloud based IoT architecture was proposed. Industrial Internet of Things (IIOT) is a subset of the IOT concept which has the potential to increase the output and amplify the working ability. The biggest concerns in this field are the interoperability, security and cost.

This study have thereby tried to developed a solution to the environmental problem posed by the textile industry waste water using cutting edge of technology by the usage of a pre-treatment system with wheat bran, then with an isolated novel strain of White Rot Fungus by usage of its advanced enzyme system. The prototype of the ETP (Effluent Treatment Plant) that we have designed is having an architecture that is pluggable with multiple heterogeneous environment. We have used REST (REpresentational State Transfer) based communication protocol to communicate with different devices like Android Mobile, iPhone, Tablet, Web bases system and Smart Client System. The design is technology independent, so the business need not have to bother about the specific technical expertise. This work will help textile industries to migrate their existing system to Cloud based IoT enable system. The entire design is independent of platform and technology. Based on business requirement the system can deploy to mobile platform too. This system can be integrated to Big Data and Data Analytics systems also.

5.2 Review of Literature

Most of the IoT based company promotes the practice of working through the concept of perceive-think - proceed cycle aiding to follow digital innovation which can ultimately contribute towards sustainability of the effluent generated from the respective industries but the legacy systems have different architectures, with different protocols which can hinder their easy interoperability, capital purchase and maintenance strategies. In the ETP, monitoring and controlling systems plays a very important role for the daily operation and maintenance. The invention has thereby endeavoured to design a platform independent IoT enabled architecture by integrating with a prototype of a physico-biological treatment method of textile effluent as an instance of an existing system to exhibit how the business can connect the existing system to such an architecture along with the ease of the device to cloud connectivity. Any vendor which provides IoT based architecture to companies require to connect a gateway to IoT which is usually a proprietary system whereby they need to configure to proprietary software or API. Thereby the legacy system requires to customize with respect to the vendor, even if customization is not done, the data that would be generated would be of a specified format which has to be converted to a format defined by the proprietary system. The superiority of our invention over others are that the data that would be generated from the legacy system can pass through our API directly, irrespective of the format whereby the major customization would not be required. It has been designed in such a way that it can be integrated to all kind of data analytic systems. It has a platform neutral architecture which can help textile industries to choose their platform like, Web, mobile, windows based or REST (Representational State Transfer) web services, based on their available technical resources. The cloud platform is also loosely associated with the system along with IoT, Android and Web application. The business users have the independence to select the cloud platform based on their budget and user volume. Different sections included in the design: The entire design has three different tires, including:

a. User Application
    i. Web Application: This application will be used to manage the device, on/off the device remotely and to check the device status.

ii. Android Application: This is Native android application, developed to on/off the device remotely and check the current device status.

b. Cloud Server
   i. Web Server for Web Site: The web application is hosted in Public Cloud, however customer can host this application to On-Premises/Private/Hybrid Cloud also.
   ii. REST Services: REST service also deployed in Cloud server, and this service can be used by multiple platforms.
   iii. Database Server: This is another integral part of the entire application and this is also hosted on Cloud environment

c. Controller Application: It would be running near the machine. All machine controllers would be connected to the computer where the controller application has to run. The application manages the below devices:
   i. Control Motors
   ii. Flow Control Valves
   iii. Control Pumps
   iv. Read Sensor Information

In this design standard motors, centrifugal pumps and aeration pump have been used as electrical components. These components are to be activated based on the input signals generated from Laptop. Sensors are to be connected to different chambers by the usage of Raspberry Pi, though consumers are independent to select their own controller board for sensors and actuators.

The proposed high-level design is based on platform and technology independent architecture. The entire design is divided into multiple technologically independent components. These components are functionally dependent to connect sensors and devices at low level. The software components are also responsible to upload data to database servers. In this design the entire data structure has been divided into two parts, first, to expose data for multiple devices like mobile phone, Bigdata platform etc. and second part to save/update transactional data into relation database. The concepts Bigdata consists of Four V's. They are:

i. Volume- Scale of Data.

ii. Variety- Multiple source data from different sensors and devices.
iii. Velocity- In/Out data rate is 1 millisecond.
iv. Veracity- Uncertainty of data.

IoT enable infrastructure has been used to control pumps, motors, rotators, valve and connected sensor information example temperature sensor, water level sensor, ph-sensor etc. The architecture is flexible enough to connect as many devices and sensor as required. The Figure 5.4 explains the high-level architectural diagram of the proposed system. The Database, Web Service and Web Site has been deployed in cloud server for high availability of infra structure. The controller system is responsible to connect with machines and sensors, communicate with server to upload and download data. The Controller Application is responsible to connect all motors and sensors based on scheduled information. For our experiment we have developed this layer using C#.Net. The proposed architecture has the flexibility to implement the controller application using any high-level language like JAVA, Python, VB.Net etc.

The user device, thus, can be attached to the plant without any external software support. The data collected can be stored in the database and can be accessed through the IoT enabled devices. The device operates with sensors and relays connected to the plant which helps in controlling the operation. The sensors to be used can monitor the temperature, pH value and the other specification. The data mining process enable through IoT which helps in to simplify the work and help in speeding up the process. This proposed IoT architecture was designed to help the small-scale textile or other industries in managing their effluent plant. The device designed works through relays and sensors which is flexible to adapt any vendor specification and user-friendly. The IoT is designed using programming languages and is not limited to any specific platform.

As reported, if, physical method is used, the process becomes expensive and chemical, alone or with physical leads to the production of significantly large amount of toxic sludge. Thus, for the elimination or reduction of cost and such sludge handling process, adsorption of the pollutants from the aqueous solution plays a very important role being of low initial cost investment as in the pre-treatment procedure, flexibility of the process, simplicity of design, operational ease and insensitivity to

toxic pollutants. Thereby in this study instead of taking activated carbon, as an extensively used adsorbent, wheat bran, a waste product of cereal wheat has been chosen as an inexpensive substance, a waste product of cereal wheat and which does not even involve higher cost in their regeneration process (Anonymous 7). Already studies have been done on wheat bran for heavy metal removal, specific dye removal but usage of wheat bran as a part of the preliminary treatment for textile effluent is a new venture which encompasses the physical treatment part of the invention.

For biological treatment of the textile effluent White Rot Fungus (WRF), is the organism of choice, as a powerful lignin degrader because of their lignocellulolytic enzymes, which make them one of the most important microbial systems for bioremediation. In one invention, the inventors have proposed a novel and sustainable process for the treatment and detoxification of liquid waste with strains of Myrothecium and Ganoderma species (Anonymous 2, 2018) proving the exploitation of the basidiomycetes strains for their efficient enzyme system for the purpose of remediation. In another invention, scientists have explored the genetic constitution of another genus within basidiomycetes (Polyporous species) for the identification of the genes and their modification for the enhanced production of laccase, laccase being the target enzyme for significance in remediation processes (Anonymous 3, 2018). In another invention US 20050067347A1, a sustainable process has been given for the treatment of and detoxification of liquid waste containing dyes has been proposed which comprises of a pre-treatment and biological treatment with fungi (white rot fungus) / active agents. They have used standard strains like *Clitocybula duSenii* DSM 11238, *Trichoderma harzanium* MUCL 29707 and *Trichoderma longibrachiatum* MUCL 39887 (Anonymous 4, 2017).

In another prior invention, WO 2016137848 A1, the invention comprised of a computer implemented method and a system for determination of the reliability of a machine that included a method of receiving one of a machine data from one or more locations through an internet of things (IOT) based machine wearable sensor network. It included the storage of the data in a distributed computer database coupled to an enterprise resource planning (ERP) system. The data extraction could have been done through a computer server, one or more entity information from the data to compare against a pre-defined baseline but this system has never spoken about the legacy to

advance conversion methodologies, no defined generic design, cloud integration methodologies (Anonymous 6, 2019).The technology thus specifically talks for Machine reliability. It had never spoken about the legacy to advance conversion methodologies. Next, no defined generic design methodologies have been talked about lastly there was no integration to the cloud methodology which has been talked about.

In another prior invention, CN106167749 A, it has given an application of Internet of Things (IoT) for an intelligent beer fermentation and its preservation barrel. It has an advantage that brewing procedures are stored in the controller, the controller calls out fermenting procedures for beer brewing after a display screen on the bar codes but the research has never spoken about the data analytics and cloud integration nor mobile device connectivity (Anonymous 5, 2019).

Thereby, after comparison of the existing system existing in the market , in this project it has been tried to develop the solution using cutting edge of technology by the usage of a pre-treatment system with wheat bran, then with an isolated novel strain of Basidiomycetes, because of its advanced enzyme system, for the treatment of the industrial wastewater. The architecture designed is pluggable with multiple heterogeneous environment. A REST (REpresentational State Transfer) based communication protocol has been used to communicate with different devices like Android Mobile, iPhone, Tablet, Web bases system and Smart Client System. The design is technology independent, so business don’t need to bother about specific technical expertise.

In another invention, Interoperability mechanisms for internet of things integration platform. The research gap which could be taken up in this present study was the conversion methodologies from Legacy system to Advance IoT based system secondly,

the integration methodologies were not disclosed which keeps an avenue open for thinking of a cost-effective designing.

The advantages and superiority over the existing prior art can be primarily based on the cost and next the simplicity and user friendliness of the architecture. Below mentioned is a price comparison few existing vendor and the present invention’s cost.

Microsoft Azure IoT		AWS IoT Core Components	
Functionality	**Monthly Price (US$)**	**Functionality (10000 Devices)**	**Monthly Price (US$)**
Azure Cosmos DB (1 Year reserved)	992.80	Connectivity Charges	345.60
Azure IoT Hub 400,000 message/day	50.00	Messaging Charges	975.00
Azure IoT Edge	0.00	Device Shadow and Registry Charges	375.00
Azure IoT Central (20 devices)	29.43	Rule Engine Charges	180.00
Total Monthly	1000	Total Monthly	1876.60

Table 5.1: Cost Comparison Azure and AWS

Server Provider	**SQL Server Database Max Size (in GB)**	**MySQL Server Max Size (in GB)**	**Cloud Server (US$)/Month**
Godaddy	1	10	16.75
SmarterASP.Net	10	10	7.95

Table 5.2: Cloud Hosting Environment

Proposed Cloud based IoT Solution			
Service Provider	hostmedia.co.uk	sqlservermart.com	rshosting.com
Web Server	NA	IIS 10	IIS Web
Bandwidth	Unlimite	Unlimited	15 GB Monthly
Storage in GB	5	50	10
Number of database	1	4	Unlimite
Database	SQL Server Hosting	SQL Server Hosting	SQL Ser
Monthly Price (in US$)	4	5	5

Existing Cloud based IoT Solutions					
Microsoft Azure IoT		AWS IoT Core Components		Kosmos IoT System	
Functionality	Monthly Price(US$)	Functionality (10000 Devices)	Monthly Price(US$)	Business	Industrial
Azure Cosmos DB (1 Year reserved)	992.8	Connectivity Charges	345.6	Upto 10 assets	Upto 25 assets and 4 assets minimum
Azure IoT Hub 400,000 message/day	50	Messaging Charges	975	One user account	3 users account
Azure IoT Edge	0	Device Shadow and Registry Charges	375	One physical Site	Single physical site
Azure IoT Central (20 devices)	29.43	Rule Engine Charges	180	Satndard Logging Interval	Satndard Logging Interval and optional machine learning insight
Total Monthly Price(in US$)	1072.23	Total Monthly Price(in US$)	1875.6	$150/per asset/per month	$250/per asset/per month

Table 5.3: Price comparison of different IoT and Cloud systems

Thus, in this invention the major aspect was to provide an environment friendly and a well-connected system which can ultimately provide a secured and a comfortable

platform to the industry so that ultimately, they do not become the major cause for the environment pollution. The cost of the proposed system was also another major concern, whereby on comparison with the existing systems a comparison provided in Table 5.1 would provide a very clear picture of the area with respect to which the cost effectiveness has been highlighted.

5.3 Material and Methods

5.3.1 Material

Borosilicate glass of width 12mm thickness glass sheets, to prepare tanks were procured from Jalandhar, Punjab. Stainless steel, industrial grade shaft, discs and stirrer procured from Phagwara, Punjab, India. Electrical and Electronic devices like three peristaltic pumps (Questquo D1-D5 Dc Dosing Pump Peristaltic Head), three motor of 12 volts (Themisto 12Volt DC Motor), three aeration pumps (Tetra 77851 Whisper Air Pump) were procured from local electrical shops in Jalandhar, India. Three ultrasound sensors (REES52 Ultrasonic Range Finder Module Sensor Distance Measuring Transducer), two pH probes (PH Sensor Module V1.1 with PH Probe for AVR 51 PH Shield with MSP430 Test Code Sensor), one Raspberry pi mother board, eight port solid state relay board (Sain Smart) were procured from Amazon, India. Software used were Visual Studio 2017 (.Net framework 4.5), Cloud server (Smartasp.net), Python 3.7.4, Linux shell script, Database SQL 2016 (Express Edition). Wheat bran (WB) was obtained from local market of Cantonment area, Jalandhar, Punjab, India.

5.3.2 Methods

5.3.2.1 Procurement of industrial effluent

Textile effluent was procured from one of the textile industries located in Ludhiana, India (name withheld), at an interval of one month for a period of 3 months (between December to March) in 2 sterelized PVC containers each of volume 5 litres. The sample collected from the inlet (final stage after dyeing), before it was sent for the effluent treatment. The sample was collected and was processed on the same day within 2 hours. If not processed on the same day the samples were preserved at 4°C for a period not more than 7days, without any pre-processing or by addition of any chemicals (Abioye et al., 2014).

5.3.2.2 Physico-chemical analysis of the effluent procured

The sample procured was subjected to analysis of COD (Chemical Oxygen Demand), BOD (Biological Oxygen Demand), TDS (Total Dissolved Solids), TSS (Total Suspended Solids), pH and Optical Density (OD) by following the APHA standard protocols (APHA 1999).

5.3.2.3 Prototype construction for effluent treatment plant

The construction materials and components differ with the usage volume. The prototype comprised of four major components, an adsorption column (Height, 108 cm; Diameter 8.5 cm and Liquid Colum Height, 36 cm), a primary treatment or equalization tank (Height, 22.40 cm., Length, 24.08 cm, Breadth 19.70 cm), a RBC (Rotatory Biological Contactor) or a secondary treatment tank (Height, 22.40 cm., Length, 35.20 cm, Breadth 19.70 cm and Disk Radius 14cm) and a precipitation tank (Height, 22.40 cm., Length, 24.08 cm, Breadth 19.70 cm) (Figure 5.2). The dimension of all the components were calculated based on disc diameter of RBC tank, on basis of the concept that 40% of the disc should be under water at a time during the operation (Cortez et al., 2013) (Figure 5.20).

For the column construction for adsorption, a column adsorption study was conducted in a small glass column with an inner diameter of 3.5 cm and 20 cm in length. Wheat bran was packed in the column above the glass wool (which filled around 1 cm height). Distilled water was passed through the column in the downward direction using a peristaltic pump, to wet the column and to ensure no space to be occupied by air. Then column was loaded with dye sample (representative dye being, Congo Red, a concentration of 100 mg/L) at a rate of 13 mL per mins. At defined intervals the samples were collected and Optical Density (OD) was measured at 420 nm (Singh et al., 2015).

For scaling up, 10 times larger glass column to the small column used in the preliminary study was constructed, by a manufacturer in Amritsar, Punjab, India. The column was constructed such that it can accumulate one third of the volume capacity to that of the RBC in its respective collector after adsorption. It was calculated such that each time the column should discharge a volume of 2071 cubic centimetre of liquid. For calculation of this an algorithm was also formulated so that it could be easily estimated even by the industries.

A stainless-steel stirrer was attached to the primary tank or an equalization tank, with a motor, to rotate at a speed of 5 rpm for uniform mixing. A stainless-steel shaft of

length (48 cm), with 5 stainless steel discs equally spaced on the shaft were attached in the secondary treatment tank. On each disc sponge of width 0.5 mm was fixed as a media for the growth of the microorganism. The choice of sponge as a media was done in a random manner to provide a surface with porosity to provide adequate amount of air for the growth of the microorganism. Each tank was supplied with air sparging system at a flow rate of 67cc/minute. (include the column packing even). Thus the different stages of the process includes, 1st stage, Adsorption (Primary treatment), 2nd Stage Equalization, 3rd stage Biological Treatment (Rotatory Biological Contactor, RBC) and the 4th stage was an extension of the secondary treatment process (after biological) which can be vendor specific process, with either sedimentation, flocculation, precipitation or centrifugation.

5.3.2.4 Architectural designing for IoT implementation on the designed prototype for effluent treatment

The architecture was implemented based on four different modules, User Application, Processing Engine (PE), Execution Control Module (ECM) and Data Logging Module (DLM). The user application operated in two modes, web application and android mobile based mode. The user application is responsible for managing the device operation like remote switching on/off and monitoring for checking status. The Processing Engine was the centre for Web application, REST (REpresentational State Transfer) based web API and database server. It was responsible to send required signal and information to responsible devices. The ECM was responsible to control the machines, pumps and motors remotely. The ECM software at ETP site was also responsible for all communication across all the connected module, like the cloud server, user application, sensor and actuator. It connected to the cloud server and executed operations as per incoming request (Figure 5.4). The DLM was responsible to capture sensors information by connecting to individual tanks and sensor controllers to capture system data, machine feedback and upload to cloud server for further processing and data analytics.

5.3.2.5 Software design and its application on the prototype for effluent treatment

There are standard design patterns available to help designers to develop application in a well- defined way and to map the different components of the software with the

physical devices. Likewise, a standard design pattern is also available for IoT ecosystems. The design patterns are divided into information models, interaction models, application programming models, infrastructure models (Koster 2014). The Information model represents the data structure of the application. In the prototype design the Processing Engine (PE) has its own internal database which was used by the ECM and DLM through REST API.

The consumer has the independence to create their own database based on available infrastructure. The REST pattern has been implemented as an interaction model. A centralized REST based JSON service has been deployed in the PE module. The services are consumed by the subscriber were as per their requirement. Separate backend services have been created for separate front-end module like, web application, android application, windows form-based application, different IoT controllers (like, Raspberry pi, Arduino etc.).

The different application programming model has been developed for different application platform like Android, web, windows-form and Raspberry pi platform. The application programming is responsible to control the execution of machines (like, water pumps, motors, aeration pump etc.) to upload sensor data. WiFi, 3G, 4G based network infrastructure has been used for machine to machine and machine to device communication (Figure 5.3). The Python programming has been used for the Raspberry Pi integration (Source Code 5.3.2.7 and 5.3.2.8).

5.3.2.6 Experimental run of representative dye sample/ industrial effluent

The initially analysed effluent (for BOD, COD, TDS, TSS, DO and Optical density by following the standard protocol of APHA, 1999) was passed through the adsorption column, after which the part collected at the bottom in the collector was transferred automatically after the collector was full. The process was automated by applying programming language (.Net) whereby the ultrasound sensor and the peristaltic pumps worked conjugatively to pass down to the equalization tank and then to the subsequent tanks in a similar manner. After each section the analysis of the effluent was done for the above parameters to check whether there was an increase, decrease or a constant nature of the values. The entire operation was co-ordinated by the relay. The sensors were operated by raspberry pi board to collect the live data for cloud migration.

5.3.2.7 Python Code to Read GPIO and Update Device Status

```
import  sys
import RPi.GPIO as GPIO
import time
import json
#import urllib.request, json
import requests


#Execute GPIO Operation based on device id
def TriggerGPIOOperation(tdata, GPIOPin):
    deviceid = tdata[0]
    status = tdata[1]
    opmode = tdata[2]
    exectime = tdata[3]
    print("GPIO Operation Started :" + deviceid + ":" + status + ":" +
opmode + ":" + exectime + GPIOPin)

    #GPIO Operation
    GPIO.setmode(GPIO.BOARD)
    GPIO.setup(int(GPIOPin), GPIO.OUT)

    if status == "ON":
         print("Switch on the device....")
         GPIO.output(int(GPIOPin),True)
         response =
requests.get("http://rbciotservice.cycastechnology.in/ControllerService
.svc/UpdateDeviceStatus/" + deviceid + "/RUNNING/"+ exectime
+"/Executed")
         print("Executed service UpdateDeviceStatus: " +
str(json.loads(response.text)))
    elif  status == "OFF":
         print("Switch off the device...")
         GPIO.output(int(GPIOPin),False)
         response =
requests.get("http://rbciotservice.cycastechnology.in/ControllerService
.svc/UpdateDeviceStatus/" + deviceid + "/OFF/0/Completed")
         print("Executed service UpdateDeviceStaus: " +
str(json.loads(response.text)))
    if int(exectime) > 0:
         print("GPIO executed for " + exectime + " sec...")
         time.sleep(float(exectime))
```

```
        GPIO.output(int(GPIOPin),False)
        print("Operation completed...")
        response =
requests.get("http://rbciotservice.cycastechnology.in/ControllerService
.svc/UpdateDeviceStatus/" + deviceid + "/OFF/0/Completed")
        print("Executed service UpdateDeviceStatus: " +
str(json.loads(response.text)))
    GPIO.cleanup()


#Get REST API Data and pass to GPIO Trigger Operation Method
def main():
    data = "NODATA"
    print('Number of arguments:', len(sys.argv), 'arguments.')
    print('Argument List:', str(sys.argv))

    if len(sys.argv) > 4:
        data =
requests.get("http://rbciotservice.cycastechnology.in/ControllerService
.svc/" + sys.argv[1] + "/"+sys.argv[2]+ "/"+sys.argv[3])
        tdata = str(json.loads(data.text)).split("-")
        #tdata = data.split("-") #split string into a list
        #print(tdata)
        if tdata[4].upper()=="REQUESTED":
            TriggerGPIOOperation(tdata, sys.argv[4])
        else :
            print("Current status is " + tdata[4].upper() + ", system
with requested status will execute operation...")
    else :
        print("No Operation")

    print(tdata)


#while 1:
main()
```

5.3.2.8 Integration with Raspberry Pi

The integrations with Raspberry Pi has been done using Python code and crontab jobs. The python code is scheduled in crontab for automatic execution. In prototype design we have configured it to execute the python code in every second (Figure 5.21).

The configuration script and commands are:

$mkdir /home/pi/WSIOTApps

$mkdir /home/pi/logs

$crontab -e

CRON Tab Configuration:

Format:

* * * * * python /home/pi/WSIOTApps/ExecuteOperation.py GetDeviceStatusLowPower <ProjectId> <DeviceId> <PinNumber> > /home/pi/logs/Device<DeviceId>.log 2>&1

$sudo /etc/init.d/cron restart

5.3.2.9 Statistical Analysis

All the experiments have been performed in triplicates. The mean values of the observed data have been presented and standard deviation (± SD) was calculated. The entire calculation was done by using Microsoft Office (version 10) Excel, 2010.

5.4 Result and Discussion

The architecture applied on each module has led to the development of an automated, remotely operated IoT enabled effluent treatment plant. The architecture led to the development of WEB API detail section; a WEB application layer section comprising of a HOME Screen, RBC Master, RBC list, RBC Assign Devices, Show/Hide Pumps and/or Valves for Processing Engine, Control RBC, Sensor Master, Sensor Project List, Assign Sensor and Sensor status. It had also led to the development of Execution Control module comprising of Login Screen, Controller Screen, describing the functionality of each section of the controller screen, integration with the Raspberry pi. The next part developed was the Mobile Application Layer, comprising of Login Screen, Controller user interface, Sensor log interface.

5.4.1 WEB API Details

Web API is part of Processing Engine (PE). The API has exposed data in JSON format. The underline architecture of the API is Representational State Transfer (REST), so that it could be consumed by all HTTP enable devices, Table 5.4 depicting the REST API details.

5.4.2 WEB Application Layer

The Web application layer is also a part of Processing Engine (PE). It is the entry point of the entire system. The user required to register their device to the portal to avail the services. The web application has the following screen like, Login, User Registration, Forgot password, Home, RBC Master, RBC list, RBC assigned devices, show/ hide pumps and/ or valves, Control RBC, Sensor Master, Sensor Base Project List, Assigned sensor, Sensor status, Log Off (Table 5.5).

5.4.3 Experimental run of the representative dye sample/ effluent sample

The small column ran had obtained its saturation within 2hr 30mins as observed through its breakthrough curve (value not given here). The scaled-up column had attained its saturation within 5 hr 45mins (value not given here). The physico-chemical analysis has shown that there was a percent reduction in the BOD, COD, TDS, TSS, pH, OD by 78.9, 52.15, 91.6, 20.3,41.5, 88.8 % respectively, after subjecting the effluent through the above prototype (Table 5.6, 5.7; Figure 5.1). Where the Table 5.6 shows the physico chemical analysis of the effluent before and

after treatment in the constructed prototype and Table 5.7 depicts physico-chemical characteristics of the effluent after each stage involved in the prototype, drawing a comparison and depicting the changes in the parameters of the effluent. The permissible limits to be reached by the effluent to be disposed-off to the environment in accordance to the BIS (Bureau of Indian Standards) are pH of the effluent should be 5.5- 9, temperature, 50ºC; Colour, None ; TDS, 2100 mg/L, COD, 250 mg/L; and BOD, 30 mg/L. The limits of the inlet effluent sample of the representative industry, as was provided was TSS- 100-150 mg/L, TDS- 1300-1800 mg/L, COD- 350-550 mg/L and BOD- 150-200 mg/L.

5.4.4 Cost effective prototype

The cost analysis shows that the entire architecture is pluggable with existing old fermenter system and to do that business one needs to spend a maximum of Rs.90000/- (Table 5.7).

The use of IoT in manufacturing industry is not very new, however it is evident from different sources the implemented IoT solution comes with full suite including cloud. Multiple Cloud based IoT solutions had been explored during analysis phase of this project some of them are Kosmos Cloud (https://blog.temboo.com/all-about-kosmos/), iMETLand Project(http://imetland.eu/project/). The high-level control flow is depicted in Figure 5.5., Figure 5.6 gives the controller log in screen, Figure 5.7 shows the controller screen. Figure 5.8 depicts the designed website login screen, Figure 5.9 depicts the website homepage, Figure 5.10 depicts the website left menu, Figure 5.11 provides the RBC project creation section, Figure 5.12 provides the select active RBC project from list, Figure 5.13 provides the RBC management interface, Figure 5.14 provides the Assign devices and /or sensors, Figure 5.15 depicts the interface to show or hide the pumps/valves used in the prototype, Figure 5.16 provides the information on interface to control RBC operation either in a local/ remote mode. The android based application is depicted in the Figure 5.17. The analysis also performed few market leading IoT and Cloud based industrials solutions such as Online Multi-parameter Analyzer solution from Forbes Marshall, ThingWorx IoT platform and Kepware industrial data collection platform etc. The analysis shows that this frame works is good but costly and closed coupled with their own cloud infra structure.

There is limited opportunity to create hybrid or multiple clod model. The above-mentioned frameworks/eco-systems are costly and difficult to integrate with legacy systems. The pricing models of existing solutions are based on number of connected devices or message volume or even depends upon more complex calculation (Table 5.3).

5.5 Reference

1. Cortez, S., Teixeira, P., Oliveira, R., Mota, M., 2013, Bioreactors: Rotating Biological Contactors, Upstream Industrial Biotechnology Equipment, Process, Design, Sensing, Control and cGMP operations, John Wiley and Sons, 2, 1013- 1032.

2. Anonymous,1, Michael Koster May 27, 2014 Design Patterns are reusable solutions to common problems, available at: https://community.arm.com/iot/b/blog/posts/design-patterns-for-an-internet-of-things, accessed on 10/10/2019.

3. Anonymous 2, Sustainable process for the treatment and detoxification of liquid waste https://patents.google.com/patent/US5091089A/en, US005091089A, accessed on 3/4/2019

4. Anonymous 3, Purified polyporus laccases and nucleic acids encoding same available at: https://patents.google.com/patent/US5770418A/en , US005770418A, accessed on 21/03/2019.

5. Anonymous 4, Sustainable process for the treatment and detoxification of liquid waste, available at: https://patents.google.com/patent/US20050067347A1/en, US 20050067347A1 accessed on 21/03/2019.

6. Anonymous 5, Internet-of-Things intelligent beer fermentation and preservation barrel https://www.google.com/patents/CN106167749A?cl=en, CN 106167749 A, accessed on 15/3/2019.

7. Anonymous 6, Internet of things based determination of machine reliability and automated maintenance, repair and operation (mro) logs, available at: https://www.google.com/patents/WO2016137848A1?cl=en,WO 2016137848 A1, accessed on 12/02/2019.

8. Anonymous 7, Interoperability mechanisms for internet of things integration platform, available at: https://www.google.com/patents/US20150019710, US 20150019710 A1, accessed on, 11/02/2019.

9. Anonymous 8, Interoperability mechanisms for internet of things integration platform, https://www.google.com/patents/US20150019710, US 20150019710 A1, accessed on 11/02/2019.

10. Anonymous 9, https://patents.google.com/patent/US5091089A/en, Sustainable process for the treatment and detoxification of liquid waste , US005091089A, accessed on 11/02/2019.

11. Anonymous 10, Flexible design – can be integrated into a process, available at: http://axiumprocess.com/membrane-filtration/typical-applications/water-recycling-andeffluenttreatment/?gclid=EAIaIQobChMI4I25r9nj1wIVqgrTCh3LHQxgEAAYAyAAEgJF3_D_BwE , Axium Process, accessed on 9/3/2019.

12. Anonymous 11, SmartINFI and Water Analytics are proprietary technology, http://www.tecoproject.eu/images/IIR/Documenti/JointWorkshop2017_Presentazioni/2Nov/2Session_7VarunSridharan.pdf, Green environment Innovation and Marketing India (P) Ltd, accessed on 9/3/2019

Tables

Table 5.4: REST API Details

API Method Name	Parameters	Description
UserLogin	{Email}: Register Email {password}: Password in integer format.	User authentication API. It returns UserId, IP Address of the Controller and Active Project Id.
GetControllerConfiguration	{IP}: Controller IP address. Presently not in use. {ProjectId}: Project ID. {IsActive}: Active projects. {UserCode}: Register use code. {status}: Device status.	Controller Configuration API. This configuration returns current status of the sensor along with other parameters. Status includes: - Created - Updated - Deleted To get all device with status as REQUESTED set STATUS parameter as REQUESTED else it will return ALL record irrespective of status. To get deleted device ID set STATUS equal to DELETED Controller IP: This is optional Parameter Active: This parameter value is either Y/N Example API: ControllerService.svc/ GetControllerConfiguration/ 10.23.22.12/ PROJID0065/N/2/Deleted ControllerService.svc/ GetControllerConfiguration/ 10.23.22.12/PROJID0065/ N/2/Requested ControllerService.svc/ GetControllerConfiguration/ 10.23.22.12/PROJID0065/ N/2/ALL
OperationMode	{ProjectId}: Project ID for registered users.	Get operation mode. There are three operation

API Method Name	Parameters	Description
		Online, Manual. Online: In this mode devices can be controlled remotely. Manual: In this mode devices can be controlled from local.
DeviceLog	{DeviceId}: Register device id. {Value}: The value of device. RUNNING/OFF	Save device log and update
ProjectId	{USERCODE}: User code.	Returns active project code
UpdateDeviceStatus	{DeviceId}: Device Id {Status}: ON/OFF/RUNNING {ExecutionTime}: Execution start time. {Flag}: Executed/Requested /Completed	This method is responsible to upload device status.
SaveSensorData	{DeviceId}: Sensor Id {DeviceLog}: Sensor value {UOM}: Unit of measure	Save sensor data and data log time is server date time.
UpdateOperationMode	{ProjectId}: Project id {OperationMode}: ONLINE/MANUAL	Update project specific operation mode. - Online - Manual
OnlineModeDeviceStatus	{ProjectId}: Project Id {deviceId}: Device Id	This method returns the device status by project id if the operation mode is Online. Device status included - ON - OFF - RUNNING Execution time in seconds.
GetdevicestatusbyId	{ProjectId}: Project Id {deviceId}: Device Id	Get device status and execution time by project id and device id for online device only.

API Method Name	Parameters	Description
SensorData	{ProjectId}: Project Id	Get all sensor information by project id. Output format is below: Sensor Id-1|Sensor Code-1|Description|Value UOM|Captured on,Sensor Id-2|Sensor Code-2|Description|Value UOM|Captured on,...
GetDeviceStatus	{ProjectId}: Project Id {deviceId}: Device Id	Get device status and execution time by project id and device id for online device only.
GetDeviceStatusLowPower	{ProjectId}: Project Id {deviceId}: Device Id	Get device status and execution time by project id and device id for online device only. This service has been designed for resource constrain controller, mobile devices.
GetSensorStatus	{ProjectId}: Project Id {deviceId}: Device Id	Get sensor value including unit of measure (UOM)(if any).
GetDeviceStatusArduino	{ProjectId}: Project Id {deviceId}: Device Id	This service has been designed for Arduino controller.
DeviceUpdatedStatus	{deviceId}: Device Id {ProjectId}: Project Id	Project id and device id specific update record count.
SaveMultipleSensorData	{DeviceId1-DeviceLog1-UOM1,DeviceId2-DeviceLog2-UOM2}	Save multiple sensor data.
SetDeviceChangeDeleteSatus Completed	{deviceId}: Device Id {ProjectId}: Project Id	Change device status.
DeviceDeletedStatus	{ProjectId}: Project Id {deviceId}: Device Id	Find deleted device status by project id and device id.
DeviceUpdatedStatus	{deviceId}: Device Id {ProjectId}: Project Id	Project id and device id specific update record count.
GetDeviceStatusMobile	{ProjectId}: Project	Returns current device

API Method Name	Parameters	Description
	Id {User Id}: User Code or user Id	status in whether it is ON/OFF.
EmergencyStop	{ProjectId}: Project Id	Enable emergency stop for all the connected devices.

Table 5.5: Controller user interface functionality details

Component Name	Description
Start Button	This button enables the different controller buttons.
Manual/Auto Button	This is toggle button to change the mode from Manual to Auto or vice versa. It reflects the status change to web and mobile application using REST API.
Stop button to interrupt/stop all operation	This button to emergency stops all operation.
Connected devices status	This area to display the status of all connect devices.
Sensor Status	This area to display the status of all connected sensors.
Wi-fi Status Icon	This is to display current Wi-fi strength.
Operation Status	It changes the color from RED to GREEN if switches are ON and from GREEN to RED if it is OFF.
Eq. Tank Liquid Level	This field will display the liquid level captured using sensors.
Eq. Tank Execution Time	Based on execution time the connected device will run. The execution time can be set from web application or mobile application. If application running in Auto mode, then controller application downloads the execution time from database using REST.
Valve or Pump between Abs. tank and Eq. tank	This button to on/off the valve. It will be enabled only in manual mode.
Pump from Eq. Tank to RBC Tank	This button to on/off the Peristaltic Pump. It will be enabled only in manual mode.
Aeration pump for Eq. Tank	This button to on/off the Aeration Pump. It will be enabled only in manual mode.
Stirrer for Eq. Tank	This button to on/off the Stirrer Motor. It will be enabled only in manual mode.
RBC Liquid Level	This field will display the liquid level captured using sensors.
RBC Tank Execution Time	Based on execution time the connected device will run. The execution time can be set from web application or mobile application. If application running in Auto mode, then controller application downloads the execution time from database using REST.

Component Name	Description
Pump from RBC Tank to Sec. Tank	This button to on/off the Peristaltic Pump. It will be enabled only in manual mode.
Aeration pump RBC Tank	This button to on/off the Aeration Pump. It will be enabled only in manual mode.
RBC Rotter	This button to on/off the RBC Rotter. It will be enabled only in manual mode
Secondary Treatment Liquid Level	This field will display the liquid level captured using sensors.
Secondary Tank Execution Time	Based on execution time the connected device will run. The execution time can be set from web application or mobile application. If application running in Auto mode, then controller application downloads the execution time from database using REST.
Aeration Pump Sec. Tank	This button to on/off the Aeration Pump. It will be enabled only in manual mode.
Stirrer Sec. Tank	This button to on/off the Stirrer Motor. It will be enabled only in manual mode.

5.6 Physico-chemical analysis of the effluent before and after treatment in the constructed prototype

S.No.	Date of collection	Parameters	Before treatment (BT)	After treatment (AT)	% Reduction
1.	**14/12/2018**	**BOD**	**197.59**	**34.39**	82.5
		COD	**539.89**	**258.32**	52.15
		TDS	**1789.25**	**675.83**	62.2
		TSS	**148.32**	**116.86**	21.2
		pH	**10.4**	**6.7**	35.6
		OD	**0.389**	**0.045**	**88.4**
3.	**16/1/2019**	**BOD**	**200.27**	**43.18**	78.4
		COD	**561.89**	**267.66**	52.4
		TDS	**1862.15**	**798.79**	57.1
		TSS	**157.38**	**125.36**	20.3
		pH	**10.7**	**6.4**	40.2
		OD	**0.586**	**0.062**	**89.4**
6.	**20/2/2019**	**BOD**	**197.89**	**47.85**	76
		COD	**549.27**	**263.89**	52
		TDS	**1775.77**	**758.43**	57.3
		TSS	**147.76**	**118.95**	19.5
		pH	**10.5**	**6.5**	38
		OD	**0.377**	**0.035**	**91**

BOD (Biological Oxygen Demand); COD (Chemical Oxygen Demand); TDS (Total Dissolved Solids); TSS (Total Suspended Solids); OD (Optical Density measured at 652nm)

5.7 Physico-chemical characteristics of the effluent after each stage involved in the prototype

	Parameters				
	BOD (mg/L)	**COD (mg/L)**	**TDS (mg/L)**	**TSS (mg/L)**	**O.D. (nm)**
Initial	198.58±1.47	550.35±11.04	1809.06±46.47	151.15±5.40	0.45±0.12
Equalization tank	166.87±0.86	479.49±1.03	1331.21±1.21	147.74±0.97	0.396±0.31
RBC TANK (2nd day)	166.28±0.79	477.13±0.99	1330.10±1.08	138.86±0.76	0.385±0.07
RBC TANK (6th day)	117.85±0.87	397.25±0.87	1154.27±1.02	131.11±0.69	0.297±0.09
RBC TANK (15th day)	63.62±0.34	279.48±1.01	687.85 ±0.98	126.86±0.38	0.079±0.02
ADDITIONAL SECONDARY TREATMENT	41.81±6.83	263.29±4.70	151.15±62.68	120.39±4.43	0.05±0.01

5.8 Average value of the parameters before and after treatment

S.No.	Parameters	Average Values (BT *[1])	Average Values (AT*[2])	Average Percent Reduction
1.	**BOD**	**198.58±1.47**	**41.81±6.83**	**78.9**
2.	**COD**	**550.35±11.04**	**263.29±4.70**	**52.15**
3.	**TDS**	**1809.06±46.47**	**151.15±62.68**	**91.6**
4.	**TSS**	**151.15±5.40**	**120.39±4.43**	**20.3**
5.	**pH**	**11.17±0.71**	**6.53±0.15**	**41.5**
6.	**OD**	**0.45±0.12**	**0.05±0.01**	**88.8**
BT *[1] : Before Treatment; AT*[2] : After Treatment				

5.9 Experimental Plant Setup Cost

Category	Description	No of Items	Total Price in INR
Fermenter & Sparger	Motor	3	4500
	Centrifugal Pumps	2	3000
	Rotator	1	3000
	Glass Boxes	3	10000
	Pre-Treatment Tank	1	5000
Software & Hardware	Cloud Server	1	2000
	Electrical Plugs and Wiring	12	3000
	Sensor (Ultra Sound) and other electronics devices (Relay)	4	6000
	Web service	1	10000
	Web Site and Mobile Application	2	20000
Other expenses	Miscellaneous		17000
Total			83500

Figures

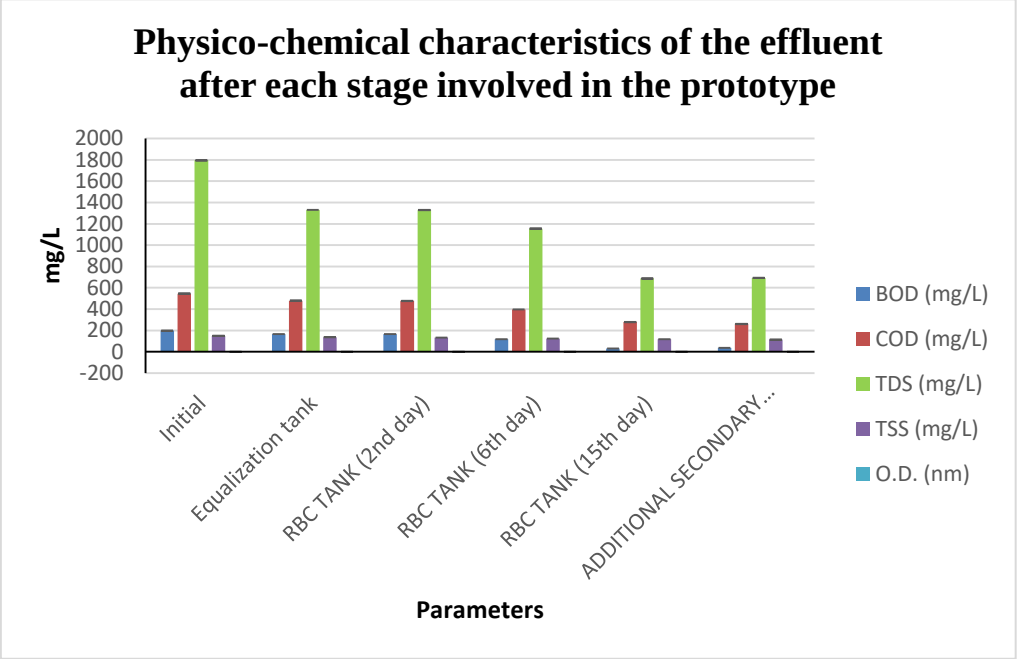

Figure 5.1 The average physico-chemical characteristics of the effluent, analysis of (a) BOD (b) COD (c) TDS and (d) TSS on initial day and during the treatment at various stages.

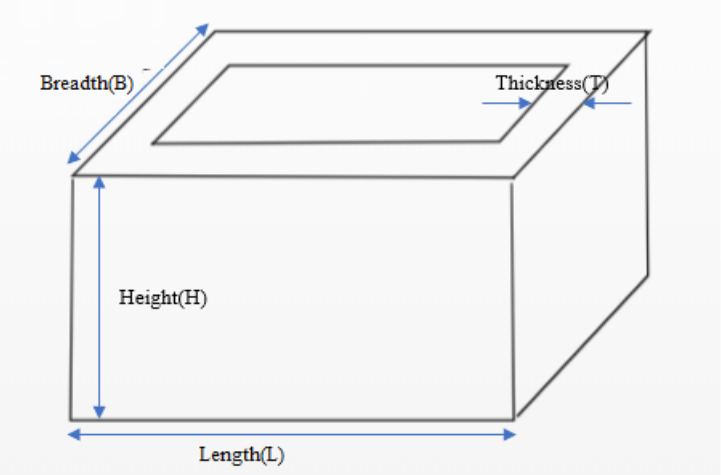

Figure 5.2: Default structure of the Glass Vessel / Container without lid

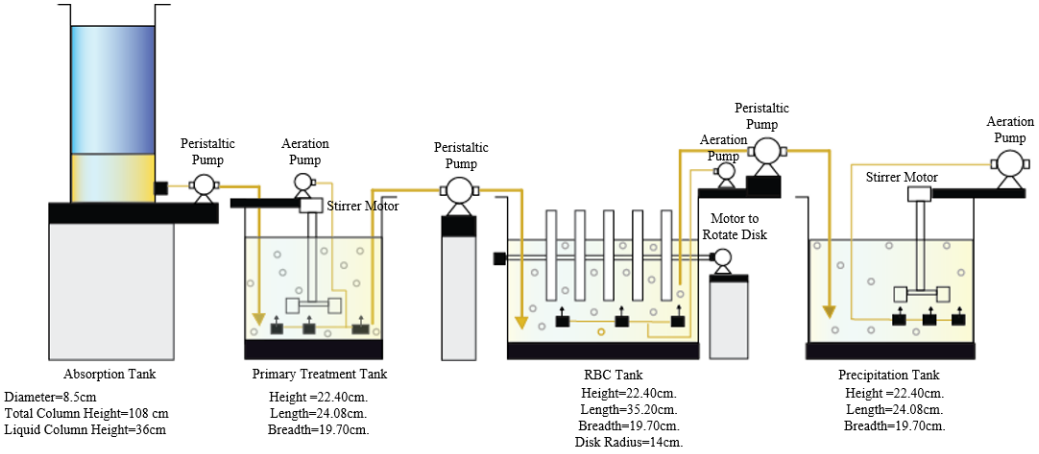

Figure 5.3: Schematic Diagram and Actual Dimension of Effluent Treatment Plant

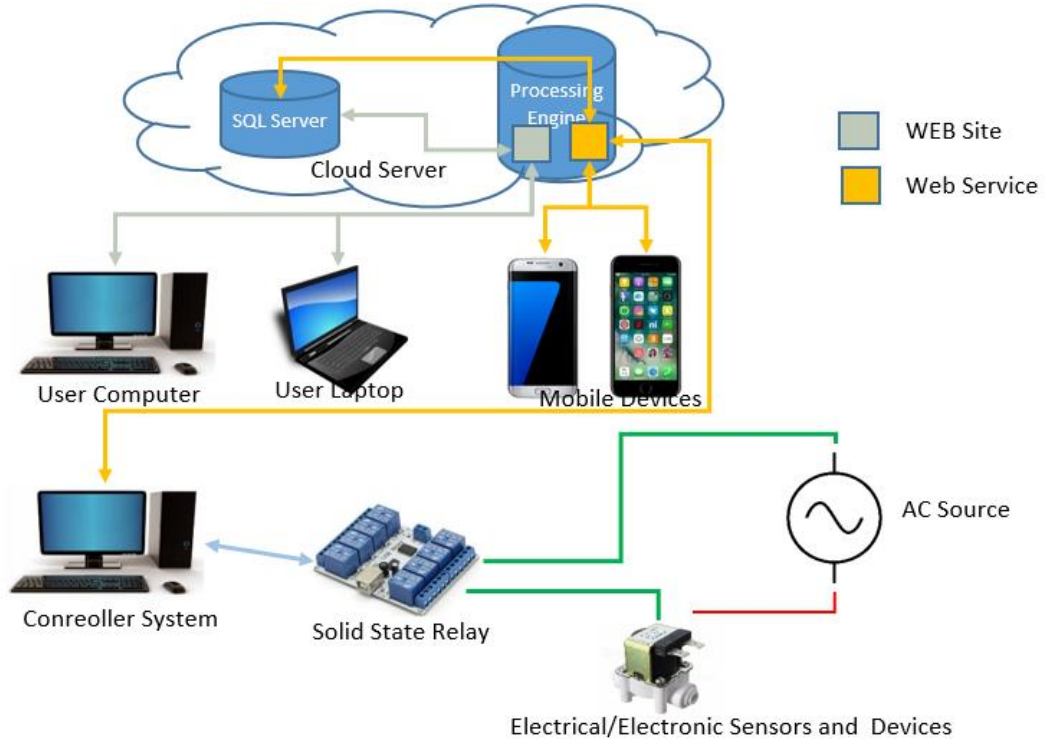

Figure 5.4: High level Architectural Diagram

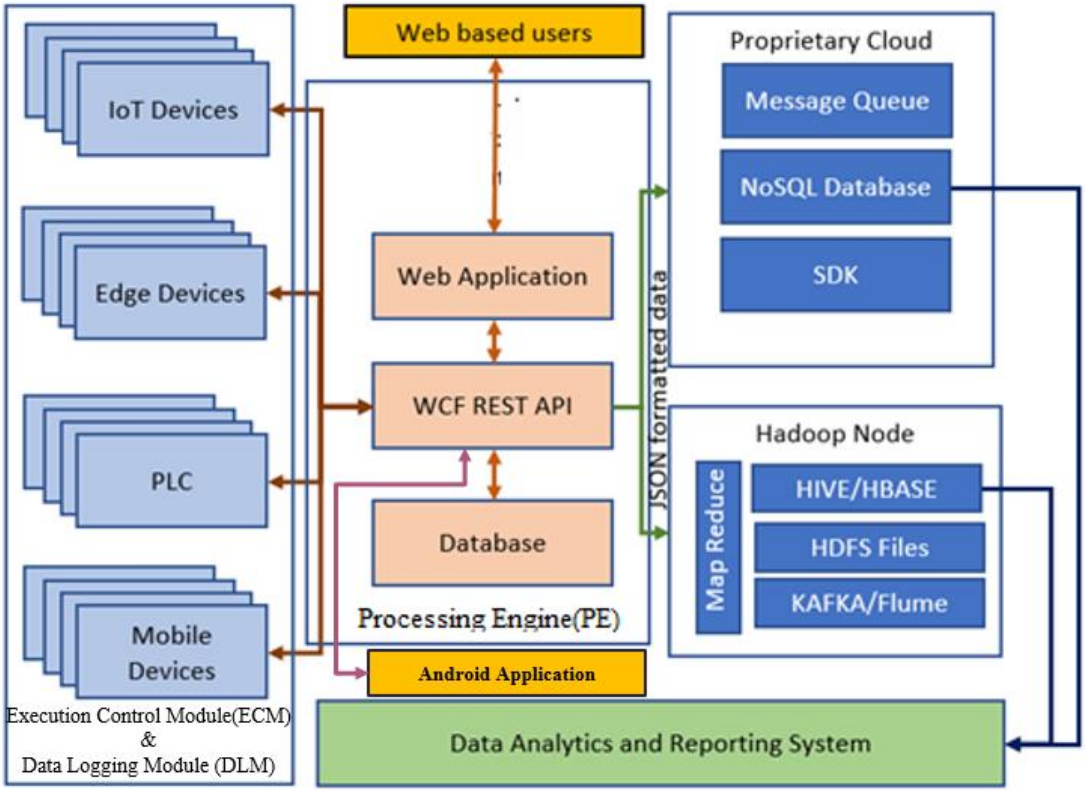

Figure 5.5: High level Control Flow Diagram

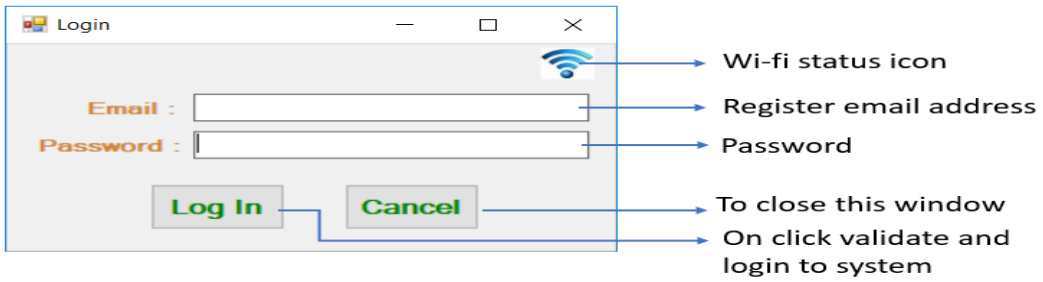

Figure 5.6: Controller Login Screen

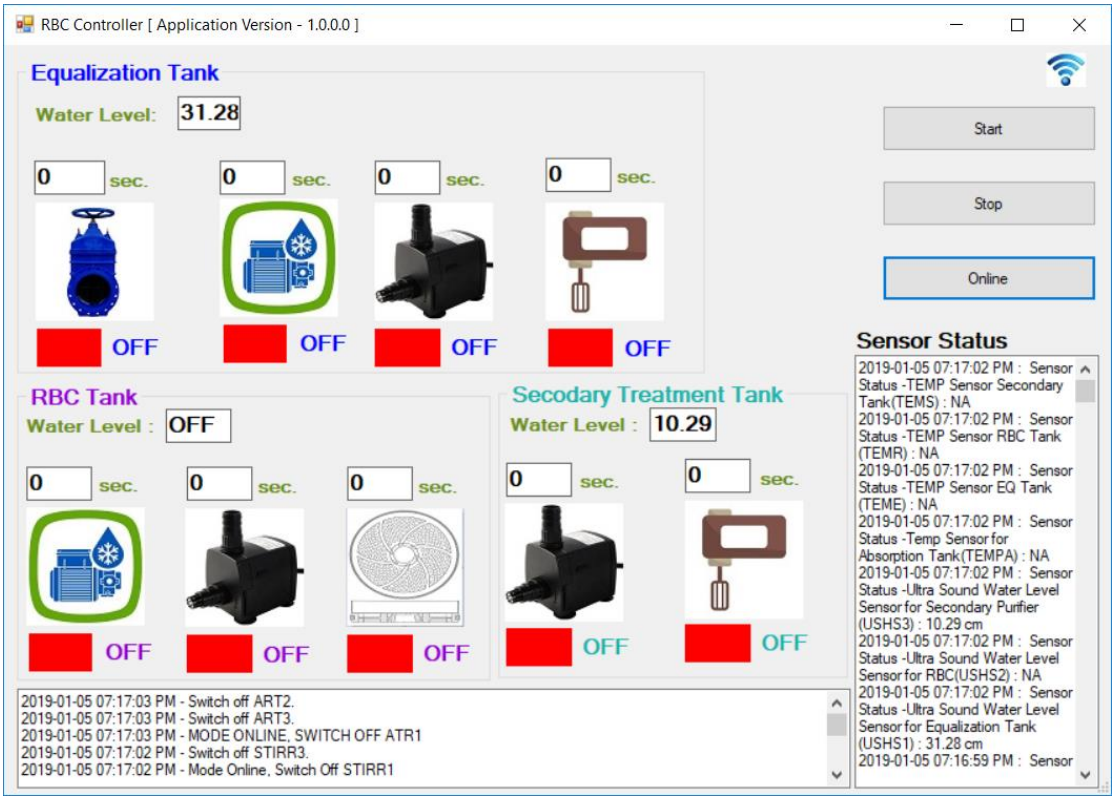

Figure 5.7: Controller Screen

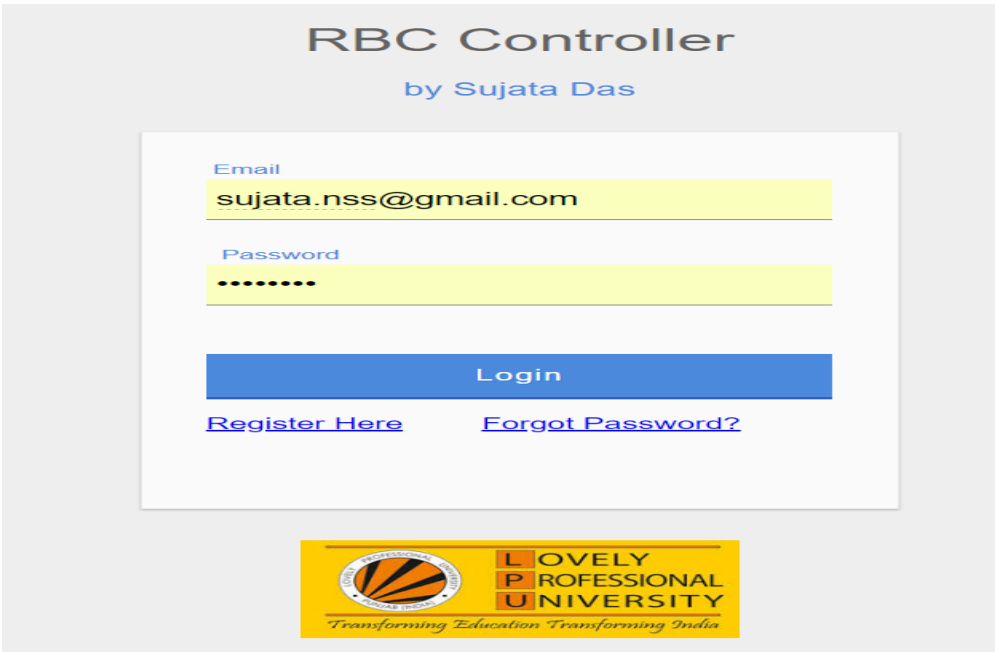

Figure 5.8: Web Site Login Screen

Figure 5.9: Web Site Home Page

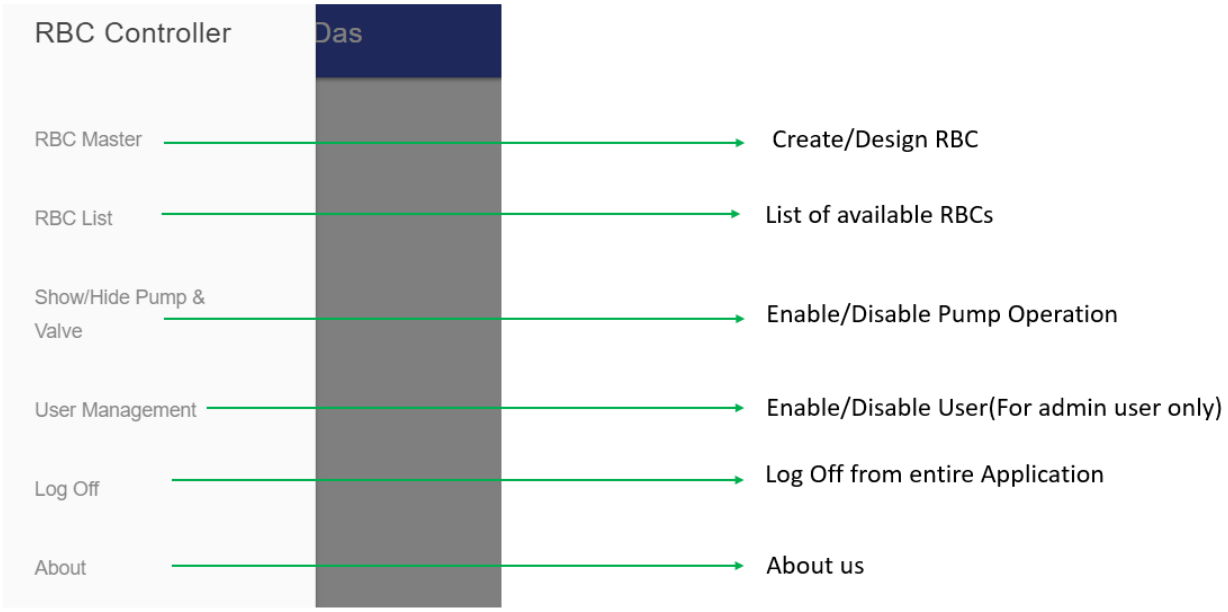

Figure 5.10: Web Site Left Menu

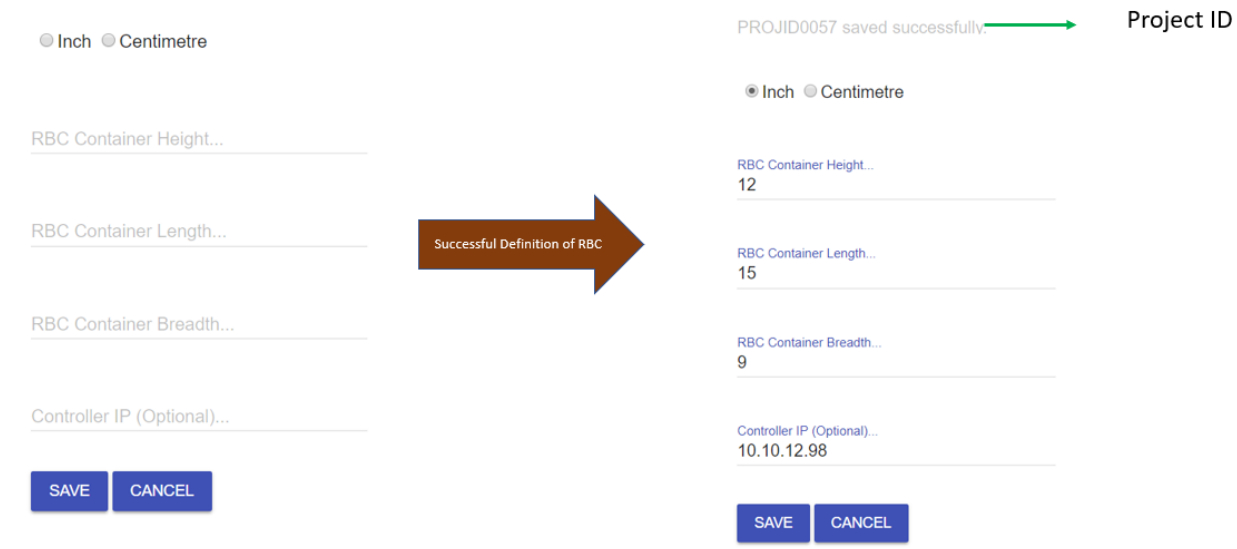

Figure 5.11: RBC Project Creation Section

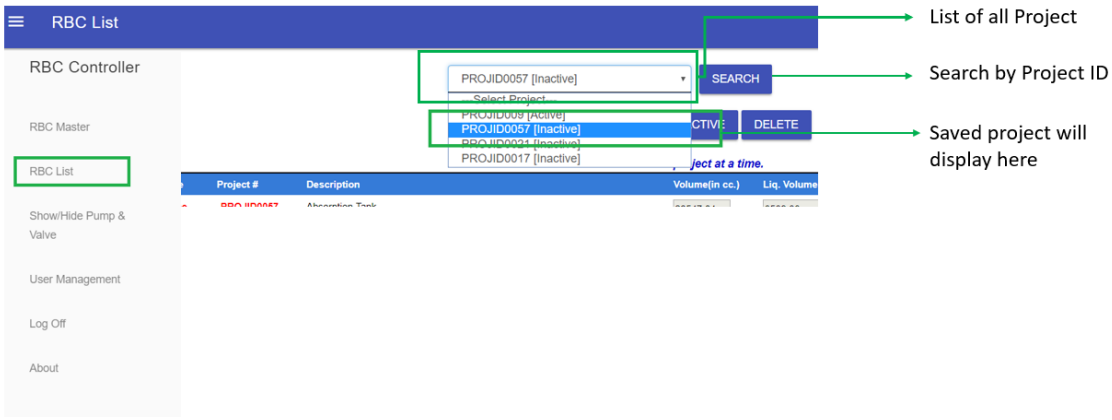

Figure 5.12: Select Active RBC Project from List

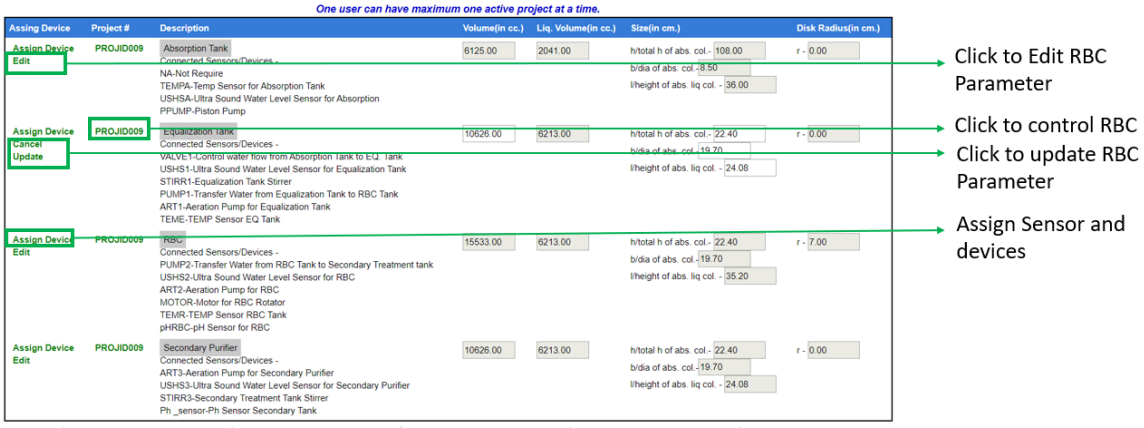

Figure 5.13: RBC Management Interface

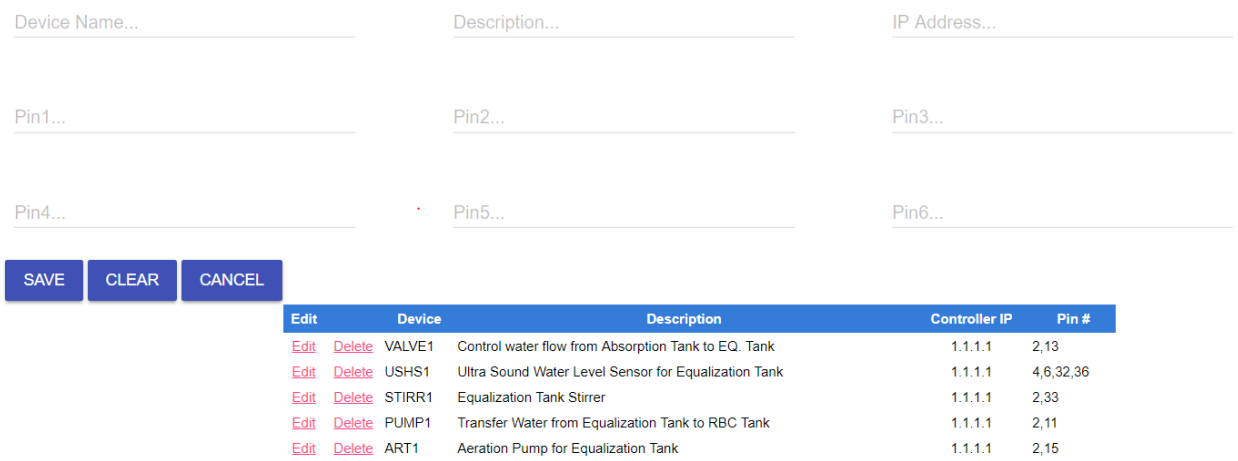

Figure 5.14: Assign Devices and/or Sensors

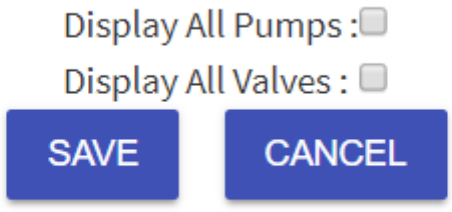

Figure 5.15: Interface to Show/ Hide the pumps/valves

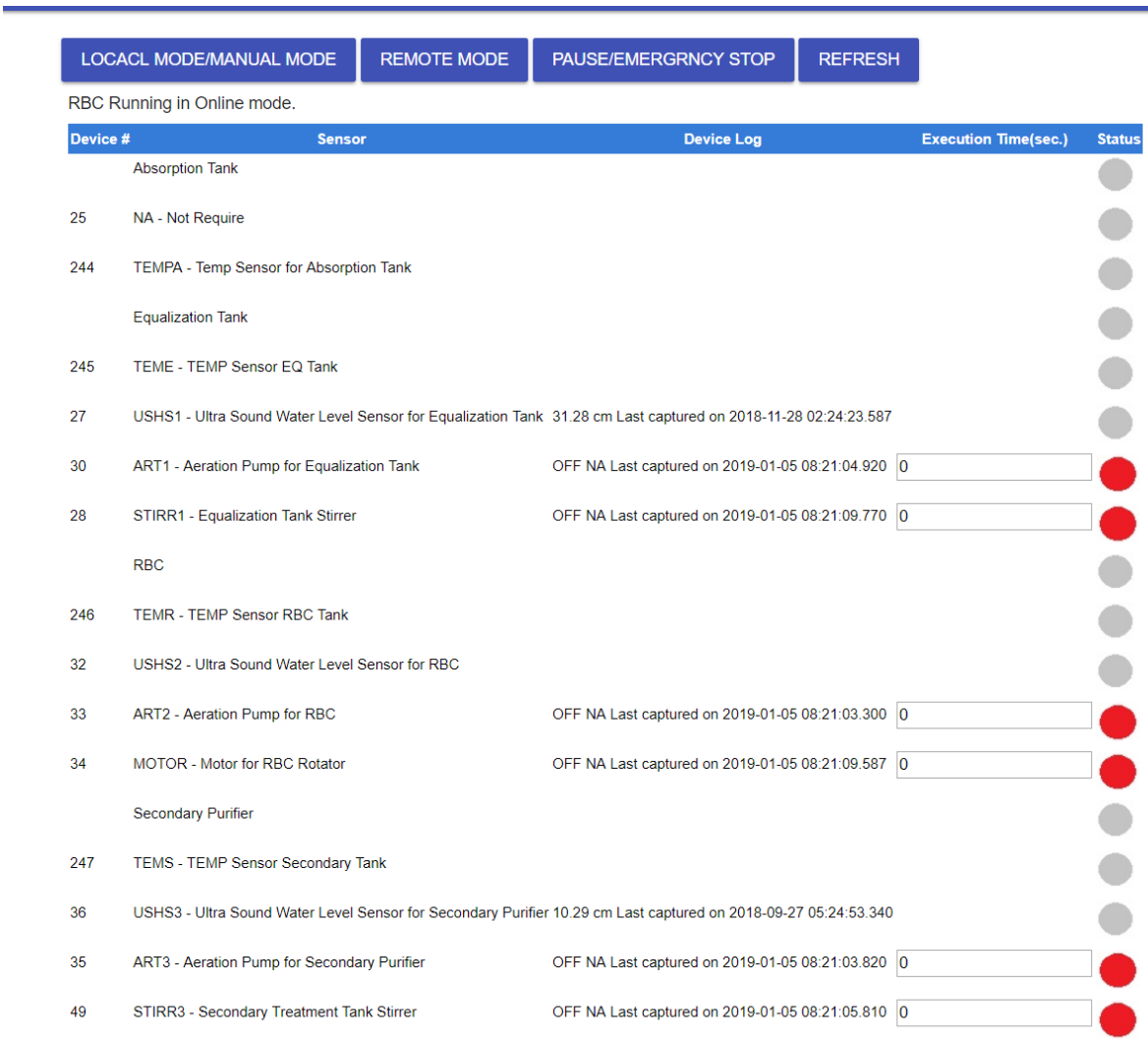

Figure 5.16: Interface to control RBC operation either in local/ remote mode

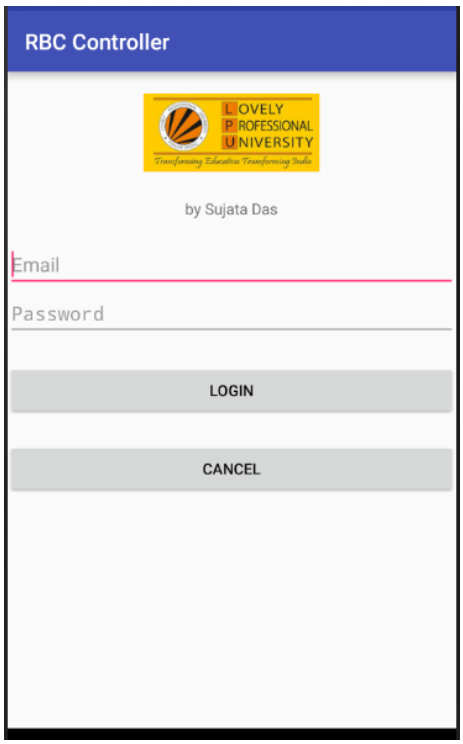

Figure 5.17: Login Screen of Android Based Mobile Application

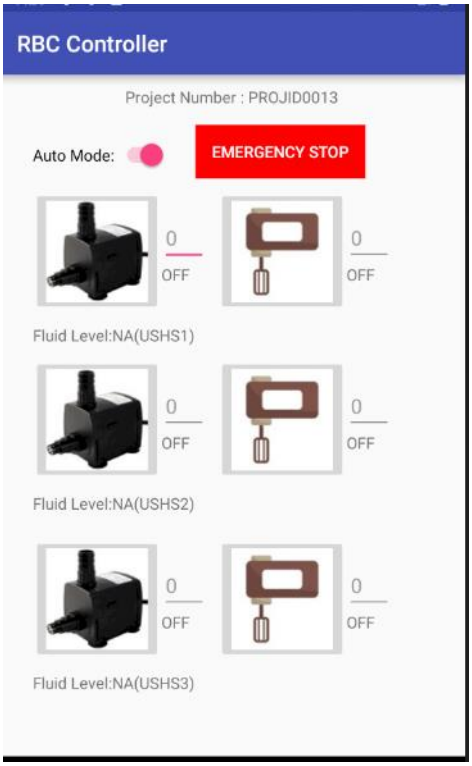

Figure 5.18: Controller Screen of Android Based Mobile Application

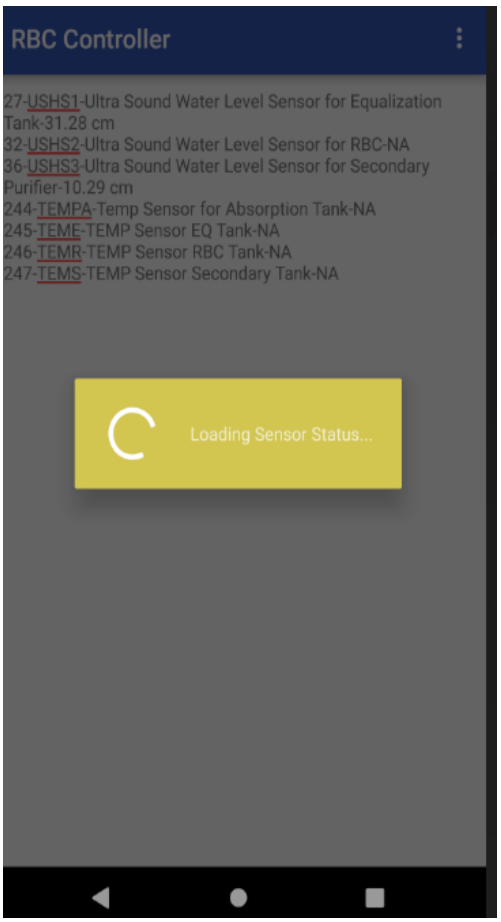

Figure 5.19: Sensor Information Panel of Android Based Mobile Application

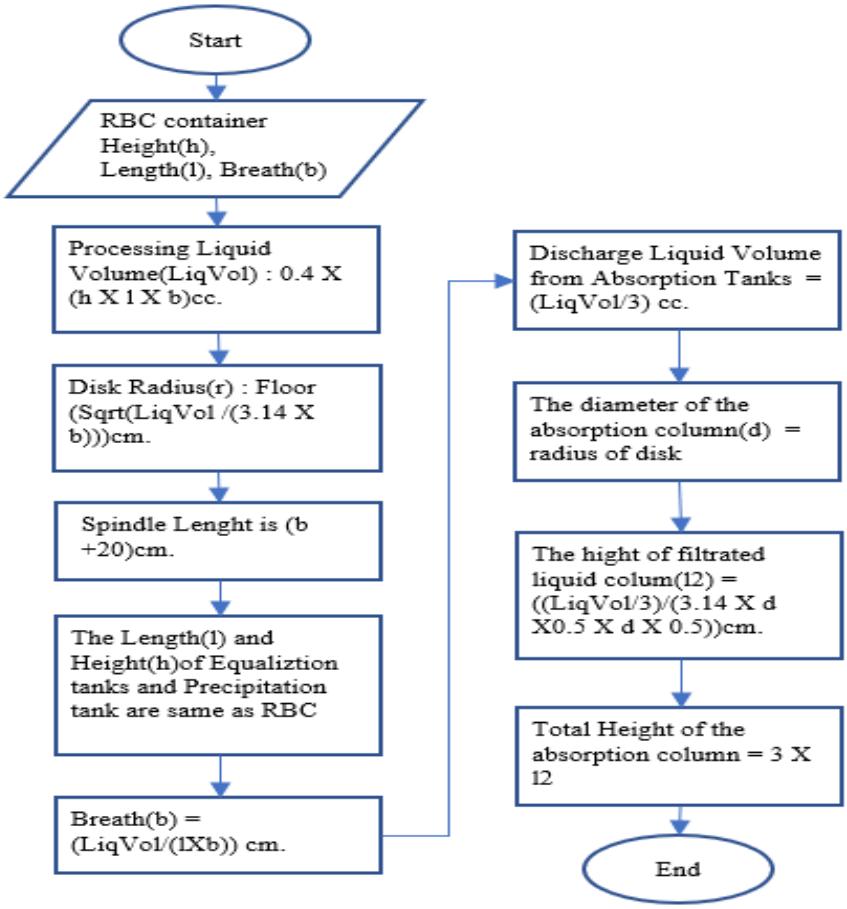

Figure 5.20: All Container and RBC Disk Dimension Calculation Logic

```
pi@raspberrypi ~/WSIOTApps $ crontab -l
# Edit this file to introduce tasks to be run by cron.
#
# Each task to run has to be defined through a single line
# indicating with different fields when the task will be run
# and what command to run for the task
#
# To define the time you can provide concrete values for
# minute (m), hour (h), day of month (dom), month (mon),
# and day of week (dow) or use '*' in these fields (for 'any').#
# Notice that tasks will be started based on the cron's system
# daemon's notion of time and timezones.
#
# Output of the crontab jobs (including errors) is sent through
# email to the user the crontab file belongs to (unless redirected).
#
# For example, you can run a backup of all your user accounts
# at 5 a.m every week with:
# 0 5 * * 1 tar -zcf /var/backups/home.tgz /home/
#
# For more information see the manual pages of crontab(5) and cron(8)
#
# m h  dom mon dow   command
* * * * * python /home/pi/WSIOTApps/ExecuteOperation.py GetDeviceStatusLowPower PROJID009 349 7 > /home/pi/logs/Device349.log 2>&1
* * * * * python /home/pi/WSIOTApps/ExecuteOperation.py GetDeviceStatusLowPower PROJID009 30 11 > /home/pi/logs/Device30.log 2>&1
* * * * * python /home/pi/WSIOTApps/ExecuteOperation.py GetDeviceStatusLowPower PROJID009 29 13 > /home/pi/logs/Device29.log 2>&1
* * * * * python /home/pi/WSIOTApps/ExecuteOperation.py GetDeviceStatusLowPower PROJID009 28 15 > /home/pi/logs/Device28.log 2>&1
* * * * * python /home/pi/WSIOTApps/ExecuteOperation.py GetDeviceStatusLowPower PROJID009 29 29 > /home/pi/logs/Device26.log 2>&1
* * * * * python /home/pi/WSIOTApps/ExecuteOperation.py GetDeviceStatusLowPower PROJID009 33 31 > /home/pi/logs/Device33.log 2>&1
* * * * * python /home/pi/WSIOTApps/ExecuteOperation.py GetDeviceStatusLowPower PROJID009 34 33 > /home/pi/logs/Device34.log 2>&1
* * * * * python /home/pi/WSIOTApps/ExecuteOperation.py GetDeviceStatusLowPower PROJID009 31 35 > /home/pi/logs/Device31.log 2>&1
* * * * * python /home/pi/WSIOTApps/ExecuteOperation.py GetDeviceStatusLowPower PROJID009 35 36 > /home/pi/logs/Device35.log 2>&1
* * * * * python /home/pi/WSIOTApps/ExecuteOperation.py GetDeviceStatusLowPower PROJID009 49 38 > /home/pi/logs/Device49.log 2>&1
```

Figure 5.21: Crontab configuration

Photograph

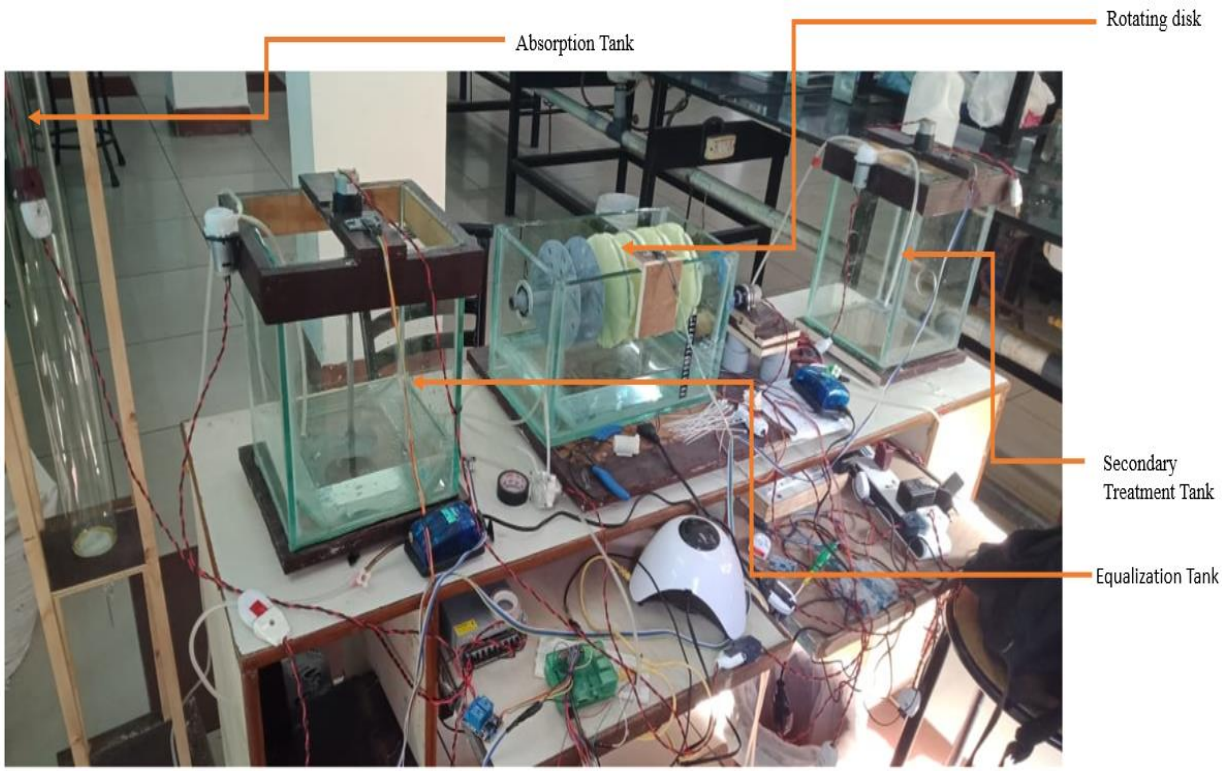

Figure 5.22: The working prototype

Summary and Conclusion

White Rot Fungus, belonging to the Basidiomycetes group was isolated. Out of 114, 3 isolates were obtained showing all the three ligninolytic enzyme activity under optimized condition of temperature (30°C), pH (8 for S1, 5.5 for both S4 and C4), days of incubation (7 days in case of S1 and 8 for both S4 and C4), substrate concentration (4gms of WB) and in presence of yeast extract (1%) and copper sulphate (0.4mM) has shown enzyme activity of S1, laccase, 8.47 ± 1.19 IU/mL, MnP, 6.72 ± 1.05 and LiP 6.12 ± 0.75 IU/mL. Whereas, S4 has produced laccase 11.84 ± 0.67, MnP 9.56 ± 0.13, LiP 8.38 ± 1.01 and C4 producing 9.46 ± 0.16, 6.65 ± 0.89, 8.79 ± 0.98 IU/mL. Thus, on the basis of the enzyme production by batch study as S4 was found to be a promising strain of basidiomycetes (white rot fungi, as produces laccase), it has been taken further for the whole genome analysis. By executing its whole genome analysis, it was found to be related to the *Schizophyllum* commune. Thereby by using *Schizophyllum* commune representative genome (Schizophyllum commune H4-8: GCA_000143185.1) as the reference to check the novelty of the sequence of the sample, 11646673 bases (~71.40% of sample length) genes were aligned with the reference genome with 1091144 mismatches and 129198 gaps. Only around 89.52% identity in the aligned region between sample and reference genome was found, suggesting the organism to be a novel species, isolated from the area of Jalandhar Cantt., Punjab, India. The isolate has shown the capacity to produce extracellular laccase enzyme around 11.84 IU/mL in the classical optimization method, whereas the statistical analysis by employing RSM has shown the organism to be able to produce 18.47 IU/mL of the same enzyme at a temperature of 30 °C at a pH 5.5.

The study has highlighted the importance of usage of wheat bran as a substrate not only for production of optimal concentration of enzyme by the isolated fungi (S4) but also as a substrate independently to act as an efficient adsorbent, to be a cost-effective alternative for the decolorization of industrial dyes. The study has used five different dyes to exhibit the maximum adsorption capacity of wheat bran for decolorization and has successfully given a result with maximum adsorption capacity (q_m mg/g) 19.79, 11.14, 15.17, 12.34 and 15.98 for CV, MG, CR, DDR and DO, respectively,

following non-Linear Langmuir adsorption isotherm model. They have followed pseudo second order kinetic model, with, q_m mg/g, values, 12.07, 13.46, 12.26, 11.88 and 13.28 for the respective dyes indicating wheat bran to be an efficient, eco-friendly alternative for the removal of dyes from the industrial wastewater.

The study has proceeded further to evaluate the synergistic activity of the adsorbent (WB) and the isolate (*Schizophyllum*-S4) obtained in the study, for the production of laccase for the purpose of dye decolorization (/ degradation) and then subsequently check the reusability of the bran and the mycelial mat obtained. The study has shown that by the use of wheat bran with microorganism, the dye removal efficiency was more in comparison to only wheat bran. As with dye adsorbed bran and microorganism the percent decolorization, it has shown 93.98, 96.57, 98.89, 87.46 and 88.12 % decolorization of CV, MG, CR, DDR and DO, respectively. With respect to reusability it has shown the alternate adsorption and desorption mechanism of the WB-F biomass could make the biomass to be used for 5 cycles with efficiency of dye removal of around 61.89, 66.28, 68.79, 61.77 and 64.38 %, respectively, depicting the involvement of the fungal mycelium as an adsorbent along with the wheat bran in the process of decolorization. Chromatographic analysis has shown that the dye of 98% has shown degradation of around 60.94%, 62.47%, 48.26%, 51.57% and 44.01% for CV, MG, CR, DDR and DO respectively after 10 days of incubation in WB-F biomass, depicting the production of laccase enzyme responsible for the degradation..

In the last part of the study by taking into consideration of the isolated novel strain, efficient lignocellulosic biomass (WB), and IoT, a cost-efficient effluent treatment plant prototype was designed. A cost effective, IoT enabled smart prototype was designed for an efficient removal of dye from the wastewater for the purpose of remediation of the effluent before their disposal. After the usage of the system, by treatment of textile effluent as a representation effluent it was observed that there was a decrease in BOD by 84.12 %, COD by, 63.92%, TDS by 54.29%, TSS by 48.23%, DO by 58.64 % and Optical Density by 93.67%. Thereby giving a unique system where a novel eukaryotic system and agro-industrial waste material could be used together for an enzyme system application in remediation purpose. Online monitoring, distribution device management and integration with a legacy system was another

uniqueness of the invention. Next, being able to connect to the surrounding system, with a boundary less information flow being able to convert the legacy system to IoT based system, compatible to Bigdata or Data analytic platform and a loose coupled customer friendly invention.

The future prospect of the project would be the study of the toxicity of the treated aqueous dye samples as well the adsorbent and the effluent obtained by following the above process. Along with the exploration of the avenues where the treated dye water and the obtained adsorbent to be reused as a fertilizer for landscaping.

Thus, it can be concluded that from this study an efficient biological, technologically advanced but cost-effective alternative could be proposed for a highly efficient toxic effluent remediation to curb down the concentration of the pollutants in the environment.

Appendix

Formula used:

1. Laccase activity is calculated by the following formula (IU/mL): E.A = A × (V/ t) × e × v
2. Dye concentration determination: $q_e = \frac{(C_0 - C_e)\, V}{W}$
3. The % decolorization of the dye was calculated using the following:

$$\% \text{ decolorization} = [D_0 - De / D_0] \times 100$$

4. Standard Curve of CV

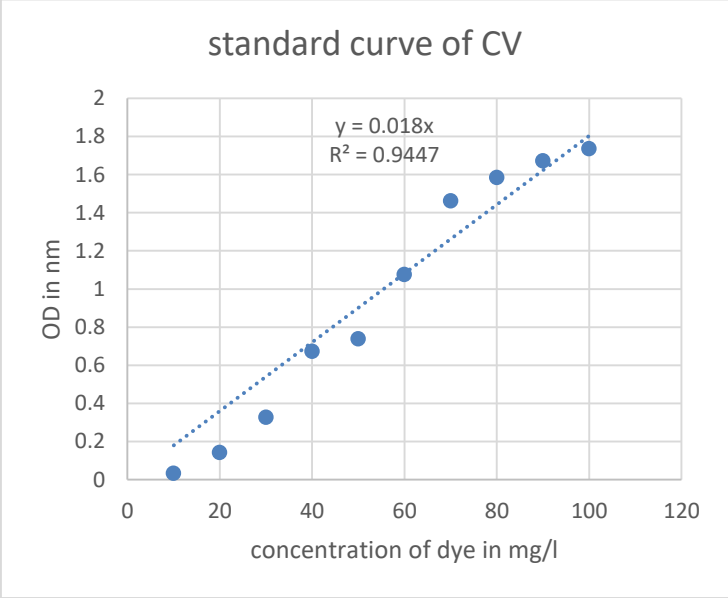

5. Standard Curve of MG

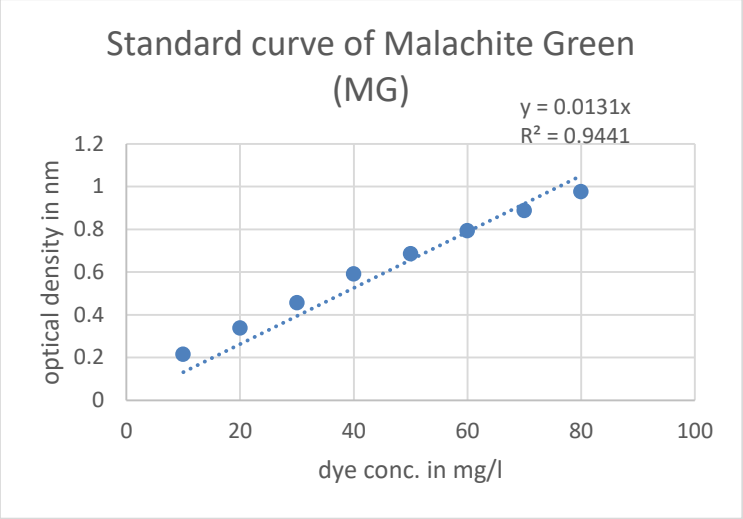

6. Standard Curve of Congo Red

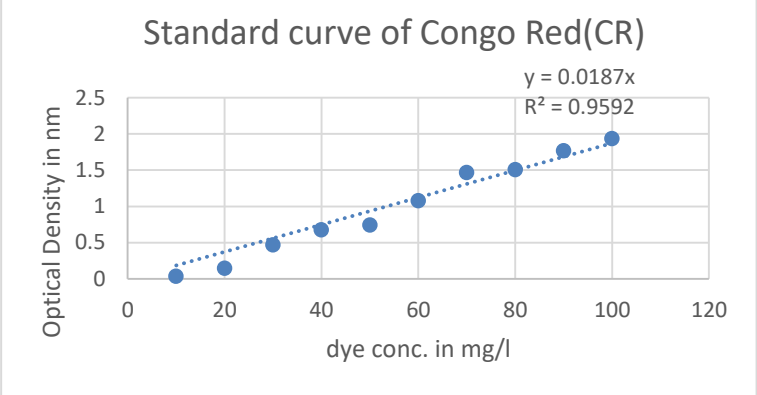

7. Standard Curve of Disperse Dark Red

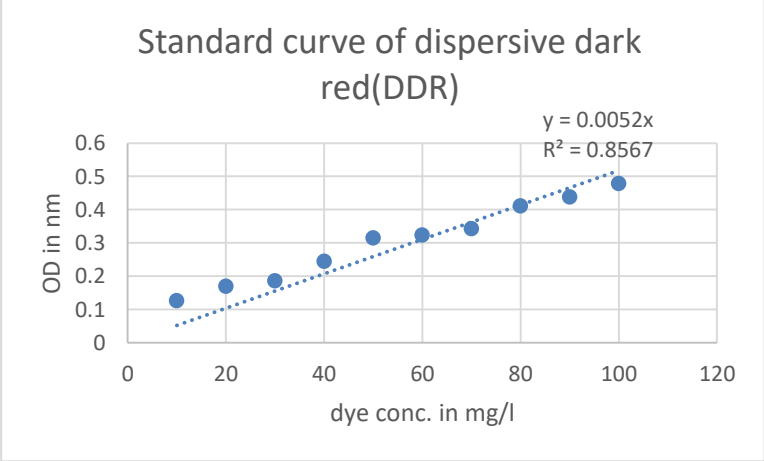

8. Standard Curve of Disperse Orange

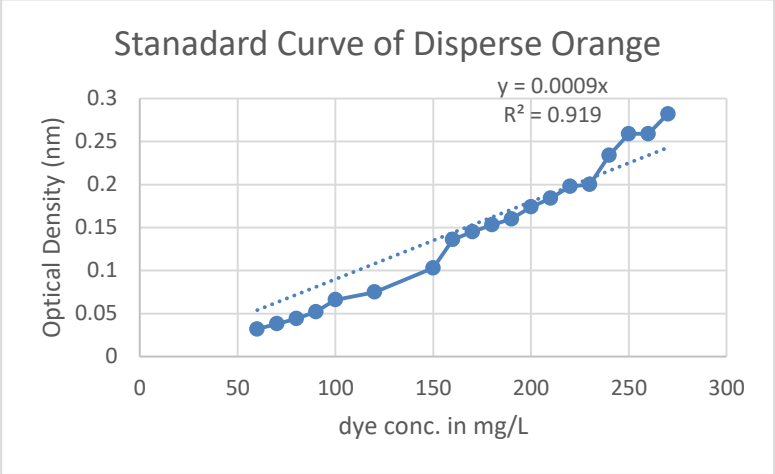

9. Flow diagram of the complete strategy of the work

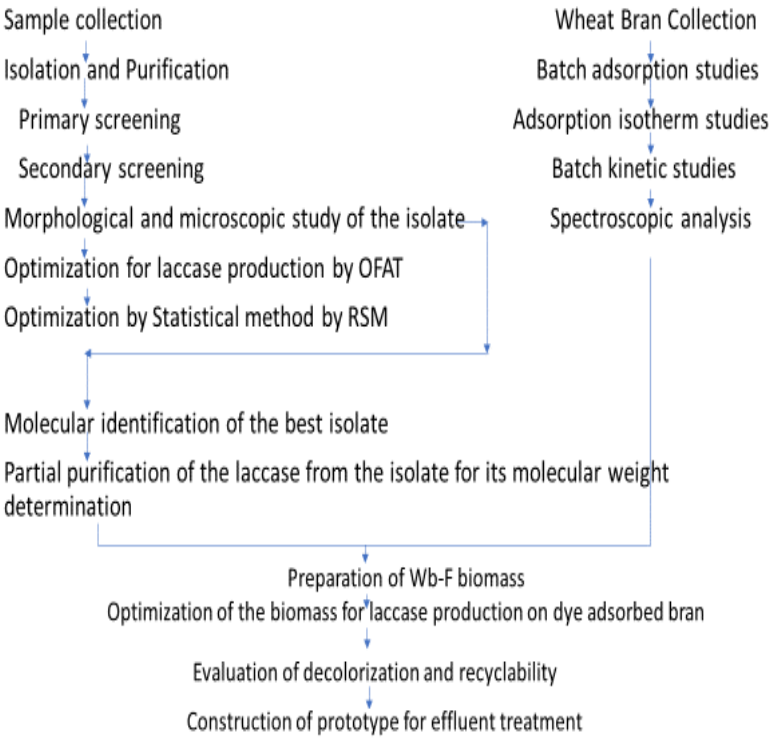

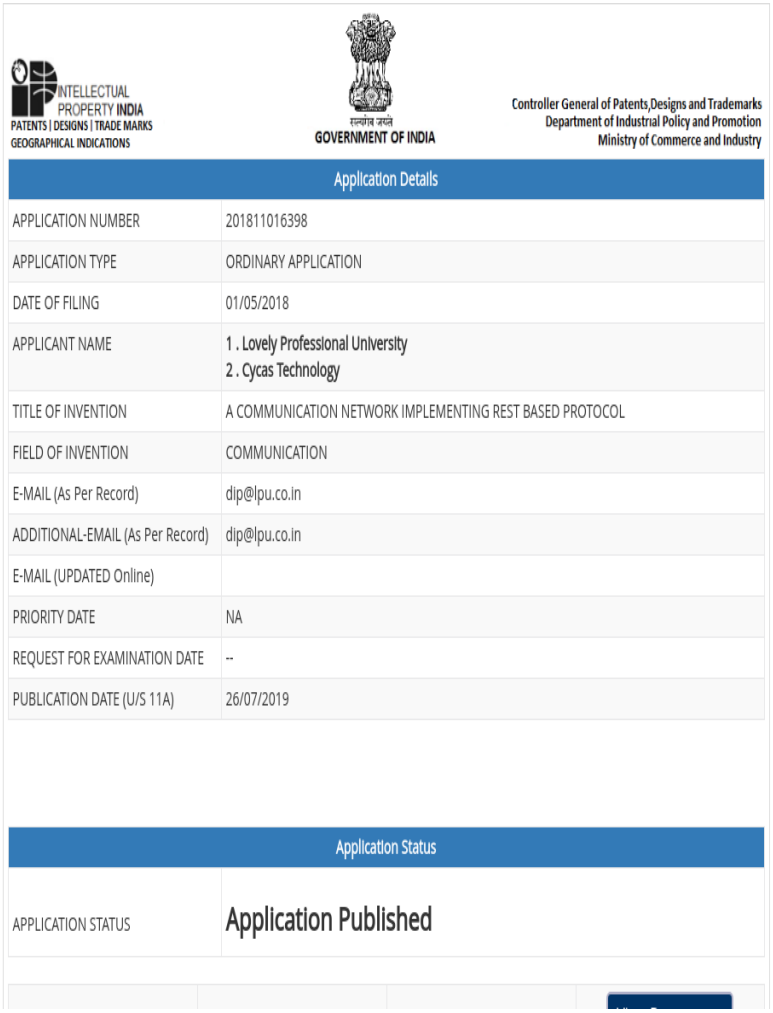

INTELLECTUAL PROPERTY INDIA
PATENTS | DESIGNS | TRADE MARKS
GEOGRAPHICAL INDICATIONS

सत्यमेव जयते
GOVERNMENT OF INDIA

Controller General of Patents,Designs and Trademarks
Department of Industrial Policy and Promotion
Ministry of Commerce and Industry

Application Details

APPLICATION NUMBER	201811016398
APPLICATION TYPE	ORDINARY APPLICATION
DATE OF FILING	01/05/2018
APPLICANT NAME	1 . Lovely Professional University 2 . Cycas Technology
TITLE OF INVENTION	A COMMUNICATION NETWORK IMPLEMENTING REST BASED PROTOCOL
FIELD OF INVENTION	COMMUNICATION
E-MAIL (As Per Record)	dip@lpu.co.in
ADDITIONAL-EMAIL (As Per Record)	dip@lpu.co.in
E-MAIL (UPDATED Online)	
PRIORITY DATE	NA
REQUEST FOR EXAMINATION DATE	--
PUBLICATION DATE (U/S 11A)	26/07/2019

Application Status

APPLICATION STATUS	Application Published

Published Patent

ORIENTAL JOURNAL OF CHEMISTRY
An International Open Access, Peer Reviewed Research Journal
www.orientjchem.org
ISSN: 0970-020 X
CODEN: OJCHEG
2019, Vol. 35, No.(5):
Pg. 1565-1573

Evaluation of Wheat Bran as a Biosorbent for Potential Mitigation of Dye Pollution in Industrial Wastewaters

SUJATA DAS[1], SHALINI SINGH[1]* and SHASHANK GARG[1]

[1]School of Bioengineering and Biosciences, Lovely Professional University, Punjab, India-144411.
*Corresponding author E-mail: shalinisingh.iit@gmail.com

http://dx.doi.org/10.13005/ojc/350514

(Received: September 11, 2019; Accepted: October 12, 2019)

ABSTRACT

Crystal violet (CV) is a basic dye that is extensively used for various industrial uses, ranging from, antimicrobial agent, paints, printing ink, biological stains, to textile dyes. Despite its many uses, it has been associated with environment pollution and toxicity, just like other chemical based industrial dyes, if not kept in check. In the current study, Wheat Bran, an agro-industrial waste reside, was tested for its adsorptive potential for removal/decrease of CV from industrial waste waters. Under optimized conditions of incubation (pH 8, temperature 30°C, adsorbent concentration 10 g/L, time 180 min and adsorbate concentration 100 mg/L), the adsorbent removed around 88% of CV from its aqueous solution, fitting appropriately adsorption model (*Langmuir isotherm*) with maximum adsorption capability (q_m) value of 25.66 mg/g, and following pseudo first-order kinetic model. Alkali treatment of adsorbent, though, showed around 4% increase in dye decolorization, but unmodified bran was preferred for further work to justify the need for cheap and environment friendly adsorbent to remediate industrial dye waste waters.

Keywords: Wheat Bran, Wheat Bran Adsorption, Crystal violet dye (CV), Isotherm, Biosorbents.

INTRODUCTION

Dyes are colored compounds, containing a chromophoric (credited for imparting color) and the auxochrome (credited for color intensity) group[1] but chemical based conventional dyes are recalcitrant and long period persistent molecules that pose threat to environmental quality as well as life forms. Hence, efficient removal/neutralization of residual dyes before their release into the environment is of utmost concern for which different methods (physical, chemical and biological) are being evaluated for reducing dye pollution in water bodies.

Various physico-chemical treatment methods, like, electro-coagulation, flotation etc. are been employed but have shown limited success in degradation of water soluble, complex structured reactive textile dyes. Improved methods like, Membrane filtration and Ion exchange (physical), Ozonation, Oxidation and Electrolysis (chemical) and microbiological (biological), alone or in different combinations, are providing some significant solutions to dye removal from wastewater. Still, the need for improved, more cost efficient and environment friendly methods to alleviate dye pollution, is ever increasing as many existing

Published Paper1

International Journal of Chemical, Environmental & Biological Sciences (IJCEBS) Volume 5, Issue 1 (2017) ISSN 2320–4087 (Online)

Bioscouring and Desizing of Textile Fabrics Using crude Enzyme Produced by White Rot Fungus (Basidiomycetes) Isolated from Rotten Wood

Sujata Das[1], Shalini Singh[2], Dhruv Sharma[3], Muhammed Anowar[4], Rajdeep Kaur[5] and SandeepKaur[6]

***Abstract*—** With an increasing demand for the reduction of pollution caused by textile industries the exploration of the microbial world has gained a special arena in the field of contemporary research. The usage of microbial enzymes is preferred to chemical processing of fibres and textiles because of their non-toxic and eco-friendly characteristics. The present experimental study circumscribed around the development of an environment friendly and an economical mean of fibre development by desizing and bioscouring with the help of crude enzyme produced from a wild variety of isolated basidiomycetes. Isolation of basidiomycetes was done from wood barks collected from eastern part of India. Plate assay for amylase, cellulase and xylanase, from the isolated organism was performed along with the determination of their respective enzyme activity. Enzyme produced on the 11 day of incubation under SSF condition at 25^{0}C was obtained to show the highest enzyme activity. A comparative study of desizing and scouring has been done subsequently on the basis of biological (with extracted enzyme from the isolate) and chemical processes whereby the biological method has shown a significant level of increase in absorbency and whiteness of the textile fibre. The liquid waste discharged from both the methods were also estimated for COD and BOD and has shown that the usage of crude enzyme for the both desizing and bioscouring was more environment friendly in nature.

***Keywords*—** Bioscouring, Desizing, cellulase, amylase, xylanase, COD, BOD.

I. Introduction

Fabrics, yarns or raw fibres includes several kinds of impurities like chemical residues, pesticides, dirt, seed coat fragments, pesticides, and metallic salts. The process which aims to improve the whiteness and absorbency of textile materials by discarding such non-cellulosic natural matter from the fabrics is called defined scouring [19, 4]. In nature, non-cellulosic materials create a physical hydrophobic barrier to protect the fibre from the environment throughout its even wettability such that these fabrics can be dyed and bleached conveniently.

In industries, sodium hydroxide, a highly alkaline chemical is generally used in scouring methods [22]. Along with the removal of the non-cellulosic impurities from the fabrics, these chemicals also attempts to damage the cellulose which results in loss of heavy strand and loss in weight of the fabrics [5]. Additionally, the use of these harmful chemicals leads to high BOD (Biological Oxygen Demand), COD (Chemical Oxygen Demand) and TDS (Total Dissolved Solid) in waste water [29].

Desizing is a process which discards a number of adhesive substances from the warp threads which is generally coated for the prevention from thread from breaking during weaving process. This method is generally carried out by treating the fabrics with a wide range of chemicals like alkali, acids or oxidizing agents [5]. In recent years, the bio-catalytic applications for enzymes have evolved immensely because of their specific properties. Enzymes have a high specificity, undergo a wide diversity of reactions, are ecologically correct and additionally present chemo-regio-enantio selectivity. A large variety of enzymes are being produced by a wide range of microorganisms which have been used in textile industry. Some of these microorganisms include: ***Bacillus subtillis***, ***Aspergillus niger*** [8], ***Aspergillus oryzae*** [8], ***Trichoderma reesei*** [9], ***Phanerochaete chrysosporium***, ***Pleurotus ostreatus*** [10]. Cellulase, amylase and xylanase are some of the potential enzymes which finds wide spread industrial applications in desizing and bioscouring [21].

Amylase comes from a family of glycoside hydrolase enzymes which acts on alpha 1, 4 glycosidic bonds and finally breaks down starch into glucose molecules. Cellulase are also known as endo-1, 4-beta-glucanase. They play a vital role in the hydrolysis of cellulosic biomass to sugars. Xylanases occurs in a broad range of fungi and bacteria. They are

Published Paper 2